GPS TECHNOLOGY TO STUDY CRUSTAL MOTIONS IN THE PHILIPPINE REGION

A thesis submitted for the degree of
Doctor of Philosophy

School of Geoinformatics, Planning and Building
Faculty of Engineering and the Environment
University of South Australia

By

David Martin Silcock
B.Surv (NSW) Honours Class 1

March 2002

CONTENTS

LIST OF FIGURES

LIST OF TABLES

ACRONYMNS

AFN	Australian Fiducial Network
AIDAB	Australian International Development Assistance Bureau
AIUB	Astronomical Institute of the University of Berne, Switzerland
AS	Anti-Spoofing
AUSLIG	Australian Surveying and Land Information Group
BCGS	Bureau of Coast and Geodetic Survey, Philippines
CEP	Circular Error Probable
CGSD	Coast and Geodetic Survey Department, Philippines
CMT	Centroid Moment Tensor
DENR	Department of Environment and Natural Resources, Philippines
DGPS	Differential GPS
DMA	Defence Mapping Agency, USA
DoD	Department of Defence, USA
DSTO	Defence Science and Technology Organisation, Australia
EDM	Electronic Distance Measurement
EOPs	Earth Orientation Parameters
ERP	Earth Rotation Parameters
EU	Eurasian Plate
FTP	File Transfer Protocol
GEODYSSEA	Geodynamics of South and South-East Asia
GFZ	German Geodetic Research Institute
GIS	Geographical Information Systems
GOP	Government of the Philippines
GPS	Global Positioning System
GSFC	Goddard Space Flight Centre
GSI	Geographical Survey Institute
HDOP	Horizontal Dilution of Precision
IAG	International Association of Geodesy
IERS	International Earth Rotation Service
IESSG	Institute of Engineering Surveying and Space Geodesy, University of Nottingham, England
IGS	International GPS Service for Geodynamics
IHO	International Hydrographic Office
IRI	International Reference Ionosphere
ISC	International Seismological Centre
ITRF96	International Terrestrial Reference Frame 1996
IUGG	International Union of Geodesy and Geophysics
JPL	Jet Propulsion Laboratory, USA
LC	Linear Combinations of the GPS Phase Observations
LDEO	Lamont-Doherty Earth Observatory
MIT	Massachusetts Institute of Technology
MOST	Multimodal Occupation Strategy

NAMRIA	National Mapping and Resource Information Authority
NASA	National Aeronautics and Space Administration, USA
NEIC	National Earthquake Information Center, USGS
NGS	National Geodetic Survey, USA
NRC	National Research Council, USA
NRMDP	National Resources Management and Development Project
NSF	National Science Foundation, USA
NSSDC	National Space Science Data Center
PGNet	Philippine Geodetic Network
PH	Philippine Sea Plate
PHIVOLCS	Philippine Institute for Volcanology and Seismology
PICMP	Philippine Islands Crustal Motion Project
PRS92	Philippine Reference System 1992
PSP	Philippine Sea Plate
QIF	Quasi Ionosphere Free
RINEX	Receiver Independent Exchange
RMS	Root Mean Square
RTK GPS	Real Time Kinematic GPS
SA	Selective Availability
SCIGN	Southern California Integrated GPS Network
SEP	Spherical Error Probable
SES	Solid Earth Science
SINEX	Solution Independent Exchange Format
SIO	Scripps Institution of Oceanography, USA
SLR	Satellite Laser Ranging
SPS	Satellite Positioning Service
SWP	SW Pacific GPS Project
TEC	Total Electron Content
TECU	TEC Units
UNAVCO	University Navstar Consortium
UniSA	University of South Australia
USCGS	US Coast and Geodetic Survey
USGS	US Geological Survey
UTC	Universal Time Coordinated
UTM	Universal Transverse Mercator
VCV	Variance-Covariance
VDOP	Vertical Dilution of Precision
VLBI	Very Long Baseline Interferometry
WGS72	World Geodetic System 1972
WGS84	World Geodetic System 1984
WSSQR	Weighted Sum of Squared Residuals

SUMMARY

The Philippine Islands Crustal Motion Project (PICMP) has evolved over the period since 1988.

The PGNet was established via the National Resources Management and Development Project 1988-91 (NRMDP) to upgrade the mapping and geodetic control of the Philippines. GPS data were mostly single frequency and processed with standard software and broadcast orbits. Thirty PGNet stations were reobserved in 1990 and 1991 following the 16 July 1990 M_s 7.8 Luzon earthquake. The adjustment of the PGNet showed an overall RMS accuracy of 3ppm and contains significant distortions. These are predominantly ionospheric effects on single frequency GPS observations made during the maximum of Solar Cycle 22.

The PICMP93 campaign established a fiducial network over the Philippine Geodetic Network (PGNet), plus a monitoring network over the earthquake-prone area of central Luzon. This Luzon network was partially resurveyed by the PICMP 96 and 98 campaigns. Therefore, three epochs of high-quality dual-frequency GPS data were available.

The Bernese V4.0 software was used to process the GPS data of the 93, 96 and 98 PICMP campaigns. Each campaign was tied to ITRF96 by co-ordinates and GPS data obtained from regional IGS tracking stations

The readjustment of the PGNet onto the ten PICMP93 (ITRF96) fiducials was undertaken to improve its accuracy as a potential framework for crustal deformation studies and for rapid response surveys of specific large earthquakes in the Philippines.

An analysis is made of the single-frequency GPS measurements taken before and after the 1990 earthquake, to constrain the faulting parameters of this major strike-slip event. The geodetic data imply fairly uniform left-lateral slip of 5.5 - 6.5 m along the well mapped part of the fault trace, in agreement with field mapping of the rupture and in general accord with seismological estimates of the fault parameters. In addition, substantial slip of about 4 - 5 m magnitude is found to have continued about 40 - 50 km northward or northwestward into the Cordillera Central beyond the end of the mapped rupture. This fault segment includes a substantial thrust component in addition to left-lateral slip. The geodetic data favour a faulting depth of at least 20 km along the central part of the rupture, unusually deep for a major

continental strike-slip earthquake.

Surface velocity fields for 1993-96 and 1996-98 of the observed stations are generated and then used to investigate preliminary postseismic deformation following the 1990 earthquake. Using an elastic half-space model with uniform slip below a sub-surface locking depth, a slip rate of 40 mm/yr and locking depth of ~15 km are found.

40 mm/yr is too high to be a steady interseismic rate as it differs from known earthquake recurrence and long-term slip rates on the Philippine fault system in central/northern Luzon. This may be partially a viscoelastic response to the earthquake and thus up to a factor of three higher than the long-term rate. A 15 km locking depth for steady interseismic slip appears to be too shallow compared to the depth of rupture computed in the earthquake. Measurements also show that northeastern Luzon is moving approximately at the Philippine Sea plate rate.

An improved network in Luzon, monitored every 5 years or so, may provide better data about the role of viscoelastic relaxation in the strike slip earthquake cycle e.g. to accurately measure temporal slowing and broadening of the strain field.

DECLARATION OF AUTHORSHIP

I declare that this thesis does not incorporate without acknowledgement any material previously submitted for a degree or diploma in any university and, to the best of my knowledge, does not contain any materials previously published or written by another person except where due reference is made in the text.

David Martin Silcock

ACKNOWLEDGEMENTS

Financial Assistance

The 1993 measurements were funded by NSF grant EAR89-15622 to Dr. J. Beavan at LDEO plus a UniSA grant and DSTO funding to Professor D. Larden.
The 1996 campaign was funded by NSF grants EAR89-15622 to LDEO and EAR93-05180 to Indiana University.
The 1998 measurements were supported by NSF grant EAR97-26024 to Indiana University.
The analysis and interpretation of the data have been funded by the previously mentioned NSF grants and by NZ Foundation for Research, Science and Technology contract CO5811. Also, D. Silcock was granted two periods of study leave by UniSA (1993 and 1999) for this purpose.

Technical Support

Sincere appreciation is offered to:

Professor D. Larden, Unisa, for arranging the availability of 1988-91 PGNet data and making the PICMP93 a possibility.
Andrew Jones, Department for Environment and Heritage South Australia, for his assistance in imparting his knowledge of the GPS processing and final geodetic adjustment of the PGNet (1988-91).
Commodore Feir, the staff surveyors and field crews of NAMRIA Philippines for their admirable support of the PICMP93, 96 and 98 campaigns.
Dr. J. Beavan, GNS New Zealand, for his expertise in geodynamics and Bernese GPS processing expertise.

Personal Support

Special thanks to:

Dr J. Beavan for being an external supervisor, his role as a mentor but more importantly his friendship.

Dr. M. Bevis (now at the University of Hawaii) for sparking an interest in GPS and geophysics in the late 1980's whilst working together in the SW Pacific.

Professor J.Gilliland, Unisa, for being the internal supervisor and for his welcomed counsel in the final production of this thesis.

The Silcock family (Vicky, Stephanie, Christopher and Michael), for their love, support and understanding throughout this research.

CONTRIBUTION TO KNOWLEDGE

Beavan, J., **D. Silcock**, M. Hamburger, and E. Ramos, Geodetic constraints on coseismic displacement and postseismic deformation associated with the 1990 M_s 7.8 Luzon earthquake, and implications for deformation at the Philippine Sea-Eurasia plate boundary, Paper presented to the GPS'99 conference (October) in Tsukuba by J. Beavan, 1999.

Beavan, J., **D. Silcock**, M. Hamburger, E. Ramos, C. Thibault, and R. Feir, Geodetic constraints on postseismic deformation following the 1990 M_s 7.8 Luzon, Philippines, earthquake, and implications for Luzon tectonics and Philippine Sea plate motion, *G-cubed, Vol. 2, paper number 2000GC000100*, 20 Sep, 2001.

Silcock, D., J. Beavan, R. Feir, and D. Larden, The Philippine Islands Crustal Motion Project, Poster presentation at the 1996 Western Pacific Geophysics Meeting (AGU) in Brisbane, 1996.

Silcock, D., and J. Beavan, Crustal motion studies in the Philippine region using GPS technology, Poster presentation at the 39th Australian Surveying Congress *(Southern Exposure)* in Launceston, November 1998.

Silcock, D. M., and J. Beavan, Geodetic constraints on coseismic rupture during the 1990 M_s 7.8 Luzon, Philippines, earthquake, *G-cubed, Vol. 2, paper number 2000GC000101*, 31 July, 2001.

Thibault, C., M. Hamburger, A. Lowry, J. Beavan, **D. Silcock**, S. Yu, E. Ramos, R. Punongbayan, and R. Feir, GPS observations of crustal deformation in the plate boundary zone of the northern Philippine Island arc, Paper presented to the spring 1999 AGU meeting in Boston, USA by C. Thibault , Indiana University, USA, 1999.

1.0 Project Overview

1.1 Introduction

This thesis details the author's contribution to the establishment of a crustal motion monitoring program in the Philippine Islands using GPS technology, and the subsequent analyses of the geodetic data for regional geodynamics. The research was named the Philippine Islands Crustal Motion Project (PICMP) for recognition purposes in the international community. As one of the inaugural researchers in this collaborative venture, it was necessary to thoroughly depict all aspects of the project that would be of future value to geophysicists and geodesists. The work received financial support from the US National Science Foundation (NSF), the Australian Defence Science and Technology Organisation (DSTO), the Government of the Philippines (GOP) and the University of South Australia (UniSA). The program is designed to maximise the scientific outcomes from PICMP with only a small injection of funds and builds upon the existing cooperation between the organisations and countries involved in the project.

The project has three principal aims:

(1) to install a superior quality "backbone" geodetic network throughout the Philippine Islands to use as a basis for future crustal motion studies;

(2) to use this backbone to enhance the accuracy of analysis of lower-order surveys done under the 1989-91 AIDAB funded National Resources Management and Development Project (NRMDP); and

(3) thereby to improve the coseismic and postseismic information on the 1990 Luzon earthquake.

1.2 Background

In the late sixties, the US National Aeronautics and Space Administration (NASA) took steps towards utilising space technologies for the measurement of tectonic plate motion and the deformation of the earth's crust. This led to the establishment of the Earth and Ocean Dynamics Program. In 1979, this program was revised and the geodesy and geodynamics elements were consolidated within a new Geodynamics Program. At the same time, the US National Research Council (NRC) commissioned a study to investigate and recommend strategies for determining present-day crustal movements, particularly in active seismic zones. This study found that [*NRC*, 1981]:

- geodetic measurements make a major contribution to the understanding of such movements and thus earthquake research;
- an increased knowledge of tectonic motion in several major seismic zones greatly improves our understanding of earthquake source mechanisms; and
- an international program of plate motion measurements is very valuable for understanding the tectonic processes that have shaped the earth's surface.

With the eighties came the recognition that a global perspective of the earth's dynamics was needed. This led to the formulation of the Solid Earth Science (SES) Program for the nineties with plate motion and crustal deformation still remaining priority areas for study [*NASA*, 1991]. A primary goal of the SES program is to investigate crustal kinematics and deformation on both local and global scales and across a variety of different plate boundaries. Two requirements were needed to study these movements:

1. a monitoring network deployed across the active zone and
2. a mechanism to tie this network to a global reference frame

It was also emphasised that new areas of interest should include the major plate convergence systems around the Pacific Basin and the regional tectonics of SouthEast Asia.

The PICMP research is a unique study of one of the world's most active seismic zones. Global Positioning System (GPS) technology and advanced geodetic techniques have been utilised to monitor crustal deformation and tectonic motion across the Philippine archipelago.

1.3 Project Aims and Significance

Recent advances in the development of high-precision GPS receiver technology and satellite orbit determination, coupled with improvements in atmospheric modelling and refinements in data acquisition and analysis techniques, are having a significant impact on the studies of crustal deformation and earthquake processes [see eg. *Dixon*, 1991; *Blewitt*, 1993; *Larson et al.*, 1997, *Segall and Davis*, 1997, *Shen et al.*, 2000]. Studies

of this nature are of major importance to earth scientists attempts to understand global seismicity and the mechanisms which accompany the release of strain in seismic zones. In this project, specific areas of the Philippine tectonic zone are monitored by high precision GPS surveying techniques and, in particular, an understanding of the kinematics of the region and the mechanisms for crustal deformation in the earthquake prone area of central Luzon are developed.

Tectonic setting of the Philippines

The Philippines is a complex junction of island arcs that lie at the intersection of four major plates; the Eurasian, Philippine Sea, Pacific and Indian-Australian. The tectonics of the area (see Figure 1.1) is influenced by many evolving systems of subduction with current deformation patterns dominated by active subduction at the Philippine and Manila trenches, rejuvenated subduction at the East Luzon trough, and major left lateral, strike slip along the Philippine fault system. This system has two main segments, which are the central section between the Bondoc Peninsula and Mindanao and the northern section in Luzon. The central section is characterised by pure left lateral, strike slip motion while the northern section is characterised by a significant thrust component in addition to the strike slip. In the south, the location is poorly known and its relation to the major plate boundaries speculative.

The Philippine fault is a classic example of a strike slip fault located behind a subduction zone. It plays an important role in the geodynamics of the region; however, its deformation pattern is still uncertain. Detailed studies of the fault zone have been scarce, although improved knowledge of Philippine geology and recent slip vector data now shed more insight on the fault motion. Estimates from localised sections along the fault predict movement at a rate of 2 to 2.5 cm/year [*Barrier et al.*, 1991; *Duquesnoy et al.*, 1994]. However, there has not yet been a comprehensive study of the fault zone and the surrounding tectonics. In particular, the kinematics and block geometry in the northern Philippines are quite complicated and new data, especially the rates and directions of movement along the active boundaries, are needed. A thorough discussion of the complexities of tectonic and earthquake monitoring in the Philippines will be covered in Chapter 6.

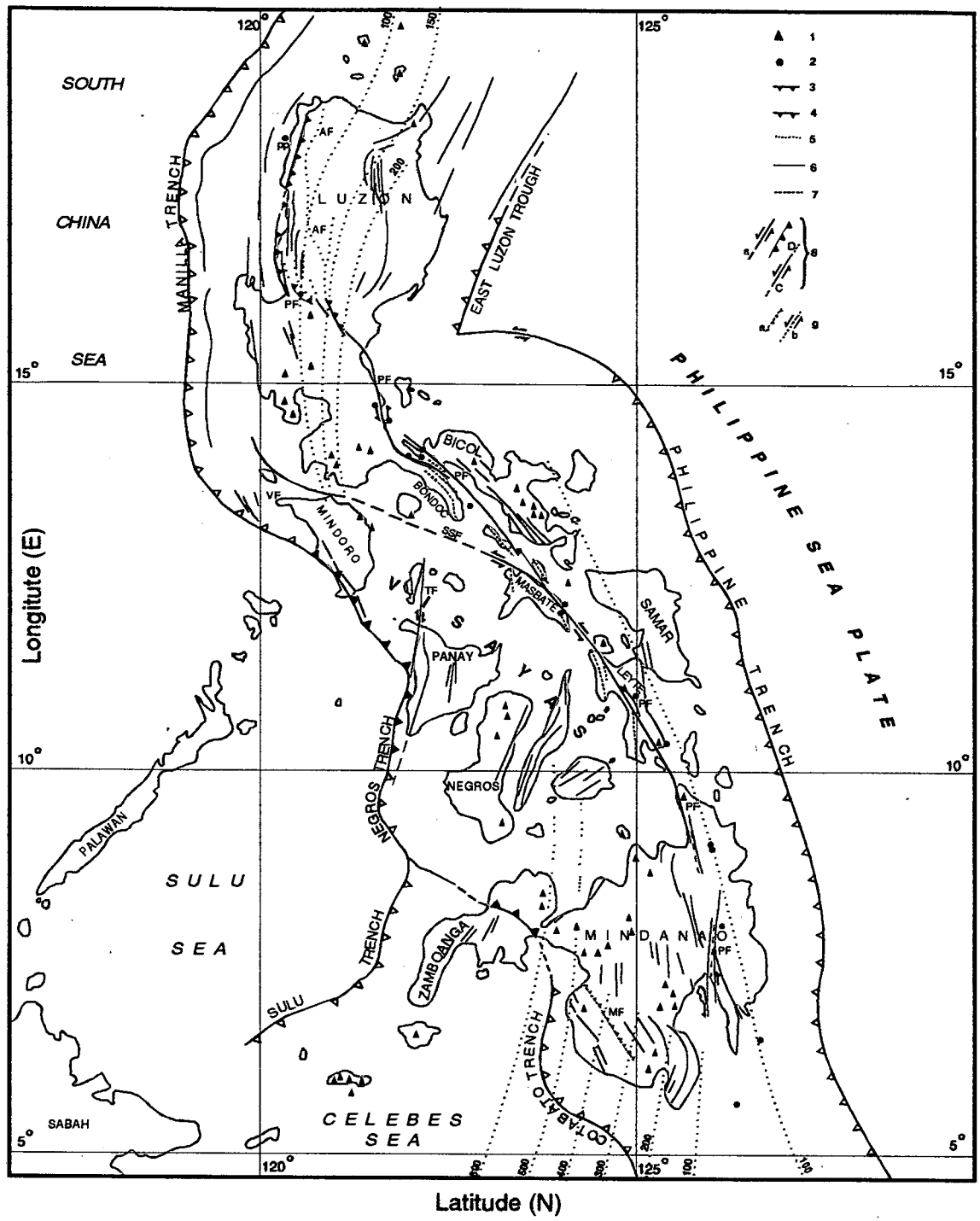

Figure 1.1 Seismotectonic map of Philippine Islands. [*Barrier et al.*, 1991]

1 = Quaternary volcanoes; 2 = epicentres of large earthquakes (M > 6.9) related to Philippine fault since 1900 [*Rowlett and Kelleher*, 1976]; 3 = active subduction; 4 = active collision front; 5 = depth contours (in km) to top of Benioff zone (dashed where uncertain) [*Cardwell et al.*, 1980]; note that Benioff zone beneath Mindanao is related to Molucca Sea subduction); 6 = axes of main Pliocene-Pleistocene fold structure; 7 = axes of main compression structures related to Philippine fault; 8 = main active faults (PF = Philippine, SSF = Sibuyan Sea, TF = Tablas, VF = Verde Passage faults; a = strike-slip, b = thrust, c = oblique thrust faults); 9 = main faults possibly active (a) or reactivated (b) (AF = Abra, MF = Mindanao faults).

The Geodetic Survey of the Philippines

A homogeneous geodetic network across the Philippine Islands is essential for the provision of new information on the complex neotectonics of the region. Fortunately, "a first order national GPS network" was established during the period 1989-91 [*AIDAB,* 1992]. This network was sponsored by the Australian International Development Assistance Bureau (AIDAB) working in conjunction with the Philippine Department of Environment and Natural Resources (DENR). The geodetic survey was performed by SAGRIC International Pty. Ltd (Australia) with the assistance in the Philippines from the National Mapping and Resource Information Authority (NAMRIA) and the Certeza Surveying Company. The Philippine Geodetic Network (PGNet) consists of 360 Primary Network stations at nominal spacings of 50 km (see Figure 1.2). The GPS observations were mostly undertaken with single frequency receivers such as Trimble 4000ST's. Because the AIDAB consultancy had a precision specification of only 10 ppm the data were successfully processed with Batch_phaser and Trimvec software using broadcast orbits. The adjustment of the network showed an overall RMS accuracy of 3 ppm. As a result, for geophysical purposes, there are significant distortions. These were mainly due to ionospheric effects on the single frequency GPS signals. These affects were worse than normal due to peak sunspot activity during the PGNet survey. GPS observations took place during the solar maximum of Solar Cycle 22. Figure 1.3 shows a historical graph of solar cycles since 1750 (see Chapter 5 for discussion of the effects of the ionosphere on the PGNet and the attempt to account for these in the readjustment onto the PICMP93 fiducials).

Given the limitations of the PGNet (ie relatively low accuracy and substandard monumentation for geophysical use), the data set would still be of immense value for long-term crustal motion studies if the RMS could be reduced to 1 ppm or less. The limitations of the PGNet would then be offset by the extensive national coverage of the network i.e. the PGNet has a nominal survey monument spacing of approximately 50km.

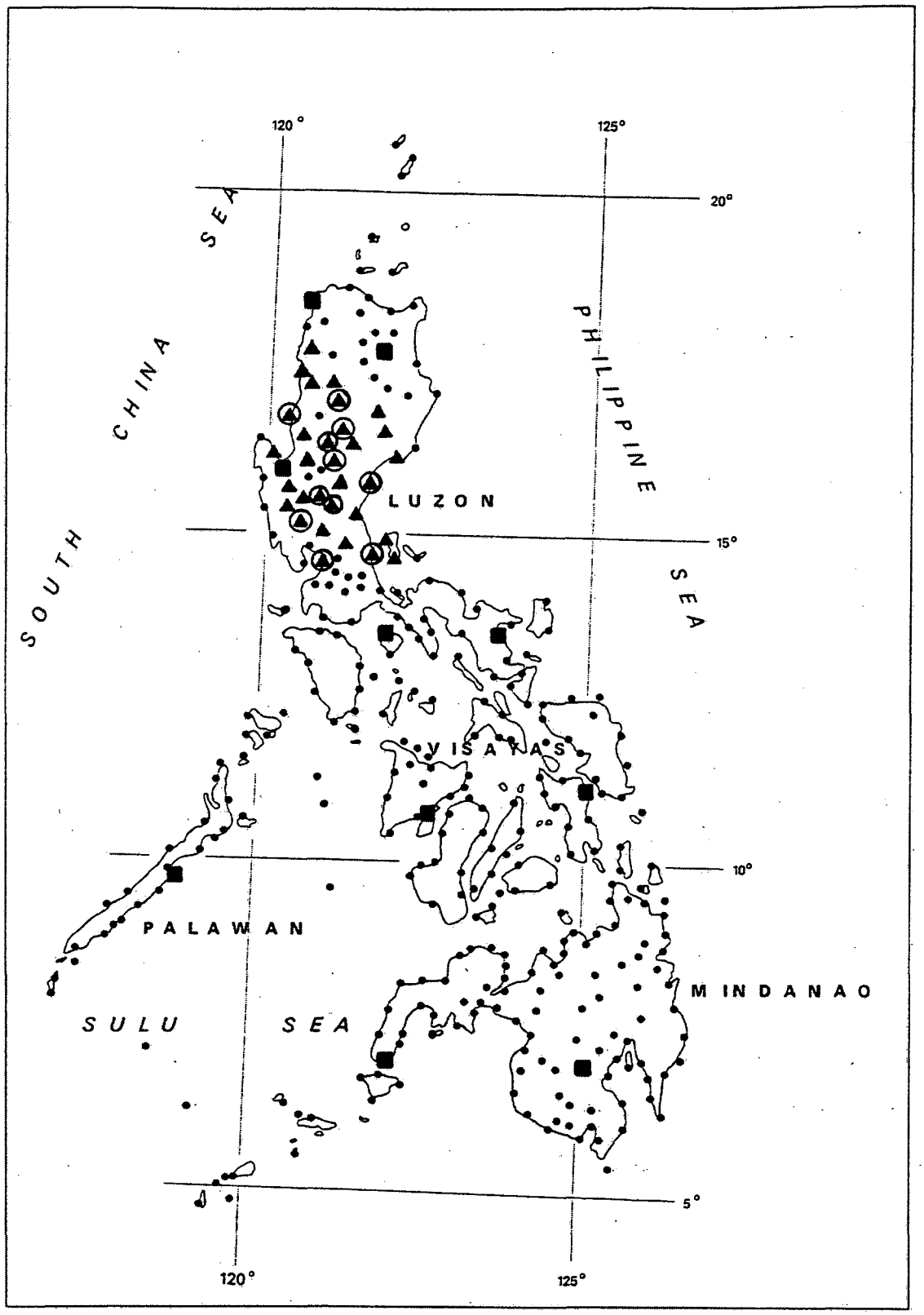

Figure 1.2 Geodetic Monitoring Network for Crustal Deformation and Regional Tectonic Plate Motion Studies in the Philippines. All stations shown on the diagram were observed as part of the AIDAB (1989-91) PGNet survey. Stations marked with a ▲ symbol were specifically observed as part of the Luzon earthquake resurvey in 1991. Stations marked with a ■ symbol were observed as part of PICMP93 to establish the fiducial network and those marked with a ◬ symbol were observed as part of the PICMP93 monitoring program in the Luzon earthquake zone.

Chapter 2 will detail and discuss:

- the PGNet GPS survey (1989-91)
- problems encountered during the survey and the GPS processing eg Solar Cycle 22
- baseline processing techniques adopted by the SAGRIC consultants
- the least squares adjustment of the PGNet, and
- the Luzon Datum definition

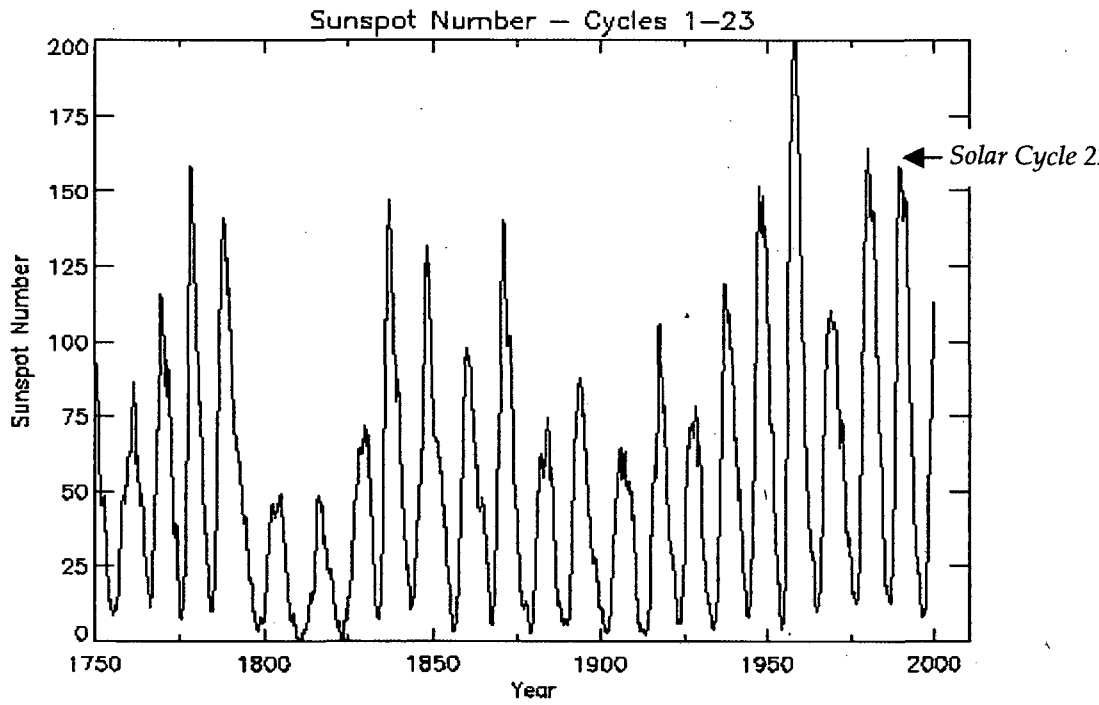

Figure 1.3 Graph of Historical Solar Cycles since 1750
[*IPS Radio & Space Services*, 2001]

The 1990 Luzon Earthquake

The potential scientific value of the network was illustrated during the (M_s = 7.8) 1990 earthquake in central Luzon which ruptured more than 100 km of the Philippine and Digdig faults causing left lateral offsets of up to 6 metres [*Yoshida and Abe*, 1992]. Figure 1.4 shows the extent of the surface rupture and also the complex nature of the Philippine Fault system in central Luzon. As a result, the PGNet suffered a major dislocation in the earthquake zone. GPS observations were repeated

(about thirty of the PGNet stations) and finally completed in May 1991 indicating metre level displacements. The 1990 Luzon earthquake is one of the great continental strike-slip earthquakes of the 20th century. All indications are that it ruptured to a surprisingly deep depth of 20 km as opposed to 10-15 km for comparable earthquakes such as 1906 San Francisco or 1976 Tangshan [*Yoshida and Abe*, 1992]. This earthquake is one of the largest ever to occur during a GPS campaign and an analysis of the coseismic and postseismic displacements will provide further insight on the geometry of the earthquake rupture, the characteristics of the deformation field and the crustal motions in the region (see Chapter 6.0).

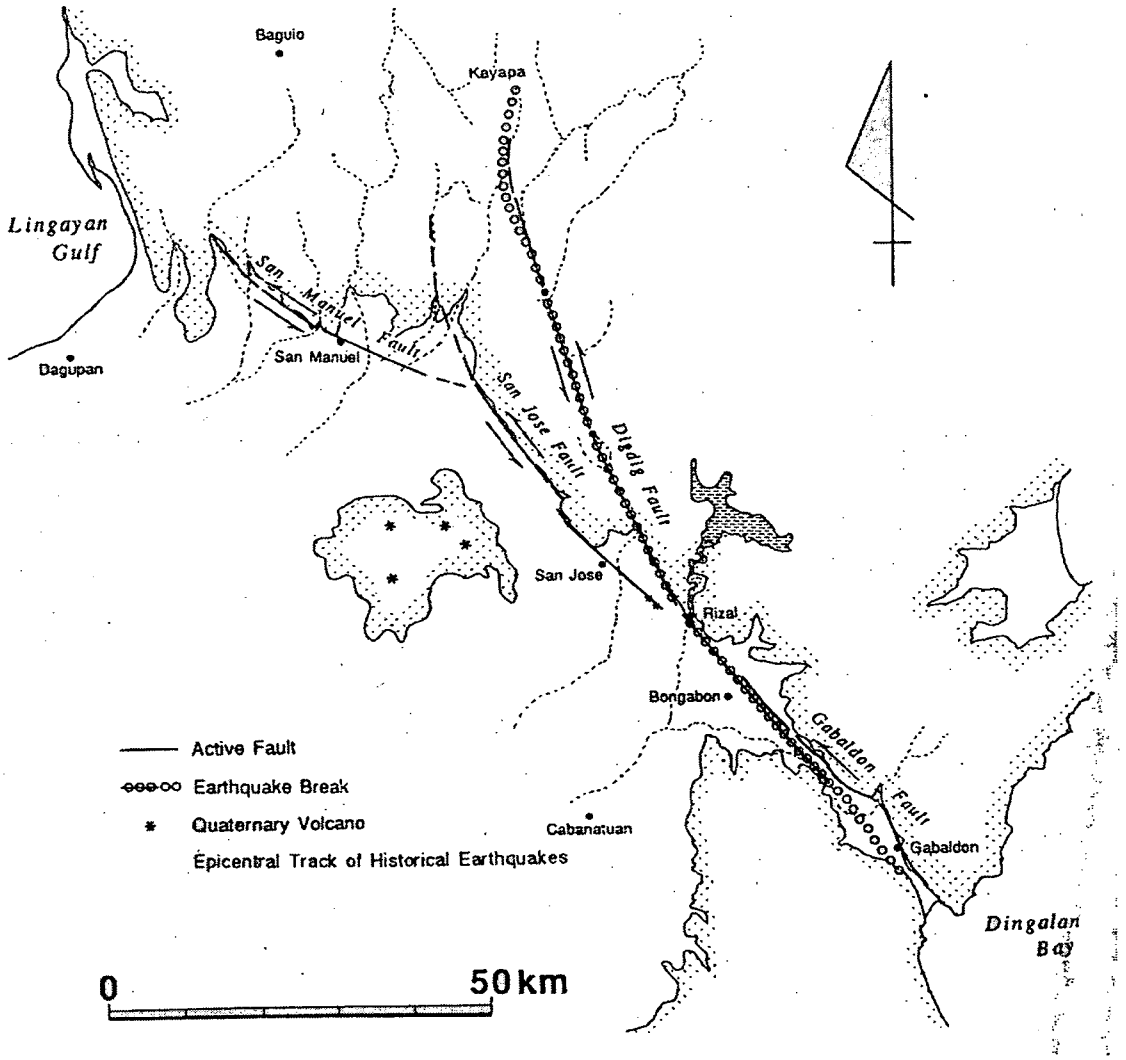

Figure 1.4 Location of the 120 km surface rupture of the 1990 Luzon earthquake. The active faults belonging to the Philippine Fault in Central Luzon are divided into several segments as shown [*Nakata et al.*, 1996].

Establishing the PICMP Network

The realisation of these objectives required a high precision fiducial network over the PGNet and a monitoring network in the earthquake zone. This was accomplished in April 1993 by the University of South Australia (UniSA) and the Lamont-Doherty Earth Observatory (LDEO) of Columbia University [*Silcock and Beavan,* 2001]. The University Navstar Consortium (UNAVCO) facility in Boulder Colorado provided ten Trimble 4000SST dual-frequency squaring receivers, ancillary equipment such as solar panels and a geodetic engineer who was responsible for the training of the Filipino surveyors and the maintenance of equipment. Data acquisition was carried out using the then standard UNAVCO procedures for crustal motion.

Prior to this first PICMP GPS campaign (PICMP93) it was necessary to make a judicious selection of the proposed fiducial stations. The PGNet station descriptions were obtained and analysed for suitability. Advice was also sought from Beavan with respect to the positioning of these stations for a high fidelity geodetic network to monitor tectonic and earthquake movements. In addition, the station sites chosen were to have the following properties:

- stability ie preferably in rock or stable solid ground and well away from fault lines
- PGNet integrity – a substantial mark within the 1989-91 network
- safe access and security for personnel/equipment

The field component of this thesis was the planning, supervision and coordination of the PICMP93. The logistical tasks were extensive and required very careful consideration. Some of the problems encountered were:

organising the entry of personnel and GPS equipment into the Philippines, the GPS training of Filipino surveyors to UNAVCO criteria, travel arrangements, access to geodetic stations, GPS battery recharging in remote areas, supply of provisions and per diems to survey parties, safety issues for personnel and equipment in regions known for terrorist activity, maintenance of GPS receivers, downloading session data onto disks, storage of disks, GPS session planning and movement schedules, debriefing survey crews, collecting and collating all disks on conclusion of the

campaign and finally organising the return of equipment to the USA.

The PICMP93 campaign involved an intensive two-week survey using high precision GPS techniques and was carried out in two stages (see Figure 1.2).

Stage 1 Philippine fiducial network

The ten 4000SST receivers were deployed nationwide on preselected stations of the PGNet. These fiducials were to provide a base network for future countrywide deformation studies, and to enable the PGNet (obtained mostly with single-frequency GPS receivers) to be adjusted onto a high precision backbone and thus to improve its accuracy. The observations were 12-hour measurement sessions for one week.

During this stage, Silcock and Beavan undertook a field reconnaissance of the 1990 Luzon Earthquake zone. The PGNet stations to be re-observed were prudently chosen and an observation schedule for Stage 2 was prepared.

Stage 2 Luzon Earthquake Zone monitoring network

On completion of Stage 1, the GPS receivers were redeployed for a regional survey of 15 sites in Luzon (10 observed in the 1990 post-earthquake survey) to enable postseismic and interseismic deformation to be monitored. The total observation period was one week with 12-hour measurement sessions. Three receivers remained stationary on stations ABY3, CGY8, PNG5 (stable PICMP fiducial stations, as shown in Figure 5.1) and the remainder were required to be moved throughout the selected PGNet stations within the earthquake zone.

The Luzon network was partially resurveyed in May 1996 (PICMP96) and May 1998 (PICMP98) using full-wavelength dual-frequency receivers with between one and six 24-hour sessions at each station (Indiana University)

Table 1.1 shows the stations observed in each PICMP campaign and the number of observational sessions in each.

NB Session lengths were 12 hours in 1993 and 24 hours in 1996 and 1998

NAMRIA STATION	GPS ID	PICMP93	PICMP96	PICMP98
ABY03	**ABY3**	12	4	-
ABY03 RM 4	**ABX3**	-	-	1
ARA01	**ARA1**	2	-	-
MAGNETICS 1995 BALER	**ARX1**	-	1	2
BLN04	**BLN4**	3	3	1
CGY08	**CGY8**	12	6	2
CTN01	**CTN1**	6	-	-
IFG01	**IFG1**	5	2	2
ILN01	**ILN1**	6	-	-
ILO01	**ILO1**	6	-	-
LUN01	**LUN1**	5	2	2
LYT08	**LYT8**	5	-	-
MMA01	**MMA1**	2	6	2
MMA08	**MANL**	-	6	15
MRQ01	**MRQ1**	6	-	4
NEJ43	**NE43**	3	-	-
NEJ44	**NE44**	2	3	3
NVY01	**NVY1**	3	2	-
NVY03	**NVY3**	1	-	-
NVY03 (mark moved between '93 & '96)	**NVX3**	-	2	-
NVY03 RM 3	**NVE3**	-	-	2
NVY04	**NVY4**	2	4	2
PLW11	**PL11**	5	-	-
PMG01 (mark moved between '90 & '93)	**PMX1**	2	4	2
PNG03	**PNG3**	-	-	1
PNG05	**PNG5**	12	6	2
QZN03 RM 2	**QZE3**	-	-	3
QZN05	**QZN5**	2	-	-
QZN07	**QZN7**	-	2	2
TRC02 RM ?	**TRE2**	-	3	2
ZGS02	**ZGS2**	6	-	-

Table 1.1 The PICMP93, 96 and 98 campaigns, the stations occupied and the number of sessions observed.

Chapter 4 details the high precision GPS processing of the 1993, 1996 and 1998 PICMP campaigns using the Bernese V4 software in the International Terrestrial Reference Frame 1996 (ITRF96). Each campaign was tied to the ITRF by co-ordinates and GPS data obtained from regional IGS tracking stations. A determination of the velocities of the observed stations will also be given.

ITRF96 was adopted for the evaluation of the PICMP campaigns because:

1. the GPS processing of all campaigns was carried out in early 1999 and ITRF96 was well accepted and adopted by the geophysical fraternity [see eg *Kouba et al.*, 1998], and

2. Beavan required all data in the ITRF96 for integration into the Philippine Sea plate (PSP) project [*Beavan et al.*, 1994].
3. Collaborative research by *Thibault* [1999] ie GPS campaigns in 1996 and '98, also utilised the PICMP93 data and eventually all were analysed using the Bernese 4.0 Processing Engine with coordinates in ITRF96.

Significance of the PICMP Research

The overall aim of the PICMP is to use GPS surveying techniques to monitor the existing fiducial network in the Philippines and the local network in the Luzon earthquake zone and determine a kinematic model for the region and the crustal deformation patterns from the geodetic data.

It is expected that the project will achieve the following specific objectives (those highlighted comprise this PhD dissertation):

i) **evaluate the errors in PGNet and improve its applicability for long-term crustal motion and earthquake studies throughout the Philippines (Chapters 2 and 5)**

ii) **determine the ground displacement vectors for the 1990 Luzon earthquake using GPS data and conduct a geophysical analysis of this displacement field (Chapter 6)**

iii) **determine the magnitude and extent of the postseismic displacements for the 1990 Luzon earthquake and analyse these displacements within the context of the earthquake model (with respect to the PICMP93 and PICMP96 campaigns) (Chapter 6)**

iv) determine the current rate and direction of movement along the Philippine fault and compare this estimate with the long-term (90 year) value obtained from an analysis of the classical triangulation and GPS data and the geological record, and

v) determine the motion of the Philippine tectonic zone with respect to the Eurasian and Philippine Sea plates and use this estimate to improve the plate motion models in the region.

The PICMP is assured of ongoing involvement and support from American and Philippine colleagues (eg PICMP96 and PICMP98). Also GPS data obtained from the Philippine Sea Plate experiment [*Beavan et al.,* 1994] is available to provide ITRF96 coordinates for the high precision GPS processing. Both the Philippine Institute for Volcanology and Seismology (PHIVOLCS) and DENR have pledged ongoing support for this study.

The magnitude of the project demanded that the tasks outlined above be shared by several researchers with specific expertise. This study within the Philippine region is unique and the research has international significance.

1.4 Research Plan, Methods and Techniques

The US Department of Defence operates GPS with a constellation consisting of about 24 satellites. Each satellite transmits a unique signal on two L-band frequencies. The carrier waves are modulated with a standard (S) code and a precise (P) code. A three-dimensional baseline vector between two points can be accurately determined with respect to a geocentric coordinate system from observations of the carrier phase. The criteria for obtaining very high precision GPS baselines include: an optimum satellite configuration, precise satellite orbits, dual frequency carrier phase data and specialised GPS processing software eg Bernese version 4.0 software. GPS surveys for geophysical purposes are now regularly yielding accuracies of better than a few parts in 10^8 of the baseline length [see eg. *Dixon,* 1991; *Blewitt,* 1993; *Segall and Davis,* 1997]. Chapter 3 presents a brief overview of GPS, some applications to geophysics and the very high precision processing techniques adopted for this research.

The PICMP research plan is comprised of two key components:

- ongoing GPS field surveys in the Philippines at fiducial stations and within the Luzon earthquake zone (PICMP93, 96 98 etc) and
- the complementary research program of data analysis and geophysical interpretation.

The strategy for measurements every two to three years is realistic based on the

knowledge of the predicted rate of 2.5 cm/yr for crustal movement along the fault and the signal to noise ratio achievable from GPS data. The PICMP96 and 98 campaigns added considerable value to the PGNet and PICMP93 and thus extended the dataset over a period of seven years. This timeframe is necessary for the detection of secular movement along the fault zone and adequately covers the period over which postseismic displacements will occur after the Luzon earthquake (Chapter 6).

An analysis of the PICMP93 data, utilising the Bernese version 4.0 software package, demonstrated that the project objectives were achievable. Figure 1.5 depicts the short-term repeatability of daily solutions at the 1-4 parts in 10^8 level for baselines ranging in length from 200 to 750 km (See Chapter 4 for full GPS processing details of each campaign).

The readjustment of the PGNet onto the PICMP93 (ITRF96) fiducials was carried out using the adjustment program NEWGAN developed by Dr. J. S. Allman from the Canadian Geodetic Survey programs GANET and HAVOC2 (Chapter 5). The rationale for this study is the potential use of PGNet for rapid response surveys of specific large earthquakes in the Philippines. The GPS observations to establish the PGNet were primarily single frequency phase measurements without tight control at long wavelengths. Although the data processing was not as rigorous as that for crustal motion research, an overall rms accuracy of 3 ppm was achieved.
A comparison of PGNet with the PICMP93 fiducial network has also confirmed this result. Even so, a more stringent analysis and adjustment of PGNet onto the fiducial framework using the method of least squares was needed to improve its accuracy to 1 ppm (if possible) for long-term crustal motion and earthquake studies. Particular attention was given to scale errors within the PGNet, which may have been introduced by:

(1) significant changes to the GPS constellation during the 1989-91 survey and
(2) ionospheric effects on the GPS signals caused by excessive sunspot activity in late 1989 and 1990 [*Larden et al.*, 1991].

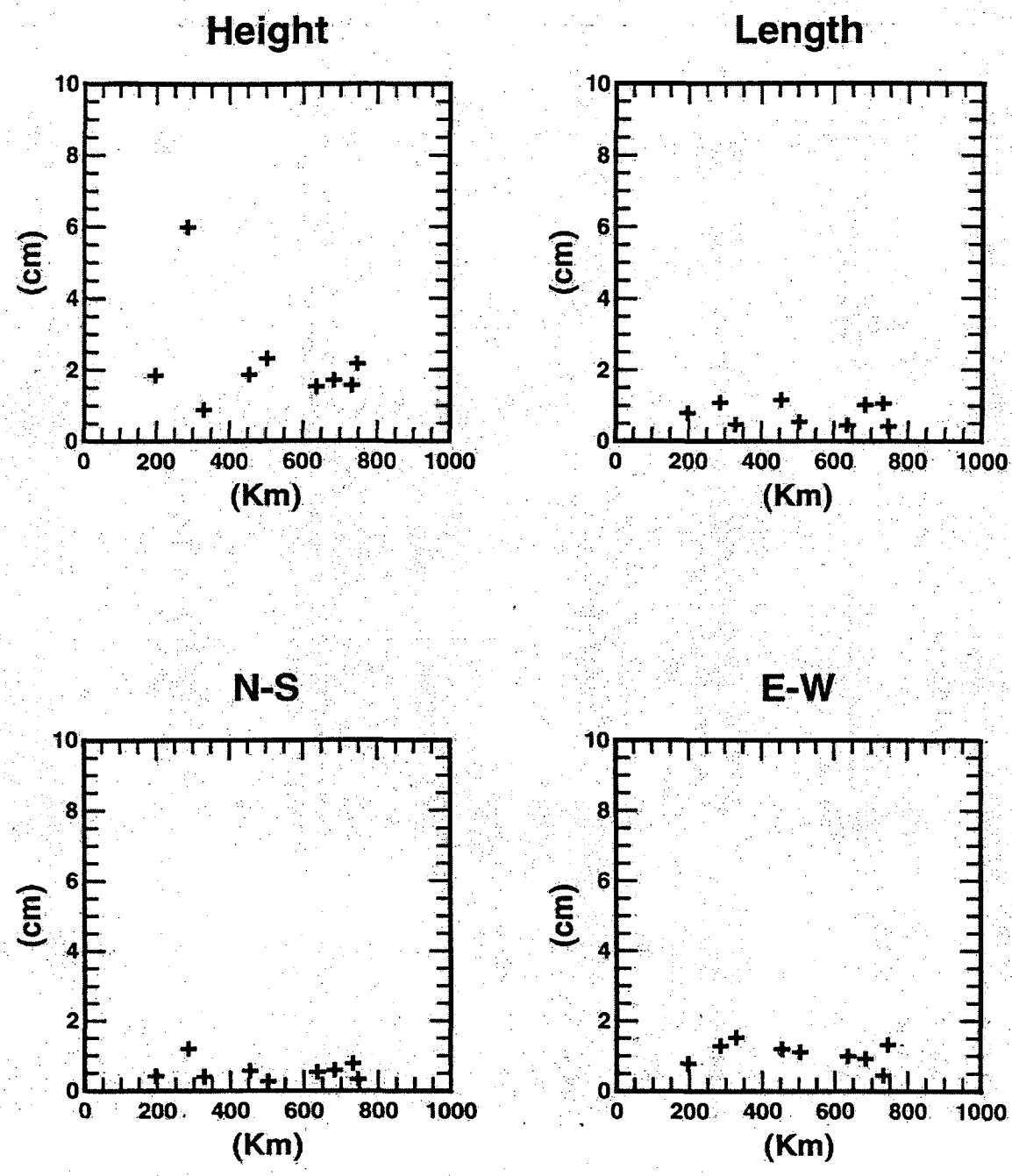

Figure 1.5 Repeatabilities of daily solutions for GPS Baselines in the PICMP93 Fiducial Network.

Verification of the analysis was attempted by comparing baselines of the readjusted PGNet (in the central Luzon region) with the results from the PICMP93. This required both a judicious selection of baselines between sites of reliable stability and some knowledge of the postseismic deformation pattern associated with the earthquake. The documentation of this adjustment has a significant historical importance with respect to the tectonics of the Philippine Islands. With the passage of time, the errors in the readjusted national net (ie the PGNet onto the PICMP93 fiducials) become smaller relative to the regional deformations that have accumulated since 1990, and thus the more valuable this data becomes to tectonic geophysicists

Chapter 5 examines the scale errors in the PGNet, illustrates the ensuing readjustment process and then documents the resulting PGNet (ITRF96) coordinate set plus the network statistics.

The U.S. Geological Survey (USGS) supplied a hard copy of the mapping results for the trace of the 1990 fault rupture. The trace survey was originally done by field and photogrammetric interpretation by *Nakata et al.,* [1990, 1996] and then by locating these points onto USGS 1:50,000 topographic maps (on the original Luzon geodetic datum). Fortunately, this matched both the scale and datum of the Philippine DENR 1:50 000 mapping. The fault line was digitised in Universal Transverse Mercator (UTM) Zone 51N coordinates (Luzon datum) and then transformed to UTM Zone 51N coordinates on WGS84. This provided a digital database of the fault rupture for input to the dislocation model and formal inversion (Chapter 6).

A preliminary comparison of the pre and post 1990 Luzon earthquake GPS data was conducted in 1993. Using the surface rupture information provided by *Nakata* (pers comm. 1993), a simple dislocation model [*Chinnery,* 1961] was created using MATLAB™ software. This particular method required the creation of the typical "butterfly" dislocation model for each depth of fault and then comparing calculated displacements with observed ones for the earthquake. These initial results showed that the measured displacement field (see Table 1.2) compared favourably with the expected model generated from a simple dislocation model [*Chinnery,* 1961] for a pure strike-slip event (see Figure 1.6 for a typical 20 km depth Chinnery model of the

Luzon earthquake). However, forward dislocation modelling of the displacement field derived from this data provided relatively poor constraints on the earthquake mechanism and slip. Therefore, it was necessary to evaluate the accuracy of this earthquake data very carefully to determine the limiting factors that restricted its use for characterising the source mechanism of the Luzon earthquake eg significant distortions at the several ppm level in the coseismic results.

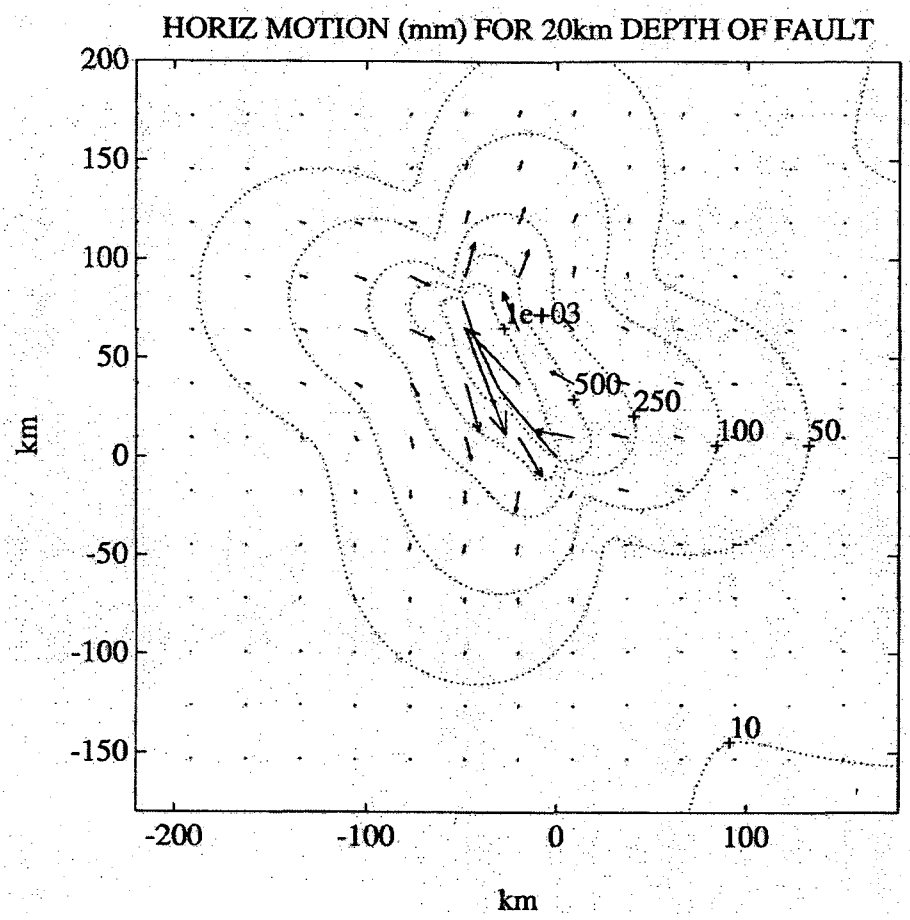

Figure 1.6: Dislocation model (Chinnery) for the Luzon 1990 Earthquake (Depth 20km). This particular method required the creation of the typical "butterfly" dislocation model for each depth of fault and then comparing calculated displacements with observed ones for the earthquake.

The displacement field had to be defined so that it could be compared with the predicted earthquake model. The following sequence was adopted:

- a free net adjustment of both the pre and post earthquake datasets of 1990 and 1991
- the analysis of a series of Helmert transformations of these pre and post

adjustments minimising station displacements in the far field

- constraining the adjustment of both the pre and post earthquake, by holding fixed at their PICMP93 values stations that are distant from the earthquake zone.

No. of Stations	Distance (km) from fault line	Average horizontal displacement vector (m)	Average value expected from the dislocation model of 20km depth (Figure 1.6)
4	3-5	2.9	2.8
1	10-20	0.7	1.0
4	20-30	0.4	0.7
5	35-45	0.3	0.3
50-80	0.2	0.1	

Table 1.2 Typical horizontal displacements measured by GPS in 1990 Luzon Earthquake zone compared to the calculated displacements of the of a simple *Chinnery* [1961] dislocation model for 20km fault depth (see Figure 1.6).

Departures in the observed displacement field from a simple dislocation model [*Chinnery*, 1961] could also be explained in terms of a complex displacement distribution, a fairly complex fault geometry and possible deficiencies in the reference frame definition. It is known that the Philippine fault is curved in the central Luzon region and that the rupture for the 1990 event was observed along the main fault and one of its splays [*Yoshida and Abe*, 1992].

Eventually it was decided to model the earthquake based on a designed surface trace that allowed a best fit with the fault trace that was mapped in 1990. Parameters such as slip, the depth, the lateral extent and to some extent the dip were variables [*Silcock and Beavan 2001*]. Chapter 6 examines the geodetic data available from the pre and post earthquake observations (PGNet) and then presents the preferred dislocation model determined by this technique.

Postseismic slip caused significant station displacements since the 1990 earthquake,

and it was not possible to separate the coseismic and postseismic effects between 1990/91 and 1993, given the lower accuracy of the earlier data set. However the PICMP96 and 98 reoccupation of the Luzon earthquake network enabled 1993-96, and 1996-98 postseismic deformations to be detected and modelled. Chapter 6 discusses the preliminary results for the postseismic slip rate interpreted using an elastic half-space model with uniform slip below a sub-surface locking depth. Using this model, the measured deformation rate implies a long-term slip rate (or far-field relative velocity) of ~40 mm/yr on the Philippine fault in Luzon ie much higher than the 25 mm/yr expected. *Beavan et al.*, [2001], suggest several lines of evidence against this high rate of slip and then offers viscoelastic relaxation models with a more realistic associated long-term slip rate of 15 - 22 mm/yr.

The rationale for the readjustment of the PGNet onto the PICMP93 (ITRF96) fiducials is to improve its accuracy to approximately 1 ppm primarily for its potential in rapid response surveys and resurveys of future large earthquakes throughout the Philippines. With the passage of time, the errors in this readjusted PGNet (ITRF96) network become smaller relative to the regional deformations that have accumulated since 1990. Therefore the more valuable this data becomes to tectonic geophysicists provided that the ground marks remain stable and undisturbed

GPS data obtained at the fiducial network sites will also provide new information on the general pattern of crustal movement within the Philippine tectonic zone. *Barrier et al.*, [1991] have analysed geological data in order to establish a simple kinematic model for the distribution of motion between the Philippine Sea and Eurasian plates in this region. Their plate rotation model predicts velocities along the Philippine fault in the Visayas and Mindanao of 1.9 to 2.5 cm/year and a subduction rate along the Philippine trench varying from 9.5 to 13 cm/year in the far south to 6.5 to 8.5 cm/year east of Samar. Their results supported the hypothesis that the Philippine archipelago is not entirely part of the Eurasian plate but also belongs to an independent block. In the south, the field and geological data fit the model quite well. However, this is not the case in the north where the kinematics and block geometry are more complex and speculative.

One of the major ongoing objectives of the PICMP was to analyse the GPS fiducial data from PICMP93/96 and 98 campaigns to provide further insight on the

kinematics of this region. Two of the fiducial sites are located on the Eurasian plate while the others straddle the Philippine fault from north to south. *Beavan et al.*, [2001], incorporated the various solutions into the ITRF96 which utilised additional data from the Philippine Sea plate and IGS stations throughout South East Asia plus Australia. The results were interpreted within the context of the NUVEL model for global plate motion [*de Mets et al.*, 1990] and the more detailed model suggested by *Barrier et al.*, [1991]. Chapter 6 gives a brief outline of these results.

Chapter 7 summarises the results of this PhD thesis, adds concluding comments on the PICMP and summarises the practical and scientific benefits of the research. Finally, recommendations are made with respect to future campaigns and international collaboration for regional tectonics and kinematics.

2.0 The Philippines Geodetic Network (PGNet)

2.1 History

The Philippines is an archipelago consisting of 7,107 islands with a combined land area of approximately 300,780 sq. km. It occupies the Western Pacific rim between latitudes 5°N and 21°N. The main island groups are Luzon, Visayas, Mindanao and Palawan (Figure 2.1)

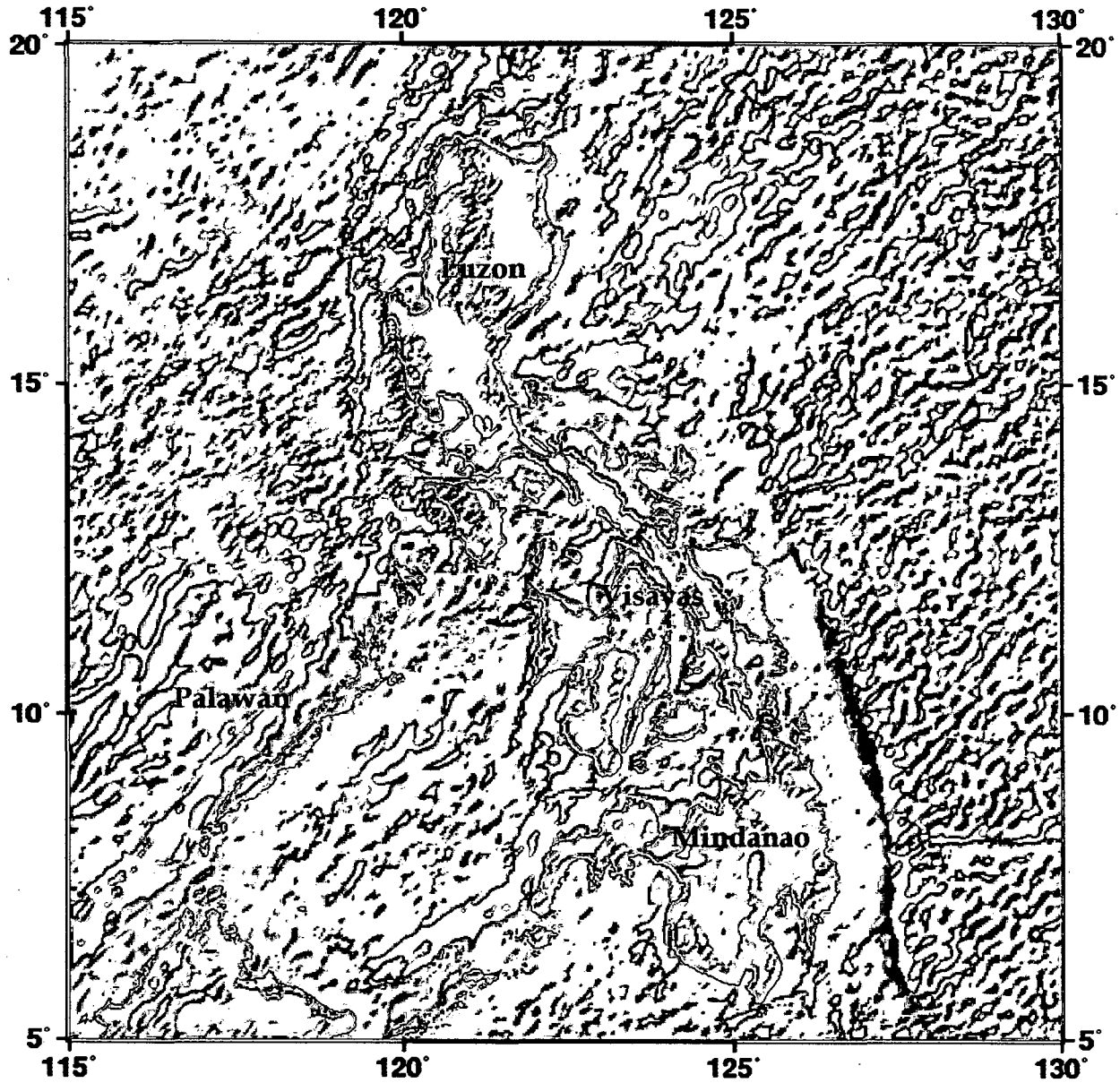

Figure 2.1 The Philippine Archipelago

The triangulation of the Philippines was started in 1901 by the US Coast and Geodetic Survey (USCGS) after Spain ceded the Philippines to the United States government under the 1898 Treaty of Paris. It was mainly comprised of narrow chains of coastal triangulation.

The network was established primarily to provide geodetic control for hydrographic surveying/nautical charting and positional coordinates. Through a logical method of planning and execution, the connections of the islands through triangulation was realised and suitable charts were published. The USCGS assessed the accuracy of the established stations as 2nd (1/10000) and 3rd order (1/5000). But by modern standards, the whole network would be rated less than third order.

The *Luzon Datum* was adopted as the national datum in 1911. The datum was purely to reference geographical positions and not for the mathematical determination of the figure of the earth. The origin was at the station MRQ-1 on Balanacan in the Marinduque province. Its geodetic coordinates on the Clarke 1866 Spheroid were adopted as:

- Latitude = 13° 33′ 41".000 N, Longitude = 121° 52′ 03".000 E

The basic USCGS network over the Philippines (*the Primary Triangulation Network)* was finished in 1927 with a total of 1692 stations, 9095 directions, 98 measured bases and 52 observed azimuths [*Bond et al.*, 1927]. After that, supplementary stations were observed on a project-by-project basis.

The USCGS utilised the most modern equipment available at that time in the execution of the surveys in the Philippines eg the Parkhurst theodolite, spirit level, invar rod, plane table and alidade. The coordinated positions were computed after a network adjustment initially using the condition equation method and then the least-squares technique. As triangulation required the stations to be intervisible most if not all of the stations are located at the highest peaks of mountains.

The original observation records and computation files were destroyed during the Second World War. The only existing records are contained in the two-volume publication *Triangulation of the Philippine Islands* published by the USCGS in 1927.

In 1950, the function of the USCGS was transferred to the Philippine Bureau of Coast and Geodetic Survey (BCGS). Eventually, the Bureau became a member of the

International Hydrographic Office (IHO) and the International Union of Geodesy and Geophysics (IUGG).

The BCGS continued the functions of the USCGS and additional control stations were added as demanded by charting and mapping requirements. In addition to geodetic surveys, the Bureau also conducted tidal observations, gravity surveys and magnetic surveys. Today, these duties are undertaken by the Coast and Geodetic Survey Department (CGSD) of the NAMRIA.

2.2 The Natural Resources Management and Development Project (NDRMP)

In 1986, the Philippine Government announced that it intended to establish a program of environmental/resource management and conservation through the development of resources. Subsequently, the Government requested the aid of Australia in 1987, to implement the initial phase of the NRMDP.

Phase I addressed [*Larden et al.;* 1991] :

- the institutional strengthening of those Government and other agencies that were charged with the developmental programs
- the identification of the appropriate methodologies to implement the programs and
- the provision of a spatial geographic framework capable of supporting these programs

AIDAB developed the project in conjunction with the Philippine DENR. Technical expertise during the design stage was implemented by the Australian Surveying and Land Information Group (AUSLIG). The contract for management and implementation of the project was awarded to SAGRIC International Pty Ltd, an Australian company. SAGRIC was assisted in the geodetic survey by CERTEZA Surveying and Aerophoto Systems Incorporated.

2.3 Geodetic Survey Component

> "A new network has been established using the Global Positioning System (GPS) under the Geodetic Survey Component of the Natural Resources Management and Development Project (NDRMP), an Australian assisted project of the Department of Environment and Natural Resources (DENR). This new network is the basic reference framework for all surveying and mapping in the country."
> [*The Philippine Geodetic Manual*, 1992]

As previously discussed, the original triangulation provided control for hydrographic surveying and charting during the early 1900's. On investigation, it was clear that this network was not capable of supporting the surveying and mapping requirements of the NRMDP programmes. Differential GPS satellite technology offered a very effective means of upgrading the first order geodetic framework of the Philippines i.e. the PGNet.

The geodetic component provided the following final outputs:

1. the PGNet - a national network, computed on an ellipsoid that mathematically approaches the form and size of the geoid
2. defined transformation parameters between WGS84 (GPS) datum and the Philippine Reference System 1992 (PRS92)
3. the geoid model definition for the Philippine islands and the geoid/ellipsoid relationship for the PRS92
4. a computerised geodetic records data base
5. training and technology transfer in modern geodetic observations, adjustment techniques and data base management

[*Larden et al.;* 1991].

The Philippines Geodetic Manual details that a total of 467 GPS stations were established as follows:

- 330 first order stations;
- 101 second order stations;
- 36 third order stations

These stations included:

- 360 for the Primary Network (adopted as the PGNet for this thesis)
- 76 for the Cebu Pilot Area
- 12 for the Nueva Ecija Pilot Area
- 19 for the Isabela Pilot Area (North)
- 11 for the Isabela Pilot Area (South)
- 6 for the Albay Supplementary
- 6 for the Zambeles Supplementary

The 360 Primary network stations have been adopted as the PGNet for the PICMP research. The other stations listed above were established for limited densification in specific areas (second and third order) and also for photo control and hydrographic projects.

Three Accuracy standards were chosen for the PGNet:

- 10 ppm for first order surveys (1 standard deviation)
- 20 ppm for second order surveys (1 standard deviation)
- 0.02 m + 50 ppm for third order surveys (1 standard deviation)

Various GPS geodetic networks established throughout the world since this time have shown that the above standards are very conservative indeed. However it must be noted that the PGNet was the first major national first-order survey undertaken anywhere in the world with the then *new* GPS technology. The limitations of the PGNet result from poor satellite availability and geometry during the late 1980's and the use of single frequency GPS receivers during peak solar sunspot activity.

2.4 PGNet Observations

Satellite Availability

PGNet observations began in January 1989. At that time there were only six fully operational satellites (Block I) available which offered a meagre five-hour window, with a maximum of four useful satellites. This contributed to poor geometric configurations and a major logistical problem when geodetic observations were restricted to the absolute minimum of four satellites.

By January 1990, the Block II satellites were being launched and hence nine fully operational satellites were available. This provided two five-hour observing windows and reduced the impact of poor satellite choice and geometric configuration. At the end of the observation schedule (December 1990), a total of fifteen fully operational satellites were in place and so three five-hour observing windows were possible per day, offering good geometry.

Atmospheric conditions

The project was undertaken during high solar activity and the peak output of solar radiation energy during *cycle 22* (a numbering system implemented since the beginning of solar radiation records). This cycle was one of the most powerful barrages of solar energy on record and before reaching its midpoint, had already surpassed *cycle 19* outputs in radiation. *Cycle 22* reached its maximum in February 1990 at which time large eruptions of energy from the visible surface of the sun caused serious disruptions in navigational satellites and disrupted satellite transmissions. Also, satellite telephone links and television broadcasts were particularly vulnerable to this solar-related interference.

The Philippine project coincided with this *11 year* solar cycle maximum and so GPS technology was tested for the first time under these conditions. Figure 2.2 illustrates the increasing number of sunspots recorded by scientists at that time. Sunspots have little direct effect on the earth but act as indicators of the more powerful magnetic storms, X-ray flares and bursts of high energy protons that emanate from the sun and shower the planet.

The GPS data recorded during the survey stage (predominantly single frequency) and subsequently processed to form the PGNet was ***not*** modelled for these ionospheric disturbances. Consequently, final results of the PGNet have been substantially biased during this period of high solar activity. These biases and the readjustment of the PGNet using the PICMP93 dual frequency campaign data are discussed in Chapter 5.

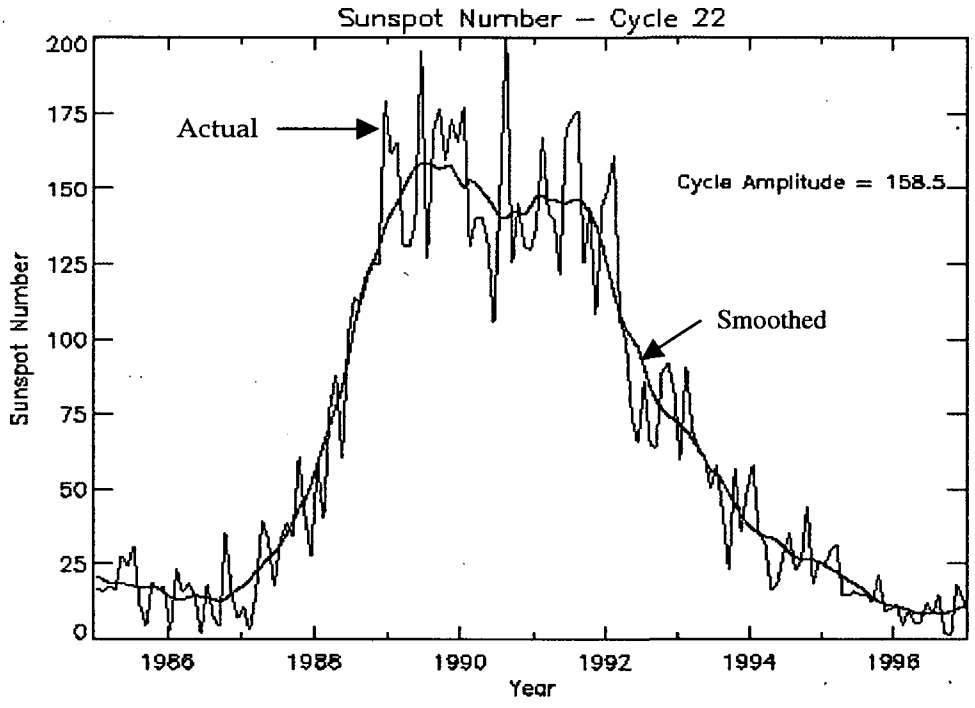

Figure 2.2 Sunspot numbers (actual and smoothed) *for Solar Cycle 22* [*IPS Radio & Space Services*, 2001]

Differential GPS Observations

A total of nine Trimble 4000S receivers were used during the geodetic survey component of the project. Single and dual frequency receivers were used and consisted of:

- 5 4000SL L1/ Geodetic;
- 3 4000SLD L1/L2 Geodetic;
- 1 4000ST L1/ Geodetic.

The network was developed using the receivers in multi-station mode with a framework of interlocking figures as depicted in Figure 2.3. This ensured an acceptable national coverage and a sufficient level of observation redundancy.

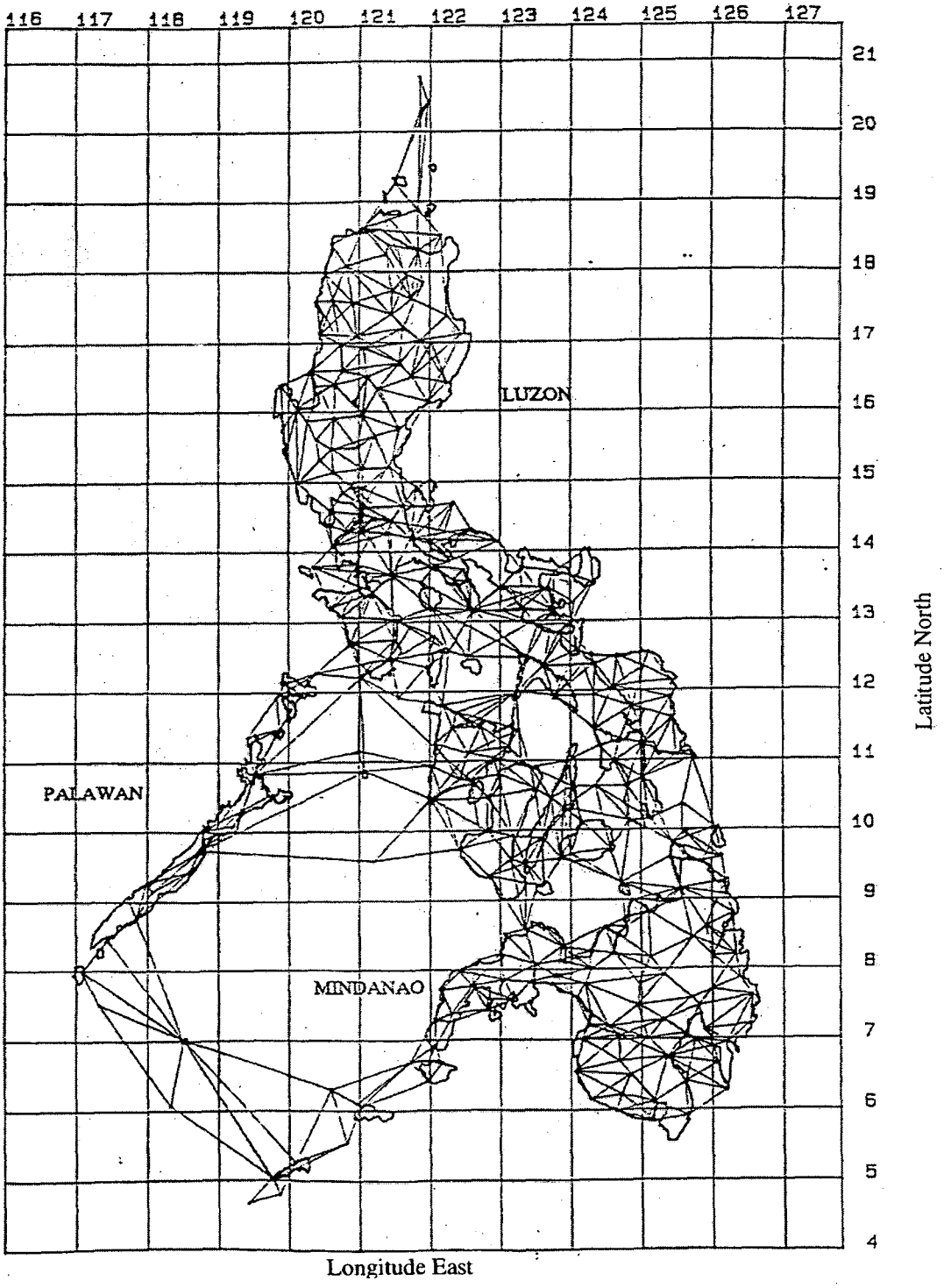

Figure 2.3 The completed PGNet WGS84 1988-1991 [*Jones*, 1991].

The observation procedure included:

- site identification, clearing and monumentation
- an observation programme for the multi station configuration - based on logistics, security and the satellite availability and geometry
- the deployment of between six and nine GPS parties with observing schedules ranging from 5-15 hours over three days
- the redeployment of observing parties to the next multi-station configurations but holding between 2-4 pivot stations

[*Larden et al.;* 1991].

Absolute GPS Observations

Pseudoranging data was collected regularly for periods in excess of six days:

1. at the main base station in Manila and
2. at regional base camp stations and key pivot points

These observations were used to determine the absolute coordinates in the WGS84 datum. A total of 104 absolute positions throughout Northern and Southern Luzon and the Central Visayas were eventually determined. These coordinates were used to provide tests of the capability of adjustment of the differential GPS Network.

2.5 The Computation and Adjustment of the PGNet

Section 2.5 is an overview of the computation and adjustment of the PGNet. The primary source of reference for this has been *Jones* [1991]. As the SAGRIC geodetic consultant for this part of the NRMDP, Jones' final report remains the definitive account of GPS processing, datum definition and PGNet adjustment.
Therefore, the summary presented here is based on his report unless otherwise referenced.

2.5.1 Processing the GPS Baselines

Overview

The reduction and adjustment of the GPS data set took place between July 1989 and October 1991 by Mr Andrew Jones of the then South Australian Department of the Environment and Natural Resources. Before day 295 of 1990 all GPS baselines were processed in Australia. However, baselines acquired after that date were reduced in the Philippines and then forwarded to Australia for adjustment. Eventually, approximately 900 GPS sessions were processed involving 4,500 data files.

An enormous amount of data was generated by the project given that:

1. usually 2 GPS sessions were observed each day of the field campaign
2. each session involved differential GPS observations employing 6-8 receivers
3. observational sessions were between 4-5 hours duration

All GPS baseline processing was carried out in batch mode to maximise the automation of the procedure. Processing methodology varied for different regions depending on the nature of the network and the accuracy achievable. However, standard procedures included:

- computing only sets of independent baseline vectors for each observation session (ie dependent vectors were not calculated as they would be highly correlated and so would distort the stochastic modelling of the network adjustment.
- all sessions were processed with the broadcast ephemeris (Jones justified this decision in his report)

a) Prior to day 295, 1990

Prior to this date, all raw GPS observations were forwarded to South Australia. The data were processed in blocks associated with a specific geographical area. Therefore the network was built up in a progressive fashion which allowed each area to be analysed before being added to the final adjustment data set.

All baselines were reduced using the BATCH_PHASER program (amended by Jones from the program PHASER developed by *Goad* [1985]) processing uncorrelated triple differences. This procedure was adopted because:

- it provided the level of precision which was required by the NRMDP,
- it offered the most efficient approach for processing the very large quantity of observations,
- it incorporated an effective data-editing mechanism especially for the baselines observed during the high solar activity periods

Network adjustments were performed frequently to confirm baseline consistency. The least squares adjustment program NEWGAN (developed by Dr. J. S. Allman from Canadian Geodetic Survey programs GANET and HAVOC2) was used for this purpose as well as the final first order network adjustment. Each geographical area was processed with the following procedure:

1. The independent vectors that were selected for each session were the shortest lines which inter-connected all the stations. Short lines were chosen to minimise atmospheric and orbital errors.
2. Each baseline was evaluated with respect to the GPS software output and rejected if analysed to be poor.
3. A regional network adjustment was carried out to check external consistency. The use of short lines and repeat observations increased redundancy and therefore assisted the analysis of the baselines.

The full BATCH_PHASER data set provided a total coverage of the Philippines.

b) After day 295, 1990

All baselines after this date were reduced in the Philippines using the Trimble GPS program, TRIMVEC (at this time a newly released commercial package). The baseline solution files were once again forwarded to South Australia for analysing and integrating into the final adjustment data set. The following processing strategy was adopted:

- uncorrelated triple difference solutions were adopted for most baselines
- double difference solutions (biases fixed) were used on some very short lines
- only independent vectors were selected for inclusion in the final network

2.5.2 PGNet Adjustment

Consolidated Primary Network

All the processed BATCH_PHASER and TRIMVEC baselines were merged and edited into a consolidated Primary Network file for the final adjustment. It comprised of:

- TRIMVEC baseline vectors for the POST 1990 Luzon earthquake area
- TRIMVEC baselines for project areas near Palawan and Manila
- BATCH_PHASER vectors for the remainder of the country

NB All BATCH_PHASER vectors observed in the earthquake area prior to the 1990 event were deleted from the adjustment file.

Network Adjustments

	Total Stations	Fixed Stations	Number of Baselines	Baselines per Station
PGNet	360	1	2691	7.5

1. The primary network was adjusted using the Canadian Section Method [*Pinch et al.*, 1974]
2. Station Balanacan (MRQ1) was the origin of the Primary Network
3. The variance-covariance (VCV) matrices associated with the baseline vectors were carefully analysed to derive appropriate population scale factors that were then applied (ie to ensure the validity of the variance estimates).

Adjustment Results

	Variance Ratio	F Test Factor
PGNet	1.062	0.9238

NB

a) The Variance Ratio Test is satisfied if the F Test Factor is approximately equal to 1.0 (and hence indicates that the post-adjustment residuals are consistent with the hypothesised mathematical model).

b) The F Test Factors are at the 99% confidence interval.

c) A statistically robust adjustment was possible because of the large volume of redundant observations.

The accuracy classifications for the PGNet are as follows:

	1st Order Stations	2nd Order Stations	3rd Order Stations	Total
PGNet	332	17	11	360

All line error ellipses were tested against the accuracy criteria to confirm the validity of the station classification. Error ellipses of relative error in the sigma semi-major axis showed 3 to 5 ppm errors between stations.

Table 2.1 summarises the final adjusted baseline residuals for the PGNet. It should be noted that all RMS values are computed around zero rather than the mean.

Line Length	No. of Baselines in Adjustment	Mean (ppm)	RMS (ppm)
< 2km	28	0.42	23.15
2 - 5 km	28	-0.38	13.44
5 - 10 km	19	-1.55	9.92
10 - 20 km	128	-0.92	5.05
20 - 50 km	1291	0.03	4.39
> 50 km	1196	0.03	3.95

Table 2.1 RMS values of chord distance residuals for the PGNet (1988-91)

2.5.3 WGS84 Datum Definition for the PGNet

It must be noted that at this time the IGS tracking network was in its infancy and so the NRMDP needed to define its own WGS84 datum and origin coordinates. Today, GPS observations would be processed simultaneously with data collected at coordinated points of the IGS network (in a known ITRF) on an easily established WGS84 datum.

In 1989, the immediate concern was the determination of the GPS datum (WGS84) plus a starting point with known coordinates (latitude ϕ, longitude λ and ellipsoidal height h) in that system. Initially, no information was available on such a point. It was decided to adopt station Balanacan (MRQ1) as the origin and the WGS84 coordinates were determined by meaning a series of observed GPS absolute positions. The amount of available data was small and so the methodology was simplistic. The mean value was obtained and this *Initial Datum* was used for the next 12-18 months to develop the network. This was required to facilitate GPS baseline processing.

As the project progressed, there was a need for a more refined estimate of the WGS84 datum. Three (3) data sets were gathered.

1. *The GPS point position file.* This was compiled from the absolute positions generated by the Trimble receivers. Mean ϕ, λ and h values were obtained at each observation epoch. The data set was very large and the final point positioning file was generated by averaging the session means for each station. Only stations which had been occupied for at least six sessions were included in the file. Also at this time, selective availability (SA) had not been instigated by the US Department of Defence (DoD).

2. *TRANSIT Doppler Observations.* TRANSIT Doppler receivers had been used to coordinate a number of stations in 1977/78. Several of these stations were re-occupied during the NRMDP GPS campaign. The Doppler coordinates were transformed from NWL-9D(WGS72) into WGS84 using the Higgins transformation parameters [*Higgins,* 1987]. Eleven Doppler absolute positions were transformed from WGS72 to WGS84. These were then added to the GPS point position file.

3. *GPS Network.* The WGS84 coordinate set generated by an interim network adjustment. The network was adjusted using the by the mean observed Balanacan WGS84 coordinate as the origin.

In September 1990, transformation parameters were generated between the GPS Network coordinate values and a combined GPS Point Position/TRANSIT Doppler set. Its purpose was to enable the GPS network to be recomputed on a relatively complex definition of WGS84 (termed the *Project Datum*).
The quality of the definition was assessed by analysing the post-transformation residuals (standard deviations). These were as follows:

Latitude residuals	5.521 m
Longitude residuals	3.834 m
Height residuals	5.244 m

Unfortunately, the results of the transformation (Table 2.2) showed that the initial estimates of WGS84 was reasonable in ϕ and λ but very poor in h, ie the GPS network

had been computed on a coordinate system that was significantly different from WGS84.

Latitude	0.1495 seconds of arc	approx 4.5 m
Longitude	0.1995 seconds of arc	approx 6.0 m
Ellipsoidal Height	22.358 m	

Table 2.2 Difference between Initial Datum and Project Datum at MRQ1

This was a matter for concern because inaccuracies in base station coordinates of more than 6 m could introduce scale and orientation errors in baselines.
As a result, Jones decided to transform the GPS Network into the *Project Datum* and then ALL baselines were reprocessed. After the network was finalised and adjusted (PGNet), the *Project Datum* (WGS84) was again checked by coordinate comparisons between:

a) Transformed TRANSIT Doppler point positions versus PGNet positions.

	ϕ	λ	h
Mean Residual (m)	-5.35	3.27	-1.39
Standard Deviation (m)	1.43	3.87	3.16

b) GPS Absolute Positions versus PGNet positions

	ϕ	λ	h
Mean Residual (m)	0.88	2.06	-1.33
Standard Deviation (m)	2.36	2.66	3.39

c) Combined TRANSIT/GPS Absolute Positions versus PGNet positions

	ϕ	λ	h
Mean Residual	0.32	2.17	-1.33
Standard Dev	2.90	2.78	3.36

Jones decided that the defined *Project Datum* of WGS84 was adequate for the task, as the mean residuals were within the 6 metre accuracy.

2.5.4 The Luzon Datum

There were several possibilities for the final geodetic datum of the Philippines. These included the adoption of:

- the GPS geocentric datum or WGS84 (ie consistent with GPS satellite technology), or
- a local datum based on the original Luzon Datum except to rename it PRS92 to account for the change in MRQ1 coordinates ie exactly the same ellipsoid but with a shift in the coordinate axis. The axis shift would take into account the best fit of the ellipsoid with the geoid

NRMDP recommended that the Philippines maintain the use of the Luzon Datum and adopt the adjusted set of the PRS92. The PRS92 was adopted over the WGS84 because:

1. GPS technology would not be universally available throughout the Philippines to justify a national change of coordinates.
2. PRS92 had exactly the same reference ellipsoid (Clarke 1866 Spheroid) as the existing Luzon Datum and hence available formula and tables (e.g. geographic to grid) could be retained.
3. PRS92 ellipsoid matched the geoid (approximately mean sea level) well and so geoid/ellipsoid separation (N) was not a major concern in traditional surveys (with WGS84 this was not the case).
4. While there were changes in the existing Luzon coordinate set by adopting the PRS92, these changes were not large and so previous mapping activities were still valid.

NB The original Luzon Datum assumed that N = 0.

Analysis of the Primary Triangulation Network of the Philippines

An analysis of the original Primary Triangulation Network of the Philippines was undertaken on behalf of the NRMDP (via SAGRIC International) by *Allman* [1991].

The Terms of Reference for this analysis were:

1. Identify and correct errors in the original data set
2. Use the corrected data set to generate
    - Point Error Ellipses for all triangulation stations that were recovered during the NRMDP GPS survey
    - A set of Position Equations (covariance matrix) containing as many of the recovered triangulation stations as possible
3. The supply of
    - corrected data set on standard computer media
    - documentation on the data format of results
    - a report concerning inconsistencies identified in the old dataset

[*Allman*, 1991]

The above data set and recommendations were incorporated into the final determination of the Luzon Datum for the PGNet.

Luzon Datum Definition

The generation of transformation parameters from the *Project Datum* (WGS84) to the Luzon Datum utilised the following two data sets:

1. the terrestrial data set (plus the variance-covariance matrix) derived from the original triangulation of the Philippines [*Allman*, 1991], and
2. the corresponding coordinates in *Project Datum* (WGS84) abstracted from the adjustment process.

Unfortunately, this process was complicated by the lack of orthometric height data in the terrestrial data set. The approach used to address this was to best fit the Clarke 1866 spheroid to the locally established geoid of the Philippines that was established by *Kearsley* [1991]. Thus at each station the geoid/ellipsoid separation value (N) was obtained. Therefore, for the common points, there was data available for ϕ, λ and N

in both the Luzon Datum and the *Project Datum* (WGS84). Transformation parameters were generated using a Helmert Transformation. Eventually, only 29 common points were used to develop the seven parameters since all other points depicted very large displacement vectors. For example, the largest residuals obtained were 56 metres in latitude and 80 metres in longitude.

Summary

> "Evaluation of the data and consideration of the implications of changing to a global geocentric datum or some other datum resulted in the decision to retain the existing Clarke 1866 spheroid. The existing horizontal datum has been retained. The vertical datum has been slightly modified by the adoption of a more realistic value of the geoid/spheroid separation at the origin in order to minimise the separation over a wide area. A new set of coordinates for stations established and integrated as part of the geodetic survey has been adopted and is referred to as the Philippine Reference System 1992 (PRS92)."
> [*The Philippine Geodetic Manual*, 1992]

2.5.5 The Philippine Reference System 1992 (PRS92)

The high volume of observational redundancy increased the final accuracy of the network from the 10 ppm level to 3-4ppm.

Results

- The final PRS92 coordinates for all 467 GPS stations (including the 360 stations of the PGNet) are listed in Appendix 1 of *The Philippine Geodetic Network Manual (1992).*
- The PGNet WGS84 coordinates abstracted from the original data set of the final adjustment (NEWGAN) can be found in *Jones* [1991].
- In addition 1700 points have been integrated into the system

Luzon Datum and Origin

The Luzon Datum is defined as:

- Clarke 1866 Spheroid: Semimajor Axis (metres) 6378206.4
  Reciprocal Flattening (1/f) 294.9786982
- Datum origin – station BALANACAN (MRQ1) in Marinduque

Latitude	13° 33′ 41.″000 N
Longitude	121° 52′ 03.″000 E
Ellipsoidal Height	271.185 metres

Geoid/Spheroid separation: +0.34 metres

Transformation Parameters

Users of GPS will use the following transformation parameters when conducting surveys in the Philippines. These figures will relate the GPS Datum (WGS84) to the Luzon Datum (PRS92). The following parameters are applied to WGS84 Cartesian coordinates to give Cartesian coordinates on the Luzon Datum, which will then be transformed into geographical coordinates of the PRS92. These parameters have been extracted from *The Philippines Geodetic Network Manual*:

Translation Parameters

Delta X	+127.62195 metres
Delta Y	+67.24478 metres
Delta Z	+47.04305 metres

Rotation Parameters

Rot X	+3.″62195
Rot Y	-4.″90291
Rot Z	-1.″57790

Scale Factor : 1.06002

NB Signs are reversed when transforming from Luzon Datum to WGS84.

The 7-paramater transformation formula that relates the two coordinates is shown as:

$$\begin{bmatrix} X_2 \\ Y_2 \\ Z_2 \end{bmatrix} = \begin{bmatrix} \Delta X \\ \Delta Y \\ \Delta Z \end{bmatrix} + [1 + Sc \times 10^{-6}] \begin{bmatrix} 1 & Rz & -Ry \\ -Rz & 1 & Rx \\ Ry & Rx & 1 \end{bmatrix} \begin{bmatrix} X_1 \\ Y_1 \\ Z_1 \end{bmatrix}$$

Where:

X_2, Y_2, Z_2	: are the transformed Cartesian coordinates
$\Delta X, \Delta Y, \Delta Z$	: are the shifts for the change in origin
Rx, Ry, Rz	: are the rotations of each axis (converted to radians)
Sc	: is the scale factor in parts per million
X_1, Y_1, Z_1	: are the coordinates to be transformed

2.6. The Luzon 1990 Earthquake and Its Effect on the PGNet

On July 16, 1990, the Philippines experienced a major earthquake of M_s = 7.8 in central Luzon which ruptured more than 100 km of the Philippine and Digdig faults. Left lateral offsets were observed of up to 6 metres. The Luzon 1990 earthquake has proved to be one of the largest events of the 20th century. A full discussion on this earthquake plus its geophysical interpretation is presented in Chapter 6. The epicentre was on the island of Luzon near Cabanatuan (See Figure 2.4).

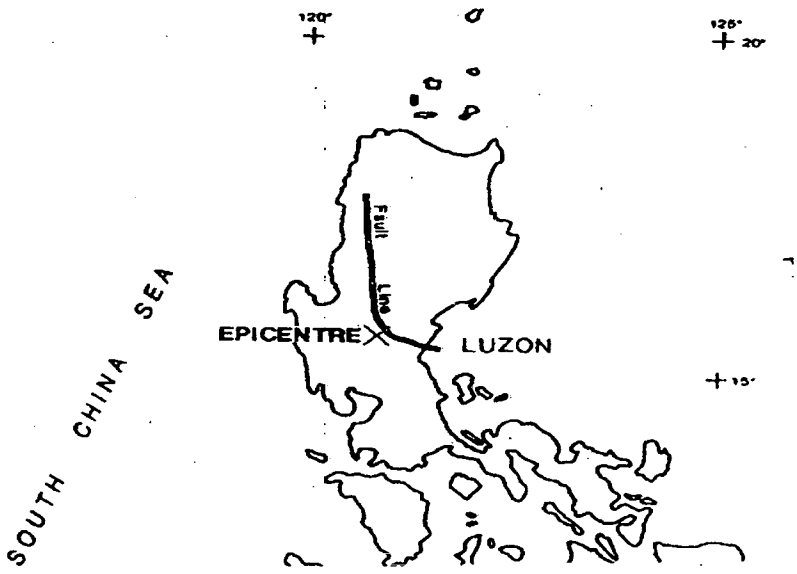

Figure 2.4 Fault Lines and Earthquake Epicentre

[*Larden et al.*, 1991]

2.6.1 Re-Observation of the Earthquake Zone

The PGNet suffered a major dislocation in the earthquake zone. GPS observations were repeated (including the 29 affected PGNet stations) and were completed in May 1991. The area covered by the re-observation extended along a 260km section of the faultline from Cabanatuan, Nueva Ecija to Bangued, Abra. Stations located up to 70 km east and west of the faultline were also connected. The extension of the survey to the north of the township of Digdig was undertaken in order to determine whether displacement occurred along the faultline in the rugged Cordillera mountain region (this is still unknown). The east-west re-survey was designed to establish the deformation in the far field away from the rupture line.

Earthquake related tasks included:

- the submission of proposals to AIDAB to obtain additional funding for the re-survey
- the design and planning of this survey
- the processing of the GPS observations
- computations and adjustment of the post earthquake network
- the evaluation and assessment of the impact of the earthquake on the PGNet
- the removal of the affected pre earthquake baselines from the existing data set
- the consolidation of the earthquake network into the final PGNet adjustment
- the presentation of the results and preliminary earthquake displacement analysis

2.6.2 Computations and Adjustment

The analysis of the *post* earthquake results was critical for the successful completion of the PGNet. It was extremely important to ensure that:

- sufficient redundancy was built into the re-observation programme and
- the WGS84 reference frame for these measurements was properly defined.

A successful merger of the *post* earthquake baselines into the Network adjustment was required and so it was necessary to:

- re-observe sufficient geodetic stations in the earthquake far field that would be unaffected by coseismic displacement and
- determine which of these stations would remain fixed during the final PGNet adjustment.

A knowledge of which stations did not move during the earthquake was essential. Therefore, several selections were tested to isolate the GPS observational errors (ie noise) from the real displacements. This involved an iterative process of analysing adjustments of the *pre* and *post* earthquake data and comparing the coordinates obtained. Initially, one station was constrained as fixed and then the number was progressively increased. Eventually, a total of six stations could be constrained in the final adjustment. The WGS84 definition did not significantly affect the results.

As previously stated the final PGNet adjustment (using NEWGAN) used a consolidated Primary Network data set that comprised the:

- TRIMVEC baseline vectors for the POST 1990 Luzon earthquake area
- TRIMVEC baselines for project areas near Palawan and Manila
- BATCH_PHASER vectors for the remainder of the country

(NB All BATCH_PHASER vectors observed in the earthquake area prior to the 1990 event were deleted from the adjustment file.)

2.6.3 Preliminary Analysis of the Earthquake Displacements

Twenty nine (29) of the stations that were surveyed in the *post* earthquake network displayed significant displacements. (See Tables 2.3 and 2.4).

The GPS observations relating to these twenty-nine stations have also been used to

determine the effects of the Ionosphere on the PGNet results (see Chapter 5). They were mostly observed with single frequency receivers. Only a few dual frequency receivers were available.

Methodology

All of the earthquake computations (plus the associated analyses) were conducted entirely independent of the PGNet results and data sets.

Jones [1991] adopted the following methodology:

1. *Pre* data was abstracted from the original PGNet adjustment file collated prior to the 1990 event.
2. *Post* data was obtained from the TRIMVEC baseline processing.
3. An independent free net adjustment (NEWGAN) was carried out on each dataset to check internal consistency and the stochastic model. The VCV matrices were weighted accordingly.
4. A network adjustment file was compiled which combined the *pre* and *post* earthquake data sets.
5. An initial adjustment of the combined data set was performed using a single constrained station TRC/01. The displacement vectors computed indicated:
    - significant horizontal and vertical movements between *pre* and *post* earthquake stations and
    - that those stations to the north and south of the zone displayed motions less than the noise level of the GPS observations.
6. As a result, it was decided to constrain two additional stations (ABR/01 and QZN/07) and then repeat the adjustment.
7. The combined earthquake adjustment was repeated to generate:
    - horizontal and vertical vectors and
    - line ellipses were computed to determine the statistical significance of the vectors at the 95% confidence interval (95% CI)

ID (Pre EQ)	Station	Azimuth (Degrees)	Distance (Metres)	95% CI (Metres)	Statistically Significant
01/01	**ABR/01**	**Fixed**	**Fixed**	**Fixed**	**N/A**
07/01	ARA/01	281	0.93	0.36	yes
07/02	ARA/02	272	0.56	0.50	yes
12/01	BGT/01	220	0.50	0.34	yes
16/01	BLN/01	108	0.02	0.4	no
16/03	BLN/03	112	0.19	0.36	no
16/04	BLN/04	213	0.32	0.31	yes
30/01	IFG/01	306	0.27	0.34	no
32/02	ILS/02	40	0.20	0.29	no
32/03	ILS/03	347	0.12	0.16	no
34/02	ISB/02	297	0.24	0.37	no
34/04	ISB/04	274	0.39	0.46	no
40/01	LUN/01	297	0.32	0.39	no
48/01	MPV/01	336	0.16	0.22	no
53/43	NEJ/43	324	2.92	0.21	yes
53/44	NEJ/44	199	0.61	0.18	yes
53/45	NEJ/45	301	2.77	0.28	yes
54/01	NVY/01	350	0.67	0.16	yes
54/02	NVY/02	336	0.64	0.19	yes
54/03	NVY/03	342	3.16	0.22	yes
54/04	NVY/04	352	2.84	0.20	yes
58/01	PMG/01	255	0.07	0.29	no
59/03	PNG/03	45	0.30	0.41	no
59/04	PNG/04	179	0.35	0.15	yes
59/05	PNG/05	341	0.12	0.17	no
60/07	**QZN/07**	**Fixed**	**Fixed**	**Fixed**	**N/A**
73/01	**TRC/01**	**Fixed**	**Fixed**	**Fixed**	**N/A**
73/02	TRC/02	33	0.18	0.20	no
73/03	TRC/03	314	0.17	0.22	no

Table 2.3 **1990 Luzon Earthquake - Horizontal Displacement Vectors**
[*Jones*, 1991]

ID (Pre EQ)	Station	Height Diff (Metres)	95% CI (Metres)	Statistically Significant
01/01	**ABR/01**	**0.00**	**Fixed**	**N/A**
07/01	ARA/01	0.35	0.2	yes
07/02	ARA/02	0.48	0.27	yes
12/01	BGT/01	0.47	0.24	yes
16/01	BLN/01	-0.20	0.21	no
16/03	BLN/03	-0.13	0.20	no
16/04	BLN/04	-0.07	0.28	no
30/01	IFG/01	0.16	0.25	no
32/02	ILS/02	0.13	0.26	no
32/03	ILS/03	0.11	0.23	no
34/02	ISB/02	0.45	0.26	yes
34/04	ISB/04	0.36	0.27	yes
40/01	LUN/01	0.49	0.25	yes
48/01	MPV/01	0.15	0.26	no
53/43	NEJ/43	0.30	0.19	yes
53/44	NEJ/44	0.17	0.19	no
53/45	NEJ/45	-0.23	0.20	yes
54/01	NVY/01	0.30	0.22	yes
54/02	NVY/02	0.37	0.23	yes
54/03	NVY/03	0.16	0.30	no
54/04	NVY/04	0.79	0.30	yes
58/01	PMG/01	-0.217	0.15	yes
59/03	PNG/03	0.07	0.26	no
59/04	PNG/04	0.34	0.20	yes
59/05	PNG/05	0.07	0.22	no
60/07	**QZN/07**	**0.00**	**Fixed**	**N/A**
73/01	**TRC/01**	**0.00**	**Fixed**	**N/A**
73/02	TRC/02	-0.05	0.15	no
73/03	TRC/03	-0.056	0.17	no

Table 2.4: 1990 Luzon Earthquake - Vertical Displacements
[*Jones*, 1991]

Results

The results of these computations are shown in Table 2.3.(Horizontal displacements) and Table 2.4.(Vertical displacement).

Jones [1991] stated that the

> "geophysical interpretation of these results is beyond the terms of reference of this report, and beyond the competence of the author."

However, he did conclude that:

- The pattern of the horizontal displacement vectors suggest a rotation of the area north-east of the fault line
- Four stations exhibited horizontal displacement vectors which exceeded 2.75 metres in length (53/43, 53/45, 54/03,54/04)
- Radial horizontal displacement vectors are evident at five stations to the south-west of the fault line (12/01, 16/04, 40/01, 53/44, 59/04)
- The north-east area of the fault line experienced significant uplift

Comments

Although the NRDMP geodetic component was highly successful and indeed innovative for that time, the final PGNet had limited use for geophysical interpretation such as tectonics. An overall PGNet precision of 1 ppm would be a more useful tool (nowadays one would expect far better than this). Chapter 5 details the readjustment of the PGNet onto the PICMP93 (ITRF96) fiducial network for this purpose.

The NRMDP analysis of the coseismic displacements (as depicted by the *pre* and *post* earthquake GPS observations) was flawed by the lack of specific knowledge of seismicity and dislocation fields eg the choice of unaffected stations in the adjustment. A preliminary analysis was carried out in 1993. Fault offset observations (acquired by Japanese, US and Filipino geologists/seismologists in 1990) were compared with the GPS displacement vectors computed by Jones. This indicated departures from the simple Chinnery-type dislocation model. These differences can

be explained in terms of:

1. a complex displacement distribution,
2. a fairly complex fault geometry, and
3. the fact that the analysis used to compute the GPS motions (horizontal and vertical) constrained as fixed a combination of points that were actually subject to relative motion ie stations TRC/01, ABR/01 and QZN/07

Vertical displacement results by Jones appeared to be extremely biased by holding three heights fixed. This cannot be justified and furthermore the results indicate that the vertical displacements of stations located in the seismic zone generally did not exceed 50 cm in magnitude and were random in nature ie that it could be concluded that were no significant vertical displacements.

WGS84 coordinates for Station PMG/01 from the PICMP93 campaign were found to be different (approximately one metre) to the 1990/91 PGNet position. This situation was confirmed by the PICMP96 results. Reasons for this include a) incorrectly sited GPS receiver in the post earthquake survey eg set up on a recovery mark instead of the main station or b) that the main mark had been disturbed and replaced without thorough relocation documentation. Therefore, coseismic results at this station required careful examination.

Since the PICMP93 campaign, further processing and computations have highlighted other aspects of the NRMDP results of the pre and post earthquake data. These required further investigation and a need for a revised methodology in the earthquake analysis eg. *pre* and *post* earthquake baselines would be analysed separately and then a series of Helmert transformations carried out. These are discussed fully in Chapter 6.

3.0 GPS and Very High Precision Positioning

3.1 GPS

3.1.1 Brief Synopsis of GPS

Introduction

The Global Positioning System (GPS) is a tool, which is becoming increasingly popular with many professions and the general public. The system's abilities are continually being enhanced by the scientific community as new techniques and products are devised to support the GPS user.

The U.S. Department of Defence (DoD) had several research and development programs in operation to design a global, all weather navigation system to be used for military applications. In 1973 these were merged into one program to develop the GPS. The first satellite was launched in 1978 and the system was declared operational in 1995, but there had been growing use of the system since the mid 1980's.

GPS cost $10 Billion (US) to design and build and it is estimated to cost the American taxpayer $500 Million per year to maintain the program. The service is available to all users worldwide free of charge [*Rizos, 1995*].

Positioning by GPS

GPS has revolutionised the science of positioning and earth measurement ie accuracy speed, simplicity and cost.

Conceptually, the satellites may be considered as control points with fixed known coordinates in space (at a particular time epoch), continuously transmitting information on their position. The GPS receiver measures its distance to each satellite. Therefore, by means of trilateration, the receiver coordinate (X,Y,Z) can be determined

The inherent accuracy of GPS can be enhanced by careful processing and by eliminating or minimising sources of error. The three critical techniques for achieving cm or mm accuracy in positioning are:

1. Differential GPS (DGPS) - two or more receivers operating simultaneously and then differential vectors are computed instead of absolute positions ie the errors that are shared by receivers will cancel when differences are formed.
2. Use of carrier phase measurements as well as or instead of code measurements.
3. Repetition of the GPS observations ie stochastically, a sequence of observations has a significantly smaller variance than a single observation.
4. Estimate or minimise each source of error in the GPS observations.

[*Strang and Borre*, 1997, p. 447]

"The key to the accuracy of GPS is a precise knowledge of the satellite orbits and the time." [*Strang and Borre*, 1997, p. 448]

As the GPS theory and technology is now well advanced there are numerous literatures available to the reader requiring comprehensive details on GPS. Therefore it is not necessary to provide a detailed description of GPS in this thesis. Further details are directed to the following texts (NB not a comprehensive list): *King et al.*, [1985], *Wells et al.*, [1987], *Hofmann-Wellenhof et al.*, [1994], *Seeber* [1993], *Webster* [1993], *Leick* [1995], *Kaplan* [1996], *Morgan et al.*, [1996] and *Strang and Borre* [1997].

3.1.2 General Applications of GPS

The civil applications of GPS and especially DGPS are extensive. Due to continual innovations in the production of GPS hardware and the development of software, there is an ever-growing community of GPS users.
Rizos [1995] summarised applications (basically positioning requirements) that range over land, sea, air and space. These include:

- Land Navigation – Initially, GPS was used for absolute point positioning using cheaper commercial hand held receivers to navigate in remote areas. This trend continues but DGPS techniques are being used for vehicle tracking systems as well as monitoring courier services, taxi's and emergency services. Geographical Information Systems (GIS), which also incorporate GPS, have

been developed to minimise the distances travelled by these vehicles and also to find the quickest path through traffic.

- Static Positioning - This technique is the most accurate compared to all other GPS techniques and involves long station occupancies and post processing of data. Static positioning is used to establish control networks and monitor land deformation across plate boundaries and volcanoes. It is used by geodesists, geophysicists and surveyors

- Marine Navigation – Techniques are virtually the same as for land navigation and cheaper GPS receivers are commonly used for recreational boating purposes. DGPS is evolving as a technique to guide ships from open sea through to final berthing positions.

- Marine positioning – GPS is used by recreational fisherman, marine rescue facilities and for more complicated work such as hydrographic surveys. The hydrographer uses GPS to position the vessel during the sounding process eg depth sounding or side scan sonar. The coordinates and soundings are combined to produce charts for a variety of purposes eg ocean, harbour and channel navigation.

- Kinematic Surveys - This GPS system involves using a base station of known coordinates, which tracks continuously throughout the survey and also a roving receiver. The rover is often in continuous movement collecting data or the rover may be stationary for a short period of time (2 mins) at a point before shifting to the next point and collecting data. Post processed kinematic surveys have been in use for many years for mapping, airborne gravimetry and various GIS applications. However, real time kinematic (RTK) GPS has become a standard surveying technique for task such as topographic, and engineering surveys where 2-3 cm precision is required.

- Air Navigation – Even though GPS is commonly available in commercial aircraft/light aircraft for enroute navigation it has yet to become accepted for landing systems at airports. This is because of the need for continuous and reliable real time GPS on aircraft. DGPS techniques have been designed for

landing systems but the aviation authorities are still insisting on further research before adopting a combined navigation/landing system that will employ GPS as one of its components.

- Attitude and Heading Determination

- Space Applications - GPS is used in the launch, orbit and re-entry phases of satellites. It is now also used for atmospheric research.

- Recreational Applications – GPS is now being used for almost any navigation purpose such hiking, four wheel driving, expedition activities and are even being installed in vehicles for incorporation with digital street directories.

As this brief summary suggests, there is an extensive range of uses for GPS. However this thesis examines the use of GPS for high precision geodynamic monitoring and as such deals exclusively with the static differential positioning technique.

Differential Positioning with GPS

Receivers and associated commercial software can routinely produce *real time* relative positions between stations with an rms of 1-2 cm over distances up to approximately 20km (RTK GPS with ambiguity resolution). Static differential GPS routinely provides 1-ppm accuracies on postprocessed baselines of any distance using only the broadcast ephemerides.

When two receivers are reasonably close together (eg 100 km), then the signals from a satellite (in an orbit of 20 200 km radius) reach both receivers along very close paths. As a result:

a) the delays in the ionosphere will be nearly identical,
b) the errors due to an incorrect satellite clock (which has been dithered to achieve SA) are essentially the same and,
c) similarly, the errors in the satellite orbits are the same.

These errors due to satellite clocks and orbits will cancel in the *difference* of travel times to the two receivers.
NB Only frequency standard variations cancel out exactly in the differencing process.

Time synchronisation, orbit errors and partly atmospheric effects are all approximately proportional to station separation. For example:

- Ionospheric gradients are typically 1 part in 10^6. Unfortunately, the use of single frequency receivers over separations of more than 20 km reflect increasing errors due to the ionosphere i.e. the effects are not negligible and do not cancel out in differencing. Sometimes these errors may even reach 10 mm over 1-2 km during periods of high solar activity. However with dual frequency these errors very nearly cancel for any distance.
- Tropospheric affects are also important in precise positioning for separation over 1-2 km. Modelling during post processing can reduce this.
- Without SA the orbital errors are about 20 m (or equating to about 1 ppm over baselines). This is critical for tectonics but not for routine surveying.

Static relative positioning implies that the receiver is stationary with the tripod/antenna set up like a permanently mounted tracking station. It also implies that various receivers are set up to simultaneously receive data from the same satellites.

Static surveys with long station occupancies allow a large quantity of many different satellite configurations to be observed. This gives:

- a large number of redundant observations, meaning that if a least squares adjustment is used, the relative baselines can be determined to a high accuracy, and
- changes in geometry, which enhances the accuracy, obtained from the survey. allows observations to a large number of satellite receiver range pairs.

Data are usually collected from thirty minutes to several days (and even weeks) depending on the required accuracy for the campaign and the technique is mainly

used for establishing survey control networks or to monitor deformations in local, regional or continental applications. Some permanently established tracking stations have been set up to monitor tectonics (see 3.1.2).

GPS phase data are downloaded from each receiver and then processed using one of the various software packages. Some of these packages may be scientific such as Bernese V4.0 or they can be commercially available products such as Trimble GPSurvey V2.50. The principle of working with differences is even more important in post processing of GPS data.

Static baseline techniques are adopted by geophysicists, geodesists and surveyors to determine a variety of high precision measurements such as:

- the detection of movements in crustal plates and earthquake displacements
- positioning requirements for geodetic and gravity observations
- the development of a geodetic datum and also the necessary coordinate infrastructure for land and resource management establishing coordinates for cadastral, engineering, hydrographic and monitoring.

3.1.3 GPS Applications for Geodynamics

Current Status

GPS has had a major impact on the earth sciences over the last decade and has become the geodetic method of choice for studying a wide range of geophysical phenomena. GPS surveying techniques are now routinely used:

- to determine the motion of the earth's tectonic plates,
- to study deformations around active faults (coseismic, postseismic and interseismic) and volcanoes,
- to measure the adjustment of the earth's surface due to the past and present changes in the mass of the world's ice sheets,
- in conjunction with tide gauges to monitor suspected changes in the sea level due to factors such as global warming, and

- to contribute to atmospheric studies.

There is a vast amount of literature available on the use of GPS for solid earth studies including the techniques used and results. *Segall and Davis* [1997] give a very useful overview of how GPS geodetic measurements have been incorporated into geophysical studies. It is interesting to compare this account with the earlier one by *Hager et al.*, [1991] and note how GPS surveying has opened up a new era in geoscience studies. The early applications were dominated by large field campaigns with significant resources spent on data processing and analysis (eg orbit improvement and ambiguity resolution strategies). It was also rightly predicted that with improvements in precise orbits, software development, atmospheric modelling and processing methodologies then very high precision GPS results would be obtainable. A typical example of a large-scale field campaign is the GEODYSSEA project [*Becker et al.*, 1996] to study the macrotectonics of SouthEast Asia
Hager et al. [1991] also effectively suggested that as the GPS system improved and matured then continuously operating networks would become more common. Examples of the many continuously operating GPS networks now operating include,

- the International GPS Service (IGS) tracking network
- the Japanese national network of over 1000 permanent GPS sites operated by the Geographical Survey Institute (GSI)
- the Australian Fiducial Network (AFN)
- the Southern California Integrated GPS Network (SCIGN)
- the SW Pacific GPS Project (SWP) - continuous GPS geodetic reference stations were used to expand an existing campaign style network using a multimodal occupation strategy (MOST) [*Bevis et al.*, 1994, *Taylor*, 2002].

Geodetic Data and GPS

Historically, surveys concentrated on position finding and mapping but as measurements became more precise it was evident that changes in position, shape, scale and orientation could also be measured. It was then realised that repeated measurements sometimes revealed changes that were not suspected and led to the discovery of new scientific knowledge (eg the relationship between seismicity and

strain in deforming regions near to tectonic plate boundaries)
Traditionally, deformation measurements were either:

1. direct - (linear and angular measurements on the object concerned)

   ✓ computations are carried out to determine characteristics such as shape, size orientation, volume and the process repeated at a later date
   ✓ any statistically significant differences in these characteristics are then used to estimate the phenomena of interest (eg seismic hazard and plate tectonics)

2. or indirect (less common today due to advances in technology)

   ✓ measurement of completely different phenomenon, changes of which are used to infer deformations eg use of gravity changes to infer vertical motions such as post-glacial uplift and solid earth tides.

GPS is a direct measurement space technique that has overtaken traditional angle and distance measuring systems in terms of both efficiency and accuracy for absolute and relative positioning in most practical situations ie no longer are accurate geodetic measurements limited to scalar strain rates or narrow zones of deformation. It has revolutionised precise measurements over short and long distances. There are some very sound reasons for the growth in crustal deformation research using GPS technology.

- GPS provides 3D relative positions with the precision of a few millimetres to about one centimetre over baseline separations of only hundreds of metres to thousands of kilometres
- The 3D nature of GPS allows the determination of vertical as well as horizontal displacements at the same time (traditionally vertical measurements were done separately by spirit levelling)
- GPS receivers are portable, operate under almost all atmospheric conditions and do not require intervisibility of sites
- The GPS technique allows an inexpensive, precise geodetic tool to be

available directly to researchers

Receivers and associated software can now deliver *Real Time Kinematic GPS* relative positions between receivers (RTK GPS) with a standard deviation of 1-2 cm over distances up to about 20 km. Collecting data for long observation periods in static mode enables the cancelling and modelling of systematic errors and can yield even higher accuracies over very long distances. For example, *Bingley* [1995] has achieved better than 1 cm accuracies over distances of 1000 km from 5 days of data. *Blewitt* [1993] states that permanently installed GPS monitoring networks can detect changes in position of a few mm over virtually any position. *Blewitt* [1993] also quotes accuracies of independent baselines of 2 mm + 2 pp billion, or better, as the achievable precision over continental distances, ie similar to Very Long Baseline Interferometry (VLBI) and better than Satellite Laser Ranging (SLR) [*Cross*, 1995].

Future of GPS Geodesy

Some of the current trends seem likely to continue and should impact significantly on the future of GPS geodesy.

The price of GPS receivers is decreasing and this should promote the growth of permanent, dedicated regional networks for geophysical studies (whether continuous or even campaign style surveys within a continuous framework). The main advantages of permanent continuous GPS networks are:

- Continuous networks can determine deformations with much greater accuracy and so measure small motions in a much shorter time (campaign style surveys assume that any motion between re-observation periods has occurred at a constant rate)
- The communication system associated with the permanent network allows the daily transmission of data to a central control to carry out monitoring and prediction continually and in quasi-real time [e.g. *Cross*, 1995]
- Many of the small periodic systematic errors that affect GPS can be modelled or will essentially cancel
- It is very efficient and convenient to establish additional differential GPS systems within the existing permanent network for whatever monitoring

or survey is required
- Campaign style GPS surveys can be carried out in specific areas with precision and in a well established geodetic datum

Further, data collected for non-research applications (eg navigational networks, regional differential GPS networks) have been available for research purposes and in the future real time plus archived data will be useful for geodynamic monitoring. In the past, permanent networks were established for temporal resolution and due to costs and logistical problems were limited in spatial distribution. However, the increased density of some GPS networks (eg Japan, SCIGN and New Zealand national network) has provided and will provide exceptional spatial and temporal sampling of crustal deformation. An enhanced spatial coverage is necessary for the detecting coherent tectonic signals.
Segall and Davis [1997] conclude that the future increase in spatial coverage will greatly enhance regional GPS studies.

- The quantity of collected GPS data should provide a tremendous improvement in our understanding of postseismic deformations
- GPS sites per tectonic plate will increase to a density needed to map the strain-rate distribution and to then associate features in the deformation field with specific tectonic structures
- The very high precision plus the increased spatial coverage and frequent sampling provided by GPS networks will reveal the complex spatial-temporal patterns of crustal deformation
- Eventually, the vast amount of information will lead to further insights into the rheology of the crust and mantle plus allow for time–dependent inversions for fault-slip distribution.

The rapid rate of advancement in GPS technology has seen an upsurge of use for research, professional, commercial and recreational purposes. Therefore, it would be realistically expected that within the next few decades virtually anything of significance would be monitored automatically eg tectonically active areas, volcanoes, earthquake zones, bridges, dams.
GPS (or other satellite system) will be permanently mounted in situ, receivers will be automatically linked to control centres, real time motion will be displayed and then

analysed with earth and engineering models to ensure the safety of those living in the region eg the Japanese nation network.

3.1.4 The International GPS Service (IGS)

The fact that such very high accuracies are now achievable is a result of several developments:

- improved instrumentation ie receivers and antennae,
- enhanced processing methodologies and physical modelling (such as the atmosphere, tidal effects, ionosphere and antenna phase centre variations) developed over the last decade, and
- the establishment of the IGS as the key global infrastructure for civilian GPS users

The IGS began operations in June 1992, was formally ratified by the International Association of Geodesy (IAG) in 1993 and considered fully operational on 1 January 1994.

"The IGS global system of satellite tracking stations, Data Centres, and Analysis Centres (*such as CODE and SCRIPPS*) puts high-quality GPS data and data products on line in near real time to meet the objectives of a wide range of scientific and engineering applications and studies.

The IGS collects, archives, and distributes GPS observation data sets of sufficient accuracy to satisfy the objectives of a wide range of applications and experimentation. These data sets are used by the IGS to generate the data products mentioned above which are made available to interested users through the Internet. In particular, the accuracies of IGS products are sufficient for the improvement and extension of the International Terrestrial Reference Frame (ITRF)" [*IGS, 2001*].

The IGS products include precise orbits (*IGS Rapid* and *IGS Final Orbits*), IGS tracking station coordinates in ITRF, earth rotation parameters, troposphere parameters, satellite clock errors, models for the ionosphere, antenna phase centre information and since 1998 the estimation of IGS station velocities. These products have been available to users via FTP for many years and more recently on the Internet. The

quality of the products is a function of the number of stations analysed, their distribution on the globe, and the quality of the processing software.

The challenge in high precision regional surveys has moved from the data collection to post-processing. The strategies adopted in the processing of GPS geodynamic networks involve making important decisions with regard to network size such as ambiguity resolution, troposphere and ionosphere modelling. Sophisticated GPS processing software such as Bernese and GAMIT offer the user the flexibility to apply these choices plus to test options via simulations.

The IGS global network contributes enormously to the quality of the final answers but has also substantially reduced the cost for investigators. In the past GPS analysts spent a great amount of time acquiring and cleaning tracking data for orbit determination. High precision orbits and global data sets can now be downloaded via the Internet and so global and regional geophysical studies can be undertaken for the cost of data analysis only.

The connection of regional networks to the global reference frame remains a key decision for analysts. This choice affects the quality of the final set of coordinates and on the definition of the reference frame to which they refer. This is of special importance in geodynamics networks as it is crucial to make a proper choice of reference system a) to be able to compare coordinates from epoch to epoch, and b) to interpret properly any coordinate differences that are noticed.

The primary goal of connecting a network to the IGS tracking stations is to determine the coordinates in a unified and homogeneous global reference frame called the International Terrestrial Reference Frame (ITRF). The connection of a network to IGS stations maintains network consistency in the same computational coordinate frame since the IGS products such as orbits and Earth Orientation Parameters (EOPs) are computed in terms of the ITRF. The *Global* tracking network of the IGS at the end of 2001 is shown in Figure 3.1. It is interesting to note that there is now an IGS tracking station in the Philippines that was not in existence during the PICMP93, 96 and 98 campaigns.

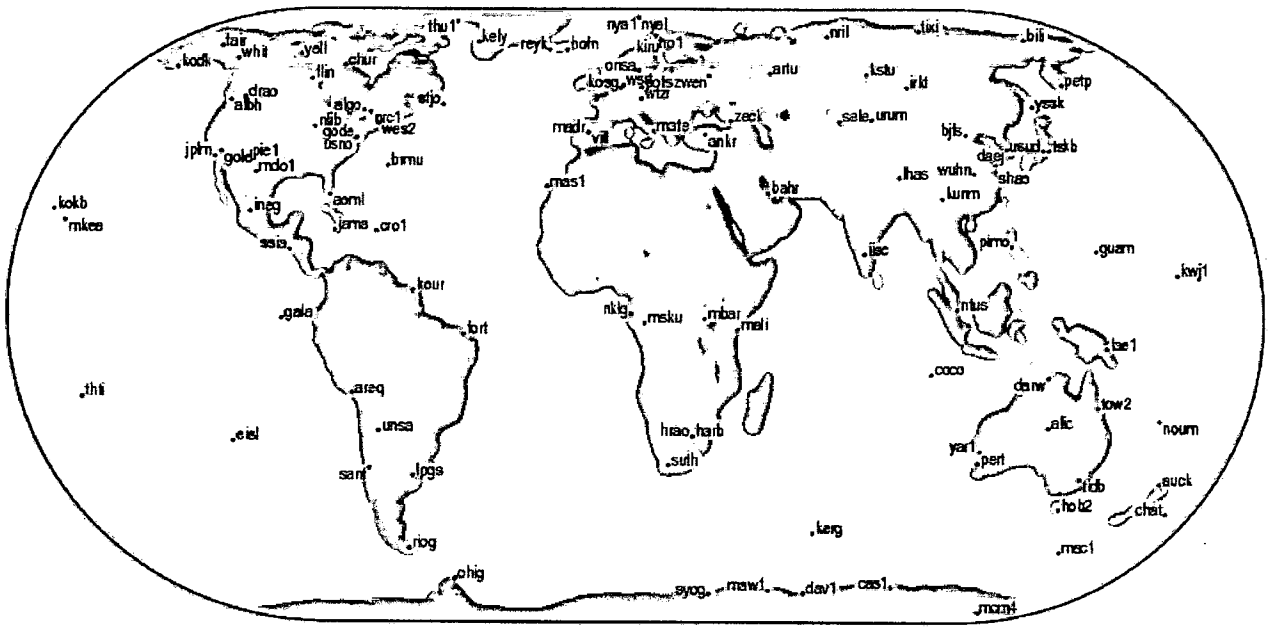

Figure 3.1 IGS Permanent *Global* Tracking Network - December 2001 [*IGS, 2001*] (NB *Global* refers to stations that have been processed by at least three IGS Analysis Centres)

3.1.5 GPS and Reference Frames

Geodynamic networks require differential GPS surveys of the highest precision plus processing using the most precise orbits available.

Differential GPS is an interferometric technique requiring good a-priori coordinates for at least one reference station to be known. All other coordinates are derived from the processed baselines relative to the reference stations. Ideally, all orbit parameters and station coordinates are in the same reference frame. Once it was also preferable to have at least three stations with accurately known coordinates (fixed or tightly constrained) to define the three translations, three rotations and scale factor of the reference frame. Nowadays, if precise orbits are used then it is no longer necessary to constrain more than one station.

IGS Final Orbits are now very precise and so the majority of GPS users do not attempt to improve the ephemerides of the GPS satellites. According to *Rothacher and Mervart* [*1996*], it is then essential that the station coordinates, the orbits and the EOPs are all in the same reference frame because:

1. the EOPs are necessary to transform the IGS precise orbits from the Earth-Fixed reference frame to the inertial reference frame, and
2. the inertial reference frame is used for the numerical integration of the orbits.

Broadcast ephemerides refer to the WGS84 reference frame whereas IGS precise orbits are in an ITRF (eg ITRF96). It should be noted that the WGS84 can only be defined to about 1 metre in geocentric position due to the quality of the broadcast orbits and satellite clock errors. However the ITRF may be determined with centimetre accuracy if IGS orbits and ITRF coordinates of the IGS stations are included in the GPS processing [*Rothacher and Mervart, 1996*]. As the two systems agree to about the 1 metre level, ITRF coordinates can be used for reference stations for either broadcast or precise orbits.
IGS orbit products indicate which ITRF is available from the information in the header of the precise orbit file. Finally, when using IGS orbits it is important to make sure that the corresponding EOP information (in the correct ITRF) is used. IGS final orbits are now created using a combined pole that is available with the orbit.

As discussed in Chapter 1, the PICMP93, 96 and 98 campaigns were all processed in the ITRF96. All Bernese GPS processing of these campaigns took place in April-May 1999. Since then, IGS has changed its realisation of the ITRF to ITRF97 in August 1999 and then to ITRF2000 in 2001.
The International Earth Rotation Service (IERS) officially accepted ITRF96 at the IAG Rio97 meeting in September 1997. On 1 March 1998, IGS announced that all of its products including the IGS Rapid and final combined orbits/EOP would be based on ITRF96 [*IGS, 2001*]. The reference frame definition of ITRF96 was nominally the same as ITRF94 and so the changes introduced only very small discontinuities. However, the 47 ITRF stations set adopted by the IGS for the ITRF96 realisation was more precise and robust than the previous ITRF94 (based on 13 ITRF stations).

Boucher [*1998*] stated that the strategy adopted for the ITRF96 solution was twofold:

1. a simultaneous combination of positions and velocities using full variance/covariance matrices, and
2. a rigorous weighting scheme based on the analysis and estimation of the variance components using Helmert method

The ITRF96 global combination was achieved with the following properties:

1. 17 selected space geodetic solutions submitted to the IERS Central Bureau in 1997
2. 70 past data files provided in Solution Independent Exchange Format (SINEX) containing positions and covariances computed from local ties
3. velocities are constrained to be the same for all points within each site
4. matrix scaling factors were estimated during the combined adjustment

[*Boucher, 1998*]

3.2 GPS Observations

3.2.1 Observables

The two composite signals at differing frequencies are transmitted from each GPS satellite. Dependent on the receiver, one or both signals may provide a type of observable, the psuedorange, while measuring the phase of a pure carrier signal will provide another observable. A third observable is that of instantaneous Doppler shift of the carrier signal, which can be measured.
However, the two main observables are the pseudorange and the carrier phase. The phase is more accurate than the pseudorange (even using the P code) because it has a much shorter wavelength.

Pseudoranges

With every human product, errors will exist. Errors in the clocks of both the satellite and the receiver are prone to drifting from the established GPS timing system, resulting in errors between the ranging. Also, the velocity of light varies because of the ionosphere and troposphere. Thus the signal is called "pseudorange". The equation relating the observable to the unknown parameters can be written as follows [Wells *et al.*, 1987]:

$$p = \rho + d\rho + c \,.\, (dt - dT) + d_{ion} + d_{trop} + \eta_p + \varepsilon_p \qquad (3.1)$$

where p is the pseudorange observation (m);

ρ is the geometric satellite-receiver range (m);

$d\rho$ is the range error due to incorrect ephemeris data (m);

c is the speed of light in a vacuum (m/s);

dt is the satellite clock offset (s);

dT is the receiver clock offset (s);

d_{ion} is the ionospheric range error (m);

d_{trop} is the tropospheric range error (m);

η_p is the error caused by code signal multipath (m);

ε_p are random measurement errors (m).

Carrier Beat Phase Observations

This type of observation is obtained by differencing the signal generated by the receiver oscillator, and the incoming Doppler-shifted carrier signal from the satellite. The equation relating it to the unknowns can be written [*Webster*, 1993]:

$$-\lambda\phi = \rho + d\rho + c\,.\,(dt - dT) - d_{ion} + d_{trop} + \eta_\phi + \lambda N + \varepsilon_\phi \qquad (3.2)$$

where λ is the wavelength of the carrier signal (m);

ϕ is the carrier beat phase measurement (cycles);

N is the cycle ambiguity (cycles);

η_ϕ is the error caused by phase signal multipath (m);

ε_ϕ are random measurement errors (m).

It should be noted that equations 3.1 and 3.2 are directly comparable except for the cycle ambiguity term (ie the unknown integer number of cycles between the satellite and receiver). The noise on these measurements for digital technology have been shown by *Meehan et al.*, [1992] to be as low as 0.13 m and 0.11 m for L_1 and L_2 respectively.

Phase observations are more precise than pseudoranges, but are only relative measures until the integer ambiguities are solved for.

Equations 3.1 and 3.2 denote the errors associated with each observable. It is

important to understand the magnitude and cause of each error so that field procedures, equipment choice and post processing techniques can eliminate or diminish them.

The observation types used in GPS plus an estimation of measurement noise is shown is Table 3.1.

Observation Type		Measurement Noise
C/A – Code	(L_1)	10-100 m
P – Code	(L_1, L_2)	1-10 m
Carrier Phase	(L_1, L_2)	1-10 mm

Table 3.1 Observation types used in GPS processing

3.2.2 Errors in the GPS Observables

Both observables include errors from many sources. Many errors can be removed, some can be reduced and others are just neglected (depending on the precision required from the survey).
Some GPS errors are systematic in nature and must be eliminated or minimised for high precision processing. These include:

- clock errors - both satellite and receiver
- errors caused by poor quality coordinates of starting point when processing baselines
- broadcast ephemeris errors
- atmospheric refraction - tropospheric and ionospheric errors
- antenna phase centre offsets
- errors associated with the determination of the carrier beat phase ambiguity

Other errors are the residual biases that cannot be modelled or differenced out (plus other effects that remain in the data). These tend to be very complex in nature and extremely unpredictable with respect to time eg uncorrected cycle slips, multipath and measurement noise.

The PICMP campaigns were processed using scientific software (Bernese version 4.0), the most precise procedures and ambiguity resolution strategies. A discussion of the GPS error sources now follows. When relevant, a brief statement will be made, detailing the technique used in the PICMP processing to reduce/eliminate the potential effect of the error described.

Selective Availability (SA).

SA is imposed by the US DoD for military reasons. This intentional degradation of the accuracy is caused by a combination of dithering the satellite clocks and by introducing errors into the broadcast ephemeris [e.g. *Hofmann-Wellenhof et al.*, 1994]. All GPS receivers encounter identical errors in the satellite clock *SA*. This affects the C/A and P code plus carrier phase measurements equally.

Differential Positioning can basically eliminate the effects of *SA* ie when precise positioning is required. However, if neglected, then *SA* induced errors will dominate all others [*Strang and Borre, 1997, pp 454-455*]. For example, it has been estimated by *Parkinson and Spilker Jr.* [1996] that the rms error in range is 20 m ie with a VDOP of 2.5 and HDOP of 2 then this implies that the rms of positional errors are 50 m vertically and 40 m horizontally.

On 1 May 2000 President Clinton announced that the United States would stop the intentional degradation of the GPS signals by SA. Therefore, after 2 May 2000 civilian users of GPS were able to obtain absolute locations up to ten times more accurately than before. The decision was made because it was felt that setting SA to zero at this time would have minimal impact on US national security. Additionally, the DOD had already demonstrated the capability to selectively deny GPS signals on a regional basis when it felt that security was threatened.

Figure 3.2 shows a plot from the GPS Support Center Web site showing the transition of SA to zero. In this plot, the circular error probable (CEP) is the circle (centred on the true position) containing 50% of all the position fixes ie horizontal errors in this case are less than 2.8 metres. There is not an exact relationship between CEP and other statistical measures and so the equivalent 95% Confidence Interval is between 6.7 and 8.4 metres.

The spherical error probable (SEP) includes the height component. The vertical accuracy works out to be roughly 10 metres (at 2-sigma or 95% probability level).

The SPS has published the standards with respect to absolute positioning using GPS since SA has been stopped (Figure 3.3).

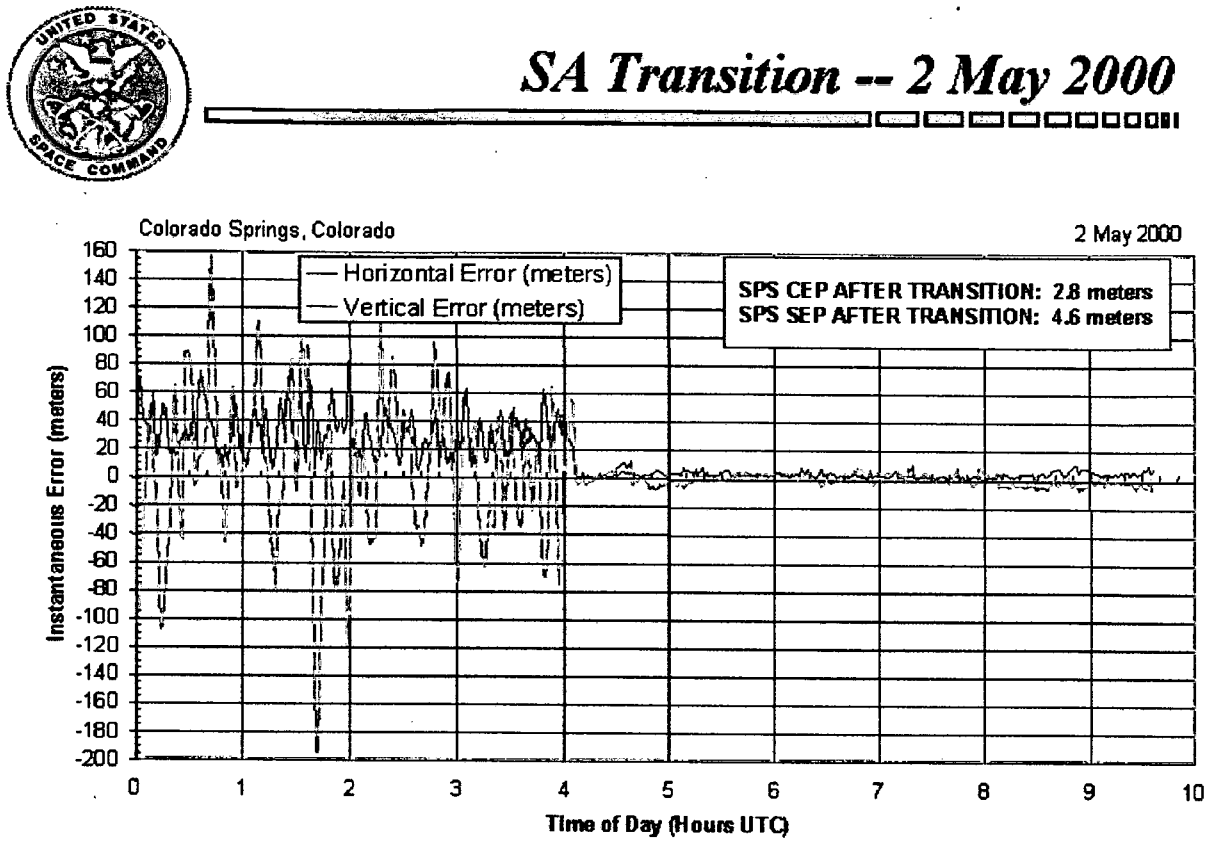

Figure 3.2 Transition of SA to zero [*GPS Support Center*, 2001]

SPS Accuracy	Global Average Accuracy*	Worst Site Accuracy
Horizontal	5 meters 95%	15 meters 95%
Vertical	8 meters 95%	26 meters 95%

SPS Availability	Global Average Availability*	Worst Site Availability
Horizontal	99.5% at 15 m 95%	92% at 15 m 95%
Vertical	99.5% at 26 m 95%	92% at 26 m 95%

SPS Time Transfer Accuracy: 20 nanoseconds 95%, Worst Site

*** Many applications will still require augmentation for better accuracy in addition to integrity and availability**

NOTES: Position Solution is All-in-View, 5° Mask Angle, SIS Only, does not include Iono, Tropo, Receiver Noise Time Transfer is All-in-View Residual Averaging

Figure 3.3 Satellite Positioning Service (SPS) Standards for GPS Positioning

Anti-Spoofing (AS)

AS is a policy implemented in 1993 whereby the P code is modulated with a secret "W" code to generate a new "Y code". This guards against "spoofing" by an enemy ie transmission of a bogus P code that would affect navigational performance of the military.

Accuracy can be maintained for precise positioning by employing differential positioning techniques.

Ephemeris (Orbital) Errors

a) Broadcast Ephemeris

The broadcast ephemerides (Keplerian elements) are transmitted by the GPS satellites. Ephemeris errors are introduced when the satellites are not at the exact positions described by the broadcasted orbits. Initially the error is small but this increases from the time of upload by the control segment until the next uploads. The error growth is slow and smooth, and only the projection of the ephemeris error along the line of sight produces an error in the range. It has been estimated by *Parkinson and Spilker Jr.* [*1996*] that, without the effects of *SA*, the rms ranging error of the broadcast orbit is about 2.1 m.

Also orbits of the satellites are affected by various factors including drag due to solar wind and gravitational changes. These factors can be reduced by differencing. The propagation of orbital error into GPS baseline length can be displayed by the rule-of-thumb derived by *Vanicek et al.*, [1985]:

$$dL / L = d\rho / \rho \qquad (3.3)$$

where
- dL is the error in the baseline;
- L is the baseline length;
- $d\rho$ is the ephemeris error;
- ρ is the satellite-receiver range (using 20200 km)

The estimate of the baseline accuracy as a function of orbit error is given in Table 3.3.

b) Precise Ephemeris

Before the International GPS Service (IGS) commenced operation in 1992, GPS ephemerides were considered as one of the primary limiting factors in the use of GPS for very high precision surveys.

This is no longer the case as extremely accurate orbits are now available via the Internet from various orbit processing centres throughout the world eg IGS, CODE (University of Berne) and SIO (Scripps Institution of Oceanography, USA).

Table 3.2 depicts the estimated accuracies of five types of orbits freely available to GPS users.

Orbit Type	**Precision (m)**	**Availability**	**Available at**
Broadcast	2.1	Real Time	Broadcast message
CODE Predicted	0.2	Real Time	CODE via FTP
CODE Rapid	0.1	after 16 hours	CODE via FTP
IFS Rapid	0.1	after 24 hours	IGS Data Centres
IGS Final	0.05	After 11 days	IGS Data Centres

Table 3.2 Estimated Quality of GPS Orbits [*Rothàcher and Mervart*, 1996, p.104]

Prior to 1992, precise orbit improvement was an important issue for high precision surveys. Precise orbits were available from the Defence Mapping Agency (DMA) but only after de-classification and a very lengthy period of time. National Geodetic Survey (NGS) precise orbits then became available. Today, due to the very high accuracy of the IGS ephemerides it is generally not recommended that orbit improvement be undertaken. It is still a consideration when processing GPS data obtained prior to 1992.

Both commercial and scientific GPS processing software usually allow the user:

- to process GPS data with the broadcast orbits, and
- to choose any of the common precise orbits available (downloaded from the internet)

Scientific software such as the Bernese V4.0 software also allows the user to estimate improved orbits commencing with broadcast or precise information.

A Priori Position Errors

A critical point in GPS processing is that an error in the fixed WGS84 coordinates of the baseline fixed station will affect the accuracy of that baseline. An error in the geocentric coordinates (WGS84) of the start position introduces a systematic scale error in the processing of GPS carrier phase observations.

By examining double-differenced equations it is possible to establish a rule-of-thumb equation similar to (3.3) for baseline errors introduced by poor start coordinates for that baseline [*Leick,* 1995]:

$$dL / L = dP / \rho \qquad (3.4)$$

where dL is the error in the baseline;
L is the baseline length;
dP is the fixed station coordinate error;
ρ is the satellite-receiver range (using 20200 km)

The estimate of the baseline accuracy as a function of the fixed station coordinate error (geocentric) is given in Table 3.3.
Table 3.3 is a combination of the approximate effects of both ephemeris errors and station location on baselines.

NB Every 20 metre coordinate error in the start position causes approximately a 1ppm error in the baselines.

Therefore for high precision GPS surveys it is critical to use the most accurate absolute positions (WGS84) available for baseline fixed stations.

The PICMP campaigns were processed using baseline processing strategies that established the most accurate coordinates via IGS global tracking stations.

Fixed Station Errors δP (m)	Orbit error $\delta\rho$ (m)	Baseline precision (ppm)
200	200	10
100	100	5
20	20	1
10	10	0.5
2	2	0.1
0.2	0.2	0.01
0.05	0.05	0.002

Table 3.3 Approximate Effects of Ephemeris Errors and Geocentric Fixed Station Location on Baselines (where ρ is approx 20,200 km) [*Leick*, 1995].

Clock Errors

GPS pseudorange and phase observables are affected by receiver and satellite clock errors. The GPS control segment monitors the condition of satellite clocks (a quadratic polynomial is used to determine the corrections for the offset). The coefficients of the polynomial are uplinked to the satellites and thus the clocks are maintained to 1 μsec of UTC. (NB GPS time does not participate in UTC's leap-second jump). The necessary data for relating GPS time and the individual satellite time are included in the navigation message. Any residual effects can be eliminated by differencing between receivers operating differentially.
An atomic clock, with a rubidium or caesium oscillator, is correct to about 1 part in 10^{12} . In a day the offset could reach 10^{-7} seconds (ie represents 26 metre rms error in range). With clock corrections being uploaded every 12 hours, an average range error of 2 m is conservative.

Receiver clock errors are generally larger than satellite clock offsets due to the lower quality in the quartz clock oscillators. Differencing between the satellites can eliminate or reduce this error. This does not mean, however, that in the differences the receiver clock error is completely eliminated. This is because to compute the geometric distance between the satellite and the receiver at time GPS time t the

receiver clock error has to be known. According to *Rothacher and Mervart* [1996] the geometric range error induced by a receiver clock error will be smaller than 1 mm if the clock error is better than 1 μsec or better. An important aspect is that the navigation solution allows this accuracy.

Atmospheric Effects on Signal Propagation

The largest errors (after the elimination of *SA*) come from the delay when the signal travels through the atmosphere. GPS signals propagate from satellite to receiver through the atmosphere, which can cause a delay and refraction of the signals, resulting in range errors. The ionosphere and troposphere are the atmospheric layers that most affect GPS measurements. The cause of this can be explained by relationship between velocity, refraction of a continually changing atmosphere and travel time ie Snell's Law

n = refractive index = c/v

where c is the speed of an electromagnetic wave in a vacuum
v is the velocity of that wave in a medium (m/s).

The concept is the same as for electronic distance measurement (EDM) devices.
The group refractive index n_{group} of the GPS modulation (superimposed on the microwave carrier wave) in a real atmosphere affects the velocity of the wave packet (and hence delays the time signal). Therefore, the scientific problem is to determine the n and n_{group} from properties of the atmosphere, the electron density in the ionosphere and the air/water densities in the troposphere [*Strang and Borre*, 1997, p. 454].

a) Ionosphere Errors

The ionising action of the sun's radiation on the earth's upper atmosphere produces free electrons. The ionosphere is the ionised upper part of the atmosphere ranging between 50 km to 1000 km above the earth.
Radio waves of frequency > 30 MHz such as GPS signals are time delayed as they pass through the ionosphere. The ionosphere is composed of free electrons and

ions. The delay is proportional to the total electron content (TEC) ie the integrated density along the signal path. The TEC is expressed in so called TEC Units (TECU), where one TECU corresponds to 10^{16} electrons per square metre ($10^{16}/m^2$). Ionospheric refraction is frequency f dependent (ie dispersive) with the density of the free electrons varying greatly with the time (day and year), high solar activity and the latitude of the observer. The variations from solar cycles, seasons and short-term effects are not predictable and difficult to model.

The effects on the pseudorange P and phase Φ are opposite in sign ie the pseudorange is delayed but the carrier phase is advanced [*Strang and Borre*, 1997]. *Brunner and Gu* [1991] estimated the ionospheric phase advance along the signal path and this is given in Table 3.4.

Phase Advance	L_1 **Signal**	L_2 **Signal**
First Order ($1/f^2$)	-16.2 cm	-26.7 cm
Second Order ($1/f^3$)	-0.8 cm *	-1.6 cm *
Third Order ($1/f^4$)	-0.3 mm *	-0.8 mm *
	* approximately	

Table 3.4 Estimated phase advance for GPS signals [*Brunner and Gu*, 1991].

The **dispersive** nature of the ionosphere can be used in actually removing most of the ionospheric delay effect by making pseudo-range and/or carrier phase measurements on both L-band frequencies, and combining them in a special linear relation that results in an "ionosphere-free" observable.

It is important to estimate the ionospheric effects so that they can be removed. A **dual-frequency** receiver can measure the pseudoranges P_1 and P_2 on both frequencies L_1 and L_2, and solve for the delay:

$$dP_{ion} = \frac{f_2^2}{(f_2^2 - f_1^2)} (P_1 - P_2) + \text{random/unmodelled errors}$$

[e.g. *Strang and Borre*, 1997].

This can then be removed from the P_1 pseudorange.

Similarly the phase correction for ionospheric delay is

$$d\Phi_{ion} = \frac{f_2^2}{(f_2^2 - f_1^2)} ((\lambda_1 N_1 - \lambda_2 N_2) - (\Phi_1 - \Phi_2)) + \text{random/unmodelled errors}$$

[e.g. *Strang and Borre*, 1997]

NB If there are no cycle slips the ambiguities N_1 and N_2 remain constants to be determined.

When using a dual frequency phase receiver, the P code observations can allow an initial estimation of the ionosphere correction. Then the improved pseudoranges can help resolve the ambiguities N_1 and N_2.

Most first order ionospheric effects are removed using dual frequency observations to form the *ionosphere-free* linear combination of phases and can be represented as follows:

$$LC_{ion-free} = \frac{f_1^2}{(f1^2 - f2^2)} * L_1 - \frac{f_2^2}{(f1^2 - f_2^2)} * L_2$$

$$(\text{i.e.} \quad L_3 = 2.546 \, .L_1 - 1.984 \, .L_2 \quad)$$

The remaining high-order terms cannot be removed [*Brunner and Gu*, 1991]. However, relative positioning techniques:

- almost entirely cancels effects over short baselines,
- removes the majority of these effects over baselines of 500 - 1000 km and
- has an expected residual error of less than 1 cm for longer baselines.

The term "ionosphere-free" is not fully correct because some approximations were involved in the derivation such as integration along the geometric path rather than the true path.

However, for short lines (< 20 km) it has been accepted that it is better to use single frequency receivers because the *ionosphere-free* phase combination is three times noisier than the corresponding single frequency measurement [*Leick*, 1995]. A good ionosphere model may then be needed to improve accuracy e.g. to avoid the scale error problem as discussed below.

Obviously, for **single frequency receivers,** both of the above equations for dP_{ion} and $d\Phi_{ion}$ cannot be resolved. Once again, differential positioning over short baselines (10 - 20 km) can almost entirely eliminate these errors when we compute the ionospheric delay. The difference in signal path produces a *slight baseline shortening,* proportional to electron content and baseline length. ie for a geodetic network incorporating predominantly single-frequency data and in which the processing disregarded ionospheric refraction, then contraction (scale error) of the network can be expected [*Georgiadou and Kleusberg,* 1988; *Strang and Borre, 1997; Komjathy,* 1996, 2001; *Rothacher and Mervart, 1996*]. This fact will be discussed at length in Chapter 5 as it applies directly to the NRMDP GPS observations and results.

Single frequency networks can be efficiently processed to remove or greatly reduce this ionosphere induced scale bias (under homogeneous and moderate ionospheric conditions) by using a dual frequency GPS derived ionosphere model to calculate dP_{ion} and $d\Phi_{ion}$.

NB The PICMP 1993, 96 and 98 campaigns were processed by the Bernese V4.0 software using the ionosphere-free linear combinations (termed L_3 by Bernese) and also the ionosphere phase advance $d\Phi_{ion}$ was calculated and then used in the so called "wide-lane" ambiguity resolution.

b) Troposphere Errors

Tropospheric refraction is the path delay caused by the electrically neutral part of the atmosphere in the region up to the start of the ionosphere (about 50 km above the earth's surface). Although most texts usually refer to this region as the *troposphere,* the neutral atmosphere is comprised of the troposphere (up to 9 km), the tropopause (9-16 km), and the stratosphere (16-50 km).

The *troposphere* is a non-dispersive medium for radio signals up to frequencies of 30 GHz [*Brunner and Welsch,* 1993]. Therefore, the delay is identical for both the L_1 and L_2 carriers i.e. affects the carrier phase and the code observables equally. As a result, it can not be eliminated using dual frequency observations. The delay reaches 2.0-2.5 m in the zenith direction and increases with the cosecant of the elevation angle, giving about 20-28m delay at a 5° angle [Leick, 1995].

The propagation temperature, pressure and humidity alter the speed of the radio waves and hence the path. Also the delay can be dependent on the variation in user height and the type of terrain below the signal path.
It is possible to separate the troposphere refractivity into a *dry* and a *wet* component. Generally about 90% of the total delay is attributed to the *dry* atmosphere component which can be effectively modelled using surface measurements of temperature and pressure or the standard atmosphere model. However the wet component is due to the water vapour content in the atmosphere and this is highly variable and hence difficult to model. Wet delay errors are the limiting factor in precise GPS heighting. NB The delay from liquid water in rain and clouds is well below 1 cm. But models of the wet delay (water vapour) using surface meteorology are often wrong by more than 1 cm [*Sprang and Borre*, 1997].

There has been much research into the creation and testing of tropospheric refraction models. Various models include:

- Saastamoinen [1972,1973],
- Hopfield [1969],
- the modified Hopfield model [*Goad and Goodman*, 1974],
- the simplified Hopfield model [*Wells*, 1974], and
- the differential refraction model based on formulae by Essen and Froome [*Rothacher et al.*, 1986]

These various models differ primarily with respect to assumptions on the vertical refractivity profiles and the mapping of the delay with elevation angle.
High precision GPS processing software (eg Bernese) tend to use an *a priori* tropospheric model (eg Saastamoinen) to account for the delay followed by various techniques to estimate the tropospheric delay parameters with respect to this a priori model.

With availability of IGS orbits, tropospheric delay can now be considered as "the *ultimate accuracy limiting factor* for geodetic applications of the GPS" [*Rothacher and Mervart*, 1996, p. 159].

There are two major troposphere biases:

- *relative troposphere biases* caused by unmodelled effects of the tropospheric refraction at one of the endpoints of a relative baseline
- *absolute troposphere biases* caused by unmodelled effects of tropospheric refraction common to both endpoints of a baseline

[*Rothacher and Mervart*, 1996]

NB *relative troposphere biases* basically cause errors in station heights whereas *absolute troposphere biases* produce scale errors of the processed baseline lengths.

For local surveys and smaller regional campaigns relative tropospheric errors are the most important but more difficult to model. *Brunner and Welsch* [1993] reported that a bias of 1 cm in differential troposphere leads to an error of about 3 cm in the computed relative height. Therefore actual surface meteorological measurements are not often used for GPS processing.
Alternatively, an absolute troposphere bias of 10 cm induces a scale bias of about 0.05 ppm. Although this effect is small it should be taken into account for baselines longer than 20 km and for high precision GPS surveys. Absolute tropospheric error is similar in effect to a scale error caused by the ionosphere. Tropospheric refraction (99% produced below 10 km in altitude) tends to be more site specific than ionospheric refraction (at a height of about 400 km).
Because tropospheric errors are larger in magnitude than the noise level of the phase observable they must be reduced for high precision GPS surveys. According to *Rothacher and Mervart* [1996] the Bernese GPS Software V4.0 has been developed with the option of reducing these effects by opting to use either of the following widely used methods:

1. model tropospheric refraction without using the GPS observable ie by using ground met measurements or water vapour radiometers
2. model the tropospheric zenith delay in the general GPS parameter estimation process.

NB the PICMP 1993, 96 and 98 campaigns were processed by modelling the

tropospheric delay in the GPS parameter estimation method (modelling for relative and absolute for each two-hour interval).

Interestingly, GPS is now being used in the ongoing research of modelling the atmosphere. *Bevis et al.* [1992] and *Dusan et al.* [1996] show that the water vapour density could be measured by GPS. Also already discussed, the electron content of the ionosphere can monitored by GPS.

Multipath Errors

Multipath is a serious type of GPS signal interference that is caused by the simultaneous arrival of a direct and a reflected signal at the receiver antenna. The signal can be reflected from buildings, objects or the ground and distorts both the code and the carrier phase observables (ie a ghosting or echo effect). Multipath signals are delayed because the reflected paths are longer than the line-of-sight path. This delay can create range errors of several metres or more. The multipath errors in the phase observable Φ range from 1-5 cm [*Strang and Borre*, 1997, p. 457].
Unfortunately, multipath is extremely difficult to model. The induced error is site-dependent and does not cancel with relative positioning.

A guide to the reduction of multipath signals includes:

- choosing an improved site for the GPS antenna ie no obstructions or nearby reflective objects
- not using observations to low elevation satellites
- the use of antennae with large groundplanes with various elements (eg dipoles, microstrip)
- the use of GPS receivers (geodetic) with a narrow correlator to block reflection or with multiple correlators to allow estimation on several paths
- careful session planning to try and estimate repeatable paths for a given satellite/receiver pair
- employ longer observation sessions so that differing satellite configurations tend to average out the multipath effects

For high precision GPS surveys it is desirable to choose sites that avoid multipath sources.

Antenna Phase Centre Errors

It should be noted that the geometrical distance between a satellite and a receiver must specify the exact physical point of GPS signal emission and of reception. These points are the antenna phase centres.

a) Satellite Antenna Phase Centre Offsets

The position of the phase centre of the GPS satellite transmitting antenna with respect to the centre of mass of the satellite is required only for very high precision surveys only.

The majority of commercial GPS software packages do not make allowance for the satellite antenna phase centres. However, in scientific software such as the Bernese V4.0 software, the precise position of the satellite antenna phase centres with respect to centre of mass is available as a file during processing. This phase centre is the same for both L_1 and L_2 and its location remains constant [*Rothacher and Mervart*, 1996, p. 215]. In most cases it is not direction dependent. However, when a satellite passes through the Earth's shadow errors result from of a mis-orientation of the antenna and a difficulty in modelling the solar radiation pressure. The Bernese software does not account for these Earth shadow effects.

NB the Bernese (CODE) and the IGS precise orbits refer to the centre of mass of the satellites and so can be used directly in the Bernese software.

b) Receiver Antenna Phase Centres

Receiver antennae are more complicated because the phase centre is dependent on the receiver type/model and the incoming signals from the satellites ie it varies with the elevation and azimuth of the satellite being observed [*Wu et al.*, 1993].

Rothacher and Mervart [1996, p. 216] term this direction dependence as *antenna phase centre variations*. The magnitude of these variations can be in the order of several centimetres. Also, the manufactured phase centre positions as well as the phase

centre variations are not identical for the L_1 and L_2 carriers.

It is critical to model phase centre variations if different antenna types are used for relative positioning eg a bias of up to 10 cm in relative station height is possible which is independent of the baseline length.

Even if the same antenna types are used, then it is possible to induce a scale error in the baselines of up to 0.015 ppm. This is because over long distances each receiver observes the same satellite with a different elevation angle. For high precision surveys this is unacceptable and must be reduced.

According to *Rothacher and Mervart* [1996], the Bernese GPS Software contains correction modelling for the antenna phase centre variation based on either a piece-wise linear function in elevation or a spherical harmonic function.

These errors can be minimised or reduced:

- for short baselines (<50 km) by using identical antennae which are similarly aligned
- for longer baselines the effect must be modelled (even with the same antenna type) because the antenna phase centre errors do not cancel in relative positioning
- for all baselines where different antenna types are used it is essential to apply a phase centre model.

Phase centre information for the most commonly used antennae has been made available by the IGS for modelling within various software packages. This is extremely useful as most geodynamic GPS surveys use IGS global tracking station data to help establish the most precise ITRF coordinates for the survey (eg ITRF96 for all PICMP surveys).

NB the PICMP 1993, 96 and 98 campaigns were processed using the Bernese GPS Software V4.0 and incorporated the satellite antenna offsets plus a piece-wise linear function model for the receiver antennae.

Earth Rotation Parameters (ERP)

For very high precision GPS it is important to incorporate variations in the earth rotation parameters including:

- the earth rotational pole coordinates
- the UT1 - UTC correction, and
- the UTC - GPS time correction

Generally, commercially available software corrects for the UTC - GPS difference BUT does not take into account the rotational pole coordinates.
The Bernese GPS Software requires an ERP *POLE-file* to be available in all orbit and processing programs. This file uses information that originates from the *IERS Bulletin A or B*. The data for this can be downloaded from the Berne anonymous ftp site (in the correct format) or from other sites such as the C04 or the IGS (then transformed into the correct format by the Berne software).

Other Sources of Errors

- A limiting factor in the precision of a GPS survey is the quality of the receivers used. For very high precision GPS surveys this is a full wavelength receiver that also has the capacity to eliminate/reduce noise eg Trimble SSI receivers. Generally, the more expensive the receiver, the lower the level of noise experienced.
- Earth tides - these are only small and can be almost completely accounted for.
- The weakest aspect of GPS positioning is the height component (which is about 3 time less accurate than horizontal positioning) primarily because of the geometry of the satellite constellation and the tropospheric delays. Another limiting factor is the difficulty in defining the geoid/ellipsoid separation (N value) ie this affects the determination of orthometric heights by GPS, but these are not necessarily required for tectonic studies.
- Residual measurement noise - "...those errors that remain after all propagation errors, clock errors, and errors related to the physical properties of the antenna have been taken into account" [*Wells and Kluesberg*, 1989].

3.3 Obtaining GPS Solutions

3.3.1 The Observation Equations

There are a number of different types of observation models that can be used to

determine GPS absolute or relative positions. Each model can use either the pseudo-range or the carrier beat phase measurement to form the observation equations.
Both techniques contain the various linear biases, which degrade the precision of the receiver position. The carrier beat phase observation equation has the added integer ambiguity bias.

When using the relative GPS technique there exists a high level of correlation among the signals received at independent sites simultaneously tracking the same satellites. By taking advantage of this physical model many of the correlated errors, such as orbit, clock, and atmospheric biases, can be reduced by forming linear combinations of either the code or phase measured ranges. Differencing the ranges in various linear combinations will lead to the computation of precise baselines. The linear combinations used in GPS reductions are:

Single Differences:	between-epoch
	between-receiver
	between satellite
Double Differences:	receiver-epoch
	receiver-satellite
Triple Differences:	receiver-satellite-epoch

As the range derived from carrier phase measurements produces more precise values than that of the pseudo-range measurements, the linear combinations of the carrier beat phase observable will be presented. Differences of the original observations allow it to eliminate or reduce some biases.

SINGLE-DIFFERENCES

The first linear combination can be constructed from the arithmetic difference between the two simultaneous phase measurements from a single satellite s_1 to two independent receivers r_1 and r_2 (at the single epoch t_1). This is known as the *single-difference* observable.

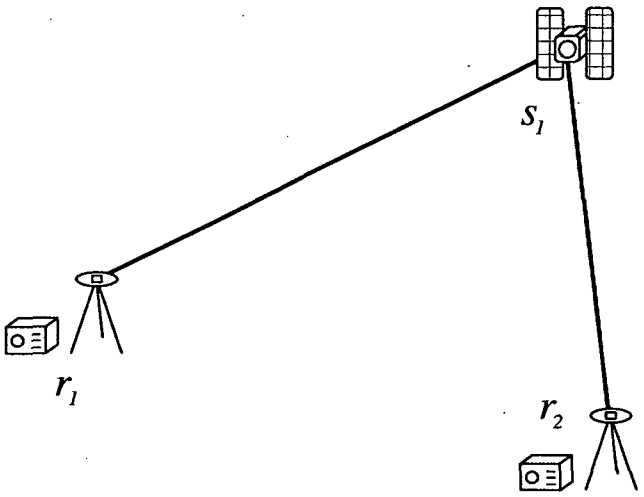

This single difference operation has removed the satellite's transmitted phase. The offset and linear drift of the satellite clock has also cancelled. It has also reduced the errors caused by path effects if the receivers are sufficiently close together (<20 km) because the signal paths will be almost the same. Thus, any bias which is equivalent at each receiver has been removed leaving a *residual noise* derived from any uncorrelated errors. This will include orbit uncertainties, and atmospheric delays. The single difference however is still contaminated by receiver clock errors.

DOUBLE DIFFERENCES

The difference between two single difference observations, constructed from simultaneous phase measurements to satellites s_1 and s_2 and receivers r_1 and r_2 is the so-called *double-difference* phase observable. This eliminates errors in both receiver and satellite clocks.

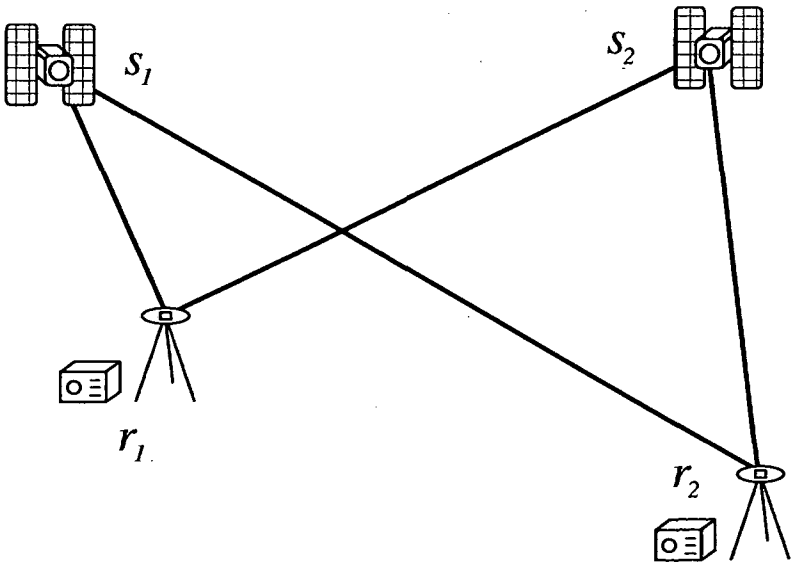

The *double difference* phase observable is formed by differencing the carrier phases measured simultaneously by a pair of receivers tracking the same pair of satellites ie by differencing 2 single difference observations.

The integer ambiguity is however still present.

TRIPLE DIFFERENCES

Since the integer ambiguity does not vary with time, the difference between two double differences observed at two epochs t_1 and t_2, will remove the unknown ambiguity except during loss of lock. This is known as the *triple Difference.*

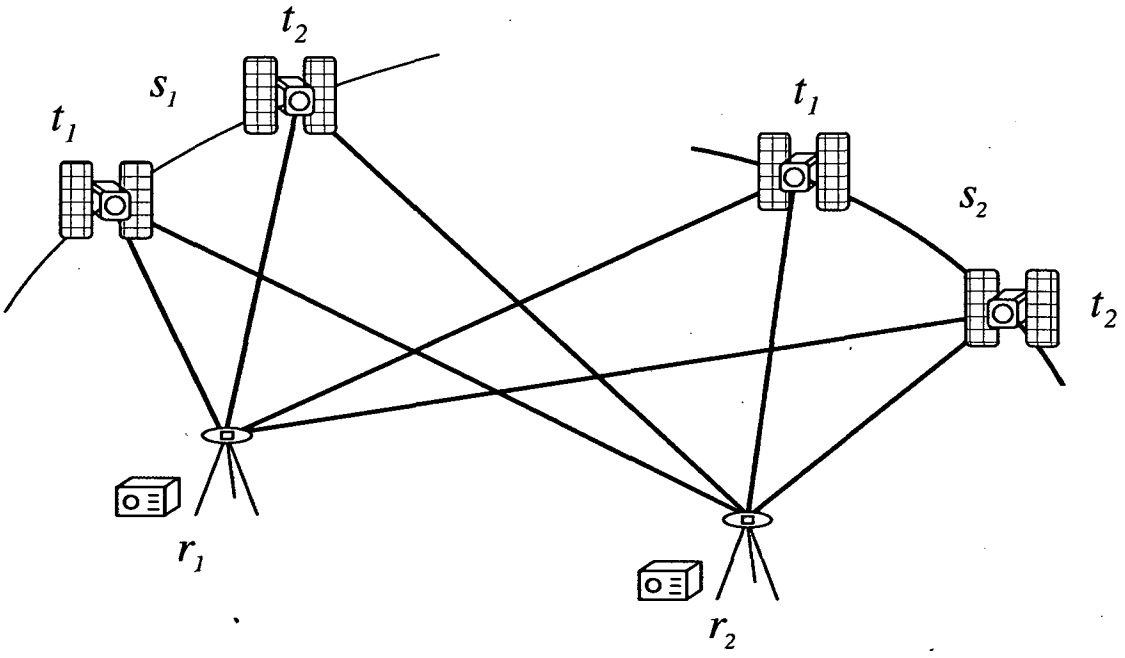

Because the triple-difference observable is independent of the integer phase ambiguity (ie the phase ambiguity is eliminated) it can be used to detect any cycle slips which contaminate the single and double difference ambiguity parameter. Also, as tropospheric refraction does not vary rapidly with time then triple differencing considerably reduces this effect.

3.3.2 Processing GPS Data

As there are usually a multiple number of phase measurements in any one static GPS survey, the baseline components derived from the differenced data set are

determined by a least squares approach.

Theoretically, any one of the differenced observation sets will yield the same solution, provided all correlations are appropriately computed. However, although the single, double, and triple differences progressively eliminate any physical correlations between observed phase data, the stochastic correlation in the least squares solution increases.

Differencing is used for removing or minimising biases, unknowns and errors. Whilst some errors can be essentially eliminated by using differenced phase observations, the primary disadvantages are:

- that there is a trade-off between removing errors by differencing and losing precision by reducing the number of observations i.e.
    a) 2 phase observations are used for one single difference,
    b) 4 phase observations are used for one double difference and
    c) 8 phase observations are used for one triple difference
- that the noise factor is increased with each difference made
- the sets of observations become correlated and then these correlations must be modelled as part of the processing of the observations.

A simple *diagrammatic* representation of the optimum processing option using single, double or triple differencing is shown in Figure 3.4.

Theoretically, there should be an exact number of whole wavelengths (ambiguities) between the receiver and the satellite i.e. the ambiguities the software solves for should be integers. Unfortunately, at this stage of the processing, the values for the ambiguities are not integers. This solution is referred to as a *double-differenced ambiguity free* solution because the ambiguities are solved as real values and are not fixed to integer values.

It is generally considered that the best baseline solution would be obtained from a double difference solution where the exact number of integer wavelengths was known between receiver and satellite i.e. *a double-difference ambiguity fixed* solution. The determination of the exact number of integer wavelengths is termed *ambiguity resolution*.

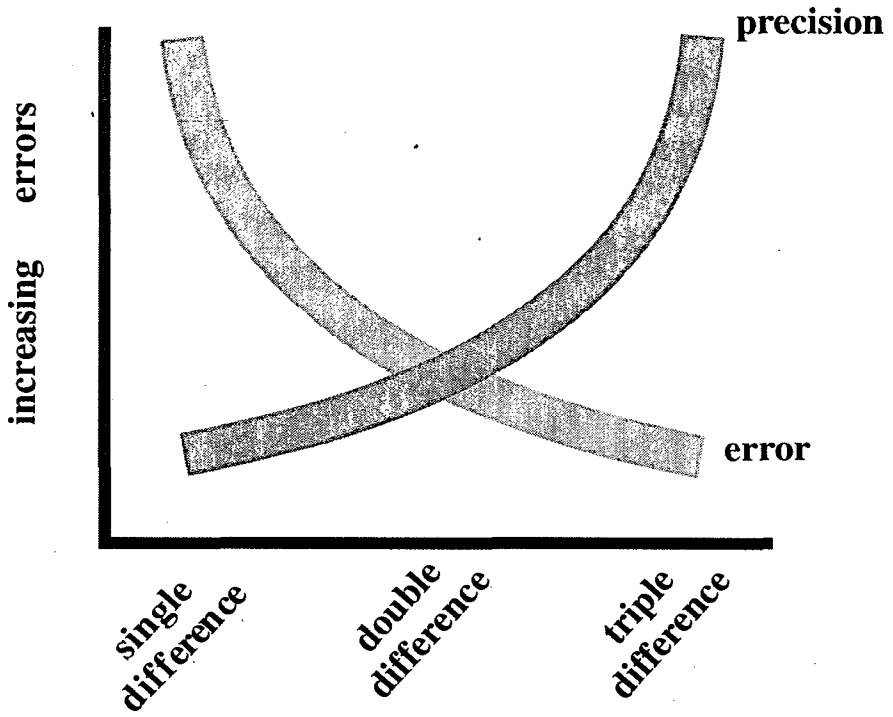

Figure 3.4 Optimum GPS Processing Option [*GPSCO, 1995*]

Ambiguity resolution is a critical process for high precision GPS surveys but it requires very careful strategies. Double-differenced ambiguity fixed solutions can be more than ten (10) times more precise than ambiguity free solutions (see Figure 3.5). However, with long observation times (>12 hours) e.g. such as those in the PICMP campaigns, this can be more like a factor of 3 in east-west and less in north-south.

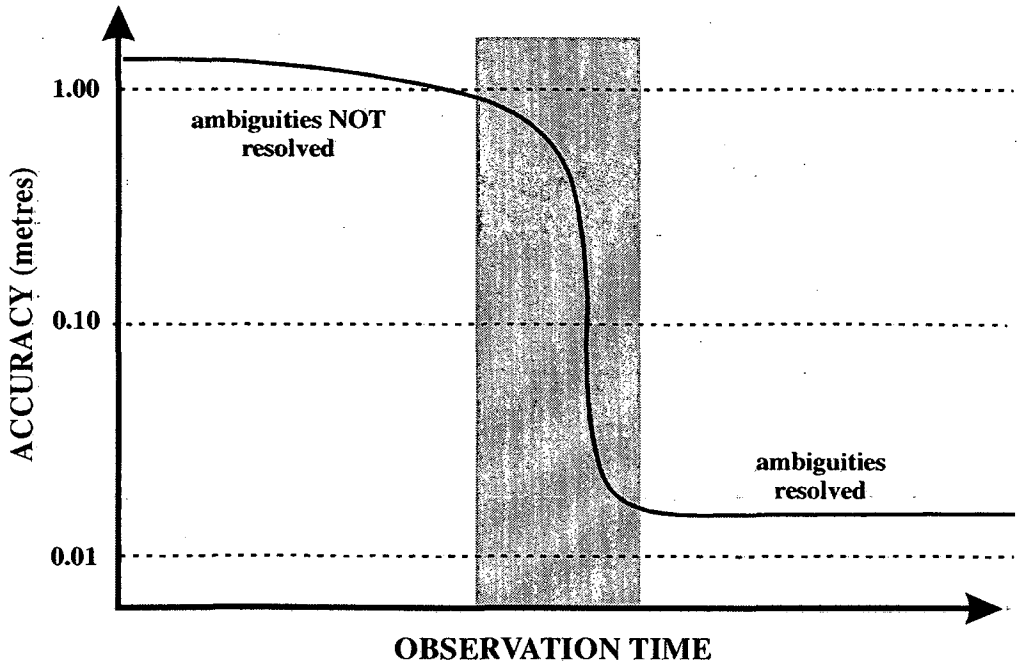

Figure 3.5 Graphical representation of successful ambiguity resolution on double differenced baselines [*GPSCO, 1995*]

However it must be stressed that if the wrong ambiguities are selected, solutions may be worse than ambiguity free or even triple difference solutions. Thus if the integer ambiguity can be correctly estimated, the double difference solution may produce the better solution. For long observation sessions e.g. 24 hours a double difference solution with *real* valued ambiguities gives similar results. However, if the ambiguity cannot be resolved adequately the triple difference solution may need to be adopted, as it is free of the unknown ambiguity term.

The residual noise, which inhibits ambiguity resolution, is a function of the baseline length. This is largely due to the spatial and temporal nature of the atmosphere. Thus longer baselines, which have receivers in differing atmospheric conditions, will usually be computed by the triple difference data set.

The chances of ambiguity resolution is increased when:

- baselines are short e.g. less than 100 km
- observation sessions are long
- processing strategies are undertaken using various L_1 and L_2 linear phase combinations

NB satellite configurations and atmospheric conditions also affect the outcomes.

$$L_3 = \frac{f_1^2}{(f_1^2 - f_2^2)} * L_1 - \frac{f_2^2}{(f_1^2 - f_2^2)} * L_2$$

$$L_4 = L_1 - L_2$$

$$L_5 = \frac{f_1}{(f_1 - f_2)} * L_1 - \frac{f_2}{(f_1 - f_2)} * L_2$$

$$fi : Frequency\ of\ carrier\ Li\ (i = 1,2)$$

$$L_1, L_2, L_3, L_4, L_5 \ \ in\ metres$$

Table 3.5 Equations for the Linear Combinations of the L_1 and L_2 observables used in the Bernese GPS Software Version 4.0 [*Rothacher & Mervart*, 1996].

3.3.3 Linear Combinations (LC) of the Phase Observations

In order to eliminate certain parameters and to improve ambiguity resolution, linear combinations of the original carrier phase or differenced measurements may be formed and used during processing. Table 3.5 shows the equations of the linear combinations used by the Bernese GPS Software V4.0 [*Rothacher & Mervart*, 1996].

The L_3 Linear Combination

The L_3 combination (see Table 3.5 for equation) practically eliminates the ionospheric path delay and is therefore commonly termed the *'ionosphere-free'* observable (as already discussed in 3.2.2). Unfortunately, the disadvantages of this combination are that the ambiguity parameters are no longer integers and the "noise" on the resultant L3 observable is higher than on either of the original L1 and L2 measurements.

The L_4 'Geometry-free' Linear Combination

The L_4 combination (see Table 3.5 for equation) is independent of receiver clocks and geometry (orbits, station coordinates). However, it contains the ionosphere delay and initial phase ambiguities, and is used for estimation of ionosphere models

The L_5 Linear Combination

The L_5 combination (see Table 3.5 for equation) has a formal wavelength of about 86 cm and is roughly 4 times longer than that for L_1 and L_2. Therefore, it is often called the *wide-lane* and the phase ambiguity deemed the *wide-lane ambiguity*. The Bernese processing software allows wide-laning for the purpose of cycle slip fixing and ambiguity resolution of double-differenced phase observations. Integer ambiguities can be solved more readily using a phase with a longer wavelength.
Disadvantages include:

- the measurement noise on the L_5 is much larger than that on L_1 and
- the ionospheric effect is also larger.

However, the ambiguities remain as integers and the long wavelength facilitates ambiguity resolution on long baselines.

NB Table 3.6 depicts the most important phase linear combinations and their characteristics.

Carrier	Description	Formal Wavelength	Noise rel to L_1	Ionosphere rel to L_1
L_1	Actual Carrier	19 cm	1	1
L_2	Actual Carrier	24 cm	1	1.6
L_3	Ionosphere-free LC	0 cm	3	0
L_4	Geometry-free LC	∞	1.4	0.6
L_5	Wide Lane	~ 86 cm	5	1.3

Table 3.6 Linear combinations of the carrier phases L_1 and L_2 used in the Bernese GPS software [*Rothacher & Mervart*, 1996].

3.4 Summary of the Procedure for Very High Precision GPS Processing

Commercial GPS software packages are generally unsuitable for very high precision processing. This is due to the fact that they have been designed to be user friendly for everyday GPS applications and can produce horizontal baseline precisions of 0.1 - 1.0 ppm using precise orbits. However for very high precision GPS surveys and crustal deformation surveys, the following procedures are essential:

1. Use a specialised scientific GPS software package that incorporates various strategies plus parameters that eliminate or reduce as many of the sources of errors that have already been discussed. For all of the PICMP campaigns the Bernese V4.0 GPS Software was used.

2. Precise orbits (preferably IGS) are a prerequisite for ALL processing.

3. It is important to use the relevant Earth Rotation Parameters (ERP) as the current POLE-file during processing.

4. Use relevant phase differencing techniques (e.g. double differencing) plus linear combination strategies (e.g. wide-laning) to resolve successfully as many integer ambiguities as possible NB ideally a *double-differenced ambiguity fixed* solution.

5. Use the most accurate coordinates (WGS84) possible for starting points on baselines to be processed eg via IGS global tracking station.

6. Incorporate ionosphere modelling plus the use of the ionosphere-free linear combinations (L_3) for baseline processing and ambiguity resolution.

7. Process campaigns by modelling the tropospheric (eg modelling for relative and absolute tropospheric effects for each 2-4 hourly interval).

8. Use established satellite antenna offsets (where possible) plus a relevant function model for the receiver antennae phase variations.

3.4.1 Scientific GPS Software Packages.

There are a number of major scientific software suites that are or have been available for high accuracy applications of the GPS. Table 3.7 shows a sample of the most well known packages and the institutions responsible for the software development.

Software Name	*Developed at*
BERNESE	Astronomical Institute of the University of Berne, Switzerland (AIUB)
EPOS	German Geodetic Research Institute (GFZ)
GEODYN	National Aeronautics and Space Administration, USA (NASA)/Goddard Space Flight Centre (GSFC)
GAS	Institute of Engineering Surveying and Space Geodesy, University of Nottingham, England (IESSG)
GIPSY/OASIS	Jet Propulsion Laboratory, USA (JPL)
GAMIT/GLOBK	Massachusetts Institute of Technology (MIT)/Scripps Institute of Oceanography, USA (SIO)

Table 3.7 Gives a sample of many of the most well known scientific GPS software suites used for very high precision processing

Chapter 4 fully describes the processing of the PICMP93, 96 and 98 campaigns using the Bernese GPS Software version 4.0, the strategies/methodologies adopted and then finally the results that are to be used for the geophysical investigations depicted in Chapter 5 e.g. coseismic, postseismic and interseismic deformations in the Luzon earthquake zone plus regional tectonics.

4.0 The PICMP GPS Processing and Analysis

PICMP93 was initially processed with Version 3.4 of the Bernese GPS Software [*Rothacher et al.*, 1993] using the CODE orbits available from the University of Berne. When GPS data became available for the PICMP 1996 and 98 campaigns it was decided to process all three set of data using the then latest Version 4.0 software [*Rothacher & Mervart*, 1996].

4.1 The Bernese GPS Software

4.1.1 Overview

The Bernese GPS Software (Astronomical Institute, University Of Berne Switzerland) was developed as a tool for the highest accuracy requirements. Typical users of the software include scientists (eg plate tectonics, geodynamics, atmospherics, general research and educational), geodetic survey agencies (zero and first order national surveys), permanent GPS arrays eg Japanese monitoring network and commercial users that require very high precision processing.

According to *Rothacher & Mervart* [1996], the software is suited for:

- Rapid processing of small-size single and dual frequency surveys
- Ambiguity resolution on medium and long baselines (up to 2000 km using precise orbits)
- Ionosphere and troposphere modelling capabilities
- Combination of different receiver types
- Full simulation capability
- Earth rotation parameter estimation
- Permanent network processing
- Orbit determination techniques (fiducial point concept/free network approach)

Also, the general features of the software include:

1. All GPS observables may be used
2. Capability of using Broadcast or Precise Orbits (IGS, CODE etc.)
3. Five different linear combinations of L1 and L2 may be used
4. Data from various receiver types may be processed and combined via the Receiver Independent Exchange (RINEX) format (including the use of receiver-type specific antenna phase centre variations)
5. Combination of single and dual frequency receivers is possible
6. Ionosphere modelling
7. Baseline/session/campaign/multiple campaign processing is allowed (incorporating full normal equations in solutions)
8. Simultaneous estimation of a large number of different parameter types is possible

The software is complex and contains more than 100 programs. However, it is generally arranged in five different components:

1. Transfer of data
2. Orbit (generation in orbit format)
3. Processing
4. Simulation Programs
5. Service Programs

The flow diagram of basic Bernese processing is shown in Figure 4.1.

NB Precise IGS orbits were used for all of the PICMP campaigns and hence no orbit relaxation was attempted. The simulation component of the software was not used.

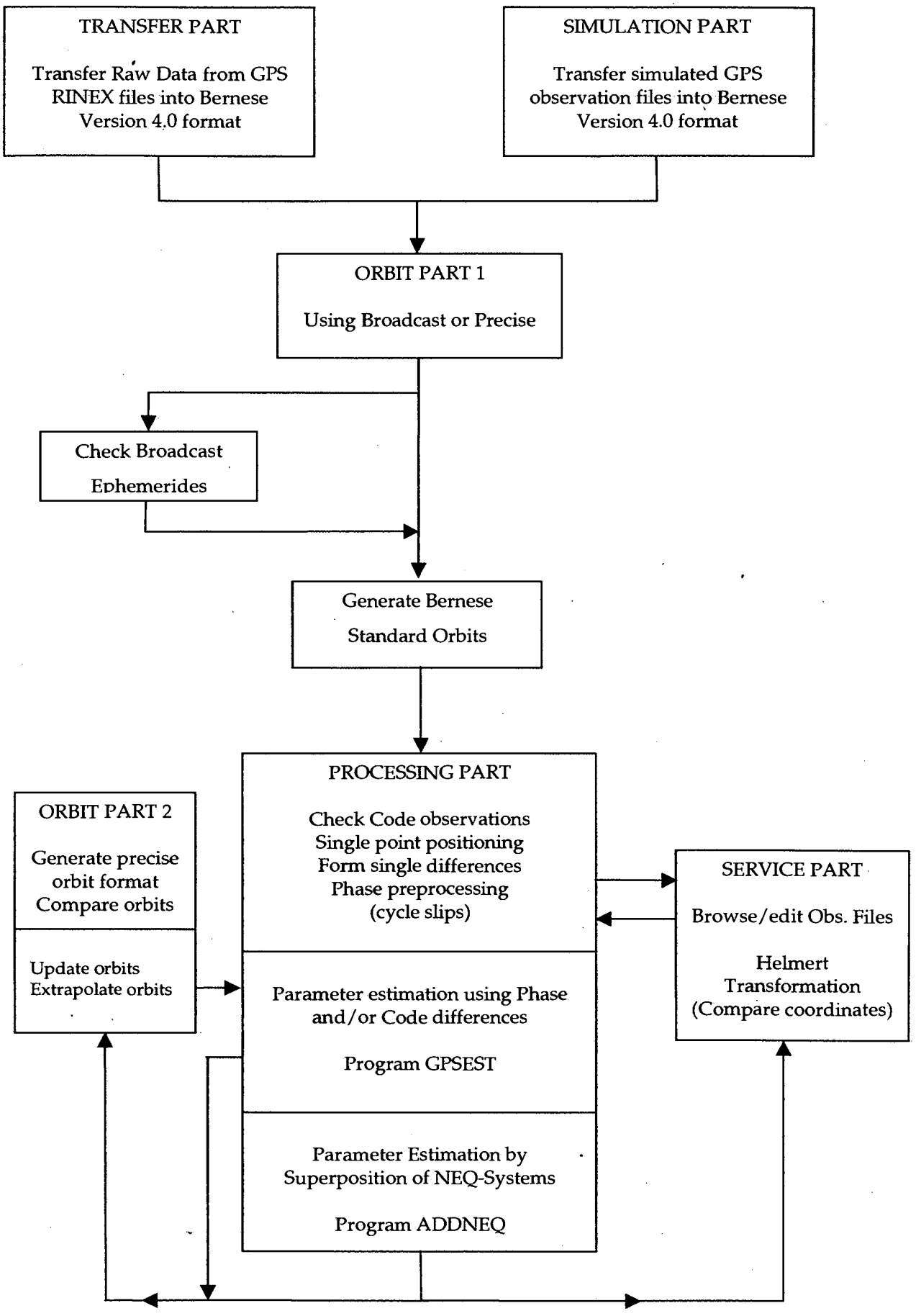

Figure 4.1 Functional Flow Diagram of Normal Processing in Bernese GPS Software Version 4.0 [*Rothacher and Mervart*, 1996].

4.1.2 Processing of GPS Measurements

The Bernese processing procedure and program options for the use of *precise orbits* (without orbit improvement) is briefly discussed. Full details plus processing options/examples can be found in *Rothacher & Mervart* [1996].

Transfer of Data

The Bernese software requires that the raw observation data is in the RINEX (Receiver Independent Exchange) format [*Gurtner et al.*, 1989; *Gurtner &Mader*, 1989]. The RINEX observation files are then converted to Bernese internal format (ie code/phase/header/observation files) by the program RXOBV3.

It should be noted that the software suite contains conversion programs for various receiver types eg TRRINEXO for Trimble receivers and ASRINEXO for Ashtech. Alternatively, independent external software may be used to convert raw GPS data in receiver format to RINEX.
NB All of the raw data from the PICMP campaigns were converted to RINEX using the *TEQC* program that was created by the UNAVCO facility in Colorado. *TEQC* can be used to check the raw data from each receiver for irregularities as well as the RINEX conversion.

Orbit Determination

Precise satellite orbits were obtained from Scripps for the 1993 campaign and then from the IGS for the 1996 and 1998 campaigns. The IGS are the preferred orbit but unfortunately were not in existence in 1993 and as a result the Scripps orbits were initially used for the processing. Eventually, the results of the PICMP93 processing were also brought into ITRF96 (as discussed in 4.2.3).
For each campaign these precise orbits are converted from the terrestrial to the celestial reference frame using the program PRETAB. This generates:

* *tabular orbit* files and
* *satellite clock* files for each satellite (determined by fitting precise orbit information with low degree polynomials) which are then used to compute satellite clock corrections for each observation epoch

The program ORBGEN generates *standard orbits* (ie source independent orbit representation files) from the satellite positions listed in the tabular orbit files. Each standard orbit consists of a standard satellite arc characterised by a start and end time and which is a solution of the equations of motion of the satellite.

Processing of Code Observations

The program CODCHK checks the code observations for outliers.
These observations are then used in the least squares program CODSPP to:

1. compute the clock corrections needed in order to synchronise the receiver clocks with GPS time and/or
2. estimate single point positions ie absolute coordinates of the receivers.

Single point positions of the GPS stations can be used as the *a priori* coordinates required in all subsequent programs. As previously mentioned the *a priori* coordinates should be as accurate as possible and so it would be preferable to use geodetic coordinates from a previous survey or from global tracking stations.

Processing of Phase Observations

The Bernese software uses double-differences as basic observables (using single-differences as the building blocks).

The phase single-differences are formed by the program SNGDIF after the receiver clock corrections, satellite clock and standard orbits have been generated. This involves forming baselines between pairs of receivers in order to eliminate errors in the satellite clocks. Single-differences are formed in such a way as to minimise baseline lengths and to maximise total data overlap.

Program MAUPRP then checks the single differenced phase observations for cycle-slips. MAUPRP uses the triple-difference observables (on L1, L2 or L3) and detects cycle-slips and where possible repairs or removes them. MAUPRP does not use code measurements.

The main parameter estimation programs GPSEST and ADDNEQ are the core of the processing engine. These programs may be used for baseline, session, or campaign processing. GPSEST allows the estimation of or use of many parameters such as station coordinates, receiver clocks, ambiguities, antenna phase centre variations, receiver antenna offsets, satellite antenna offsets, orbital elements, radiation pressure parameters, earth rotation parameters, earth's centre of mass, station specific tropospheric parameters, local troposphere models and ionosphere models.
For typical GPS campaigns, baselines are generated as well as the double-difference residuals. Once again an external program such as the UNAVCO graphical tool *GT* can be used to examine these residuals and if necessary mark and manually fix cycle slips or remove bad data.

After phase preprocessing, all baselines should be free of cycle-slips. GPSEST is used to a) attempt phase ambiguity resolution and b) to then combine the baselines to form daily network solutions.

Ambiguity Resolution Strategies

Phase ambiguities are resolved in the GPSEST program using the double-difference observables.
Ambiguities can be resolved either in baseline mode or in the session mode. According to *Rothacher & Mervart* [1996] it is more efficient to resolve the ambiguities in the baseline mode (ie processing each baseline separately) and then introducing them as known quantities into the subsequent processing of each session.
The optimal ambiguity resolution strategy is dependent on the phase data available (dual or single frequency), the length of the baseline and the GPS session duration.

If only **single frequency** (L1) data are processed then most ambiguities can be

resolved if the baselines are only short (ie < 15 km). The Bernese strategy for single frequency data would be to use double-differences employing:

a) the SEARCH algorithm (a fast ambiguity resolution approach) for short observational sessions or,
b) the SIGMA algorithm (an iterative least squares approach using rms ambiguity errors) for long sessions.

If **dual frequency** data are available then the options are:

1) For surveys with baselines < 10 km

⇒ where the ionospheric effects are similar at both ends it is possible to resolve ambiguities on L1 and L2 separately rather than using the relatively noisy L5 observable
⇒ site specific tropospheric delay parameters can be estimated every 2-6 hours
⇒ final site coordinates are then calculated as part of a final L3 solution.

NB This method is useful for processing sessions where faults in the receiver or antenna causes disruption to the L2 phase data.

2) Longer baselines (up to 2000 km)

⇒ fix coordinates to those obtained from the L3 float solution
⇒ then attempt to resolve ambiguities simultaneously on L1 and L2 using the Quasi Ionosphere Free (QIF) method for long sessions/arbitrary baseline length **OR** the SEARCH algorithm for short sessions/short baselines
⇒ final site coordinates are then calculated as part of a final L3 solution introducing these resolved ambiguities, pre-eliminating others and solving for site specific tropospheric delay parameters (2-6 hours)

3) Wide-lane /Narrow-lane Ambiguity Fixing
(NB This is the strategy used for all PICMP processing)

⇒ initially enhanced *a priori* coordinates are obtained from the daily ionosphere-free (L3) float network-solutions (NB "float" means that there is no attempt to resolve the ambiguity parameters)

⇒ calculate an ionosphere model (estimated by program IONEST using the geometry-free L4 observable)

⇒ this model is then introduced into the wide-lane (L5) ambiguity resolution process holding all stations fixed at their best available coordinates ie resolving as many L5 ambiguities as possible to integers

⇒ final site coordinates are then calculated as part of a final L3 solution introducing resolved L5 ambiguities, solving for the narrow-lane (L1) ambiguities and solving for site specific tropospheric delay parameters (2-6 hours)

NB L2 ambiguities are automatically resolved whenever both of the corresponding L5 and L1 ambiguities are resolved.

Final Campaign Solution

The Bernese GPS software V4.0 has two programs that can be used to combine solutions:

1. COMPAR - based only on the variance-covariance information of the processed coordinates ie GPSEST. It is used to compare different coordinate sets (eg individual daily solutions or daily network solutions) but does not allow additional Helmert transformations between data sets. There is no flexibility to change constraints, to change geodetic datums or to combine data sets which are weighted differently.

   The program is useful to study coordinate repeatabilities (geocentric/geodetic coordinates) and baseline results. Final results include the weighted and unweighted rms values of the combinations.

2. ADDNEQ - based on normal equations and capable of handling all types of unknowns. ADDNEQ is more flexible than COMPAR and should be used when a statistically correct combination is required eg to compute multi-session solutions from the combination of a set of single-session solutions [*Rothacher and Mervart*, 1996]. The program can handle different parameter types/input which are identical to GPSEST (eg coordinates, troposphere, orbits, centre of mass etc). The features that are unique to ADDNEQ are:

    * velocity estimation of sites over long time span observations
    * creation of Software Independent Exchange format (SINEX) files
    * free network solutions (including transformations etc)
    * specialised long-arc orbit computations
    * special earth rotational parameter calculations

The output results from ADDNEQ are usually in terms of:

- *combined solution for station coordinates* -(similar to GPSEST results) showing coordinate estimates plus the rms of residuals, 3D and 2D error ellipses
- *mean values of geocentric coordinates (XYZ)* -summary of coordinate estimates plus formal and weighted rms values
- *comparison of station coordinates* - compares each individual solution with the combined solution ie displays the unweighted rms values of residuals (also weighted rms if appropriate)
- *comparison of baseline lengths* - baseline statistics showing residuals in ϕ, λ, h and length
- *outlier detection*

It should be note that the formal rms values obtained from the network solutions do not necessarily give a true estimate of the actual errors. Oversampling during campaign observations (eg 15-30 seconds intervals for 24 hours) creates processed phase data that are not truly independent ie introduces unmodelled correlation effects.

Therefore, error estimates output from the GPS processing package are usually scaled to account for these unmodelled errors. The scaling factor is derived from the

repeatability of daily coordinate estimates of a campaign using network adjustment software.

4.1.3 Bernese V4.0 Processing Procedures for the PICMP Campaigns.

The PICMP 1993, 1996 and 1998 data were processed using the Bernese V4.0 software and the same basic procedures was used for each campaign.
The key procedures are:

- Precise orbits were downloaded and used ie SIO for 1993 and IGS for 1996 and 1998.
- The use of IGS_01 elevation dependent antenna phase centre models.
- SATELLIT.TTT files were used to model each satellite antenna phase centre.
- Single-differences were formed using a strategy that minimised baseline lengths.
- Phase data were processed at 30 second intervals until the completion of the MAUPRP program and then decimated to a 120 second epoch in order to increase the speed of processing and to reduce the oversampling correlations.
- The UNAVCO graphical program, GT, was occasionally used to visually check double-differenced phase residuals for cycle slips. In some cases cycle slips were repaired and noisy data deleted.
- Double-differenced phase ambiguities were estimated at both the L1 and L2 frequencies. Ambiguities were resolved to integer values using the wide-lane/narrow-lane strategy.
- Ionospheric models were estimated to assist with ambiguity resolution.
- Tropospheric delay parameters estimates were made every 2 hours.
- Coordinate and covariance files are produced from network solutions of each GPS session using program GPSEST.
- These are then combined using the ADDNEQ program to obtain final coordinates, comparisons and statistics for each campaign.

4.2 PICMP 1993, 1996 and 1998

4.2.1 GPS Observations.

The April 1993 (PICMP93) campaign comprised two phases. The first consisted of a GPS survey of ten PGNet stations distributed nationwide designed:

(1) to provide a base network for future national deformation studies, and
(2) to enable the PGNet single-frequency survey to be adjusted onto a high precision backbone and thus to improve its accuracy.

The second phase was a regional survey of 15 PGNet sites in Luzon. Of these stations, 10 had been observed in the 1990 post-earthquake survey and were included to monitor postseismic and eventually interseismic deformation.
The 1993 measurements used dual-frequency squaring receivers (Trimble 4000SST) and 12-hour measurement sessions.
The Luzon network was partially resurveyed in May 1996 (PICMP96) and May 1998 (PICMP98) using full-wavelength dual-frequency receivers with between one and six 24-hour sessions at each station.
The number of sessions observed during each of the PICMP campaigns is shown in Table 4.1.

4.2.2 GPS Processing

The 1993, 1996 and 1998 data were processed using the Bernese V4.0 software and the standard techniques based on the double-difference phase observable, including atmospheric modelling, and fixing wide-lane and narrow-lane double difference ambiguities to integers where possible.
It should be noted that the error estimates output from the Bernese GPS processing were scaled by a factor of six (6) to account for unmodelled correlations between the successive 120-second GPS phase samples used in the last stage of the analysis. This factor of 6 was derived from the repeatability of daily coordinate estimates within each survey, using the geodetic network adjustment software ADJCOORD [*Bibby*, 1982; *Crook*, 1992] and does not account for longer term correlations likely to be

present in the GPS data [eg *Zhang et al.*, 1997]. Outliers in the coordinate estimates were also identified during this step.

A summary of the GPS processing for each of the PICMP campaigns follows.

NAMRIA STATION	GPS ID	PICMP93	PICMP96	PICMP98
ABY03	**ABY3**	12	4	-
ABY03 RM 4	**ABX3**	-	-	1
ARA01	**ARA1**	2	-	-
MAGNETICS 1995 BALER	**ARX1**	-	1	2
BLN04	**BLN4**	3	3	1
CGY08	**CGY8**	12	6	2
CTN01	**CTN1**	6	-	-
IFG01	**IFG1**	5	2	2
ILN01	**ILN1**	6	-	-
ILO01	**ILO1**	6	-	-
LUN01	**LUN1**	5	2	2
LYT08	**LYT8**	5	-	-
MMA01	**MMA1**	2	6	2
MMA08	**MANL**	-	6	15
MRQ01	**MRQ1**	6	-	4
NEJ43	**NE43**	3	-	-
NEJ44	**NE44**	2	3	3
NVY01	**NVY1**	3	2	-
NVY03	**NVY3**	1	-	-
NVY03 (mark moved between '93 & '96)	**NVX3**	-	2	-
NVY03 RM 3	**NVE3**	-	-	2
NVY04	**NVY4**	2	4	2
PLW11	**PL11**	5	-	-
PMG01 (mark moved between '90 & '93)	**PMX1**	2	4	2
PNG03	**PNG3**	-	-	1
PNG05	**PNG5**	12	6	2
QZN03 RM 2	**QZE3**	-	-	3
QZN05	**QZN5**	2	-	-
QZN07	**QZN7**	-	2	2
TRC02 RM 1	**TRE2**	-	3	2
ZGS02	**ZGS2**	6	-	-

IGS Station and DOMES Number		PICMP93	PICMP96	PICMP98
GUAM	50501M002		6	15
SHAO	21605M002	-	6	12
TAEJ	23902M001	-	4	14
TAIW	23601M001	11	6	-
TIDB	50103M108	11	6	15
USUD	21729S007	5	6	15
YAR1	50107M004	9	5	14

Table 4.1 Numbers of sessions observed during each GPS campaign. Session lengths were 12 hours in 1993 and 24 hours in 1996 and 1998. The DOMES number is a unique identifier for space-geodetic monuments, maintained by the International Earth Rotation Service (IERS).

Step	Program	Description of Process
001	*RXOBV3*	RINEX translation
002	*SATCLK*	Creates clock file
003	*PRETAB*	Creates tabular orbit file
004	*ORBGEN*	Creates standard orbit file
005	*CODCHK*	Checks code observations
006	*CODSPP*	Writes clock correction to phase file
007	*SNGDIF*	Creates single difference file. Uses pre-defined baseline files baseline files
008	*MAUPRP*	Corrects cycle slips
009	*GPSEST*	Uses the ionosphere free data combination to calculate point positions. Ambiguities are not resolved.
010	*GPSEST*	Ionosphere modelled using the L4 data combination. Points are held fixed at those found in previous run of GPSEST
011	*GPSEST*	Solves for L5 integer ambiguities. Points are held fixed to those found in the first run of GPSEST.
012	*GPSEST*	The point position are calculated and the L1/L2 integer ambiguities resolved by introducing the L5 integer ambiguities
013	*GPSEST*	The Normal equations (NEQs) and covariance matrices are written.
014	*ADDNEQ*	All baseline NEQs are then combined from Step 13 to get one NEQ solution. Final coordinates, comparisons and statistics are also obtained for each campaign.

Table 4.2 Bernese GPS processing routine adopted for the PICMP93, 96,98 campaigns.

Daily sessions are processed automatically using Steps 1-13 to obtain NEQs and covariances for daily baselines. A single campaign solution is then obtained by combining the NEQ files (from Step 13) using the ADDNEQ program (Step 14) ie one NEQ solution plus final coordinates, comparisons and statistics.

Each campaign result can then be compared to investigate velocities eg PICMP 93-96 and PICMP 96-98.

PICMP93

Survey

- The data were collected between day 107-119 of 1993 by NAMRIA staff under the direction of Silcock (UniSA) and Beavan (LDEO).

Equipment

- Receivers: TRIMBLE 4000SST
- Antennas: Trimble geodetic (SST)

- Observation Session - most sessions began at 21:30 UT and ran for 12 hours at 15 sec sampling. It was attempted to introduce data from regional stations (e.g., TAIW, USUD, see Table 4.1) to improve reference frame definition, but without much success.
- Orbits - Scripps Institute of Oceanography (SIO) reprocessed orbits in the ITRF93 reference frame were used.
- Pole file - IGSFINAL.ERP (April 1999), but with the values corresponding to the SIO orbits included over the period of the campaign.
- Phase Eccentricity file - PHAS_IGS.01 (obtained April 1999)
- Single difference files - Single difference files were created such that the number of observations were maximised while keeping the baselines as short as possible, and ensuring that poorer quality stations are used on only one baseline.
- Constrained Coordinates - PNG5 was constrained throughout the processing, at a value determined from a one-day analysis using several regional IGS stations (e.g., TAIW, TIDB see Table 4.1). This value is very close to a value determined later by fitting a velocity to all the 1993-96-98 data and propagating the 1998 coordinates back to 1993 using this velocity.
- Data rate - Initial runs (up to and including MAUPRP) were made at 15 or 30 second interval while succeeding runs were made at 120 second interval.
- Troposphere - The troposphere parameters were estimated at 120 minute intervals at each station.
- Processing procedure

  - The daily sessions of GPS data were processed automatically, then Normal Equations (NEQs) and covariance matrices obtained using Steps 1-13 of the Bernese process control routine shown in Table 4.2.
  - To obtain a single campaign result, the entire daily baseline NEQs were

combined to get one NEQ solution using program ADDNEQ (Step 14 shown in Table 4.2). Final campaign coordinates, station comparisons and statistics are obtained.

PICMP96

Survey

- Data collected between days 137 and 142 of 1996 by PHIVOLCS, NAMRIA and Lamont and Indiana University staff.

Equipment

- Receivers: TRIMBLE 4000SSE
- Antennas: Mixture of Trimble geodetic and compact/ground-plane.

Data Processing

- Observation Session - Sessions generally began at 00:00 UT and ran for 24 hours at 30 sec sampling. Data from regional stations were introduced to help define the reference frame.
- Orbits - IGS orbits in the ITRF96 reference frame were used. The original ITRF94) orbits and polar motion were transformed to ITRF96 using global average parameters derived by *Kouba and Mireault* [1997]. The orbit files contain the satellite clock corrections.
- Pole file - IGSFINAL.ERP (obtained April 1999).
- Phase Eccentricity file - PHAS_IGS.01 (obtained April 1999).
- Single difference files - Single difference files were created such that the number of observations were maximised while keeping the baselines as short as possible, and ensuring that poorer quality stations are used on only one baseline.
- Constrained Coordinates - The following regional stations were constrained to 5 mm rms in each component: TAIW, USUD, TIDB, GUAM, TAEJ and YAR1 (see Table 4.1).

- Data rate - Initial runs (up to and including MAUPRP) were made at 30 second interval while succeeding runs were made at 120 second interval.
- Troposphere - The troposphere parameters were estimated at 120 minute intervals at each station.
- Processing procedure

  - The daily sessions of GPS data were processed automatically, then Normal Equations (NEQs) and covariance matrices obtained using Steps 1-13 of the Bernese process control routine shown in Table 4.2.
  - To obtain a single campaign result, the entire daily baseline NEQs were combined to get one NEQ solution using program ADDNEQ (Step 14 shown in Table 4.2). Final campaign coordinates, station comparisons and statistics are obtained.

PICMP98

Survey

- Data collected during 19 days between days 141 and 172 of 1998 by PHIVOLCS, NAMRIA and Indiana University staff.

Equipment

- Receivers: TRIMBLE 4000SSi
- Antennas: Trimble Dorne-Margolin/choke-ring antennas

Data Processing

- Observation Session - Sessions generally began at 00:00 UT and ran for 24 hours at 30 sec sampling. Data from regional stations were introduced to help define the reference frame.
- Orbits - IGS orbits in the ITRF96 reference frame were used. These orbit files contain the satellite clock corrections.
- Pole file - IGSFINAL.ERP (obtained April 1999)

- Phase Eccentricity file - PHAS_IGS.01 (obtained April 1999)
- Single difference files - Single difference files were created such that the number of observations were maximised while keeping the baselines as short as possible, and ensuring that poorer quality stations are used on only one baseline.
- Constrained Coordinates - On most days, the following regional stations were constrained to 5 mm rms in each component: TAIW, USUD, TIDB, GUAM, TAEJ, and YAR1 (see Table 4.1).
- Data rate - Initial runs (up to and including MAUPRP) were made at 30 second interval while succeeding runs were made at 120 second interval.
- Troposphere - The troposphere parameters were estimated at 120 minute intervals at each station.
- Processing procedure

  - The daily sessions of GPS data were processed automatically, then Normal Equations (NEQs) and covariance matrices obtained using Steps 1-13 of the Bernese process control routine shown in Table 4.2.
  - To obtain a single campaign result, the entire daily baseline NEQs were combined to get one NEQ solution using program ADDNEQ (Step 14 shown in Table 4.2). Final campaign coordinates, station comparisons and statistics are obtained.

4.2.3 Establishing ITRF96 for the PICMP Campaigns

IGS ITRF96 orbits were used for the 1996 and 1998 analysis, and Scripps Institution of Oceanography (SIO) reprocessed ITRF93 orbits for 1993. It was necessary to convert the original IGS ITRF94 orbits for the 1996 data to ITRF96 using the global-average parameters derived by *Kouba and Mireault* [1997]. However the *Kouba and Mireault* parameters were not used to convert SIO ITRF93 orbits to ITRF96 because it is uncertain whether the IGS and SIO implementations of ITRF93 are consistent. Regional IGS stations (see Figure 4.2 and Table 4.1) were added to the 1996 and 1998 processing so that the results could be formally tied into the ITRF96 reference frame.

It was also attempted to use regional IGS stations TAIW, USUD, TIDB and YAR1 for the 1993 processing but it was not possible to solve these long baselines sufficiently accurately to improve the reference frame definition.

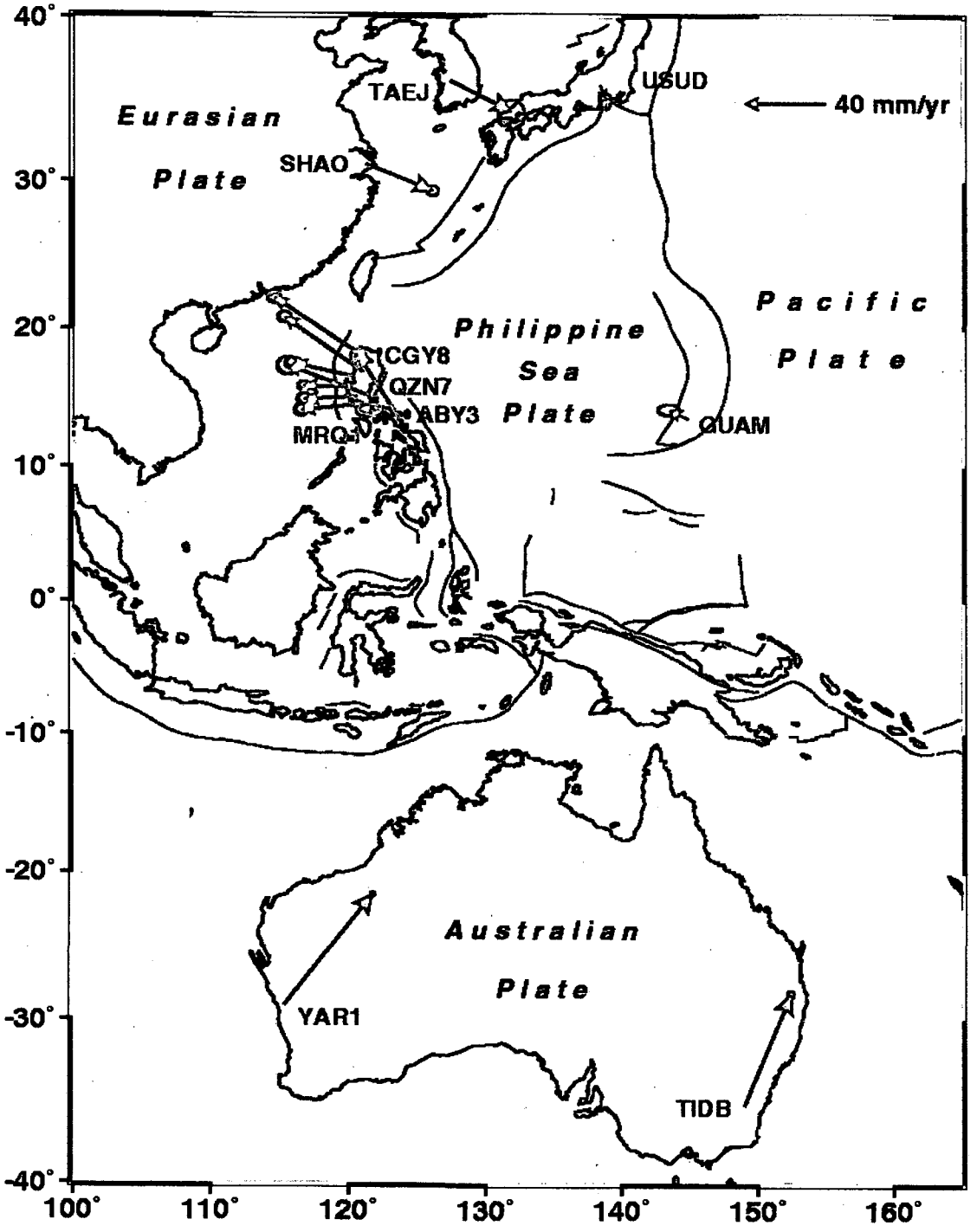

Figure 4.2 Velocities in the ITRF96 reference frame of the IGS stations were used to define the reference frame (blue arrows), plus the velocities in this frame of a selection of the PICMP stations (red arrows).

In Chapter 6 it will be shown that the velocities of stations in the Philippines, even those in the 1990 earthquake zone, do not change significantly between 1993-96 and 1996-98. Therefore a *least-squares combination* program VELFRAME was used (with full covariance propagation) to estimate the ITRF96 coordinates and velocities of all stations observed during more than one epoch (shown in Figures 4.2). VELFRAME (a least squares velocity fitting program) was written by Dr J. Haines of Cambridge University.

This adopted method:

(1) held the IGS stations (see Table 4.1) to their ITRF96 coordinates and velocities [*IGS*, 1998] within their assigned errors,

(2) allowed a 7-parameter transformation of each day's coordinate/covariance results to best fit the reference frame definition, and

(3) assumed that the velocities of other stations are constant (or slowly varying with a time-constant of tens of years) within the uncertainties of the daily coordinate estimates.

By using this procedure, the stations measured only in 1993 were put strictly into the ITRF96 reference frame, even though the 1993 analysis used ITRF93 orbits and no regional IGS stations were incorporated in that analysis. This was possible because:

- both the 1996 and 1998 coordinates were in the same reference frame, and
- sufficient stations were measured in each of 1993, 1996 and 1998 that this reference frame can be propagated back into the 1993 data (assuming constant velocities at the stations that appear in all three data sets).

Therefore all three PICMP campaigns are in a consistent reference frame and thus can be compared. Table 4.3 gives the ITRF96 coordinates of the 1993 stations, which were used to transform the PGNet into ITRF96 (See Chapter 5).

Coordinates are obtained by propagating final coordinates and velocities from 1993-96-98 VELFRAME run back to April 1993.

Coordinate errors are taken from the VELFRAME run just after the end of the 1993 processing, and have been scaled by • (1.212), where 1.212 was the variance parameter at the time.

Name	Latitude (North)			Longitude (East)			Height	σ_N	σ_E	σ_U
	°	'	"	°	'	"	m	mm	mm	mm
ABY3	13	28	36.03044	123	40	33.32067	161.740	7.5	7.8	13.9
ARA1	15	45	25.80087	121	33	47.22259	47.517	7.7	8.7	27.2
BLN4	15	11	23.95888	121	2	39.55035	119.516	7.5	7.9	22.6
CGY8	17	37	2.56789	121	43	35.42473	82.055	7.4	7.7	13.5
CTN1	7	0	44.44612	125	5	30.85745	367.189	10.2	18.4	22.0
IFG1	16	55	14.10929	121	3	5.53716	1406.975	7.4	7.8	18.7
ILN1	18	23	41.34389	120	35	49.04971	41.120	8.8	11.2	16.5
ILO1	10	42	36.55294	122	33	53.57658	84.001	9.5	14.5	17.8
LUN1	16	34	57.20362	120	18	15.94163	84.091	7.4	7.7	18.5
LYT8	11	15	4.95018	125	0	19.32520	88.229	9.4	15.7	21.1
MMA1	14	32	13.81754	121	2	23.13336	69.384	8.5	9.0	33.2
MRQ1	13	33	36.03296	121	52	7.98220	319.029	8.9	12.2	16.2
NE43	15	56	27.23615	121	2	40.41242	437.455	7.5	8.3	24.2
NE44	15	29	29.58224	120	58	10.44346	100.567	7.7	8.1	24.2
NVY1	16	30	8.20378	121	6	45.50527	419.280	7.6	8.0	22.1
NVY3	16	7	59.15221	120	55	48.05075	979.027	8.1	8.9	32.6
NVY4	16	9	31.58059	120	54	26.86845	1141.612	7.6	8.1	25.3
PL11	9	42	27.86143	118	42	51.58254	55.774	9.6	13.8	20.0
PMX1	15	8	24.80350	120	37	59.56880	107.116	7.8	8.4	26.1
PNG5	15	52	3.65030	120	15	13.27447	139.874	7.2	7.4	7.6
QZN5	14	39	54.06837	121	36	19.15216	47.643	7.9	8.6	27.9
ZGS2	6	55	21.09463	122	4	8.81316	77.155	10.0	16.7	20.7

Table 4.3 PICMP93 coordinates in ITRF96 reference frame, epoch 1993 April 22. (Coordinates are obtained by propagating back to April 1993 the final coordinates and velocities from the least-squares combination of the 1993-96-98 PICMP data).

Table 4.4 gives the final ITRF96 coordinates of the PICMP96 stations and Table 4.5 the final ITRF96 coordinates of the PICMP98 stations. Appendices 1, 2 and 3 give an extract of the final coordinate residuals from the ADDNEQ Bernese output for the PICMP 93, 96 and 98 campaigns respectively.

In Chapter 6, the ITRF96 velocities of all stations observed in more than two epochs are shown. Also the determination of the Euler vector for using this data

PICMP96 APRIL'99 PROCESSING WITH IGS STATIONS 01-MAY-99 17:13

LOCAL GEODETIC DATUM: ITRF96 EPOCH: 1996-05-16 23:59:45

NUM	Station Name	X (M)	Y (M)	Z (M)
1	ABY3	-3439974.1392	5162722.4957	1476777.2034
3	BLN4	-3175082.8905	5274978.8200	1660428.2207
4	CGY8	-3197753.6962	5172251.0847	1918090.9213
6	IFG1	-3149063.9618	5230260.3371	1844836.5543
9	LUN1	-3085400.0515	5279092.9358	1808629.9741
11	MMA1	-3184192.3095	5291065.9427	1590599.1577
12	MANL	-3177118.4101	5293321.8456	1597133.1710
15	NE44	-3163645.9249	5271531.4980	1692603.2385
16	NVY1	-3161030.3785	5237487.4177	1800208.9822
18	NVY4	-3148101.5543	5258540.0585	1763928.0688
20	PMG1	-3137880.6450	5298853.7265	1655110.0822
21	PNG5	-3091887.4765	5300963.2677	1732686.5988
26	QZN7	-3208785.2846	5253747.9612	1662667.7498
27	TAIW 23601M001	-3024781.9458	4928936.8685	2681234.4419
28	USUD 21729S007	-3855262.9654	3427432.5346	3741020.3333
30	TIDB 50103M108	-4460996.1358	2682557.0831	-3674443.7733
31	GUAM 50501M002	-5071312.8124	3568363.5346	1488904.2897
35	NVX3	-3150497.9354	5257844.3822	1761151.6602
36	ARX1	-3213885.0183	5231702.4877	1720905.5356
37	TRE2	-3116046.4608	5305708.6836	1674673.8567
38	SHAO 21605M002	-2831733.2205	4675666.0772	3275369.4985
39	TAEJ 23902M001	-3120422.8759	4086355.4829	3761769.5942
40	YAR1 50107M004	-2389025.5285	5043316.8674	-3078530.8096

Table 4.4 ITRF96 coordinates of the PICMP96 campaign from the Bernese GPS Version 4.0 Software using IGS stations (NB the original ITRF94 orbits for the 1996 data were converted to ITRF96 using global-average parameters derived by *Kouba and Mireault* [1997]).

PICMP98 APRIL'99 PROCESSING WITH IGS STATIONS (ITRF96 IGS Orbits)-MAY-99
LOCAL GEODETIC DATUM: ITRF96 EPOCH: 1996-05-16 23:59:45

NUM	Station Name	X (M)	Y (M)	Z (M)
3	BLN4	-3175082.8404	5274978.8142	1660428.2143
4	CGY8	-3197753.6340	5172251.0982	1918090.9879
6	IFG1	-3149063.9086	5230260.3384	1844836.6024
12	MANL	-3177118.3415	5293321.7850	1597133.1459
13	MRQ1	-3274407.3791	5266929.0812	1485778.4615
15	NE44	-3163645.8881	5271531.4767	1692603.2335
18	NVY4	-3148101.5165	5258540.0660	1763928.1075
21	PNG5	-3091887.4633	5300963.2659	1732686.6040
26	QZN7	-3208785.2448	5253747.9854	1662667.7832
28	USUD 21729S007	-3855263.0055	3427432.5381	3741020.3331
30	TIDB 50103M108	-4460996.2525	2682557.1044	-3674443.6695
31	GUAM 50501M002	-5071312.7964	3568363.5179	1488904.2949
37	TRE2	-3116046.4518	5305708.7238	1674673.8676
38	ZBS3	-3062287.8067	5320172.7810	1726061.1118
39	CASP	-3101294.4235	5327157.7932	1633148.9535
40	DAUP	-3132573.1343	5300872.5351	1658832.6285
41	DIZP	-3110744.6700	5320758.5172	1636458.3383
42	GUMP	-3125510.6358	5311601.4063	1637568.2124
43	LODP	-3123723.3546	5299409.1774	1679948.4534
44	MACP	-3124235.4198	5305540.6461	1660249.5165
45	NABP	-3122720.9151	5311994.8892	1642442.8450
46	UODP	-3112859.6212	5308496.0565	1671899.5117
47	ZBS9	-3086604.3483	5332455.0511	1643419.2018
48	ALAT	-3185461.0864	5307063.6263	1534073.2343
49	BIGT	-3189051.5722	5304122.0829	1536758.2737
50	MCLT	-3187184.0956	5306004.4139	1534146.9073
51	PRPT	-3188942.9043	5303923.2405	1537692.8282
52	BUAN	-3439450.7543	5168328.3216	1458974.6723
53	PNG3	-3075374.5534	5303613.3194	1753482.3973
54	QZE3	-3248981.9152	5238686.9988	1632131.2987
55	BALT	-3197694.2531	5299481.5519	1535068.8022
56	PNKT	-3186808.5491	5305558.1208	1536521.4813
57	SALT	-3186770.4361	5307049.5867	1531545.6019
58	TBGT	-3187768.3258	5304902.2292	1536722.6329
59	TGYT	-3181411.9353	5307495.1495	1543636.5725
60	TLY2	-3188771.1196	5302405.8663	1543265.6836
61	BLG4	-3183307.9194	5308689.8333	1533067.8101
62	CALT	-3189360.3323	5304966.1182	1533329.8570
63	CAPT	-3189210.5758	5305288.4444	1532427.7283
64	CCA5	-3194157.4499	5305606.7607	1522197.4650
65	KAYT	-3186179.6325	5307362.7745	1531588.1073
66	MTBT	-3186177.7756	5307071.5590	1532741.7875
67	PINT	-3189372.7453	5304678.7484	1534542.6527
68	TVST	-3187757.3971	5304935.3450	1536648.4718
81	NVE3	-3150498.3870	5257845.6235	1761146.2922
82	TRCP	-3115707.6823	5305843.9724	1674786.4385
84	SHAO 21605M002	-2831733.3152	4675666.0419	3275369.4797
85	TAEJ 23902M001	-3120422.9620	4086355.4471	3761769.5771
86	YAR1 50107M004	-2389025.6547	5043316.8825	-3078530.6844

Table 4.5 Final Bernese ITRF96 coordinates of the PICMP98 campaign.

5.0 Readjustment of PGNet using PICMP93 Results

5.1 Introduction

The rationale for the readjustment of the PGNet onto the PICMP93 (ITRF96) fiducials is to improve its accuracy to approximately 1 ppm (if possible) primarily for its potential in response surveys and resurveys of future large earthquakes in the Philippines. This readjusted network, the PGNet (ITRF96), can be useful for earthquake response surveys at the 20-30 cm accuracy if the ground marks remain stable and undisturbed. With the passage of time, the errors in the PGNet (ITRF96) network become smaller relative to the regional deformations that have accumulated since 1990. Therefore, the PGNet (ITRF96) may become valuable for regional deformation studies but not for at least 40 years since 5mm/year accuracy is the minimum that would be useful and there are 20-30 cm errors within the PGNet.

The GPS data of the PGNet were primarily single frequency phase measurements without tight control at long wavelengths and the baseline processing was not as rigorous as that for crustal motion research (Chapter 2). However, the PICMP93 (with an overall rms precision of about 0.03 ppm) had dual frequency phase measurements and baselines were processed to a very high precision (Chapter 4).
Using the Bernese V4.0 program HELMR1, seven Helmert transformation parameters are computed for the PGNet to PICMP93 (ITRF96) conversion. The scale factor parameter determined $\cong$ -3.1 ppm (see section 5.2) and this highlights a possible scale bias where the PGNet has suffered a substantial systematic "contraction". This is also confirmed by comparing the 1990 post-earthquake observations with the PICMP93 fault zone survey (NB this includes reprocessing some of the raw GPS post-earthquake data using the commercial package GPSurvey [Trimble]).
The nature of this $\cong$ -3.1 ppm scale bias is investigated and particular attention is given to the cause of this error within the PGNet. Ionosphere variations during the 1989-91 PGNet GPS survey are examined over the Philippine region using data available from the National Space Science Data Center (NSSDC)
It is determined that everything is consistent with the scale error being caused by the ionospheric effects on the single frequency GPS signals which were exacerbated by

the sunspot activity in late 1989 and 1990 during the solar maximum of Sunspot Cycle 22. It is uncertain what effects were caused by the significant changes to the GPS constellation during the 1989-91 survey (Chapter 2).

A piece-meal readjustment of the PGNet (e.g. Northern, Central and Southern Philippines) was considered. This would have required the reanalysis of all of the original PGNet data including some sort of ionospheric modelling for the single frequency GPS observations. Eventually, this was considered impractical due to:

- the vast quantity of data for the PGNet i.e. over 3000 disks
- the problem of lost data (original floppy disks) that had been destroyed, damaged or misplaced at the NAMRIA office in Manila (NB Disks were stored in boxes in an office area),
- the original work by Jones to process GPS baselines and to adjust the whole of the PGNet had been a very difficult and arduous one – over a period of 2-3 years (see Chapter 2), and
- finally, the complexities in determining individual baseline contractions due to the ionospheric effects (or even localised networks) during the PGNet

As are result of these issues, it was decided to take a national Helmert transformation approach.

The readjustment of the PGNet onto the PICMP93 fiducials was then carried out using the geodetic least-squares adjustment program NEWGAN (developed by Dr. J. S. Allman from Canadian Geodetic Survey programs GANET and HAVOC2) incorporating the seven transformation parameters determined. The adjustment results in the PGNet (ITRF96) geodetic coordinate set.

The analysis of the ionospheric effects justifies the adjustment of the PGNet onto the PICMP93 (ITRF96) fiducial framework. Verification of the adjustment is attempted by comparing baselines of the readjusted PGNet (in the central Luzon region) with the results from the PICMP93 Luzon survey. This requires both a judicious selection of baselines between sites of reliable stability and some knowledge of the postseismic deformation pattern associated with the earthquake.

The documentation of this adjustment has a significant historical importance with respect to the tectonics of the Philippine Islands.

5.2 Comparison of the PGNet and the PICMP93 (ITRF96)

The PGNet WGS84 Adjustment

A copy of the original PGNet consolidated Primary Network Adjustment File (*Primary Network 2.6*) was supplied by Jones (see Chapter 2). This file comprised:

- the TRIMVEC baseline vectors for the post 1990 earthquake observations and other areas near Palawan and Manila, plus
- the BATCH_PHASER baseline vectors for the remainder of the country

Other files made available included the final WGS84 coordinates of the PGNet and the pre and post 1990-earthquake baseline vectors. It should be noted that the coordinates published in the Philippine Geodetic Manual are based on the Philippine Reference System 1992 (PRS92) and not WGS84.
The program NEWGAN was then used to reproduce the final network adjustment of the PGNet in the WGS84 datum defined by the NRMDP. The coordinates obtained were entirely consistent with the final PGNet WGS84 results. The reasons for this reproduction of the 1991 adjustment were:

1. to become familiar with the NEWGAN software so that further adjustments could be carried out of the PGNet and also the pre/post earthquake observations, and
2. to ensure that the correct data set of the PGNet baseline vectors was used

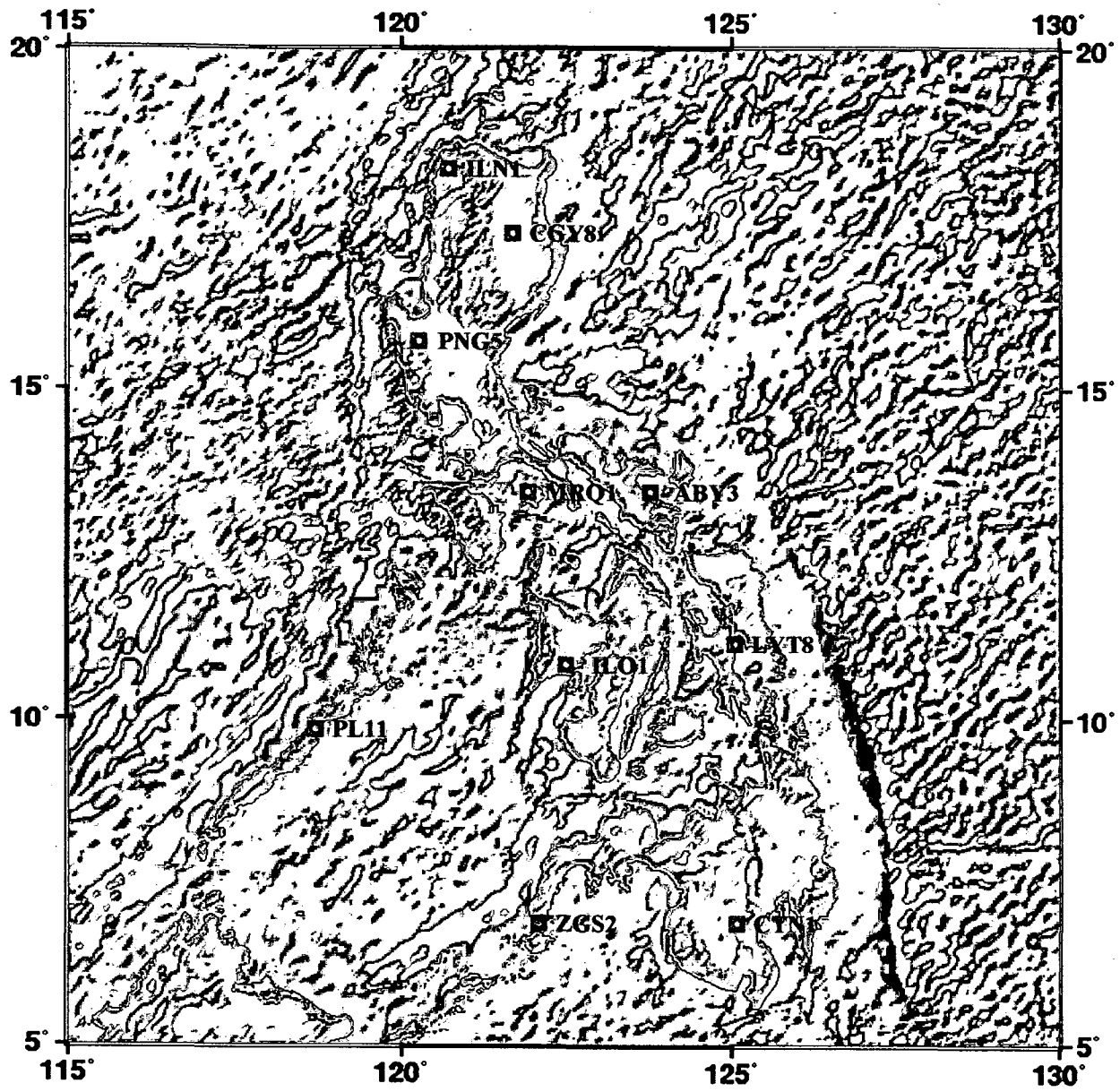

Figure 5.1 The PICMP93 (ITRF96) fiducial sites used for the readjustment of the PGNet

Helmert Transformation

LOCAL GEODETIC DATUM: WGS84 EPOCH: 1993- 4-22 12:00:00

Station Name	X (m)	Y (m)	Z (m)
ABY3	-3439974.2638	5162722.5001	1476777.1253
ARA1	-3213914.8883	5231687.1719	1720894.9481
ARX1	-3213885.1498	5231702.3931	1720905.4564
BLN4	-3175083.0489	5274978.7925	1660428.2494
CGY8	-3197753.8992	5172251.0586	1918090.8546
CTN1	-3639688.4612	5180308.4882	773534.2194
IFG1	-3149064.1107	5230260.2848	1844836.4839
ILN1	-3081613.0864	5211354.5665	1999911.2662
ILO1	-3373689.9827	5282422.4323	1177534.5051
LUN1	-3085400.1825	5279092.9187	1808629.9779
LYT8	-3589024.8887	5124636.7762	1236306.7814
MANL	-3177118.5803	5293321.8877	1597133.2261
MMA1	-3184192.4461	5291065.9260	1590599.1755
MRQ1	-3274407.4421	5266929.1465	1485778.4610
NE43	-3163764.1234	5256124.1817	1740560.5414
NE44	-3163646.0772	5271531.5041	1692603.2745
NVE3	-3150498.5268	5257845.5256	1761146.2445
NVX3	-3150498.0902	5257844.3050	1761151.6824
NVY1	-3161030.5547	5237487.4091	1800208.9051
NVY4	-3148101.7061	5258540.0404	1763928.0377
PL11	-3020765.1030	5514266.1096	1068408.8552
PMG1	-3137880.7817	5298853.7357	1655110.1160
PNG5	-3091887.5858	5300963.2371	1732686.6170
QZE3	-3248981.9044	5238686.9517	1632131.4245
QZN5	-3234384.2117	5256322.8453	1604282.6399
QZN7	-3208785.4278	5253747.9020	1662667.7200
TRCP	-3115707.5515	5305844.0460	1674786.4162
TRE2	-3116046.5633	5305708.6003	1674673.8718
ZGS2	-3361937.1842	5365810.2730	763638.8131

Table 5.1 Final ITRF96 Cartesian Coordinates of the PICMP93. (Converted from those presented in Table 4.3)

The next step was to compare the PICMP93 (ITRF96) coordinates for the ten (10) fiducial sites (as shown in Figure 5.1) with the corresponding stations of the PGNet WGS84 (see Table 5.2 for the geographical coordinates from the NEWGAN software and Table 5.3 for these converted to cartesian coordinates).

Station Name	Latitude			Longitude			Ellipsoidal Height (m)
	°	'	"	°	'	"	
ABY3	13	28	35.90103 N	123	40	33.28848 E	161.789
CGY8	17	37	02.37536 N	121	43	35.38491 E	84.335
CTN1	7	00	44.39289 N	125	05	30.85211 E	365.205
ILN1	18	23	41.13485 N	120	35	49.02541 E	44.086
ILO1	10	42	36.46780 N	122	33	53.59304 E	83.433
MRQ1	13	33	35.89849 N	121	52	07.97811 E	319.740
PNG5	15	52	03.48353 N	120	15	13.27588 E	141.744
ZGS2	6	55	21.02390 N	122	04	08.83333 E	77.239
LYT8	11	15	04.87253 N	125	00	19.31458 E	86.797
PL11	9	42	27.75802 N	118	42	51.64595 E	56.553

Table 5.2 WGS84 Geographical Coordinates of the PGNet Fiducials

30-NOV-93 15:21 LOCAL GEODETIC DATUM: WGS - 84

Station Name	X (m)	Y (m)	Z (m)
ABY3	-3439973.9970	5162723.8490	1476773.2690
CGY8	-3197754.9840	5172255.0490	1918085.9030
CTN1	-3639687.3080	5180307.1350	773532.3540
ILN1	-3081614.9360	5211359.0990	1999906.1030
ILO1	-3373690.3640	5282422.1030	1177531.8290
MRQ1	-3274408.2130	5266930.6230	1485774.6100
PNG5	-3091889.2330	5300965.9810	1732682.1970
ZGS2	-3361937.8910	5365810.2380	763636.6660
LYT8	-3589024.0850	5124636.1930	1236304.1620
PL11	-3020767.4230	5514266.3250	1068405.8550

Table 5.3 WGS84 Cartesian Coordinates of the PGNet Fiducials

The two cartesian coordinate solutions for the fiducials from Table 5.1 and 5.3 were then used with the Bernese V4.0 program HELMR1, to compute the seven Helmert transformation parameters for the PGNet to PICMP93 (ITRF96) conversion ie three translations, three rotations and a scale factor. The residuals for all common stations used and the transformation parameters derived are shown in Table 5.4.

HELMERT TRANSFORMATION

FILE 1: PGNet WGS84 Fiducial Coordinates
FILE 2: PICMP93 ITRF96 Fiducial Coordinates

TRANSFORMATION IN EQUATORIAL SYSTEM (X, Y, Z):
RESIDUALS IN LOCAL SYSTEM (NORTH, EAST, UP)

Num	Station	Flag	Residuals in Metres (m)		
			North	East	Up
6	**ABY3**	M.M	0.2073	0.2102	0.0907
1	**CGY8**	M M	0.2341	0.2264	-0.3810
8	**CTN1**	M M	0.2311	0.1661	-0.1874
2	**ILN1**	M M	0.1927	0.0341	-0.4464
3	**ILO1**	M M	-0.4224	-0.3251	0.4918
9	**LYT8**	M M	-0.3668	-0.4327	0.4405
5	**MRQ1**	M M	-0.0339	-0.0011	0.2118
10	**PL11**	M M	-0.1436	-0.2055	0.4929
7	**PNG5**	M M	-0.2147	-0.0283	0.2506
4	**ZGS2**	M M	0.3167	0.3597	-0.9635
	RMS		0.2727	0.2559	0.4833

NUMBER OF PARAMETERS: 7
NUMBER OF COORDINATES: 30
RMS OF TRANSFORMATION: 0.3823 metres
NUMBER OF ITERATIONS: 2

TRANSFORMATION PARAMETERS (PGNet to PICMP93):

TRANSLATION IN X: **-12.0431** ± 3.3338 m
TRANSLATION IN Y: **-27.3482** ± 2.5977 m
TRANSLATION IN Z: **-18.2150** ± 1.9265 m
ROTATION AROUND X-AXIS: **- 0 0 0.58761** ± 0.06581"
ROTATION AROUND Y-AXIS: **- 0 0 0.15441** ± 0.05460"
ROTATION AROUND Z-AXIS: **0 0 0.85912** ± 0.12385"
SCALE FACTOR: **3.091739** ± 0.254753 mm/KM

Table 5.4 Calculated Helmert Transformation (Bernese V4.0) between fiducial stations in PGNet WGS84 and in PICMP93 (ITRF96).

Comments

Therefore, the NEWGAN readjustment of the PGNet WGS84 observation set onto the ITRF96 required the use of the following additional input data:

1. the calculated seven Helmert transformation parameters as shown in Table 5.4, and
2. the PICMP93 (ITRF96) coordinates of the ten fiducial sites as tightly constrained stations in the adjustment.

It was initially considered that the justifications for incorporating the transformation and constrained coordinates included:

- the unknown errors introduced by the poor geometry of the GPS satellite constellations during the NRMDP,
- that there was a WGS84 datum definition problem created by the poor accuracy of the absolute positioning techniques of that time (see Chapter 2), and
- the known limitations of using mostly single frequency GPS receivers especially during a period of high solar activity.

The limitation of the WGS84 datum definition was well documented by Jones. Unfortunately, the errors introduced by poor satellite geometry could not be realistically estimated due to the large observation set and the changing nature of the constellations. The GPS data recorded during the survey stage (predominantly single frequency) and subsequently processed to form the PGNet was ***not*** modelled for these ionospheric disturbances. Consequently, final results of the PGNet have been substantially biased during this period of high solar activity. It was therefore necessary to try and quantify the ionospheric errors introduced into the PGNet WGS84 adjustment.

In Chapter 3 it was shown that for a geodetic network incorporating predominantly single-frequency data and in which the processing disregarded ionospheric refraction, then contraction (scale error) of the network can be expected [*Strang and*

Borre, 1997; *Rothacher and Mervart*, 1996; *Henson and Collier*, 1986; *Georgiadou and Kleusberg*, 1988; *Komjathy*, 1996, 2001]. Therefore, it was expected that the ionospheric delay error introduced into the PGNet would show a contacted scale bias when compared with the PICMP93 campaign ie the ionospheric refraction would cause the baselines of single frequency GPS to be shorter.

Table 5.4 shows that the PGNet is significantly contracted by a scale factor of ≅ 3.1 ± 0.3 ppm when compared with the PICMP93 fiducial coordinates.
This appeared to support the hypothesis that the whole of the PGNet had been affected by ionospheric delay during the NRMDP 1989-91.

It was therefore necessary to investigate the scale bias further to establish whether this was an acceptable value to estimate ionospheric delay effects on baselines.

5.3 PGNet and Unmodelled Ionospheric Errors

Scale Bias Analysis

The post earthquake data file supplied by Jones was processed with the NEWGAN software and a set of free net adjustment WGS84 coordinates was produced (see Appendix 6). Transformation parameters were computed between this coordinate set and the comparable PICMP93 (ITRF96) earthquake zone stations (from Table 5.1). The results and residuals of this Helmert Transformation (Bernese 4.1 software) are shown in Table 5.5.
The translations and rotations depicted may be ignored because they basically display the arbitrary nature of the free net adjustment coordinates of the post earthquake data. However, the resulting scale bias (**3.1** ± 0.7 ppm) once again depicts a contraction of the PGNet data when compared with the PICMP93 (ITRF96). This is very similar to the regional scale factor of **3.1** ± 0.3 ppm determined in Table 5.4.

HELMERT TRANSFORMATION

FILE 1: POST_EARTHQUAKE (Arbitrary WGS84) - Earthquake Zone Coordinates
FILE 2: PICMP93 ITRF96 - Earthquake Zone Coordinates

TRANSFORMATION IN EQUATORIAL SYSTEM (X, Y, Z):
RESIDUALS IN LOCAL SYSTEM (NORTH, EAST, UP)

Num	Station	Flag	Residuals in Metres (m)		
			North	East	Up
22	**ARA1**	M M	0.2442	0.0150	-0.1425
19	**BLN4**	M M	-0.1269	-0.1592	0.3193
15	**IFG1**	M M	0.1418	0.1006	0.0861
17	**LUN1**	M M	-0.1529	-0.0648	-0.2012
20	**NE43**	M M	0.1249	0.1187	0.0818
11	**NE44**	M M	-0.1646	0.0246	0.0533
14	**NVY1**	M M	0.1285	0.1585	-0.0484
21	**NVY4**	M M	0.0747	0.1347	0.0640
13	**PMG1**	Not	-0.3144	-0.9329	0.0004
7	**PNG5**	M M	-0.3690	0.0344	-0.0827
18	**QZN5**	M M	0.1453	-0.0865	-0.3751
25	**QZN7**	M M	-0.0454	-0.2733	0.2454
	RMS		0.1853	0.1346	0.1985

NUMBER OF PARAMETERS : 7
NUMBER OF COORDINATES : 33
RMS OF TRANSFORMATION : 0.1879 metres
NUMBER OF ITERATIONS : 2

TRANSFORMATION PARAMETERS (POST_EARTHQUAKE to PICMP93 ITRF96):

TRANSLATION IN X : **13.7753** ± 7.8901 m
TRANSLATION IN Y : **-14.9889** ± 6.6119 m
TRANSLATION IN Z : **-10.8726** ± 5.7188 m
ROTATION AROUND X-AXIS: - **0 0 0.59279** ± 0.19786"
ROTATION AROUND Y-AXIS: **0 0 0.31724** ± 0.14354"
ROTATION AROUND Z-AXIS: **0 0 0.00922** ± 0.29215"

SCALE FACTOR : **3.136840** ± 0.671590 mm/KM

Table 5.5 Calculated Helmert Transformation (Bernese V4.0) between earthquake zone stations in POST_EARTHQUAKE (Arbitrary WGS84) and in PICMP93 (ITRF96).

It should be noted that the transformation excluded the use of station PMG1. After careful analysis, it was determined that the PMG1 station observed during the PICMP93 campaign was not the same as the original mark placed for the PGNet (1988-91). Checks of redundant observations for each survey showed a consistency for each time frame. The station mark is atop a small concrete wall on the approaches to a road overbridge. It appears most likely that the wall may have been damaged and repaired without notifying NAMRIA.

As part of an undergraduate student project at the University of South Australia and also to further confirm the scale bias, it was decided to reprocess baselines from the 1990-91 post-earthquake re-observation of the Luzon Earthquake area. The Trimble GPSurvey software package was used instead of BATCH_PHASER processing used for the PGNet. Results were then compared with the PICMP93 Earthquake zone results.

This was a more difficult task than anticipated and it soon became very evident that the original work by Jones to process GPS baselines and to adjust the whole of the PGNet had indeed been a very complex and arduous one (Chapter 2). In fact, given all the advantages of hindsight, more sophisticated processing software and computer power, this small exercise in reprocessing did not significantly improve baseline selection criterion and processing by Jones at all. The other main problems encountered included:

- Data Volume – the large number of floppy disks ie over 500 floppy disks
- Disk Availability – many PGNet GPS sessions were missing
- Disk Quality – the disks had been stored in cardboard boxes in an office in Manila and had been subject to dust, temperature and moisture
- Data Quality – as was expected the GPS data were very poor due to the observations being undertaken during the peak of sunspot activity of Sunspot Cycle 22
- Baseline Processing - where possible the best L1 Fixed solutions were sought but the majority of solutions were L1 Float. Jones' decision to use triple difference solutions was more than justified.

Due to the poor quality of the data, few results could be obtained for analysis. No reasonable analysis was productive for the pre-earthquake data. However the results obtained for the post-1990 and 1991 GPS data were sufficient to give some useful comparisons with the PICMP93 (Table 5.6). It was significant that the single frequency baselines reprocessed from the PGNet were indeed shorter than the PICMP93 solutions ie a systematic baseline shortening.

Post EQ	Stations used (max 29)	Baselines processed	Best Solutions (L1 Fixed/Float) ppm	**Mean ppm**
1990	17	67	-1.5	
1991	16	68	-5.1	**-3.3**

Table 5.6 Baseline length comparisons between reprocessed post-earthquake PGNet observations and PICMP93 observations.

Due to the nature of the undergraduate project it is necessary to state that some of the baseline solutions that were incorporated into the L1 Float solutions were indeed very marginal and could have been rejected. However, the purpose of the project was to independently prove the existence of a systematic scale error throughout the earthquake zone i.e. a mean value of *-3.3 ppm* as seen in Table 5.6. This small sample has therefore provided results that confirm the existence and consistency of a systematic contraction of the PGNet relative to the more accurate PICMP93 coordinates.

Therefore, a major component of the re-adjustment of the PGNet onto the PICMP93 (ITRF96) fiducials must be an expansion of the network ie the application of a positive scale factor to the PGNet.

The next section examines whether **the proposed scale factor transformation parameter of *+3.1 ppm*** is indicative of values that could be expected under the solar conditions experienced during the PGNet GPS surveys throughout the Philippines (between latitudes 6-18 degrees North).

It was therefore necessary to try and quantify the actual ionospheric errors introduced into the PGNet from the 1988-91 GPS surveys. Once again, this was not an easy task due to a combination of the following factors:

- the vast amount of original GPS observations ie over 3000 data disks that were not wholly available for analysis
- the GPS surveys were carried out over a large regional area (ie between latitudes 5°N and 21°N plus longitudes 117°E and 127°E) and it is known that ionospheric effects fluctuate with geographical position
- the poor satellite constellation geometry of this era in GPS history (1988-91) meant that sessions were observed when possible (ie day or night) and sometimes with an absolute minimum of satellites available
- GPS single frequency observations (L1) were undertaken continually throughout the 1988-91 period which included the peak time for the 11 year sunspot cycle (the maximum occurred in November 1989)
- the time of day of GPS observations varied and therefore the daily fluctuations of the ionospheric effects varied
- the GPS survey of Luzon was carried out first and it should be noted that this occurred during 1989 and the peak of the sunspot cycle - therefore the collection of the Luzon data was severely hampered by the worst satellite geometry/configuration and peak ionospheric effects in the most northerly region of the Philippines
- after the Luzon Earthquake on July 6 1990, affected geodetic stations were re-observed throughout the rest of 1990 and into 1991

All L1 frequency GPS baselines observed for the PGNet were being contracted by the effects of the ionosphere in a systematic but also a temporal fashion. These effects vary during daily ionospheric fluctuations as well as over the 11-year sunspot cycle. **Therefore, the expected baseline shortening (scale factors), due to the effects of the ionosphere, changed constantly over the 2.5 years of the GPS survey phase of the PGNet.**

Georgiadou and Kleusberg [1988] state that for single frequency GPS, the mean resulting baseline length reduction caused by the ionosphere amounts to 0.25 ppm per 1 metre vertical delay. However, it is also claimed that for practical GPS observations this baseline reduction would be different to some extent because the satellite coverage is not homogeneous and also since vertical ionospheric delay actually varies along the paths of the satellites.

Therefore, having accepted this premise, in low latitude regions, during high solar activity times with no geomagnetic disturbances, the baseline shortening can be about 4-5 ppm [*Komjathy*, 1996]. For example, in the above conditions, a typical value of 100 vertical TECU relates to 16 meter vertical delay on L1, and this would correspond to (16 meters * 0.25 ppm) about 4 ppm baseline length reduction [*Komjathy*, 2001].

To test this hypothesis for the PGNet GPS survey, the International Reference Ionosphere (IRI-95) Model was used to calculate the number for vertical TECU during the 1988-91 GPS survey. The model was found at the National Space Science Data Center (NSSDC) web site http://nssdc.gsfc.nasa.gov/space/model/models/iri_n.htm. It should be noted that the IRI-95 is only a climatological model and produces monthly median values for the TEC eg 50-60 TECU. Therefore in actuality these values could be multiplied or divided by 2 [*Komjathy*, 2001]. For calculations using this model the height of the ionosphere was set at 1000 km.

TECU values from the IRI-95 model were obtained for the following parameters:

1. various times during the 1988-91 GPS geodetic survey including the start, end and at the peak of Sunspot Cycle 22
2. various latitude profiles (between latitudes 5°N and 19°N) at a mean longitude of 122°E
3. one longitude profile (between 117°E and 127°E) at a mean latitude of 13°N – this profile demonstrated that changes in the longitude range resulted in very little variation in the TEC

Figures 5.2, 5.3, 5.4 and 5.5 show graphical summaries of the latitude profiles created above. Note that in each graph, the TEC values were substantially higher from latitudes 13°N - 19°N ie predominantly the Luzon island region.

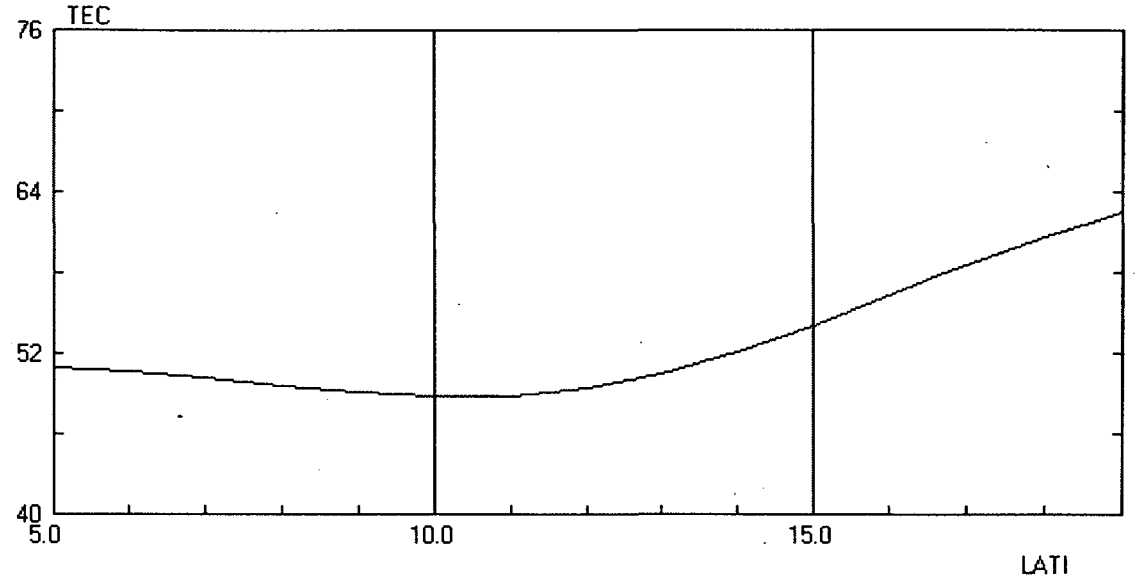

Figure 5.2 Latitude profile of TECU for January 1989 using Longitude 122°E
TECU range 48.88 to 62.52 and for ϕ 13°N TECU = 50.61
(International Reference Ionosphere (IRI-95) Model)

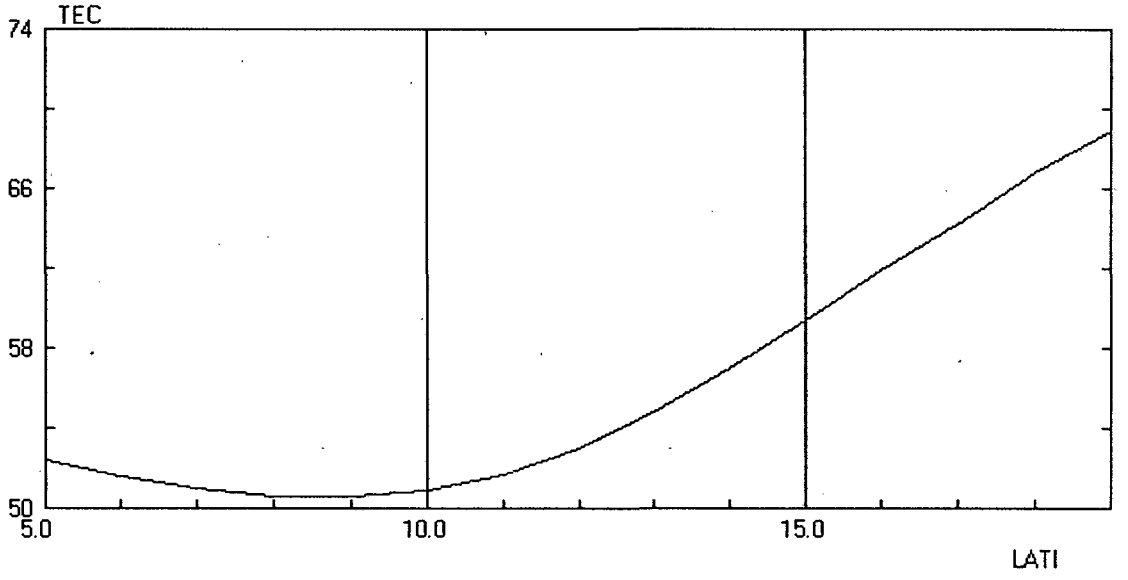

Figure 5.3 Latitude profile of TECU for July 1989 Peak of Sunspot Cycle 22 using Longitude 122°E
TECU range 50.64 to 68.93 and for ϕ 13°N TECU = 54.90
(International Reference Ionosphere (IRI-95) Model)
Note that the maximum possible TECU variation with latitude is $\approx$ 40%

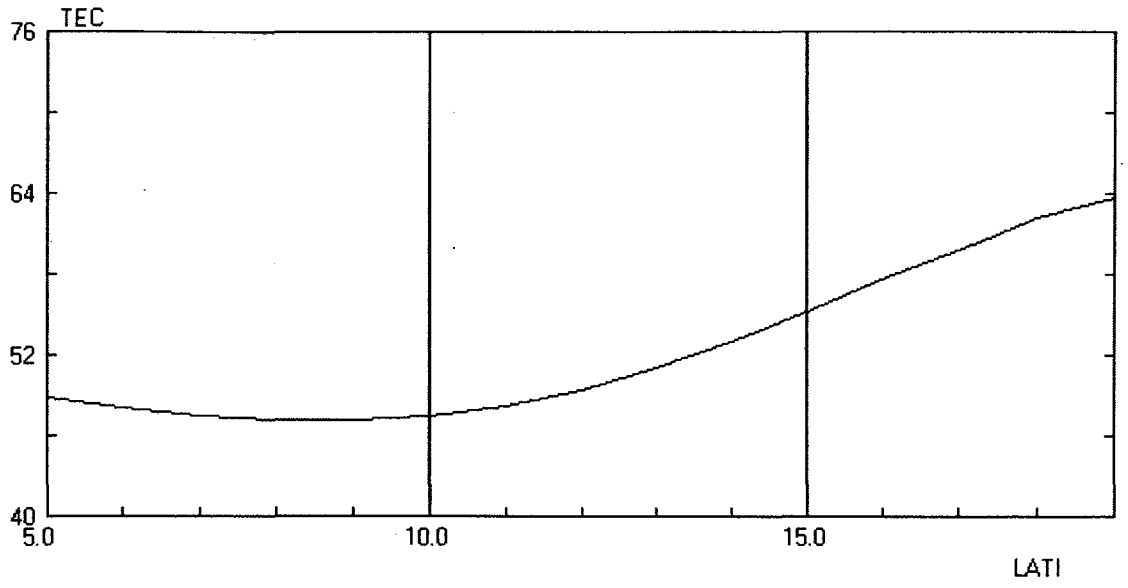

Figure 5.4 Latitude profile of TECU for the day of the Luzon Earthquake, July 6 1990 using Longitude 122°E
TECU range 47.21 to 63.70 and for ϕ 13°N TECU = 51.19
(International Reference Ionosphere (IRI-95) Model)

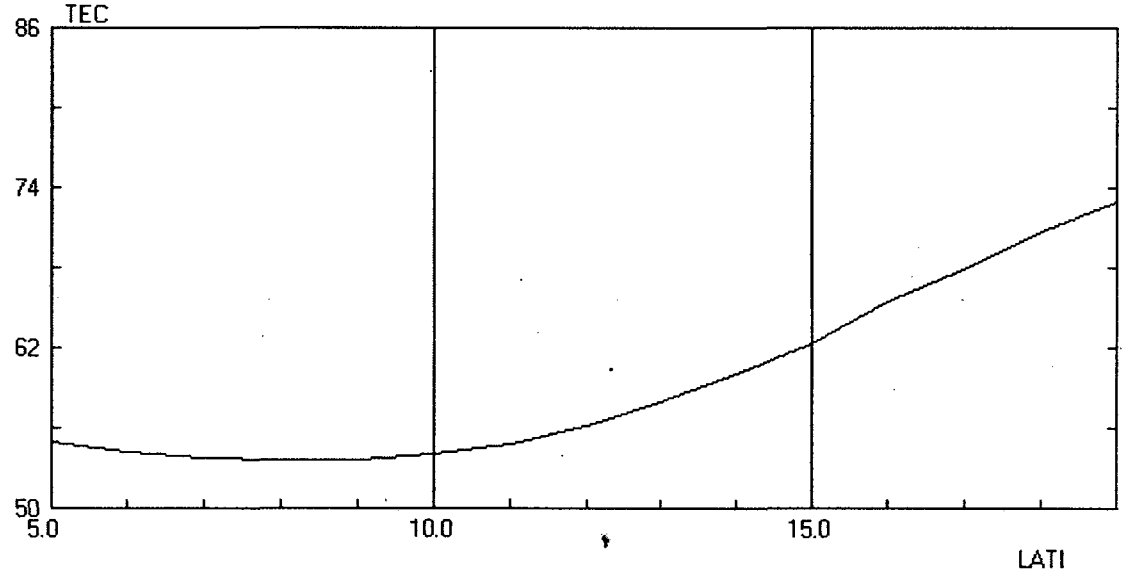

Figure 5.5 Latitude profile of TECU for June 1991 using Longitude 122°E
TECU range 53.62 to 73.01 and for ϕ 13°N TECU = 57.96
(International Reference Ionosphere (IRI-95) Model)

Table 5.7 shows the median and possible maximum TEC values over the 2.5 years of the GPS surveys for the PGNet.

Date	Median TEC ϕ 13°N, λ 122°E	ppm shortening ϕ 13°N, λ 122°E		Range Median TEC ϕ 5°-19°N, λ 122°E	Max real life ppm shortening ϕ 19°N, λ 122°E
		median	max possible		
	(TECU)			(TECU)	
Jan 1989	50.61	2.02	4.04	48.88 to 62.52	5.00
Jul 1989	54.90	2.20	4.40	50.64 to 68.93	5.51
Jul 6 1990	51.19	2.05	4.10	47.21 to 63.70	5.10
Jun 1991	57.96	2.32	4.62	53.62 to 73.01	5.84
Mean	**53.66**	**2.15**	**4.30**		5.36

Table 5.7 Median and possible maximum TEC values over the 2.5 years of the GPS surveys for the PGNet. Longitude 122°E was adopted as an average meridian for computations (IRI-95 Model)

The very large range of possible values highlights the difficulty in determining the ionospheric errors that occurred during the PGNet survey.

Table 5.7 is based on the median values obtained from the NSSDC IRI-95 Model for the period 1989-91. It can be seen that for a central geographical position (ϕ 13°N, λ 122°E), then a mean vertical TEC value would be 53.66 TECU. From the previous discussion on the relationship between vertical TECU and vertical delay on L1, then this would correspond to a baseline reduction in length of approx 2.15 ppm.

Note that the IRI only produces monthy median values for the TEC and is only a climatological model. In actuality, this could be multiplied or divided by 2. Therefore at certain times during the 2.5 years of GPS single frequency observations the TEC could be up to 107.21 TECU. This corresponds to baseline shortening of approx 4.30 ppm.

Similarly, at a position ϕ 19°N, λ 122°E, a standard median TEC value of 67.04 TECU corresponds to baseline shortening of 2.68 ppm and a possible real life TEC value of 134.08 TECU which relates to about 5.36 ppm in base reduction in length. In fact, *Jones* [1991] states that the worst baseline errors of 10-13 ppm exist in the very

northern areas of Luzon which were mostly observed during 1989.

Conclusion

It has been shown that the realistic range of possible baseline contraction due to the ionospheric effects during the 1989-91 GPS programme is anywhere between 1.0 ppm up to 5.4 or more.
It would be an extremely difficult and tedious task to determine scale biases for individual baselines (or maybe localised networks) throughout the whole of the PGNet. The procedure would require an exhaustive evaluation of each baseline based on the following factors:

1. the geographical position – vertical TEC values vary over throughout the Philippines and in fact the Luzon region was seen to have the highest values during the survey period
2. the epoch in the Solar Cycle at which the GPS observations were taken
3. the time of day of GPS observations eg the maximum ionospheric effects occur during mid afternoon and at a minimum throughout the night

It was decided that for the re-adjustment of the PGNet, once the mean effect or bias was removed then the remainder of the ionosphere error would be largely noise that would tend to be eliminated in the least squares adjustment.

The median value of 56 TECU gives baseline shortening of 2.3 ppm but with different latitudes/longitudes plus time of day of observerations this could be as high as 4-5 ppm baseline shortening.
The purpose for examining the ionosphere was to corroborate the scale bias discovered between the PGNet and the PICMP93 (ITRF96) from the Helmert transformation ie a contraction of 3.1 ppm.
There is no doubt that this value is indicative of values that could be expected under the solar conditions experienced during the PGNet GPS surveys throughout the Philippines (between latitudes 6-20 degrees North).
Therefore, **the proposed readjustment scale factor transformation parameter of *+3.1 ppm* is well justified.**

5.4 PGNet Readjustment Procedure, Results and Analysis

PGNet Readjustment onto the PICMP93 (ITRF96) Fiducials

The PGNet was readjusted onto ITRF96 using the NEWGAN software incorporating the following conditions:

1. using the PGNet WGS84 data file as originally provided by Jones,
2. adopting the seven transformation parameters computed for PGNet WGS84 to ITRF96 as shown in Table 5.4 ie taking into account the change from the WGS84 to ITRF96 datum and the apparent contraction due to the ionosphere on the single frequency observations during 1989-91,
3. tightly constraining the ITRF96 coordinates of the ten fiducial stations of the PICMP93 as shown in Table 5.1, and
4. adopting a 99% Confidence Interval for the adjustment

NB the errors introduced by the poor constellation/geometry of satellites of that era would be unlikely to be improved by a transformation. Noise due to poor constellation would remain in the data.

Results

The final readjusted PGNet (ITRF96) coordinate set (plus the position error ellipses) from the NEWGAN adjustment is attached at Appendix 4.

The summary from the NEWGAN software of the least squares adjustment results is shown in Table 5.8.

As a check on this adjustment process, a Helmert Transformation (Bernese V4.0) was calculated between stations in the re-adjusted PGNet (ITRF96) post-earthquake survey and in the PICMP93 (ITRF96). This is as shown in Table 5.9.
The resulting network scale factor of **-0.003 ppm** shows an acceptable outcome of substantially less than 1ppm. This result helps to justify the decision to correct for the

systematic scale bias of the original PGNet caused by ionospheric effects on the predominantly single frequency GPS network of 1988-91.

The resulting average RMS station residuals of 0.18 m (N), 0.12 m (E) and 0.17m (U) are indicative of overall positional accuracy of the PGNet in Luzon.

PHILIPPINE PRIMARY NETWORK (PGNet) ITRF96 DATUM

THE ESTIMATE OF THE VARIANCE FACTOR AFTER ADJUSTMENT IS **1.120**
THE A PRIORI VARIANCE FACTOR WAS **1.000**
THIS GIVES A VARIANCE RATIO OF **1.120**

7023 DEGREES OF FREEDOM
10 CONSTRAINT STATIONS
0 TERRESTRIAL OBSERVATIONS
30 POSITION EQUATIONS
0 POINT POSITIONS
0 MULTI-STATION FIGURES
0 MULTI-BASELINE FIGURES
2691 BASELINES
86.7 PER CENT REDUNDANCY
360 FREE STATIONS
19.51 DEGREES OF FREEDOM PER FREE STATION
6.50 RATIO OF REDUNDANCIES/PARAMETERS

4 ITERATIONS REQUIRED FOR CONVERGENCE

THE VALUE OF THE MINIMUM IS **7866.**

*THE VARIANCE RATIO TEST IS SATISFIED AT THE **99 %** CONFIDENCE LEVEL*
AND HENCE RESULTS ARE CONSISTENT WITH THE MATHEMATICAL MODEL

F TEST FACTOR = **0.9740**

1) THE TAU REJECTION VALUE IS **4.846** BASED ON A CONFIDENCE LEVEL OF 99 %
STANDARDISED CORRECTIONS GREATER THAN THIS VALUE WILL BE MARKED

2) THE STANDARDISED CORRECTIONS HAVE BEEN SCALED BY THE CALCULATED SECOND MOMENT. FACTOR = **1.0149**
VALUES GREATER THAN THE VALUE OF TAU **(4.8455)** WILL BE MARKED

THE NUMBER OF BASELINES DETECTED AS 'POSSIBLE' OUTLIERS WAS **10**

Table 5.8 NEWGAN software summary of the results of the readjustment of the PGNet WGS84 on the ITRF96

HELMERT TRANSFORMATION

FILE 1: PGNet ITRF96 Earthquake Zone Coordinates
FILE 2: PICMP93 ITRF96 Earthquake Zone Coordinates

TRANSFORMATION IN EQUATORIAL SYSTEM (X, Y, Z):
RESIDUALS IN LOCAL SYSTEM (NORTH, EAST, UP)

Num	Station	Flag	Residuals in Metres (m)		
			North	East	Up
22	**ARA1**	M M	0.2475	0.0042	-0.1735
19	**BLN4**	M M	-0.1387	-0.1058	0.2728
15	**IFG1**	M M	0.1402	0.1070	0.0564
17	**LUN1**	M M	-0.1862	-0.0659	-0.1726
20	**NE43**	M M	0.1580	0.1226	0.0846
11	**NE44**	M M	-0.1611	0.0576	0.0488
14	**NVY1**	M M	0.1260	0.0811	-0.0094
21	**NVY4**	M M	0.0980	0.1144	0.0941
13	**PMG1**	Not used	*-0.3249*	*-0.8458*	*-0.0006*
7	**PNG5**	M M	-0.3201	0.0721	-0.1013
18	**QZN5**	M M	0.0943	-0.1461	-0.3019
25	**QZN7**	M M	-0.0571	-0.2387	0.2019
	RMS		0.1805	0.1219	0.1727

NUMBER OF PARAMETERS : 7
NUMBER OF COORDINATES : 33
RMS OF TRANSFORMATION : 0.1724 metres
NUMBER OF ITERATIONS : 2

TRANSFORMATION PARAMETERS (PGNet_EQ ITRF96 to PICMP93 ITRF96):

TRANSLATION IN X : **21.2633** ± 7.2364 m
TRANSLATION IN Y : **8.8605** ± 6.0640 m
TRANSLATION IN Z : **11.2817** ± 5.2450 m
ROTATION AROUND X-AXIS: **0 0 0.12157** ± 0.18147"
ROTATION AROUND Y-AXIS: **0 0 0.52144** ± 0.13164"
ROTATION AROUND Z-AXIS: - **0 0 0.65516** ± 0.26794"

SCALE FACTOR : **-0.003204** ± 0.615938 mm/KM

Table 5.9 Calculated Helmert Transformation (Bernese V4.0) between stations in the re-adjusted PGNet (ITRF96) Earthquake zone and in the PICMP93 (ITRF96).

Comments on the Readjusted PGNet (ITRF96)

The readjustment of the PGNet onto the ITRF96 using the PICMP93 fiducials was an attempt to upgrade the accuracy of the 1988-91 NRMDP GPS network The positional error ellipses for the 99% Confidence Interval show that most positions are still within an overall precision of about 3ppm.

The original PGNet had a precision requirement (under the NRMDP) of only 10-ppm and regionally this was successful completed to about 3ppm [*Jones,* 1991]. It was also noted from the original PGNet adjustment that there are a few areas of the Philippines where some individual GPS baselines had very large errors of 10-13 ppm e.g. the northern provinces of Luzon were observed during 1989 (time of high solar activity and the worst satellite availability/configuration) and also some baselines that were re-observed after the 1990 earthquake.

The readjusted PGNet (ITRF96) data set has been corrected by the scale factor of +3.1 ppm to account for the mean effect of the ionosphere on the predominantly single frequency GPS data of the PGNet.

Table 5.9 shows an attempt to check the resulting network scale factor based on a comparison of readjusted PGNet (ITRF96) with the PICMP93 (ITRF96) Luzon Earthquake monitoring stations. The resulting scale factor of -0.003 ppm suggests that the systematic errors introduced by the ionosphere in the PGNet (1989-91) have been reduced and that therefore the accuracy of the network has been improved. Unfortunately, the reality is that:

- the final residuals after the readjustment have not varied significantly from Table 5.5, and
- the precision of the PGNet has not been improved much and some individual baselines within the Philippines would still have baseline errors of up to 10 ppm.

It is recommended that, before PGNet (ITRF96) coordinates are used, the available position error ellipses are examined to determine station quality and possible baseline precision (Appendix 4).

To have improved the precision (i.e., reduced the size of the uncertainty ellipses), the PGNet GPS data would have had to be readjusted with the PICMP93 data, either using some sort of ionosphere model for the earlier data or perhaps by relaxing the scale constraints on the baseline lengths. As discussed in section 5.1, the Helmert transformation approach was adopted due to the logistical problems involved in reprocessing the PGNet GPS data.

Finally, it must be remembered that the PGNet of 1988-91 was one of the first GPS national geodetic networks. The contract for the NRMDP geodetic component required a precision of only 10-ppm. In recent times, using broadcast orbits, dual frequency receivers plus the complete satellite constellation, it would have been quite easy to achieve a network precision of 0.5-1 ppm.

The new PGNet (ITRF96) data set may however become very significant for long-term geophysical analyses, only if the marks remain stable and the network is not going to be totally reobserved for more than another 30 years.

5.5 Transformation Parameters for the PRS92 to ITRF96

The Philippine Reference System 1992 (PRS92) is the geodetic datum for the coordinates published in *The Philippine Geodetic Network Manual 1992*. The PRS92 is based on the Clarke 1866 Spheroid and not the WGS84 or ITRF96.

It would be very useful (eg for future regional tectonic monitoring etc) to be able to transform any survey with PRS92 coordinates into the PICMP93 (ITRF96) reference frame. This would enable PRS92 data sets to be in a common reference with the high fidelity GPS surveys of the PICMP93, 96 and 98 campaigns.

The Bernese V4.0 program HELMR1 was once again used to compare the PICMP93 (ITRF96) coordinates for the ten (10) fiducial sites with the PRS92 results for the same stations. The seven transformation parameters were computed ie three translations, three rotations and a scale factor.

Procedure and Results

Table 5.10 shows the geographical PRS92 coordinates as published in the manual.

LOCAL GEODETIC DATUM: PRS92 (CLARKE 1866 Spheroid)

Philippine Geodetic Network Manual 1992

Station Name	Latitude			Longitude			Ellipsoidal Height (m)
	°	′	″	°	′	″	
ABY3	13	28	40.83363 N	123	40	28.31567 E	108.591
CGY8	17	37	08.41491 N	121	43	30.74950 E	48.214
CTN1	7	00	47.54584 N	125	05	25.31805 E	293.628
ILN1	18	23	47.42681 N	120	35	44.44843 E	13.208
ILO1	10	42	40.81004 N	122	33	48.37076 E	25.916
MRQ1	13	33	41.00000 N	121	52	03.00000 E	271.185
PNG5	15	52	09.25114 N	120	15	08.48584 E	103.733
ZGS2	6	55	24.43016 N	122	04	03.26680 E	13.019
LYT8	11	15	09.14182 N	125	00	14.15966 E	24.574
PL11	9	42	32.18317N	118	42	46.31722 E	6.296

Table 5.10 PRS92 (Clarke 1866) Geographical Coordinates of the PICMP93 Fiducials

These were then converted into PRS92 Cartesian coordinates are shown in Table 5.11.

LOCAL GEODETIC DATUM: PRS92 (CLARKE 1866 Spheroid)
Philippine Geodetic Network Manual 1992

Station Name	X (m)	Y (m)	Z (m)
ABY3	-3439845.6240	5162800.9210	1476816.8970
CGY8	-3197636.7710	5172323.7150	1918135.8970
CTN1	-3639542.2960	5180396.2120	773570.7510
ILN1	-3081498.2460	5211425.7020	1999959.5270
ILO1	-3373553.8920	5282503.2450	1177578.4960
MRQ1	-3274279.0810	5267006.4050	1485823.7330
PNG5	-3091765.5160	5301036.7300	1732736.4260
ZGS2	-3361790.9310	5365897.5340	763684.4130
LYT8	-3588890.4460	5124717.9430	1236343.4260
PL11	-3020626.2090	5514346.6350	1068464.2420

Table 5.11 PRS92 (Clarke 1866) Cartesian Coordinates of the PICMP93 Fiducials

The PRS92 cartesian coordinates were then compared with the matching PICMP93(ITRF96) fiducial stations (from Table 5.1). The results and residuals of this Helmert Transformation (using Bernese 4.1 software) are shown in Table 5.12.

The following 7 transformation parameters (from Table 5.12) may therefore be adopted generally for relating PRS92 coordinates within the Philippines to the ITRF96 reference frame based on the PICMP93 (ITRF96):

TRANSLATION IN X : **139.7** metres
TRANSLATION IN Y : **94.6** metres
TRANSLATION IN Z : **65.3** metres

ROTATION AROUND X-AXIS: **- 2.48** "
ROTATION AROUND Y-AXIS: **5.06** "
ROTATION AROUND Z-AXIS: **0.72** "

SCALE FACTOR : **-2.03** ppm

HELMERT TRANSFORMATION

FILE 1: PRS92 Geodetic manual Coordinates
FILE 2: ITRF96 Coordinates of the PICMP93

TRANSFORMATION IN EQUATORIAL SYSTEM (X, Y, Z):
RESIDUALS IN LOCAL SYSTEM (NORTH, EAST, UP)

			North	East	Up
6	**ABY3**	M M	-0.2072	-0.2099	-0.0913
1	**CGY8**	M M	-0.2347	-0.2264	0.3804
8	**CTN1**	M M	-0.2312	-0.1664	0.1867
2	**ILN1**	M M	-0.1926	-0.0342	0.4474
3	**ILO1**	M M	0.4230	0.3251	-0.4919
9	**LYT8**	M M	0.3666	0.4323	-0.4394
5	**MRQ1**	M M	0.0343	0.0010	-0.2119
10	**PL11**	M M	0.1433	0.2054	-0.4928
7	**PNG5**	M M	0.2151	0.0285	-0.2511
4	**ZGS2**	M M	-0.3170	-0.3594	0.9640
	RMS		0.2729	0.2558	0.4834

NUMBER OF PARAMETERS : 7
NUMBER OF COORDINATES : 30
RMS OF TRANSFORMATION : 0.3824 M

TRANSFORMATION PARAMETERS (PRS92 Geodetic to PICMP93 ITRF96):

TRANSLATION IN X : **139.6561** +- 3.3344 M
TRANSLATION IN Y : **94.5835** +- 2.5981 M
TRANSLATION IN Z : **65.2689** +- 1.9267 M
ROTATION AROUND X-AXIS: **- 0 0 2.4797** +- 0.0658 "
ROTATION AROUND Y-AXIS: **0 0 5.0572** +- 0.0546 "
ROTATION AROUND Z-AXIS: **0 0 0.7193** +- 0.1239 "
SCALE FACTOR : **-2.0316** +- 0.2548 MM/KM

Table 5.12 Calculated Helmert Transformation (Bernese V4.0) between fiducial stations in PRS92 (*Philippine Geodetic Manual 1992*) and in PICMP93 (ITRF96).

Comments

The result is a usable transformation of PRS92 points into ITRF96 – while ignoring tectonic motion between 1990-1993. The poor WGS84 datum definition of the original PGNet was created by the poor accuracy of the absolute positioning techniques of that time. These transformation parameters give the best available conversion of the PRS92 into the modern reference frame of the ITRF96.

The limitations to the use of these parameters include:

- the limited number of common points in the transformation computations ie only ten PICMP93 fiducial points over the whole archipelago, and
- the errors introduced by the continual seismic/volcanic/tectonic displacement of all the geodetic stations (including the fiducial points) over time ie from the original GPS observations of 1988-91 until the high fidelity PICMP93 survey and then over the ensuing years since 1993.

These derived parameters would be of significant precision for regional long-term tectonic movements or rapid response monitoring displacements associated with large earthquakes.

If a future earthquake happens before the PRS92 points are resurveyed with more precise GPS, then these parameters are the best possible set for the pre-earthquake positions of the affected stations. But, if the points are re-surveyed before a future earthquake, then the PRS92 data become redundant as long as the ground marks remain intact.

However, it is unlikely that a high precision GPS resurvey of the whole PGNet will take place in the Philippines in the foreseeable future.

6.0 The 1990 M_s 7.8 Luzon Earthquake and Regional Tectonics

6.1 Introduction

The Philippine Islands form part of the complex boundary between the Philippine Sea and Eurasian plates as can be seen in Figure 6.1.

In the central and southern Philippines most of the deformation is partitioned between approximately trench-normal westward-directed subduction at the Philippine trench and left-lateral strike slip motion on the intra-arc Philippine fault [*Fitch*, 1972; *McCaffrey*, 1996]. Both the trench and the fault are quite recent, with their activity beginning between 2 and 4 Ma [*Cardwell et al.*, 1980; *Aurelio et al.*, 1991; *Barrier et al.*, 1991.

At the latitude of Luzon, the east-dipping Manila trench to the west of Luzon has been the primary plate boundary since the late Miocene [*Karig*, 1973; *Murphy*, 1973] but it does not presently show high levels of seismic activity [*Cardwell et al.*, 1980]. It has been proposed [*Fitch*, 1972; *Karig*, 1973] that subduction east of the Philippine islands is propagating northwards along the East Luzon trough, which is connected to the Philippine trench by a left-lateral trench-trench transform, and which will eventually take over from the Manila trench as the primary plate boundary.

There is no evidence for active subduction north of ϕ 17N°-18N° at the East Luzon trough [*Bowin et al.*, 1978; *Cardwell et al.*, 1980; *Hamburger et al.*, 1983; *Lewis and Hayes*, 1983, 1989], so that the present convergence rate across the trough cannot be very rapid. Supporting this, *Hamburger et al.* [1983] find no marine geophysical evidence for substantial recent slowing of subduction at the Manila trench.

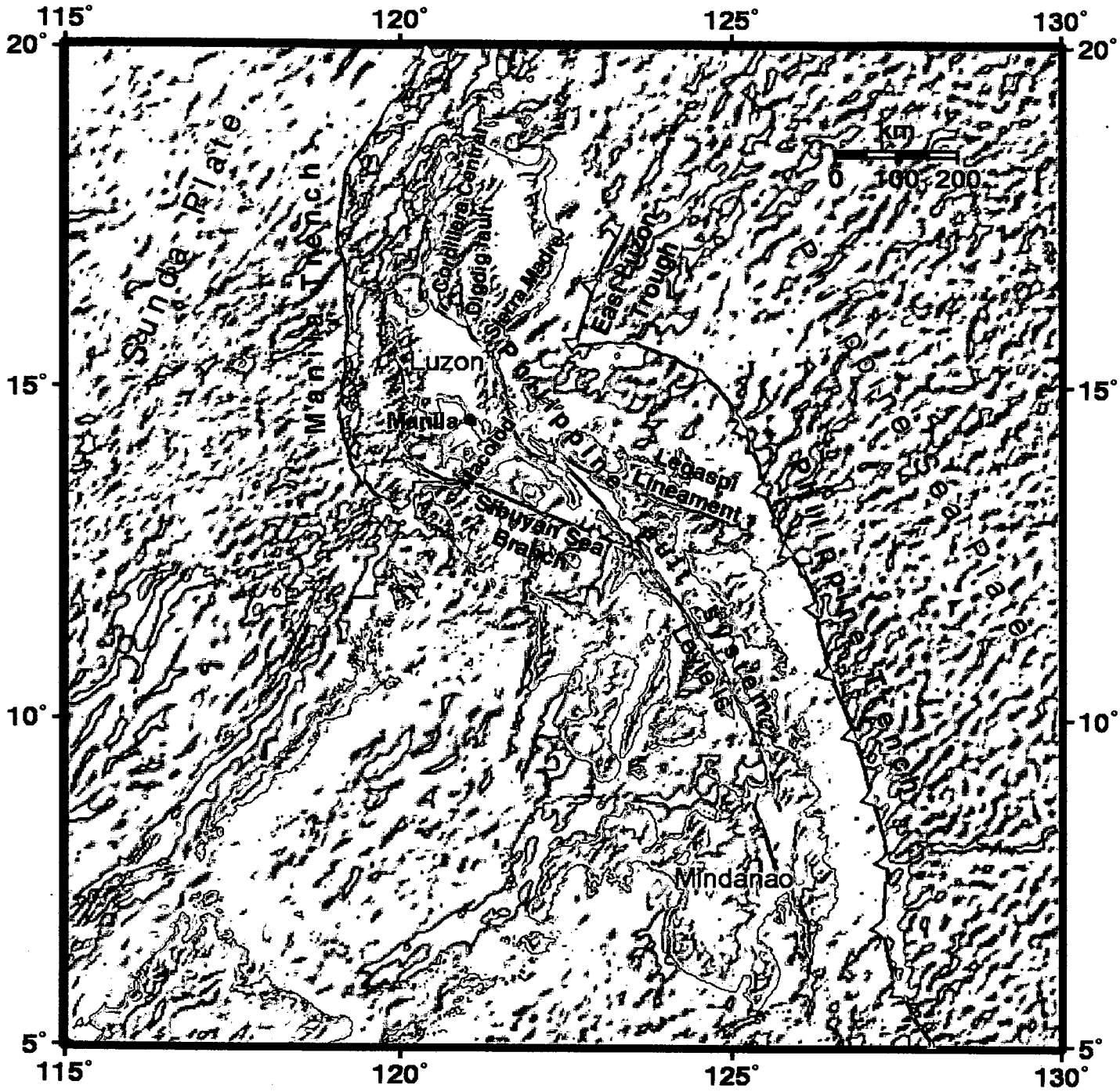

Figure 6.1 Topography and bathymetry of the Philippine region showing major tectonic features in our region of interest, superimposed on a shaded relief image of topography and bathymetry lit from the southeast. Faults with filled triangles are active subduction zones. The fault shown with open triangles in western Luzon is the active convergence zone of *Barrier et al.* [1991]. The Philippine fault system is a predominantly left-lateral system that splits into several splays in central Luzon. The "Sunda Plate" (comprising SE Asia and the South China Sea) is moving at some 10 - 15 mm/yr east or southeast relative to stable Europe and central Asia [*Michel et al.*,2001].

The nature of the Philippine fault as one of the world's great continental strike-slip faults was first properly recognised by *Allen* [1962], but its long-term slip rate and earthquake recurrence history remain poorly known. A number of large earthquakes have been relocated close to the Philippine fault [*Rowlett and Kelleher*, 1976], suggesting it is currently active through most of its length. The left-lateral slip rate on an apparently creeping section of the fault on Leyte Island has been measured at 26±10 mm/yr [*Duquesnoy et al.*, 1994], adding to the evidence of slip partitioning between the Philippine fault and Philippine trench.

Further north, in Luzon Island, the situation is more complex, with active subduction to the west of the island and active convergence to the east, and with the Philippine fault system separating into several splays and trending more northerly in the northern half of the island (see Figure 6.1). Prior to the M_S 7.8 1990 earthquake, only one large historical earthquake, the 1973 Ragay Gulf event well to the south, had been unequivocally associated with the Philippine fault in Luzon [*Morante and Allen*, 1973; *Morante*, 1974].

Using historical records, geomorphological expression and radiocarbon ages of wood in offset terraces, *Hirano et al.* [1986] estimate that the most recent historical earthquake to have broken the central Luzon section of the Philippine fault occurred in 1645. It is believed that the historical record in the region is complete since 1645 for events of more than Intensity MM7 [*Daligdig*, 1997; E. Ramos, pers. comm., 1999] so it is unlikely that there have been intervening major events on this section of the Philippine Fault. Paleoseismic investigations, including trenching, of the Digdig and Philippine faults subsequent to the 1990 quake [*Daligdig*, 1997] provide the most recent information on slip rate and earthquake recurrence interval. *Daligdig* [1997] finds evidence for six or seven past events on the fault sections that broke in the 1990 earthquake. Radiocarbon dating of the two events prior to 1990 provides good evidence to identify the 1645 earthquake with this fault segment, and places the previous event in the range 1190 - 1390 AD. *Daligdig* [1997] estimates from his trenching studies that the average earthquake recurrence interval on the Digdig Fault is 300 - 400 years, with a long-term slip rate of 9 - 17 mm/yr. He also notes that most estimates by other authors of slip rate based on faulted rock units and geomorphic data place the rate in the range 6 - 25 mm/yr, both on the Digdig Fault and the Philippine Fault to the south. For example, *Hirano et al.*, [1986] estimate the long-term

slip rate of the Philippine fault in this region to be 1.5—5 mm/yr, while *Newhall et al.* [1990] quote the long-term rate as "probably in the order of 10-20 mm/year".

However, a convincing geomorphic estimate by *Daligdig* [1997] based on a carbon-dated stream offset near the 1990 epicenter and gives a rate of 15±3 mm/year.

The 1990 Luzon earthquake was one of the largest continental strike-slip earthquakes of the 20th century [*Yoshida and Abe*, 1992]. It caused observed ground rupture along 110 km of the Philippine Fault and one of its northern splays, the Digdig Fault, with 5 - 6 m of predominantly left-lateral surface offset [*Abe*, 1990; *Nakata et al.*, 1990, 1996; *Newhall et al.*, 1990]. Figure 6.2 shows the mapped surface rupture and the three planar fault sections adopted to approximate the southern 100km of the rupture. It should be noted that *Daligdig* [1997] refers to the whole section that ruptured in 1990 as the Digdig Fault, while other authors including *Nakata et al.* [1996] refer to the northern part as the Digdig Fault and the southern part as the Gabaldon Fault.)

The most reliable hypocentral depth is estimated from pP-P phases as 25±0.9 km by the International Seismological Centre [*ISC*, 1992]; this agrees with the 25 km hypocentral depth estimate of *Yoshida and Abe* [1992], while the Harvard CMT solution uses a constrained centroid depth of 15 km.

Mapping of the surface rupture ended near Kayapa (see Figure 6.2) because of difficulties of access to the mountainous terrain of the Cordillera Central further north [*Nakata et al.*, 1996]. However, distributed aftershocks indicate that the rupture could have continued a further 50-100 km north [*Newhall et al.*, 1990].

Using centroid moment tensor (CMT) inversion of long-period surface waves, *Yoshida and Abe* [1992] estimate the scalar moment of the earthquake to be 3.9×10^{20} N m, while the Harvard CMT catalogue gives 4.1×10^{20} N m. Also, *Yoshida and Abe* [1992] estimate the fault length, width and average slip as 120 km, 20 km and 5.4 m, respectively, with nearly pure left-lateral strike slip on a nearly vertical fault. Their estimate of 20 km fault width was based on the fact that almost all well-located aftershocks were shallower than 20 km [*Newhall et al.*, 1990; *Yoshida and Abe*, 1992].

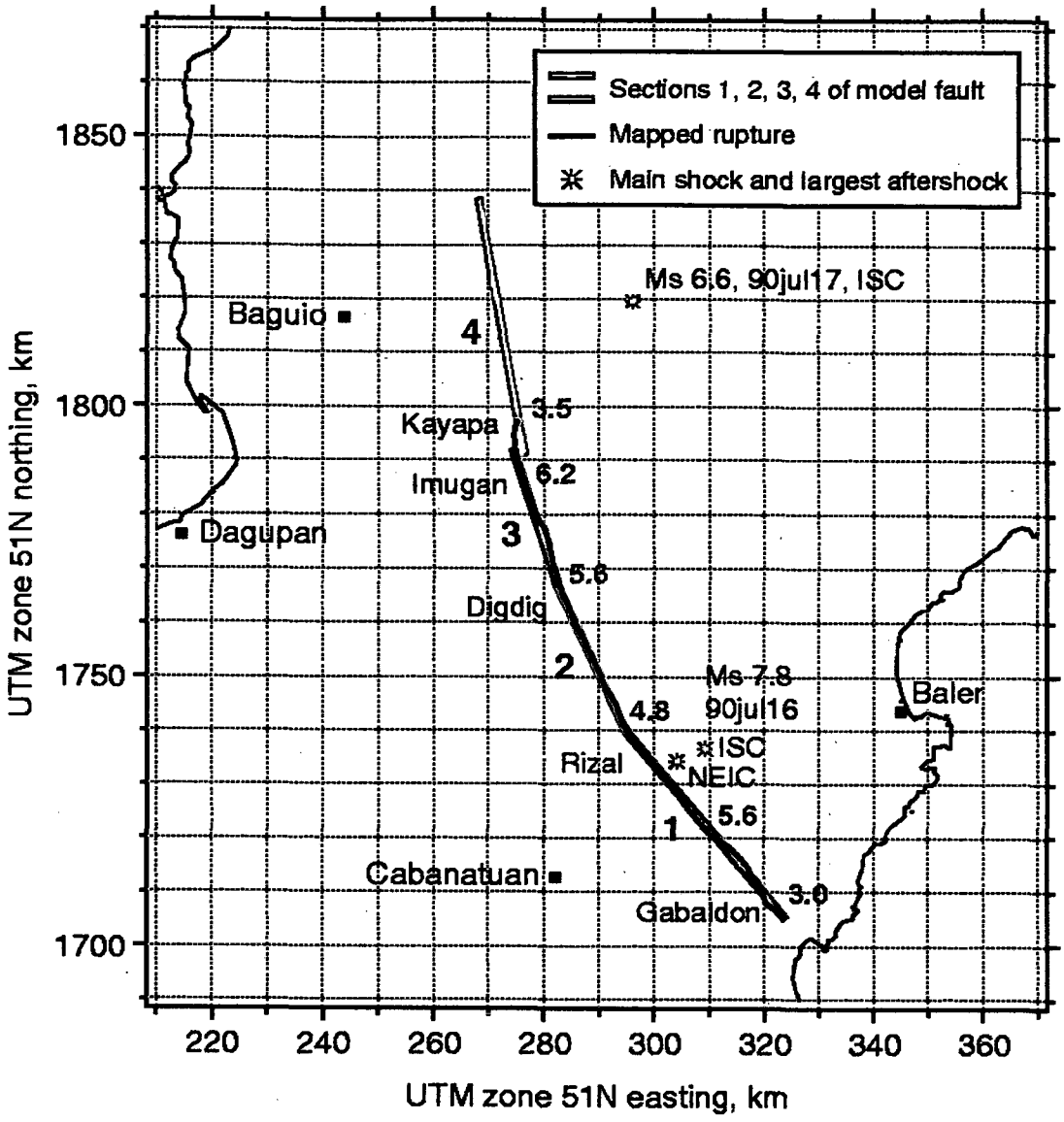

Figure 6.2 Mapped surface rupture of the 1990 Luzon earthquake from *Nakata et al.* [1990, 1996] (black line) and the three planar fault sections (1, 2, 3) adopted to approximate the southern 100 km of the rupture. The decimal numbers to the east of the fault trace are mapped coseismic surface offsets in metres. Also shown is the modelled northern extension of rupture (section 4). The existence of this extension about 45 km north of the mapped rupture is well constrained, though its strike is not. Note that a right-stepping jog near the north end of the mapped rupture is favored by the geodetic data. Also shown are several Philippine cities and various locations along the surface rupture. Both the ISC and USGS NEIC epicentral locations are shown, as well as the ISC epicenter of the largest aftershock.

No significant post-seismic creep was observed on a small-scale geodetic array crossing the fault between days 13 and 20 after the quake. Twenty millimeters of motion was observed on the following day, and this may have been related to a nearby strong aftershock [*Newhall et al.*, 1990].

In this chapter, evidence is presented from the PGNet GPS geodetic measurements that support the observed coseismic offsets and seismological estimates of the fault parameters of the 1990 earthquake. This will include data justifying the claim that significant faulting took place to 20 km depths along the central section of the fault. Also strong evidence will show that the rupture continued 45±5 km north or northwest of the mapped surface trace.

Additionally, results from the geodetic measurements show the left-lateral strike-slip rate on the Philippine fault system in Luzon between 1993 and 1998 has been close to 40 mm/yr. However, *Beavan et al.*, [2001] have now shown this to be a partially viscoelastic response to the 1990 earthquake and thus up to a factor of three higher than the long-term rate.

Silcock and Beavan [2001], and an associated paper, *Beavan et al.*, [2001] use the GPS data collected i.e. for the PGNet under NAMRIA, the PICMP93, 96, 98 campaigns and later on for the 1994 Philippine Sea Plate campaign (PSP94). The comprehensive results of this research include:

- the geodetic constraints on coseismic rupture and postseismic deformation due to the 1990 M_s 7.8 Luzon Earthquake and implications for Philippine Sea-Eurasian plate motion, and
- implications for Luzon tectonics, Philippine Sea Plate motion and additional information on the tectonic setting.

6.2 Data Available for the 1990 M_s 7.8 Luzon Earthquake

6.2.1 GPS observations of the 1990 earthquake

The 1990 earthquake occurred as the primary geodetic survey (PGNet) of the Philippines was being completed [see Chapter 2 and *Jones*, 1991] and a section of the network in central Luzon was remeasured over a period between 4 and 9 months after the earthquake. As already discussed, both the pre- and post-earthquake surveys used predominantly single-frequency GPS receivers and broadcast orbits at a time of poor satellite geometry and high ionospheric activity, with these effects being particularly severe during the pre-earthquake survey of Luzon.

Partially offsetting these problems, the surveys were done area-by-area with overlapping stations between areas, and stations were observed multiple times. 55% of baseline lengths were < 50 km and most of the rest were < 70 km. The GPS data were processed as independent baseline vectors, generally using triple-difference processing, but with bias-fixed double-difference processing on some of the shortest lines [*Jones*, 1991]. The baselines were then combined in a geodetic least squares adjustment using program NEWGAN (developed by Dr. J. S. Allman from Canadian Geodetic Survey programs GANET and HAVOC2).

6.2.2 Fault Rupture Trace

Nakata et al., [1996, and pers comm. 1993] mapped the 1990 fault rupture trace as soon as possible after the earthquake (see Figures 6.3 and 6.4). Copies of these trace diagrams as well as documented field displacements were provided by Nakata in 1993. Unfortunately, the trace diagrams were only diagrammatic in nature and were of little use for coordinating the rupture trace. However, the USGS supplied a hard copy of the mapping results for the trace of the 1990 fault rupture. The trace survey was done by photogrammetric interpretation and then by locating these points onto USGS 1:50,000 topographic maps (on the Luzon geodetic datum). Fortunately, this matched both the scale and datum of the Philippine DENR 1:50,000 mapping.

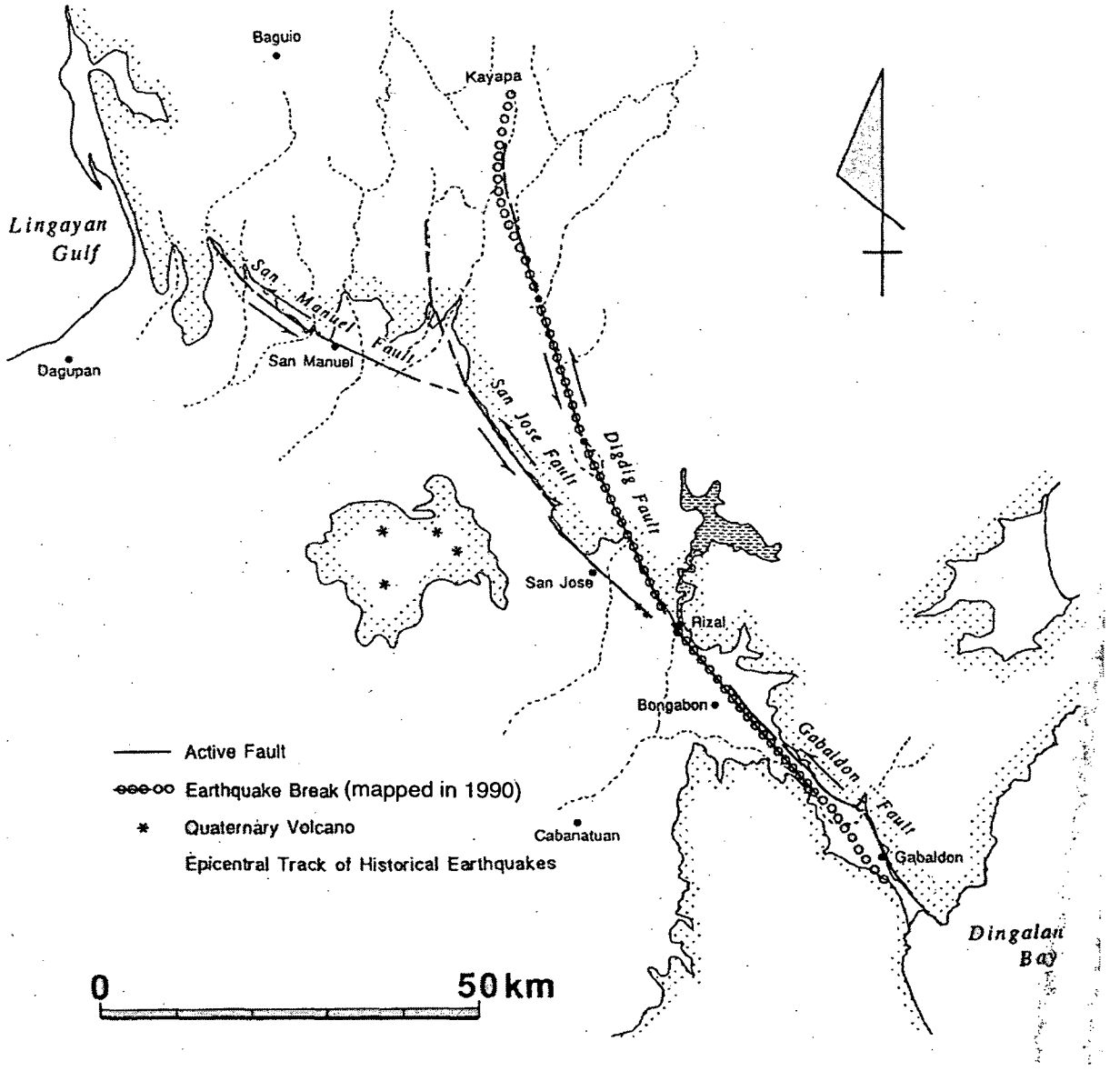

Figure 6.3 Location of surface fault ruptures of the 16 July 1990 Luzon earthquake with active fault traces *Nakata et al.*, [1996].

To obtain a useful digital database of the fault rupture (for input to the dislocation model and formal inversion) it was necessary to:

- trace the identified 1990 points from the 1:50,000 USGS map onto the corresponding DENR map.
- join these points into a continuous trace of the fault rupture
- digitise (using surveying software GEOCOMP®) grid ticks on each DENR map sheet as control for the fault trace digitising (UTM zone 51N coordinates on the Luzon datum)

- digitise the entire fault trace using GEOCOMP software
- having obtained the digitised coordinates perform a seven parameter transformation plus UTM projection to obtain final coordinates (UTM Zone 51N coordinates on the WGS84 datum)

Nakata et al., [1996] and the USGS [pers comm. 1993] maintain that the trace coordinated points are within about +-50 metres but obviously the digitising process for the remainder of the trace would not be to this precision ie subject to errors of interpretation, plotting and digitising.

Figure 6.5 shows the horizontal and vertical displacements observed by *Nakata et al.*, [1996]. This information was extremely useful in determining the preferred dislocation model. A table of the final Zone 51N UTM (WGS84) coordinates for the visible fault rupture trace of the 1990 earthquake is shown in Appendix 7.

6.3 Preliminary Tectonic Analysis

The preliminary analysis shown here was an attempt to determine the tectonics with respect to the Eurasian (EU) plate fixed. *Beavan et al.*, [2001] furthers this analysis with additional GPS data (1994 PSP campaign), which was not available at the time when the GPS processing and earthquake modelling was undertaken for this thesis. The ITRF96 coordinates of the 1993 stations, used to transform the PGNet into ITRF96 were shown in Chapter 4. From the procedure described, the ITRF96 velocities of all stations observed in more than two epochs were also calculated and are shown in Table 6.1.

The ITRF96 velocities (see Figure 6.6) may then be transformed into a reference frame fixed to stable Eurasia by calculating the Euler vector of Eurasia relative to ITRF96 from the ITRF96 velocities published by the *IGS* [1998]. Using the stations in Table 6.2 to define stable Eurasia, a Euler vector of 61.5°N, 93.7°W, 0.283°/Ma was calculated, with velocity residuals < 2 mm/yr at this set of stations. Applying this Euler rotation to the ITRF96 velocities of Table 6.1 also gives velocities relative to stable Eurasia (EU fixed). These are shown diagrammatically in Figure 6.7.

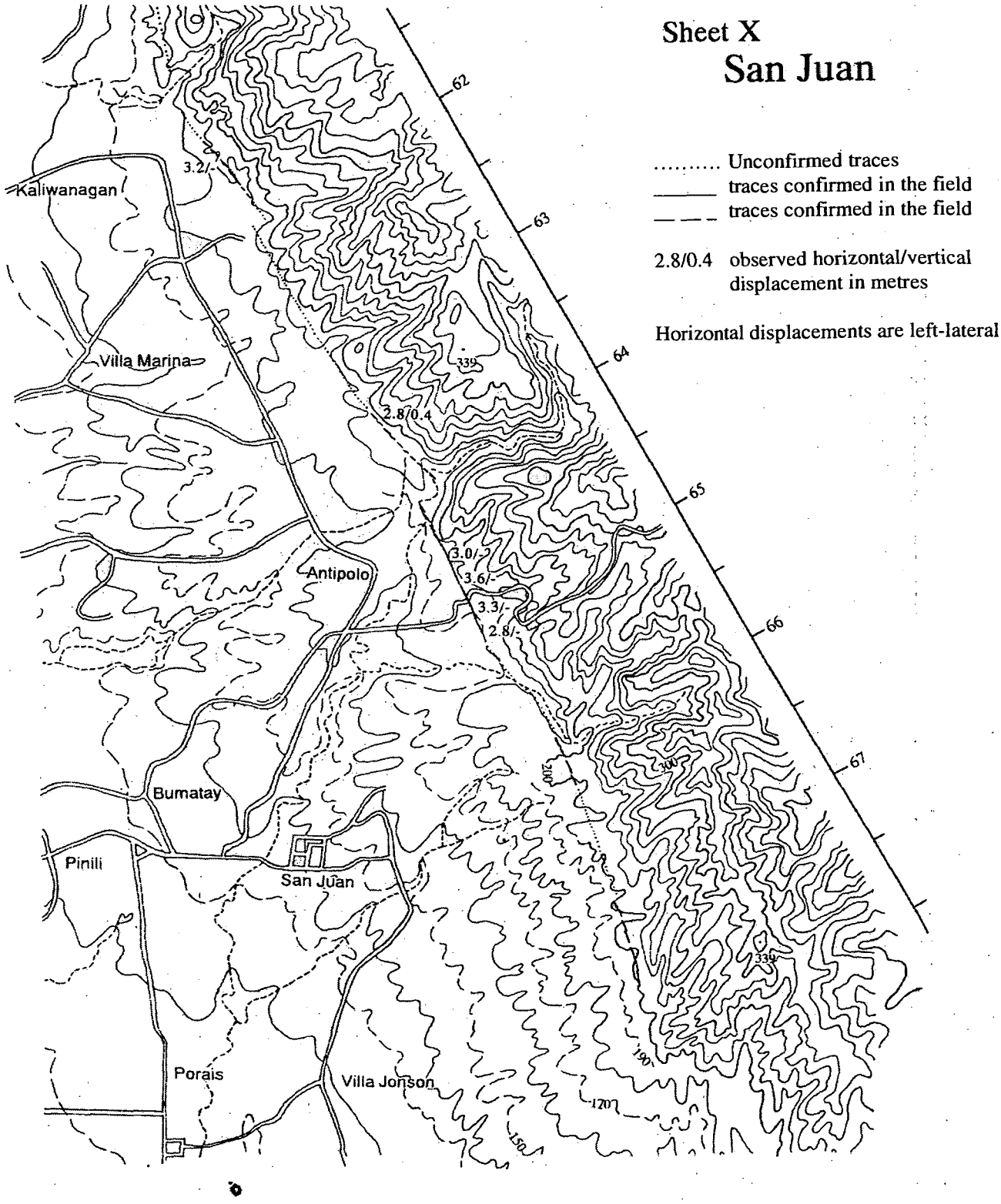

Figure 6.4 One of the 17 map sheets by *Nakata et al.*, [1996] produced for the 1990 earthquake. Each sheet contains data originally plotted in the field on 1:12,500 enlargements created from the Philippine DENR 1:50,000 topographic maps.

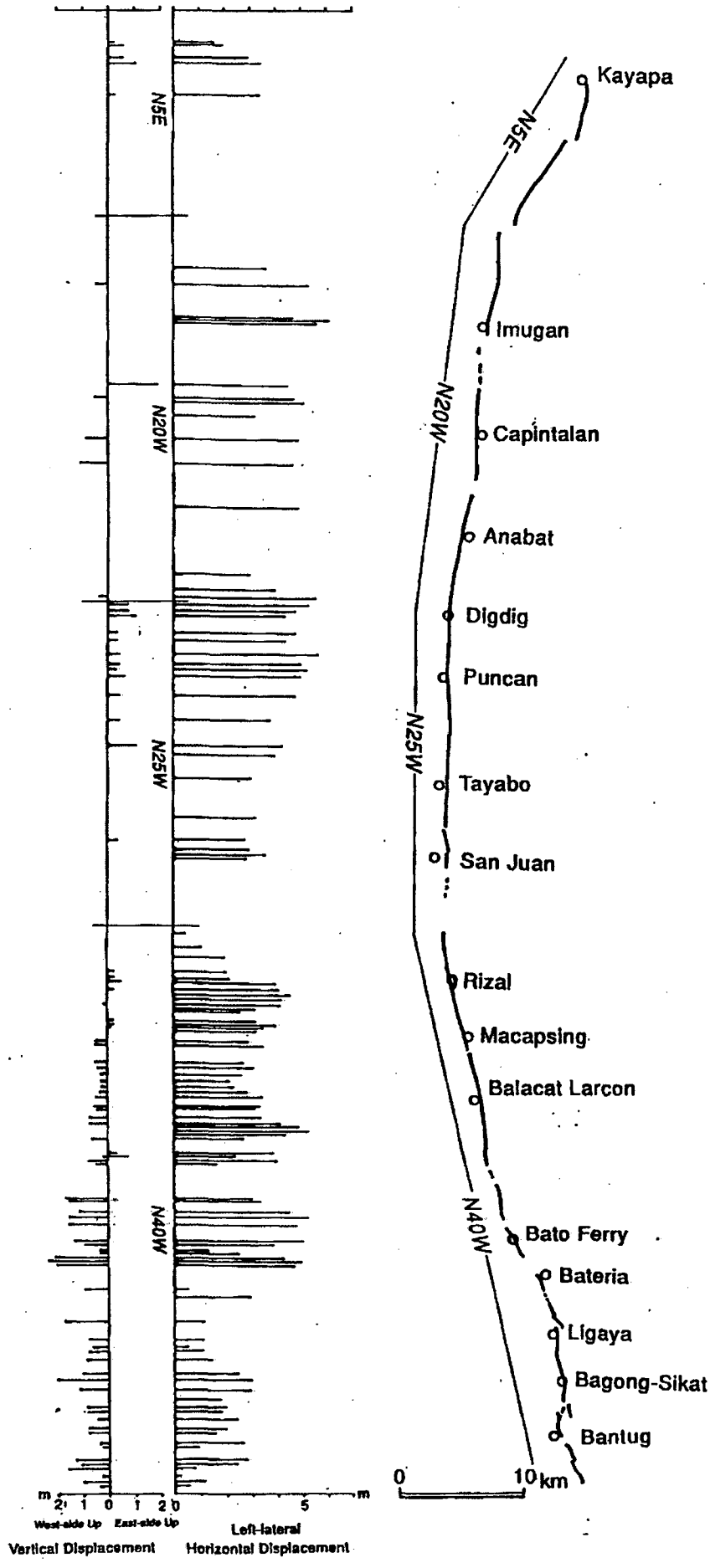

Figure 6.5 Horizontal and vertical displacements observed by *Nakata et al.* [1996] along the surface fault ruptures of the 1990 Luzon earthquake, Philippines.

Name	Lon (E) °	Lat (N) °	ITRF96 Ve mm/yr	ITRF96 Vn mm/yr	• Ve [b] mm/yr	• Vn [b] mm/yr	EU fixed [a] Ve mm/yr	EU fixed [a] Vn mm/yr
ABY3	123.676	13.477	-30.6	48.2	1.7	1.5	-54.3	47.8
ARX1	121.563	15.757	-54.7	39.9	3.7	2.5	-73.8	40.6
BLN4	121.044	15.190	-49.3	5.0	1.6	1.4	-69.5	12.5
CGY8	121.727	17.617	-63.5	46.0	1.4	1.2	-81.0	45.7
IFG1	121.052	16.921	-51.3	40.0	1.5	1.2	-71.1	40.7
LUN1	120.304	16.583	-39.5	14.2	1.6	1.4	-61.7	19.7
MANL	120.973	14.598	-39.4	1.4	1.2	1.2	-61.3	9.5
MMA1	121.040	14.537	-39.5	9.0	1.7	1.6	-61.4	15.8
MRQ1	121.869	13.560	-7.2	12.2	2.2	1.2	-35.5	18.6
NE44	120.970	15.492	-39.4	5.4	1.4	1.2	-61.5	12.8
NVY1	121.113	16.502	-51.7	49.5	1.9	1.6	-71.5	48.3
NVY4	120.907	16.159	-45.3	29.3	1.5	1.4	-66.3	32.0
PMX1	120.633	15.140	-35.4	4.6	1.5	1.4	-58.3	12.2
PNG5	120.254	15.868	-32.6	6.4	1.2	1.2	-56.1	13.5
QZN7	121.415	15.211	-51.5	23.9	2.0	1.9	-71.1	27.8
TRE2	120.426	15.323	-41.1	2.5	2.7	2.7	-62.8	10.3

[a] using EU-ITRF96 Euler vector from Table 6.2.

[b] The errors are standard errors, scaled by 1.5 to attempt to account for non-white noise in the GPS time series

Ve is velocity in the east component
Vn is velocity in the east component

Table 6.1 PICMP velocities in various reference frames

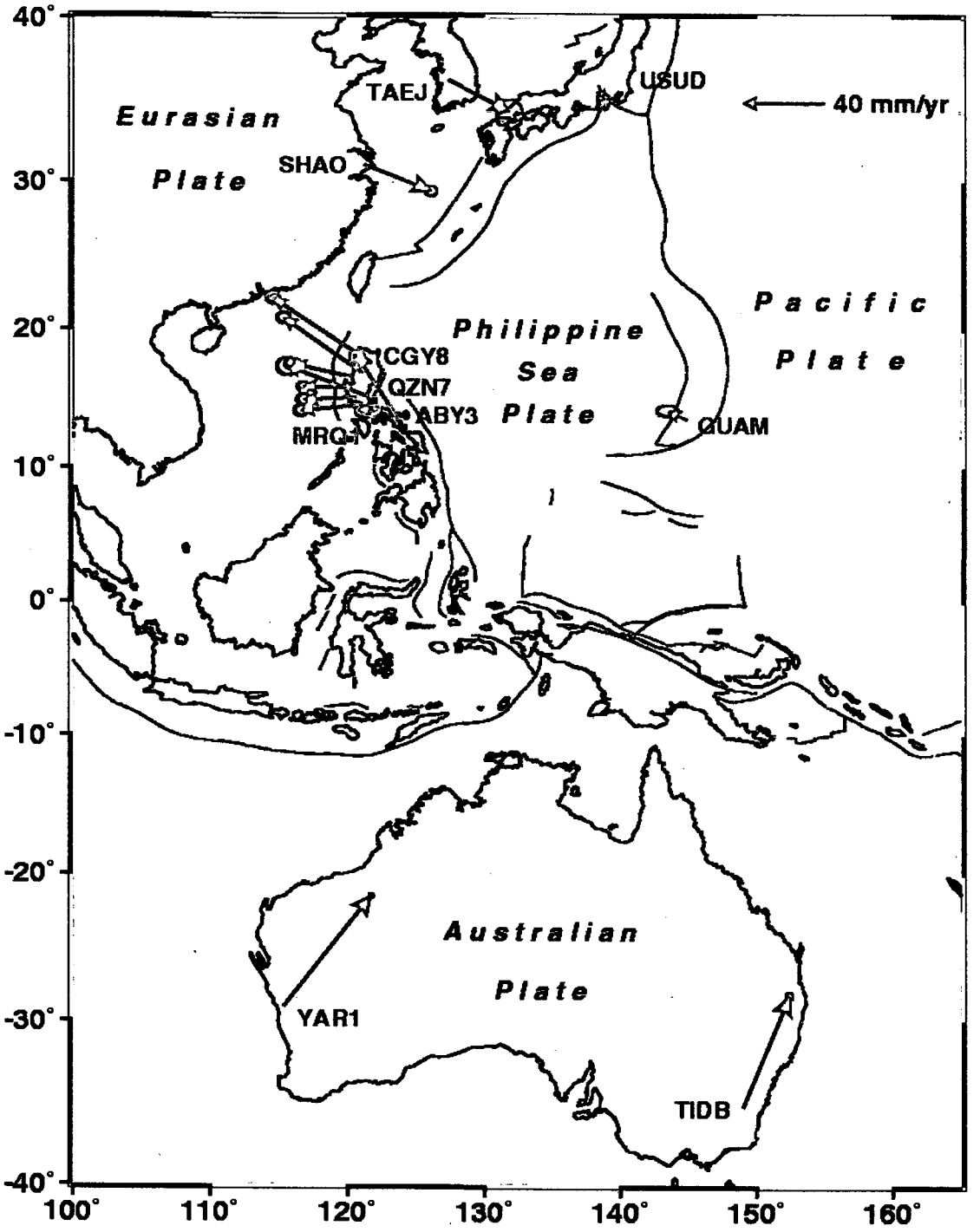

Figure 6.6 Velocities in the ITRF96 reference frame of the IGS stations that were used to define the reference frame (blue arrows), plus the velocities in this frame of a selection of the PICMP stations (red arrows). It should be noted that there is no differentiation of the Sunda and Amurian plates from the Eurasian on this figure. (This figure, initially shown in Chapter 1, has been reproduced due to its relevance to the tectonic analysis of the Philippines region).

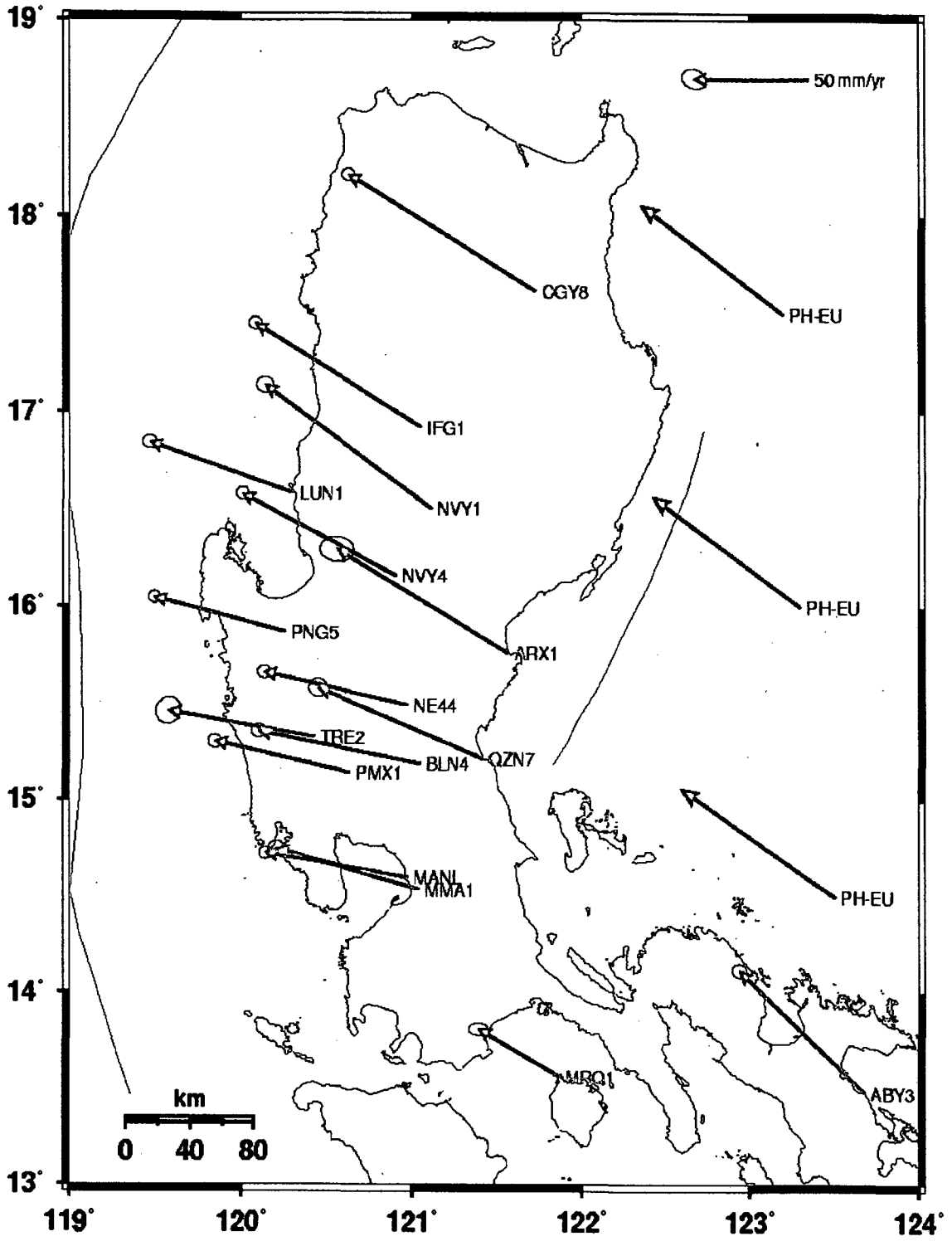

Figure 6.7 Velocities of the PICMP 1993-98 Luzon stations relative to stable Eurasia, using the EUR-ITRF96 Euler vector from Table 6.2 are shown in red. The PH-EU velocities from the *Seno et al.*, [1993] model are shown in blue.

NAME	DOMES NO.[a]	N residual mm/yr	E residual mm/yr
Misfits to best-fit Euler vector [b]			
NYAL	10317M001	-0.84	-1.31
HERS	13212M007	1.63	1.18
KOSG	13504M003	0.69	-0.23
MADR	13407S012	-0.38	-1.49
TROM	10302M003	1.66	1.3
WETT	14201M009	-1.25	-0.67
ONSA	10402M004	-0.73	-0.3
METS	10503S011	-2.04	0.89
MDVO	12309M001	-1.53	0.6
KIT3	12334M001	0.95	-0.48
IRKT	12313M001	-1.6	0.4
POL2	12348M001	2.38	0.37
RMS misfit		1.49	0.92
Velocities relative to stable Eurasia			
TAIW	23601M001	-2.67	11.98
SHAO	21605M002	-2.6	7.72
WUHN	21602M001	-3.37	8.86
TAEJ	23902M001	-5.69	7.58

[a] The DOMES number is a unique identifier for space-geodetic monuments, maintained by the IERS.

[b] The calculated Euler vector between ITRF96 and stable Eurasia is

rate	0.282°/Ma
latitude	61.5° N
longitude	-93.7° E

Euler vectors give the counter-clockwise rotation of the first-named plate relative to the second

Table 6.2 Euler vector between ITRF96 and stable Eurasia (EU)

6.4 Dislocation models of the 1990 Luzon earthquake

Jones [1991] undertook the preliminary earthquake analysis [see 2.6.2]. It was decided that the pre and post data files from the PGNet survey would be used as a starting point for the dislocation model of the 1990 earthquake.

6.4.1 Inversion of GPS surface displacement data

The following methodology was adopted:

1. the *Pre* data was abstracted from the original PGNet adjustment file collated prior to the 1990 event.
2. the *Post* data was obtained from the TRIMVEC baseline processing, and then
3. an independent free net adjustment (NEWGAN) was carried out on each data set to obtain coordinates based on the same local WGS84 datum (ie not the ITRF96 datum) and the weighted VCV matrices.

The coordinates of the pre and post data set can be found in Appendices 5 and 6 respectively.

The resulting standard errors in the 1990 pre- and post-earthquake surveys are quite large (0.1 - 0.2 m) compared to present-day accuracies attainable with dual-frequency GPS measurements. In addition, the worldwide GPS tracking network was in its infancy in 1990 so it is impossible to put the pre- and post-earthquake survey results into a consistent global reference frame.

The coordinates and covariances from these pre- and post-earthquake NEWGAN geodetic adjustments were then used as data to model the 1990 Luzon earthquake by uniform slip on a number of rectangular patches. There was no attempt to correct the data for steady interseismic motion between the two surveys, since any relative motion was likely to be less than 10 cm over the 18 months between surveys, whereas the estimated errors of the coordinates are on the order of 20 cm.

Firstly, the ADJCOORD program [*Bibby*, 1982; *Crook*, 1992] was used to solve separately for the coordinates of all pre-earthquake and all post-earthquake stations, holding one station fixed as a minimal constraint. The horizontal coordinates from each survey were then projected onto a local cartesian system (UTM zone 51N) and used to form an inner-coordinate displacement solution [e.g., *Prescott*, 1981] that minimises the displacements of all stations except those closest to the observed earthquake rupture. It is also necessary to solve for a scale change and rotation of the reference frame between surveys (Figure 6.8).

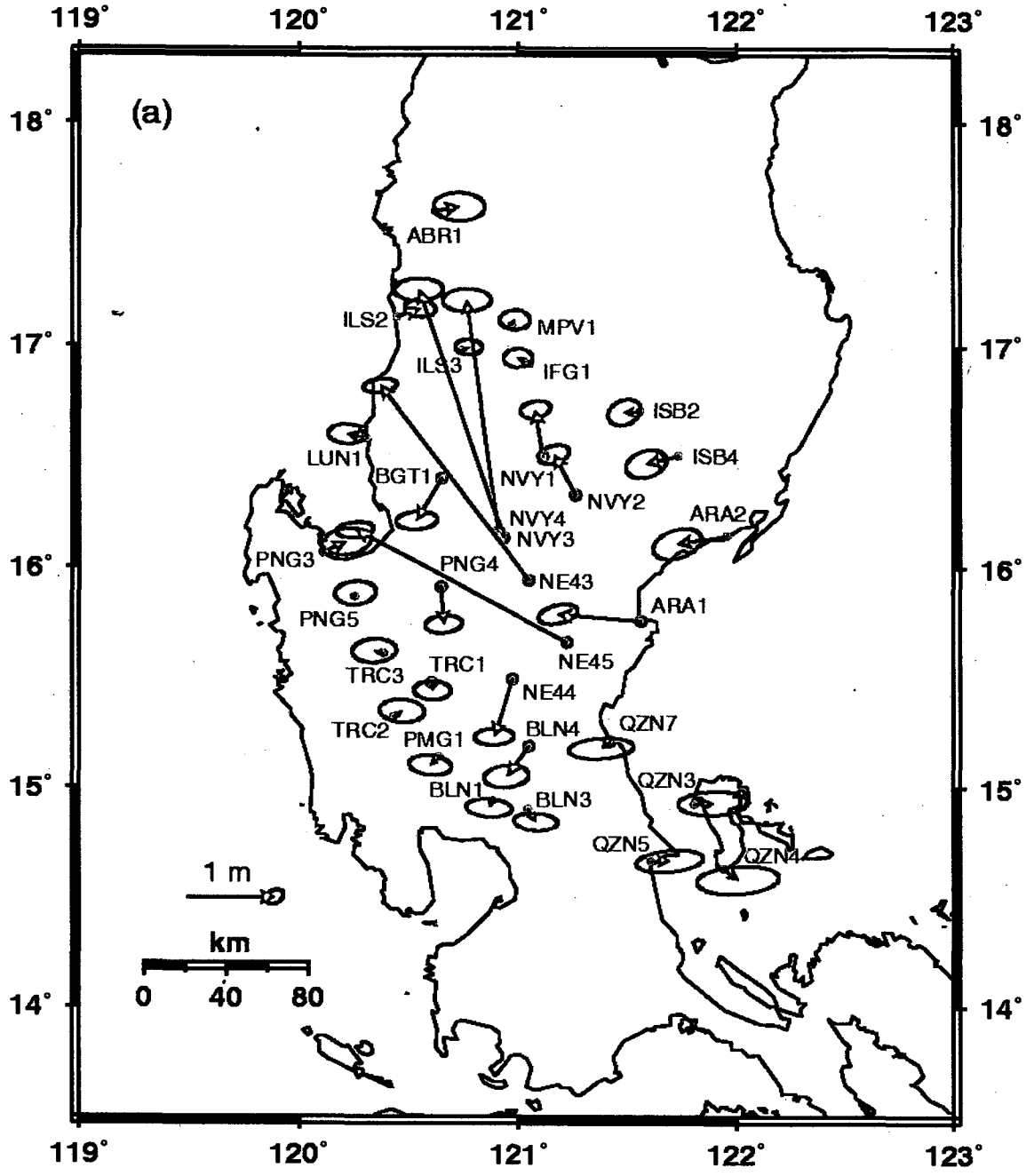

Figure 6.8 Estimated 1990 coseismic displacements derived from PGNet pre-earthquake and post-earthquake single-frequency GPS data, with 68% confidence two-dimensional error ellipses. (The linear dimensions of 95% confidence ellipses would be 1.62 times the linear dimensions of the 68% confidence ellipses). The reference frame is chosen by minimising the RMS velocities of stations far from the rupture and solving for a scale change, rotation and mean displacement between surveys. Stations NVY1, NVY2, NVY3, NVY4, NE43, NE44, NE45, ARA1, BLN4, QZN7, PNG4, TRC1 and BGT1 are not included in the minimisation.

In this analysis, station ABR1 in the north and stations QZN3, QZN4 and QZN5 in the southeast show displacements larger than other stations closer to the earthquake rupture (e.g., ILS3, MPV1, IFG1 in the north, and BLN1, BLN3, QZN7 in the south). It seemed apparent that the four stations were affected by distortions in the GPS solutions (most probably in the pre-earthquake solution) that were totally unrelated to the earthquake and so these four stations were omitted from the earthquake modelling. Computations showed that these omissions made little difference to the derived earthquake fault parameters

Using the surface displacement data, a non-linear least-squares inversion [*Dennis et al.*, 1981a,b; *Darby and Beavan*, 2001] was then carried out to:

- determine a model consisting of one or more uniform-slip rectangular dislocations buried in an elastic half-space of equal Lamé constants [*Chinnery*, 1961; see also *Okada*, 1985 and *Cohen*, 1999], and
- retain the full variance-covariance matrix of the data

The preferred solution (Model *M4a*) is shown in Figure 6.9 and explained in Section 6.4.2.

In Figure 6.8, a group of stations was constrained to determine the translation, rotation and scale of the post-earthquake survey relative to the pre-earthquake survey. However, given the earthquake displacements and the known uncertainties in the surveys (particularly the pre-earthquake survey) it was felt that the rotation, scale and translations determined by that method were not optimal. Therefore, the transformation parameters (i.e. the rotation, scale and horizontal translations) were allowed to be additional unknowns in the dislocation inversion. Relative to the reference frame in Figure 6.8, the reference frame in Figure 6.9 has thereby been shifted by 65 mm south and 203 mm west, and is rotated and scaled by –1.5±0.6 μrad and –0.3±0.5 ppm, respectively, where 1 sigma uncertainties are quoted. These were quite reasonable values given the various uncertainties in data and reference frame.

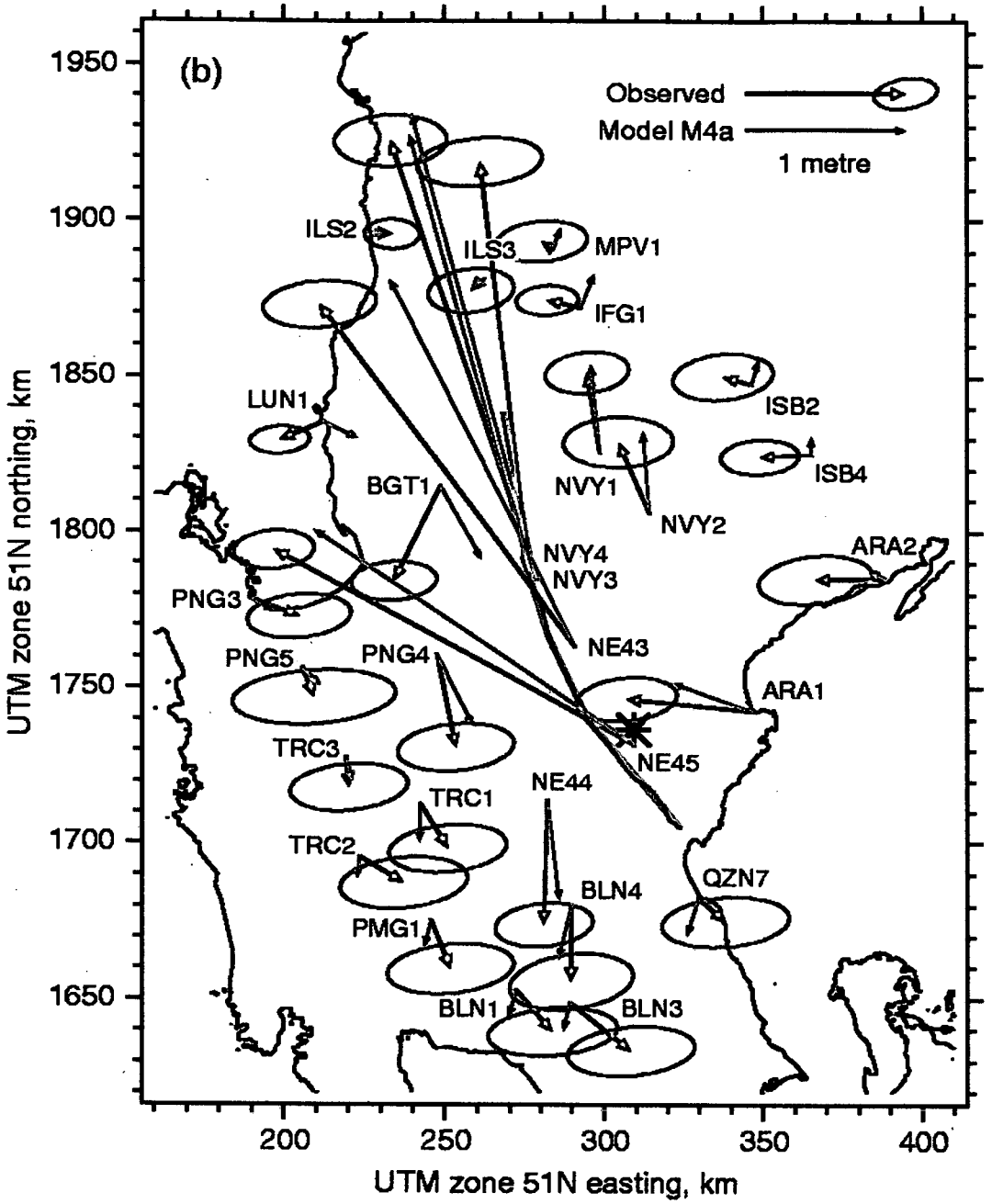

Figure 6.9 Estimated displacements (thick blue arrows with 68% confidence 2-D error ellipses) and dislocation model ***M4a*** discussed in Sections 6.4.2 (thin red arrows). A rotation and displacement of the reference frame are solved for during the dislocation inversion, so the reference frame is slightly different from that shown in Figure 6.8.

6.4.2 Dislocation modelling and analysis

The modelling was an iterative process. It was not possible to find a single rectangular dislocation that fits the data, which is not surprising in view of the curved nature of the observed surface trace plus the close proximity (~400 m) of some of the geodetic stations to the trace. Experiments with two or more unconstrained dislocations were also unsuccessful because of the limited amount of data and the relatively large errors in the observed displacements. Therefore, the surface trace of the model dislocation was constrained to closely follow the observed surface trace of the fault as shown in Figure 6.2.

An investigation into the possible northern extension of the mapped fault

Table 6.3 shows the principal details of the various fault models for the 1990 Luzon earthquake.

The observed trace was initially fitted with three dislocation patches (ie 1, 2 and 3 on Figure 6.2) from a few km south of Gabaldon to a few km south of Kayapa. These patches were very similar to the three southern sections of *Nakata et al.* [1996]. In the first trial, the bottom of the faulting was fixed at 20 km, and the data was inverted for uniform slip on each of the three fault sections (model *M1a*).

Then a less-constrained fourth fault section was allowed north of Kayapa, where rupture was considered to have occurred but no detailed post-earthquake field mapping observations were made (ie patch 4 in Figure 6.2). In addition to solving for slip on patches 1, 2 and 3, the uniform slip, length, strike, rake and northing (north component of position) of patch 4 were solved for, while fixing the fault bottom to 20 km, its dip to 80° west, and also fixing its easting (model *M1b*). In model *M1b*, the steep dip to the west was based on a number of tests with varying dips, while fixing the easting allowed some variation in the length and position of fault patch 4 without letting it be entirely free. An F-test on the weighted sum of squared residuals (WSSQR) from these inversions was used to determine whether the addition of the fourth patch significantly improves the solution (see Table 6.3).

Model	Slip magnitude, fault patches 1-7				Parameters for fault patch 4			Bottom depth fault patches 1-7							
	1 5 m	2 6 m	3 7 m	4 m	*length* *km*	*strike* °	*rake* °	1 5 km	2 6 km	3 7 km	4 km	M_0	*SS*	*P* %	*Ref*
Can a northern fault segment be detected?															
M1a	5.4±0.4	6.1±0.4	5.8±0.4	-	-	-	-	20	20	20	-	3.5	261	-	-
M1b	5.5±0.3	5.5±0.3	6.4±0.3	3.6±1.0	50±10	170±2	38±15	20	20	20	20	4.6	114	99.99	M1a
Can slip below 10 km be detected?															
M2a	7.0±0.4	7.4±0.4	7.1±0.5	7.6±2.1	47±8	169±2	26±20	10	10	10	10	3.3	170	-	-
M2b	7.0±0.4	7.4±0.3	7.1±0.5	7.6±1.0	47	169	26	10	10	10	10	3.3	170	-	-
M2c	6.0±0.9 -0.6±7.8	4.4±0.7 17±7	6.2±0.4 14±4	4.1±1.6	47	169	26	10 15	10 15	10 20	12±7	4.3	106	99.97	M2b
M2d	6.1±0.7 -0.3±4.0	5.2±0.6 8.5±3.8	6.4±0.4 9.5±3.0	4.7±1.7	47	169	26	10 20	10 20	10 25	11±6	4.4	112	99.91	M2b
Can slip below 15 km be detected?															
M3a	6.0±0.3	6.1±0.3	6.7±0.4	5.0±1.4	47±8	170±2	32±15	15	15	15	15	3.9	130	-	-
M3b	6.0±0.3	6.1±0.3	6.7±0.3	5.0±0.6	47	170	32	15	15	15	15	3.9	130	-	-
M3c	5.5±0.4 -	5.2±0.4 10±7	6.3±0.3 19±8	3.9±0.7	47	170	32	15 -	15 20	15 20	15	4.6	106	98.9	M3b
M3d	5.5±0.4 -	5.4±0.3 5.5±4.1	6.4±0.3 8.8±4.8	4.1±0.7	47	170	32	15 -	15 25	15 25	15	4.7	109	98.1	M3b
Comparing unconstrained northern extension against favored model															
M4a	**6.0±0.3**	**5.8±0.3**	**6.5±0.4**	**4.6±1.3**	**49±9**	**170±2**	**40±15**	**12.5**	**20**	**20**	**15**	**4.1**	**113**	-	-
M4b	6.0±0.3	5.8±0.3	7.6±0.4	6.0±1.5	38±1	133±1	65±5	12.5	20	20	15	4.3	86	99.9	M4a

Parameters for each fault patch (1, 2, 3, 4) are given from south to north, and are labelled as in Figure 6.2. Patches 5, 6, 7 are down-dip extensions of patches 1, 2, 3, respectively.

Entries with associated standard errors are solved for, others are fixed. The quoted uncertainties are the formal standard errors scaled by the square root of WSSQR/dof.

M_0 (the total geodetic moment) is derived from the slip, length and width of the individual fault patches assuming a rigidity of 3×10^{10} Pa. It is given in units of 10^{20} N m.

SS is the weighted sum of squared residuals (WSSQR) of the model fit to the data, and is referred to as WSSQR in the text.

P is the probability level at which the model is statistically superior to the reference model listed in the final column ("Ref")

dof means degrees of freedom

Table 6.3 Summary of determined dislocation models of 1990 Luzon earthquake (These models are fully explained in Sections 6.4.2)

The reduction in WSSQR was significant at better than 99.99% probability. The modelled slip is 3.6±1.0 m with a rake of 38°±15° on a fault section of length 50±10 km striking 170°±2° (the low uncertainty in strike is because of the partial constraint mentioned above). Thus there is a significant thrust component as well as strike slip on the northern extension of the fault. The rupture on patch 4 was modelled reaching the surface, but the data are not sensitive to whether the rupture actually reached the surface or simply to within a few km of the surface.

The detection of depth of slip on the fault plane

Current methods for the inversions of high quality deformation data for the spatial distribution of coseismic fault slip include

- splitting the inferred fault plane into many small elements and then,
- solving for the slip on each element, subject to some smoothing constraint to overcome the under-determined nature of the problem

  [e.g., *Segall and Harris*, 1987].

However, a simpler approach was adopted for this inversion. The procedure was as follows:

1. find the best solution with the fault bottoms fixed to a certain value D1
2. keeping the geometry and slip directions fixed, a down-dip extension of the fault between depths D1 and D2 was added
3. then solve for the slip magnitude on both the shallow and deep patches (no smoothing constraints were applied in the inversion), and finally
4. use the F-test to determine whether inverting for slip on the deep patches significantly improved the solution

The results from testing the various dislocation models were:

1. For D1 = 10 km the best solution was model *M2a*. Keeping the geometry of this model constant the four shallow slips only were inverted, to give model *M2b*. Then *M2b* was used as the basis against which to compare more complicated models. In model *M2d* inversion was also for deep slip between 10 - 20 km on fault sections 1 and 2, and 10 - 25 km on section 3. Other restraints included:

    - rather than adding a deep extension beneath section 4 the bottom depth was solved for.
    - a deeper D2 on section 3 was used in order to keep its slip magnitude at a reasonable level (compare model *M2c* which has D2=20km).

    Deep slip was detected on sections 2 and 3, but not on sections 1 and 4. The reduction in WSSQR between models *M2b* and *M2d* is significant at better than 99.9% probability, demonstrating clearly that slip below 10 km is required by the data, at least on fault sections 2 and 3.

2. For D1 = 15 km the best solution was Model *M3a*, while model *M3b* was an inversion for the four shallow slips with the other parameters of *M3a* held fixed. Also two other models were inverted, where:

    - in model *M3c*, slip was solved for between 15 - 20 km depths on fault sections 2 and 3, plus
    - in model *M3d*, slip was solved for between 15 - 25 km depths on fault sections 2 and 3.

The reduction in WSSQR between model *M3b* and either *M3c* or *M3d* was significant at better than 98% probability, making it likely that slip occurred below 15 km on the central fault sections, 2 and 3. The derived deep slips for model *M3c* are very high, suggesting that slip may have occurred throughout the 15 - 25 km depth range.

3. However, a similar test to the *M2* and *M3* tests using D1 = 20 km and D2 = 25 km did not find statistically significant improvement to the solution when slip below 20 km was added to the model.

4. Finally, model *M4a* combined the statistically significant improvement information gained from the previous inversions into a model with just four uniform-slip fault patches. The maximum depth of faulting was set to 12.5 km on section 1, 20 km on sections 2 and 3, and 15 km on section 4.

Other fault parameters

Unfortunately, the data cannot be used to solve for many additional fault parameters other than those described above. Numerous inversions were attempted to solve for the dip and rake on the southern three sections of the rupture but were unsuccessful. The -20° rake on the southern mapped section was chosen because constraining this rake to 0° always gave a significantly poorer fit to the data. A rake of -20° on a 320° striking fault implies relative vertical displacement down to the northeast. This section of the fault was the only one on which consistent vertical displacement was observed [*Nakata et al.*, 1990, 1996; *Newhall et al.*, 1990], with displacement down to the northeast as in our model.

It was also attempted to let the position of the northern extension (patch 4) be completely unconstrained, by solving for the easting as well as the northing of the centre of the fault patch. The tendency in this solution was for the northern extension to trend more northwesterly and for the slip to become more nearly pure thrusting. Interestingly, when allowed to be completely free (see model *M4b*), the far end of patch 4 was close to station BGT1, with the model fault evidently tending to this

position in order to reduce the large displacement residual at this station. While this model appeared to be significantly better than *M4a* (see Table 6.3), the improvement was coming entirely from the single station BGT1 and so model *M4b* may not be a reliable solution. Therefore, it was preferred to constrain fault patch 4 to have a more northerly strike as this tended to agree better with existing fault maps [e.g., *Philippine Bureau of Mines*, 1963]. However, it is still possible that the northern extension of the 1990 rupture did run northwest toward BGT1, and that this could help to explain the high level of coseismic damage experienced in Baguio City [*Newhall et al.*, 1990].

In general the solutions for the northern extension require between 4 and 5 metres of slip and a rake of 25° to 40°, implying oblique thrusting with the west side upthrown, consistent with the tectonics in this region [*Barrier et al.*, 1991; *Bureau of Mines and Geosciences*, 1982].

All the models analaysed find a right-stepping jog (see Figure 6.2) between the northern mapped section of the fault and the northern extension, consistent with geological maps of the faults in this area [*Philippine Bureau of Mines*, 1963]. The strike of the northern extension is calculated as 169° - 170° in our modeling, but this is constrained by the right-stepping jog favoured by the available data and by the fact that the easting of the fault was fixed. By fixing the easting to a smaller value (i.e. further west), the strike would be correspondingly more counterclockwise, as shown in model *M4b*).

The preferred dislocation model for the 1990 earthquake

The preferred model is *M4a* where the bottom depths adopted for the faulting was based on the earlier inversion tests (see Table 6.1 and Figure 6.9). The rake is set to -20° on section 1 of the fault, and to 0° on sections 2 and 3, and the slip on each of these sections was solved. It was possible to solve for the slip, rake, strike, length and northing of the northern extension, but the dip was fixed to 80° and where the easting was constrained so that the fault runs slightly west of due north from the end of the mapped rupture.

The results (see Table 6.3) are:

1. 5.9±0.3 m of slip on the southern two sections and 6.5±0.4 m on the northern mapped section
2. the northern extension, with its dip fixed at 80°, extends for ~48 km with 4.6±1.3 m average slip, strike 170°, and rake 40°, implying convergence with the west side upthrown in addition to right-lateral strike slip motion
3. the reduced χ^2 statistic (WSSQR/dof) of the solution is 2.6 (showing that there remain substantial misfits of the model to the observed displacements, which may be attributed to the relatively low quality of the single-frequency GPS data as well as to inadequacies of the model)
4. the inferred fault displacements are consistent with the observed surface rupture, with the maximum model slip occurring on the northern mapped section in agreement with field observations [*Nakata et al.*, 1990, 1996; *Newhall et al.*, 1990]

6.4.3 Discussion

From the coseismic modelling plus other observations, it can be stated confidently that ~150 km of the Philippine and Digdig faults ruptured in the 1990 earthquake. This was with quite uniform and predominantly left-lateral slip of 5.5 - 6.5 m, decreasing to 4 - 5 m on the northern ~45 km of the rupture. The dislocation models presented resolve the average slip on the mapped part of the fault quite accurately, with standard errors of ~0.4 m (and > 1 m on the northern extension) after scaling by the square root of the reduced χ^2 statistic of the fit. Also the inferred slip agrees closely with the maximum mapped fault offsets (see Figure 6.2).

Faulting north of the mapped surface rupture had been suspected [*Newhall et al.*, 1990; *Nakata et al.*, 1996], and the geodetic data implied that the rupture propagated into the Cordillera Central mountains ~45 km beyond the mapped rupture. There is a significant thrust component on this section, with the west side upthrown in accord with the contractional tectonics of the region.

On the remainder of the rupture (fault sections 1-3) slip is nearly pure left-lateral strike slip on a near-vertical plane. However, there is a significant vertical component on the more NW-SE trending southern 45 km of the fault (section 1), in accord with the observed subsidence to the northeast in this region. The contractional component at the north end and the extensional component at the south end of the rupture are also consistent with the curved geometry of the fault trace.

It was confidently resolved that the maximum depth of faulting is 10 km or greater all along the fault. Faulting depths significantly greater than 15 km are required along the central sections (2 and 3) of the fault, and it cannot be discounted that significant slip below 20 km may have occurred on these two sections. This result is consistent with the 25±0.6 km hypocentral depth inferred by the ISC from pP-P phases, and with the 20 km estimate based on well-located aftershocks [*Newhall et al.*, 1990; *Yoshida and Abe*, 1992].

The 20 km or greater depth of slip on the central section of the fault is unusually deep for a continental strike-slip earthquake. *Yoshiba and Abe* [1992] find inferred faulting depths of 10 - 15 km in the literature for four other such earthquakes of $M_s >$ 7.5. The Luzon post-earthquake survey was undertaken 4 - 9 months after the earthquake. As a result, afterslip may have occurred on the down-dip extension of the coseismic rupture during that period.

It is of interest that the epicentre is close to the junction between fault patches 1 and 2, since the preferred model suggests that faulting to the south of the epicenter terminated at substantially shallower depth than faulting to the north.

Yoshida and Abe [1992] used body-wave inversion to estimate locations and sizes of subevents during the coseismic rupture. The sequence was as follows:

1. a small subevent near the epicentre
2. the major moment release propagated northward along the central section of the fault
3. two smaller subevents further north, and
4. finally a modest subevent near the southern end of the fault.

The release of the majority of the moment on the central section of the fault is consistent with this section having the deepest slip, either as a result of deep slip during the coseismic rupture or as afterslip induced by coseismic stress changes.

The geodetically determined moment of model *M4a* is 4.1×10^{20} N m. This value is modestly higher than the seismologically determined moment, 3.9×10^{20} N m, of *Yoshida and Abe* [1992], and is in close agreement with the Harvard determination. Some of the other appealing dislocation models have moments up to 20% larger than the seismically determined moment, however none are smaller. A larger geodetically determined moment is not unusual for an earthquake of this size, since there may be slow deformation that is not detected seismically (e.g., the afterslip discussed above) and because there may be a contribution from aftershocks.

6.5 Observed deformation following the 1990 earthquake

During 1999 the PICMP93, 96 and 98 GPS campaigns were processed and the coordinates and velocities of each campaign placed into the ITRF96 reference frame. A preliminary analysis of the observed deformation following the 1990 earthquake was also undertaken as part of the collaborative research.

Beavan continued this research into post-seismic deformation (elastic plus viscoelastic models) and regional tectonics using additional data from the PSP94 campaign. *Beavan et al.*, [2001] present these results and explain:

1. the generation of horizontal velocity fields at the Earth's surface for the 1993-96 and 1996-98 periods
2. how these velocities, plus 1996-98 GPS velocity results reported by *Yu et al.* [1999] (ie 13 additional stations in Luzon) were used, to show that present-day deformation in Luzon is dominated by strike-slip motion along the Philippine fault system
3. how the measured strike-slip rate across central Luzon is faster than the expected long-term slip rate on the fault, which is then attributed to

postseismic deformation following the 1990 earthquake

4. that the 1993-96 and 1996-98 deformation patterns can be interpreted using an elastic half-space model with uniform slip below a sub-surface locking depth, resulting in:
   - a fault slip rate of 40 mm/yr (too fast to be a steady interseismic rate as it disagrees with what is known from paleoseismic and other evidence about earthquake recurrence and long-term slip rate on the Philippine fault system in central and northern Luzon)
   - and a locking depth of ~15 km for steady interseismic slip (probably too shallow compared to the depth of rupture in the 1990 earthquake)

5. that the deformation can also be interpreted with two types of viscoelastic models and that the observed velocities fit well for a range of values of lower lithosphere viscosity and long-term slip rate e.g., for a 2D viscoelastic coupling model, the minimum allowable lower lithosphere viscosity is 0.5×10^{19} Pa.s, with an associated long-term slip rate of 15 - 22 mm/yr
6. other implications of the computed 1993-98 surface velocities to regional tectonics e.g., the Philippine Sea-Eurasia (PH-EU) plate motion and convergence rates estimated from the GPS velocities

Differences in the final PICMP93 (ITRF96) coordinates

Beavan et al., [2001] show a slightly different set of PICMP93 (ITRF96) coordinates from those used for the readjustment of the PGNet described in Chapter 5 (i.e. those shown in Table 4.3). This is simply explained since *Beavan et al.*, [2001] used the additional PSP94 GPS data. Thus, the new coordinates were obtained by propagating back to April 1993 the final coordinates and velocities from the least squares filtering procedure of the 1993-94-96-98 data.

The coordinates would be expected to change slightly when introducing additional

data (ie the 1994 data) and changing the reference stations. (TAIW was omitted as a reference station in *Beavan et al.*, [2001] but was used in the earlier calculations in Chapter 4.0). The two sets of coordinates do not differ by more than two standard deviations, and much of the difference is a uniform shift of about 0.0006" in latitude, -0.0005" in longitude, and 0.015 m in height. The uncertainty estimates relative to the ITRF96 reference frame are smaller in the earlier calculation. The uncertainties shown in Table 4.3 are relative to the ITRF96 reference frame, rather than relative errors within the regional survey. The errors in relative coordinates within the Philippines are only about half the size.

It should be noted that even with much higher quality data of recent surveys, different analyses disagree at the centimetre level in "absolute" coordinates. Consequently, standard errors of a few cm relative to ITRF96 seem quite reasonable given that in the PICMP93 campaign squaring receivers were used and observation sessions were only about 12-hours in length.

As a result there were slight differences in the two analyses and the coordinate differences are within the expected range.

6.5.1 Preliminary post seismic elastic modelling

As an ending to this Chapter, a summary of the elastic modelling of the post-seismic deformations that were commenced in 1999 will be presented. The final research and analysis shown in *Beavan et al.*, [2001] is beyond the scope of this thesis. However, the initial elastic modelling results are of interest to demonstrate the connection between this thesis and the ongoing research.

NB The PICMP93 (ITRF96) coordinates calculated in Chapter 4 were used for these preliminary computations and not the ones used by *Beavan et al.*, [2001].

Modelling sequence for the 1993-98 deformation

1. The generation of horizontal velocity fields at the Earth's surface in Luzon for the 1993-96 and 1996-98 periods.

- The ADJCOORD software (previously described) was used to solve simultaneously for the coordinates and velocities of all the Luzon stations observed in the 1993-1996 interval (see Figure 6.10), and then in the 1996-1998 interval (see Figure 6.11). The PGNet geodetic station (CGY8) in the northeast of Luzon was held fixed as a minimal constraint with full covariance information being retained throughout the inversion.
- The 1993-1996 and 1996-1998 horizontal velocity solutions were projected into UTM zone 51N for dislocation modelling. The reference frame is therefore orientated to ITRF96, but with a translation applied in order to set the velocity of station CGY8 to zero.
- In the initial modelling, the velocities were left in a frame rotating with ITRF96, while solving for the azimuth of the model fault

2. The 1993-96 and 1996-98 velocities were then modelled using the dislocation method first described by *Savage and Burford* [1970, 1973] in which uniform steady slip is applied to a vertical strike slip fault below a locking depth. Rather than a forward model, the data were formally inverted using the same non-linear least-squares algorithm described earlier.

- The data were quite sparsely distributed and so not all of the fault parameters could be solved for. It was therefore assumed based on the observed 1990 coseismic deformation that it is possible to adopt a single, long, strike-slip fault slipping at a steady rate below the locking depth.

- The long model fault was used for simplicity, and was an adequate assumption to estimate slip rate and to test the velocity data for changes in slip rate with time. Also, only a single, planar fault was adopted despite the facts that the Philippine fault splits into several splays in central Luzon and that the surface trace of the 1990 rupture was substantially curved. Modelling was for the slip rate at depth, rather than coseismic slip cutting the surface and

therefore the displacements at surface stations were less sensitive to details of the fault model, including the precise position of the slipping fault

- The above assumptions were supported by the fit of the models to the data. For the **preliminary** elastic model, 90° dip and 0° rake were assumed (from the slip parameters for the coseismic model already described). Also the projection of the fault plane of the model was constrained to cut the surface at the 1990 earthquake fault trace near its 1990 epicentre. The slip rate, the locking depth and the strike of the fault model was then solved for. Figures 6.10 and 6.11 show the dislocation models for 1993-96 and for the 1996-98, respectively.

Results and Discussion

Table 6.4 shows the preliminary results for the postseismic slip rate interpreted using an elastic half-space model with uniform slip below a sub-surface locking depth.

Period	**Slip Rate** mm/yr	Locking Depth km	**Strike** degrees	**Dip** degrees
1993-96	40.2 ± 7.7	15 ± 14	152 ± 5	96 ± 25
1996-98	38.8 ± 5.4	14 ± 10	151 ± 2	85 ± 14

Table 6.4. Elastic dislocation model results for post-seismic/inter-seismic slip on the Luzon Philippine fault system

The mean fault slip rate for the entire 1993-98 period is ~40 mm/yr with a mean locking depth of ~15 km. The results show that the locking depth has been poorly constrained. Also it is clear that the slip rate is almost constant over that time.

This high rate is unlikely for several reasons. It implies a repeat time of about 120 - 150 years for 6-m displacement earthquakes, yet at least 300 - 400 years elapsed between the 1645 earthquake and the 1990 event, and between the ~1300 event and 1645 [*Daligdig*, 1997].

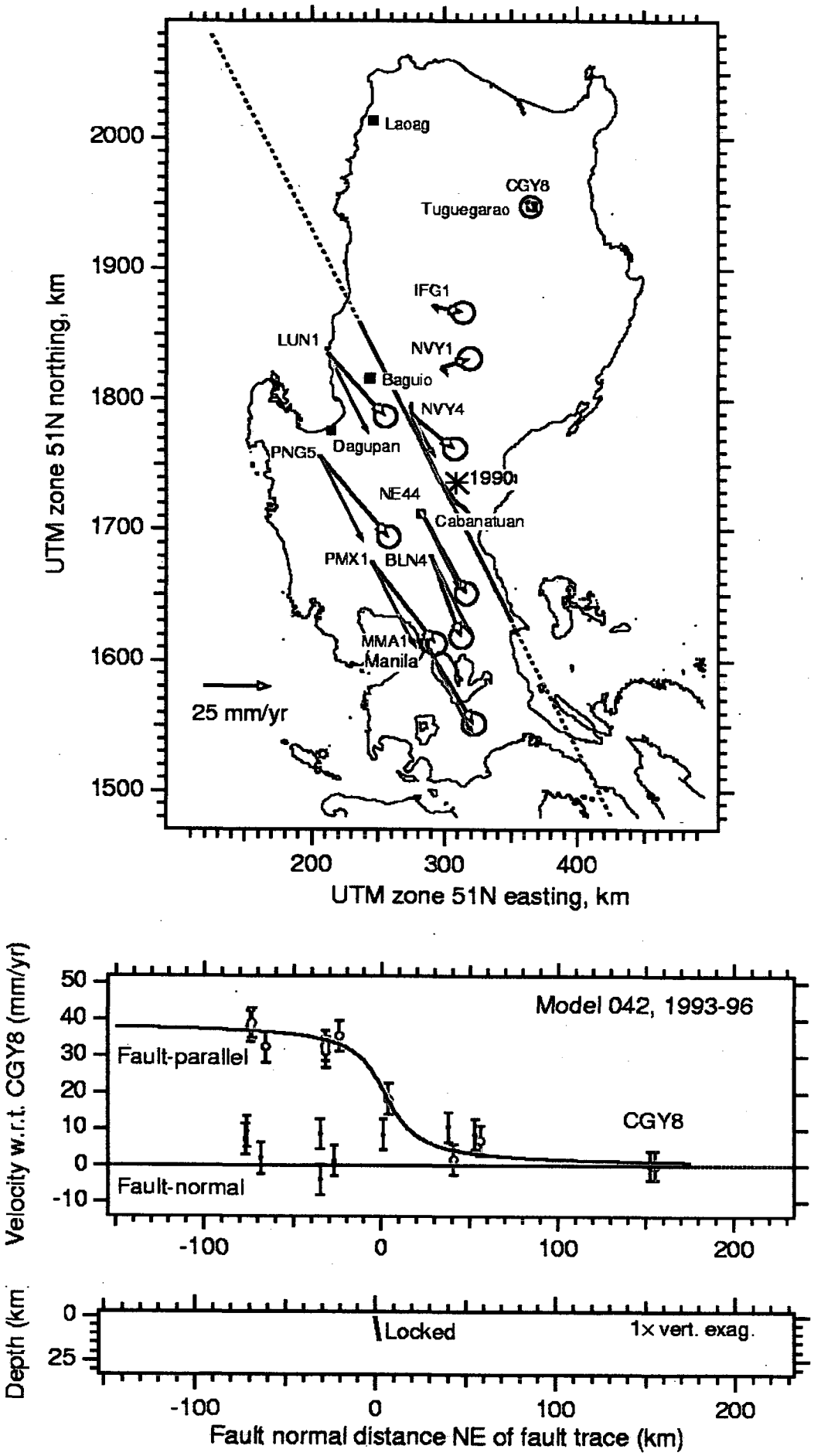

Figure 6.10 1993-96 Elastic dislocation model for post-seismic/inter-seismic slip *Beavan et al.*, [2001]

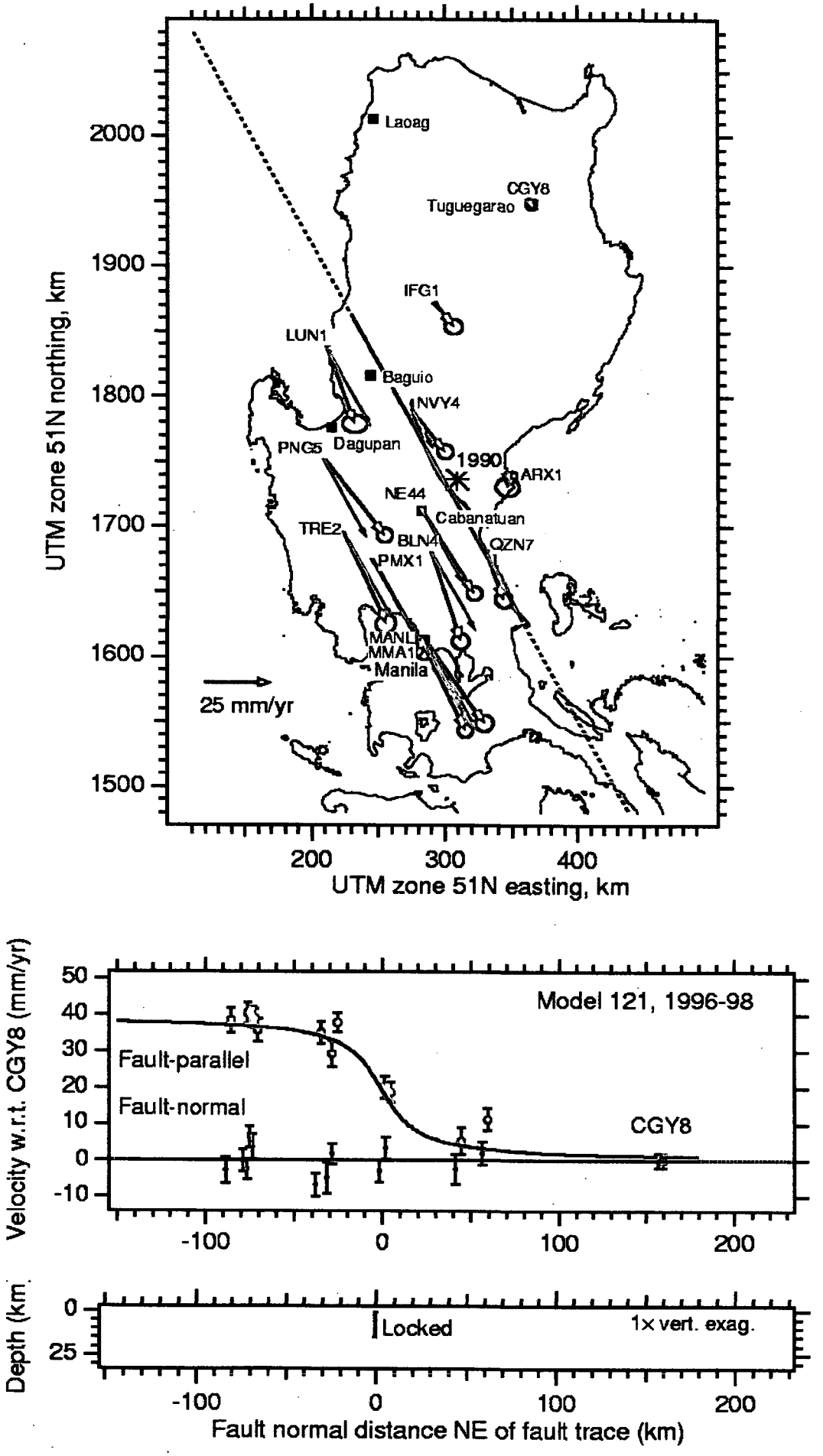

Figure 6.11 1996-98 Elastic dislocation model for post-seismic/inter-seismic slip *Beavan et al.*, [2001]

7.0 Comments and Conclusions

7.1 Objectives Achieved from the Research

The main objectives of this research was to 1) develop a crustal motion-monitoring program in the Philippine Islands using GPS technology, and 2) to carry out preliminary analyses of the geodynamics in Luzon and the region.
The overall results can be summarised as follows:

- The PICMP93 has provided a high quality "fiducial" network that can be used as a basis for these future crustal motion studies.
- The lower-order PGNet, done under the 1989-91 NRMDP, was readjusted onto the PICMP93 (ITRF96) fiducial network to enhance the accuracy for geodynamic purposes.
- The PGNet single-frequency GPS measurements taken before and after the 16 July 1990, M_S 7.8, Luzon earthquake were used to determine the geodetic constraints on the coseismic rupture.
- The PICMP 93, 98 and 98 campaign data are used to determine initial postseismic information on the 1990 Luzon earthquake and also regional tectonics over the period.

The results of this research provide a strong framework for ongoing crustal motion studies in the Philippines to help develop an understanding of the kinematics of the region.

7.2 Summary of the Thesis Findings

7.2.1 The NRMDP PGNet

Chapter 2 detailed thoroughly the establishment of the Philippine geodetic datum between 1989-91 under the NRMDP. The geodetic survey of the Philippines was an extremely ambitious exercise at that time due to the poor satellite geometry available at this early stage of the GPS constellations. It was the first major national first order survey undertaken anywhere in the world with the then *new* GPS technology Also, the GPS field operation coincided with the eleven year solar cycle maximum.

Unfortunately, the PGNet surveys used mostly single-frequency GPS receivers during the high ionospheric activity between 1989-91. This caused severe logistical problems in the field due to data loss and also complicated the GPS baseline processing.

The PGNet, adopted for the PICMP research, includes the 330 GPS survey stations of the primary geodetic network of the Philippines. A total of 467 survey stations were established as the geodetic component of the AIDAB funded NRMDP but these included those established for pilot areas and mapping control points. The GPS surveys (1988-91) were done area-by-area with overlapping stations between areas, and stations were observed multiple times.The accuracy standard adopted for the PGNet contract was 10 ppm for first order surveys (1 standard deviation). Overall, 55% of baseline lengths were < 50 km and most of the rest were < 70 km.

The GPS data were were processed as independent baseline vectors, generally using triple-difference processing, but with bias-fixed double-difference processing on some of the shortest lines.

The baselines were then combined in a geodetic least-squares adjustment using the program NEWGAN.

The July 1990 M_S 7.8 earthquake occurred as the PGNet of the Philippines was being completed. A section of the network in central Luzon was remeasured over a period between 4 and 9 months after the earthquake

Although the NRDMP geodetic component was highly successful and indeed innovative for that time, the final PGNet had limited use for geophysical interpretation such as tectonics. An overall PGNet precision of about 3 ppm was achieved and an investigation was made to improve this to a more useful 1ppm.

The existing Clarke 1866 spheroid horizontal datum was retained and the vertical datum was slightly modified by the adoption of a more realistic value of the geoid/spheroid separation at the origin in order to minimise the separation over a wide area. A new set of coordinates for stations established and integrated as part of the geodetic survey has been adopted and is referred to as the Philippine Reference System 1992 (PRS92).

7.2.2 High Precision GPS for Geodynamics

Commercial GPS software is suitable for general survey applications including first order geodetic networks. However for very high precision GPS surveys such as zero order networks and crustal deformation, specialised procedures are required. These include:

- ✓ specialised scientific GPS software package (e.g. Bernese V4.0 GPS Software) that incorporates various strategies plus parameters that eliminate or reduce as many of the sources of GPS errors
- ✓ using precise orbits (preferably IGS) for ALL processing; incorporating relevant Earth Rotation Parameters (ERP) as the current POLE-file during processing
- ✓ the use of relevant phase differencing techniques (e.g. double differencing) plus linear combination strategies (e.g. wide-laning) to resolve successfully as many integer ambiguities as possible (ideally a *double-differenced ambiguity fixed* solution is accepted as the best)
- ✓ adopting the most accurate coordinates (WGS84) possible for starting points on baselines to be processed eg via IGS global tracking station
- ✓ incorporating ionosphere modelling plus the use of the ionosphere-free linear combinations (L_3) for baseline processing and ambiguity resolution
- ✓ processing campaigns by modelling the tropospheric (eg modelling for relative and absolute tropospheric effects for each 2-4 hourly interval), and
- ✓ always using established satellite antenna offsets plus a relevant function model for the receiver antennae phase variations.

7.2.3 PICMP 93, 96 and 98 GPS Processing plus ITRF96 Realisation

The PICMP93 survey took place in two parts. The first consisted of ten stations distributed nationwide designed (1) to provide a base network for future country-wide deformation studies, and (2) to enable an earlier 1989-90 survey using single-

frequency GPS receivers to be adjusted onto a high-precision backbone and thus to improve its accuracy. The second part was a regional survey of 15 sites in Luzon, 10 of which had been observed in the 1990 post-earthquake survey to enable postseismic and eventually interseismic deformation to be monitored. The 1993 measurements used dual-frequency squaring receivers (Trimble 4000SST) and multiple 12-hour measurement sessions. The Luzon network was partially resurveyed by the PICMP96 and 98 campaigns using full-wavelength dual-frequency receivers (Trimble 4000SSE and 4000SSi) with between one and six 24-hour sessions at each station.

The 1993, 1996 and 1998 PICMP data were processed using the Bernese V4.0 software adopting the standard techniques based on the double-difference phase observable, including atmospheric modelling, and fixing wide-lane and narrow-lane double difference ambiguities to integers where possible. The key procedures were detailed in Chapter 4. The result of each day's processing was a set of coordinate and covariance files for the stations observed that day. The error estimates output from the GPS processing package were scaled by a factor of 6 (derived from the repeatability of daily coordinate estimates within each survey, using geodetic network adjustment software ADJCOORD) to account for the unmodelled correlations between the successive 120-second GPS phase samples used in the last stage of the analysis

IGS ITRF96 orbits were used for the 1996, and 1998 analyses, and SIO reprocessed ITRF93 precise orbits for 1993. Regional IGS stations were added to the 1996 and 1998 processing so that the results could be put strictly into the ITRF96 reference frame.

The velocities of stations in the Philippines, even those in the 1990 earthquake zone, do not change significantly between 1993-96 and 1996-98. Therefore, a least squares filtering procedure was used, as discussed in Chapter 4, with full covariance propagation to estimate the ITRF96 coordinates and velocities of all stations observed during more than one epoch. Using this procedure, the stations measured in 1993 are put strictly into the ITRF96 reference frame, even though the 1993 analysis used ITRF93 orbits and no regional IGS stations were incorporated in that analysis. This was possible because PICMP96 and 98 coordinates were all in ITRF96, and also because sufficient stations were measured in each year that ITRF96 could be propagated back into the 1993 data. The ITRF96 velocities of all stations observed in

more than two surveys, including IGS regional stations, were also calculated, tabulated and graphically represented in Chapter 4. Therefore all three PICMP campaigns are in a consistent reference frame and could thus be compared for post-seismic and tectonic studies.

The resulting ITRF96 coordinates of the observed PICMP93 stations were also used in Chapter 5 to transform the 1989-90 PGNet single-frequency results into ITRF96.

7.2.4 Readjustment of the PGNet onto the PICMP93 (ITRF96) Fiducials

PGNet Scale Bias

The readjustment of the PGNet onto the ITRF96 using the PICMP93 fiducials was an attempt to upgrade the precision of the 1988-91 NRMDP GPS network, primarily for its potential in response surveys and resurveys of future large earthquakes in the Philippines

Seven Helmert transformation parameters were computed for the PGNet to PICMP93 (ITRF96) conversion. The scale factor parameter determined showed a scale bias contraction $\cong$ 3.1 ppm in the PGNet.

Ionospheric Effects on the Single frequency GPS Data of the PGNet (1989-91)

Various research has shown that for single frequency GPS:

1) the mean resulting baseline length reduction caused by the ionosphere amounts to 0.25 ppm per 1 metre vertical delay
2) in low latitude regions, during high solar activity times with no geomagnetic disturbances, the baseline shortening can be about 4-5 ppm, and
3) a typical value of 100 vertical TECU relates to 16 meter vertical delay on L1, and this would correspond to (16 meters * 0.25 ppm) about 4 ppm baseline length reduction.

An investigation (discussed in Chapter 5) was made into the effects of the ionosphere on the single frequency GPS baselines observed during the 1989-91 NRMDP (including the peak period of Solar Cycle 22). The purpose of this was to corroborate the scale bias discovered between the PGNet and the PICMP93 (ITRF96) and to

justify a network expansion in the readjustment.

To test this hypothesis for the PGNet GPS survey, the International Reference Ionosphere (IRI-95) Model was used to calculate the number for vertical TECU during the 1988-91 GPS survey. The IRI-95 is only a climatological model and produces monthly median values for the TEC eg 50-60 TECU. The median value determined of 56 TECU for the Philippines gives baseline shortening of 2.3 ppm but with different latitudes/longitudes plus time of day of observe rations this could be as high as 4-5 ppm baseline shortening.

It was concluded that this value was indicative of values that could be expected under the solar conditions experienced during the PGNet GPS surveys throughout the Philippines (between latitudes 6-20 degrees North).

Therefore, the proposed readjustment scale factor transformation parameter of *+3.1 ppm* was considered justified. Once the bias was removed then the remainder of the ionosphere error would be largely noise that would tend to be eliminated in the least squares adjustment of the PGNet

Readjusted PGNet (ITRF96)

To have improved the precision (i.e., reduced the size of the uncertainty ellipses), the PGNet GPS data would have had to be readjusted with the PICMP93 data, either using some sort of ionosphere model for the earlier data or perhaps by relaxing the scale constraints on the baseline lengths. This approach was ruled out as impractical due to factors such as the vast quantity of data, the logistical problems involved in reprocessing the PGNet GPS baselines, the complexities of realistically modelling ionospheric errors for all baselines throughout the Philippines, and the problem of missing raw data.

Accordingly, the Helmert transformation readjustment approach was adopted. This puts the PGNet into a modern reference frame i.e. the PGNet (ITRF96). However, it does not significantly improve the precision of PGNet (the uncertainty ellipses are not reduced in size) since no distortions in the original survey are corrected. It does, however, improve the accuracy since a systematic error (the average ionosphere scale error) in the original PGNet is significantly reduced.

The readjustment of the PGNet onto the ITRF96 using the PICMP93 fiducials was undertaken using the program NEWGAN and statistical results presented. The 330 readjusted PGNet (ITRF96) coordinates plus the positional error ellipses for the 99% Confidence Interval are attached in Appendix 5.
The documentation of this adjustment may have significant historical importance with respect to the long-term tectonics of the Philippine Islands.

Transformation parameters from the PRS92 to the ITRF96

The PRS92 is the geodetic datum for the coordinates published in *The Philippine Geodetic Network Manual 1992*. The PRS92 is based on the Clarke 1866 Spheroid and not the WGS84 or ITRF96.
It would be very useful (eg for future regional tectonic monitoring etc) to be able to transform any survey with PRS92 coordinates into the PICMP93 (ITRF96) reference frame. This would enable PRS92 data sets to be in a common reference with the high fidelity GPS surveys of the PICMP93, 96 and 98 campaigns.
The seven transformation parameters were computed and presented in Chapter 5. These transformation parameters may therefore be adopted generally for relating PRS92 coordinates within the Philippines to the ITRF96 reference frame based on the PICMP93 (ITRF96). The result is a usable transformation of PRS92 points into ITRF96 – while ignoring tectonic motion between 1990-1993.
These derived parameters would be of significant precision for regional long-term tectonic movements or rapid response monitoring displacements associated with large earthquakes.

Comments

The PGNet (ITRF96) data set may be useful for further geophysical research.

1. It can be used for response surveys following large earthquakes - but only large ones, since PGNet has only 20 cm accuracy at best (see Chapter 5.
2. With the passage of time, PGNet (ITRF96) errors decrease relative to regional deformation.

3. However, they are still substantial errors compared to regional deformation - the errors are not much smaller than would have been obtained from high quality traditional geodetic methods.
4. So it will take perhaps 30-40 years before a resurvey of PGNet could provide a regional deformation signal with a geophysically useful accuracy (say 5 mm/yr- now routinely better results are achieved with just a few years between GPS measurements).
5. The signal over such a long time interval would probably be hard to interpret, as it would be likely to contain a mix of long-term deformation and earthquakes.
6. If various authorities were interested in measuring the deformation of the country (either for geophysical purposes or for dynamic cadastral purposes) they would be better off to do two modern GPS surveys separated by a few years (rather than do anything further with PGNet).

7.2.5 Geodynamic Analyses from the PICMP

Silcock and Beavan [2001] and *Beavan et al.*, [2001] published the results of the 1990 Luzon Earthquake modelling, the subsequent postseismic deformation and the implications for Philippine Sea-Eurasian plate motion of 1993-1998 GPS-determined surface velocities. These results were possible due to data collected via the collaborative efforts of the PICMP 93, 96 and 98 campaigns.

Coseismic

In Chapter 6, a formal inversion was undertaken using the PGNet GPS geodetic data collected before and after the 1990 M_s 7.8 Luzon earthquake in order to solve for faulting parameters. This was also to investigate the lateral and depth extent of the faulting.

The results are largely consistent with field mapping and with seismological estimates of the faulting, but several additional features are revealed. The fault slip along the mapped part of the rupture is 5.5 - 6.5 m, predominantly left-lateral, and on a nearly vertical plane. The most likely depth of faulting is 10 - 15 km along the

southern and northernmost parts of the rupture, and deeper than 15 km along the central part with our preferred depth being at least 20 km. The deeper slip could have occurred partly as afterslip in the 4 - 9 months following the earthquake. The observed subsidence to the northeast on the southernmost part of the rupture is matched by the model.

The final dislocation solution has a slightly larger moment (0-5%) than the seismic moments estimated by *Yoshida and Abe* [1992] and the Harvard CMT solution. This is not unexpected given that the displacement data include the effects of some aftershocks and an unknown amount of pre- and post-seismic displacement.

It is found that the rupture extended 40 - 50 km north of the mapped 1990 fault break into the mountainous Cordillera Central, as had been previously proposed. The strike of this northern extension is between north and northwest, the slip is 4 - 5 m rather than the 5.5 - 6.5 m further south, and there is a significant component of thrusting, as might be expected from the contractional tectonics of the Cordillera Central.

Postseismic

Between survey epochs of 1993 and 1998 substantial strike-slip deformation was detected sub-parallel to the faults that ruptured in the 1990 Luzon earthquake. There also appears to be no detectable time dependence in this deformation. If the observed velocities are interpreted using an elastic half-space model, the measured deformation rate implies a long-term slip rate (or far-field relative velocity) of ~40 mm/yr on the Philippine fault in Luzon. Paleoseismic data and historical observations suggest that 40 mm/yr is far too high as a long-term slip rate.

Beavan et al., [2001], show several lines of evidence against this high rate of slip and then offers viscoelastic relaxation models with a more realistic associated long-term slip rate of 15 - 22 mm/yr. In particular, it is shown that the long-term rate of earthquake recurrence along the Philippine fault system in central and northern Luzon from paleoseismic data and historical observations (even though quite poorly documented) suggests that 40 mm/yr is far too high a long-term slip rate.

7.3 Future monitoring

In Chapter 5, the readjustment for the PGNet (ITRF96) was documented. The noted incurred errors of using single frequency GPS receivers during high ionospheric activity, poor satellite geometry and earthquake/tectonic activity will eventually be reduced relative to the regional deformations that have accumulated since 1990. Therefore the more valuable this data may become to tectonic geophysicists.

The availability of pre and post earthquake GPS data from the PGNet made it possible to present in Chapter 6 a coseismic model for the 1990 Luzon event. This data was obtained purely by chance. However, more useful information could be gained through a programme of continual GPS monitoring nationally and within various islands of the Philippine Archipelago.

Also, if the PICMP93 ITRF96 fiducials could be monitored regularly (in conjunction with regional tracking stations) then this may have significant historical importance with respect to the tectonics of the Philippine Islands.

A network with improved spatial distribution of points in Luzon, monitored even as infrequently as every 5 years as an ongoing project, promises to provide better data about the role of viscoelastic relaxation in the strike-slip earthquake cycle than any existing data set (though future data from the region of the similar-sized 1999 Izmit, Turkey, earthquake [*Reilinger et al.*, 2000] will also be valuable, as may data from the region of the much smaller Landers earthquake). In particular, it should be possible to accurately measure temporal slowing and broadening of the strain field.

The tectonics of Luzon are dominated by strike-slip motion along the Philippine fault system, not by rapid (5.5°/Ma) large-scale counter-clockwise rotation of Luzon as has been suggested in a recent paper by *Rangin et al.* [1999] based on very limited GPS data. *Beavan et al.*, [2001] estimate that Luzon is rotating counter-clockwise at 1 - 2°/Ma relative to PH.

There is strong evidence that a large majority of the present day motion convergence between the Philippine and Sunda plates at the latitude of Luzon is occurring at the Manila Trench, despite the absence of large 20th century earthquakes at the trench.

7.4 Ongoing Role of the PICMP

The PICMP basic framework was established in 1993 and has already proved it's scientific worth with the results from the PICMP93, 96 and 98 campaigns [see eg *Silcock and Beavan* 2001; *Beavan et al.*, 2001; *Thibault* 1999]. Other regional GPS projects (eg Taiwan-Luzon campaigns, 1994 DMA survey and the PSP campaigns) occupied some of the sites established for the PICMP. Future use of the network will add to the historical value of the data obtained and will help resolve the complexities of kinematics in the Philippines.

Luzon Fault Zone Monitoring

Perhaps the most exciting future results will come from:

- on going study of the postseismic displacement field of the 1990 deep strike-slip event
- the strain rates in the near-field of the fault
- the long term slip rates of the fault
- a monitoring network available for future large earthquakes in Luzon

PGNet (ITRF96) for Rapid response for Earthquake throughout the Philippines

AS discussed in section 7.2.4, the rationale for the readjustment of the PGNet onto the PICMP93 (ITRF96) fiducials is to improve its accuracy for its potential in response surveys and resurveys of future large earthquakes in the Philippines. With the passage of time, the errors in this readjusted PGNet (ITRF96) network become smaller relative to the regional deformations that have accumulated since 1990. Therefore the more valuable this data becomes to tectonic geophysicists provided that the ground marks remain stable and undisturbed.

Thibault [1999] examined present-day crustal deformation within the Philippine island arc based on multiple campaign-style GPS geodetic measurements on the northern island of Luzon i.e. the PICMP96 and 98 campaigns. The network, consisted of four subnetworks surrounding zones of active deformation:

1. the Philippine Fault, a major left-lateral strike-slip fault extending the length of the Philippine Islands (18 sites),
2. the Marikina Fault, a dextral structure that transects Metro Manila (15 sites),
3. Mount Pinatubo Volcano (10 sites), and
4. Taal Volcano (18 sites), with a common station operating continuously in Manila.

Many of these sites were occupied during the PICMP93 and as part of annual Taiwan-Luzon campaigns in '96, '97, and '98. All processing was in the ITRF96.'s Results [*Thibault, 1999*] showed:

(1) in a Eurasian plate-fixed reference frame, 60 mm/yr westward convergence accommodated by subduction at the Manila Trench and divergence south of the Philippine Fault

(2) in a Philippine Sea plate-fixed reference frame, 20 mm/yr oblique convergence partitioned between subduction at the East Luzon Trough and strike-slip shear at the Philippine Fault

(3) approximately 20-30mm/yr sinistral shear along the Philippine Fault, with significant variability along strike, including evidence for fault-normal compression in the Sierra Madre and Cordillera Central

(4) large, aseismic deformation near the Marikina Fault, possibly associated with ground water withdrawal

(5) small motions radially outward from Mount Pinatubo, possibly indicative of inflation

(6) large, radially inward motion toward Taal caldera, indicating a phase of significant volcanic deflation in the aftermath of the 1993-94 volcanic crisis at Taal

(7) sites located on the margin of Taal caldera show negligible movement, while

those located on the volcano island show significant motion, with rates in excess of 20 mm/yr.

In 1999 Taal was instrumented with a telemetered continuous GPS network consisting of three dual-frequency stations relaying data that were processed in near real time.

Regional Tectonic Research

GPS data obtained at the fiducial network sites will also provide new information on the general pattern of crustal movement within the Philippine tectonic zone. *Barrier et al.*, [1991] have analysed geological data in order to establish a simple kinematic model for the distribution of motion between the Philippine Sea and Eurasian plates in this region. Their plate rotation model predicts velocities along the Philippine fault in the Visayas and Mindanao of 1.9 to 2.5 cm/year and a subduction rate along the Philippine trench varying from 9.5 to 13 cm/year in the far south to 6.5 to 8.5 cm/year east of Samar. Their results supported the hypothesis that the Philippine archipelago is not entirely part of the Eurasian plate but belongs to an independent block. In the south, the field and geological data fit the model quite well. However, this is not the case in the north where the kinematics and block geometry are more complex and speculative.

One of the major ongoing objectives of the PICMP was to analyse the GPS fiducial data from PICMP93/96 and 98 campaigns to provide further insight on the kinematics of this region. Two of the fiducial sites are located on the Eurasian plate while the others straddle the Philippine fault from north to south. *Beavan et al.*, [2001], incorporated the various solutions into the ITRF96 which utilised additional data from the Philippine Sea plate and IGS stations throughout South East Asia plus Australia. The results were interpreted within the context of the NUVEL model for global plate motion [*De Mets et al.*, 1990] and the more detailed model suggested by *Barrier et al.*, [1991] (see Chapter 6).

7.5 Benefits Of Research

The benefits, which will accrue from the PICMP, have both a practical and scientific basis and are summarised as follows:

- Studies of tectonic motions in active seismic zones are of particular importance in terms of society's ability to respond, cope, manage and, therefore, mitigate the impact of natural geological hazards.

- This project combines the disciplines of geodesy, geology and geophysics in order to improve the understanding of complex crustal deformation processes at active plate boundaries. This cross-disciplinary interaction will strengthen the knowledge base already obtained.

- This research will lead to a broader understanding of earthquake mechanisms and will provide an improved knowledge of the kinematic behaviour of a tectonic zone within a major plate convergence system.

- The various agencies and universities involved regard GPS applications for geophysics as a priority area of research. This multi-lateral initiative involves scientists from the Philippines, New Zealand, the United States and Australia. It utilises an extensive international network of contacts and hence allows exchange of expertise and knowledge.

The PICMP research is a unique study of one of the world's most active seismic zones. There is no doubt that GPS technology and newer advanced geodetic techniques will continue to be utilised to monitor crustal deformation and tectonic motion across the Philippine archipelago.

REFERENCES

Abe, K., Seismological aspects of the Luzon, Philippines earthquake of July 16, 1990 (in Japanese), *Bull. Earthq. Res. Inst. Univ. Tokyo, 65*, 851-873, 1990.

Allen, C. R., Circum-Pacific faulting in the Philippines-Taiwan region, *J. Geophys. Res., 67*, 4795-4812, 1962.

Allman, J.S., An analysis of the primary triangulation network of the Philippines, Report to SAGRIC International, NRMDP Philippines, Adelaide, South Australia, 29 pp. 1991.

Aurelio, M. A., E. Barrier, C. Rangin, and C. Muller, The Philippine fault in the late Cenozoic tectonic evolution of Bondoc-Masbate-N. Leyte area, central Philippines, *Jour. S. E. Asian Earth Sci., 6, 3/4*, 221-238, 1991.

Aurelio, M. A., W. F. W. Simons, R. L. Almeda, et al., Present-day plate motions in the Philippines: Interpretation of GPS results of GEODYSSEA,), in: The Geodynamics of S and SE Asia (GEODYSSEA) Project, eds. P. Wilson and G. W. Michel, Sci. Tech. Rept. STR98/14, GeoForschungsZentrum, Potsdam, 251-263, 1998.

Australian International Development Assistance Bureau, Natural Resources Management and Development Project, Implementation Document, Manila, Philippines, 68 pp. 1989.

Australian International Development Assistance Bureau, The Geodetic Survey of the Philippines, Final Report (3 vols.), Canberra, Australia, 1992.

Barrier, E., P. Huchon, and M. Aurelio, Philippine fault: a key for Philippine kinematics, *Geology, 19*, 32-35, 1991.

Bureau of Coast and Geodetic Survey, Triangulation of the Philippine Islands, Manila, Philippines, (2 Vols.), 1927.

Beavan, J., C. H. Scholz, I. Murata, T. Kato, H. Ishii, D. M. Davis, S. W. Roecker, K Hirahara and T. Tamaka, A GPS Study of the Philippine Sea Plate, *EOS (71), 857, 1990.*

Beavan, J. et al., Determination of the Philippine Sea plate velocity from Global Positioning System observations and effects of the 1993 Guam earthquake, *EOS Trans. Am. Geophys. Un. (Supp), 59*, 1994.

Beavan, J., D. Silcock, M. Hamburger, E. Ramos, C. Thibault, and R. Feir, Geodetic constraints on postseismic deformation following the 1990 M_s 7.8 Luzon, Philippines, earthquake, and implications for Luzon tectonics and Philippine Sea plate motion, *G-cubed, Vol. 2, paper number 2000GC000100*, 20 Sep, 2001.

Bevis, M., R. Reilinger, T. Herring, C. Rocken, R. Anthes, and T. Ware, GPS Meteorology: Remote Sensing of Atmospheric Water Vapour using the Positioning System, *J. Geophys. Res., 97*, 15,787-15,801, 1992.

Bevis, M., R. Reilinger, Y. Bock, J. Stowell, A Multimodal Occupation Strategy for Regional GPS Geodesy, UNAVCO FY95-99 NSF Proposal, 1994

Bibby, H.M., Unbiased estimate of strain from triangulation data using the method of simultaneous reduction, *Tectonophysics, 82(1-2)*, 161-174, 1982.

Bingley, R. M., From WWW GLOSS Bulletin 2

(http://www.pol.ac.uk/psmsl/gb/gb2/bingley.html), October 1995.

Bischke, R. E., J. Suppe, and R. del Pilar, A new branch of the Philippine fault system as observed from aeromagnetic and seismic data, *Tectonophysics, 183,* 243-264, 1990.

Blewitt, G., Advances in Global Positioning System technology for geodynamics investigations: *1978-1992, JPL Geod. and Geophys. Rep. No. 232,* Pasadena, California, 16 pp, 1993.

Bowin, C., R. S. Lu, C.-S. Lee, and H. Schouten, Plate convergence and accretion in the Taiwan-Luzon region, *Am. Assoc. Petr. Geol. Bull., 62,* 1645-1672, 1978.

Boucher, C., ITRF96 and follow on for 1998, IGS Reference Frame Realization, IGS Analysis Centre Workshop Proceedings, Darmstadt, 173-176, 9-11 Feb., 1998.

Boucher, C., Z. Altamimi, and P. Sillard, Results and Analysis of the ITRF96, *IERS technical note 24, Observatoire de Paris,* 1998.

Brunner, F. K. and M. Gu, An improved model for the dual frequency ionospheric correction of GPS observations, *Manuscripta Geodaetica, Vol. 16,* 205-214. 1991.

Brunner, F. K. and W. M. Welsch, Effect of the troposphere on GPS measurements, *GPS World, Vol. 4, No. 1,* 42-51, 1993.

Bureau of Mines and Geosciences, Geology and Mineral Resources of the Philippines, Vol. 1, Geology, 406 pp, Ministry of Natural Resources, Manila, 1982.

Calais, E. et al., Southeast Asia kinematics and the International Terrestrial Reference Frame from GPS, *EOS Trans. Am. Geophys. Un. (Supp),* Fall Meeting, San Francisco, CA., 194, 1993.

Cardwell, R. K., B. L. Isacks, and D. E. Karig, The spatial distribution of earthquakes, focal mechanism solutions, and subducted lithosphere in the Philippine and northeastern Indonesian islands, in The Tectonic and Geological Evolution of SE Asian Seas and Islands, ed. D. Hayes et al., *AGU Monograph, 23,* 1-35, 1980.

Chen, Z., B. C. Burchfiel, Y. Liu, R. W. King, L. H. Royden, W. Tang, E. Wang, J. Zhao, and X. Zhang, Global Positioning System measurements from eastern Tibet and their implications for India/Eurasia intercontinental deformation, *J. Geophys. Res., 105:B7,* 16,215-16,228, 2000.

Chinnery, M. A., The deformation of the ground around surface faults, *Bull. Seism. Soc. Am., 50,* 355-372, 1961.

Cohen, S. C., Numerical models of crustal deformation in seismic zones, *Advances in Geophysics, 41,* 133-231, 1999.

Crook, C. N., ADJCOORD: a Fortran program for survey adjustment and deformation modelling, N. Z. Geol. Surv. Earth Def. Sec. Report, 138, Dept. Sci. Indust. Res., Lower Hutt, N. Z., 22 pp, 1992.

Cross, P. A., Surveillance and monitoring: from millimetres to megametres, Keynote address, SAMS'95, 3rd symposium on surveillance and monitoring surveys, Department of Geomatics, University of Melbourne, Australia, November 1-2, 1995.

Daligdig, J. A., Recent faulting and paleoseismicity along the Philippine fault zone, north central Luzon, Philippines, PhD thesis, Faculty of Science, Kyoto University, 1997.

Darby, D. J., and J. Beavan, Evidence from GPS measurements for contemporary plate coupling on the southern Hikurangi subduction thrust and for partitioning of strain in the upper plate, *J. Geophys. Res., accepted subject to revisions,* 2001.

DeMets, et al., Current plate motions, *Geophys. J. Int., 101*, 425-478, 1990.

DeMets, C., R. G. Gordon, D. F. Argus, and S. Stein, Effect of recent revisions to the geomagnetic reversal time scale on estimates of current plate motions, *Geophys. Res. Lett., 21*, 2191-2194, 1994.

Dennis, J. E., D. M. Gay, and R. E. Welsch, An adaptive non-linear least-squares algorithm, *ACM Trans. Math. Software, 7*, 348-368, 1981a.

Dennis, J. E., D. M. Gay, and R. E. Welsch, Algorithm 573 NL2SOL - an adaptive non-linear least-squares algorithm [E4], *ACM Trans. Math. Software, 7*, 369-383, 1981b.

Dixon, T.H., An introduction to the Global Positioning System and some geological applications, *Rev. Geophys., 29, (2)*, 249-276, 1991.

Dixon, T. H., M. Miller, F. Farina, H. Wang, and D. Johnson, Present-day motion of the Sierra Nevada block and some tectonic implications for the Basin and Range province, North American Cordillera, *Tectonics, 19*, 1-24, 2000.

Duan, J., M. Bevis, P. Feng, Y. Bock, S. Chiswell, S. Businger, C. Rocken, F. Solheim, T. van Hove, R. Ware, S. McClusky, T. A. Herring, and R. W. King, GPS meteorology: direct estimation of the absolute value of precipitable water, *Journal of Applied Meteorology, 35:* 830-838, 1996.

Dusquenoy, T., Contribution de la géodésie à l'étude de grand décrochements actifs associés à des zones de subduction à convergence oblique, Exemple de la grand faille de Sumatra et de la faille Philippine, thèse, Université de Paris Sud, Orsay, 1997.

Duquesnoy, Th., E. Barrier, M. Kasser, M. Aurelio, R. Gaulon, R. S. Punongbayan, C. Rangin, et al., Detection of creep along the Philippine fault: first results of geodetic measurements on Leyte Island, central Philippines, *Geophys. Res. Lett., 21*, 975-978, 1994.

Fitch, T. J., Plate convergence, transcurrent faults, and internal deformation adjacent to southeast Asia and the western Pacific, *J. Geophys. Res., 77*, 4432-4460, 1972.

Fuller, M., R. McCabe, I. S. Williams, J. Almasco, R. Y. Encina, A. S. Zanoria, and J. A. Wolfe, Paleomagnetism of Luzon, *AGU Geophys. Monograph, 27*, 79-94, 1983.

Geodyssea, http://www.geologie.ens.fr/%7Evigny/geodyssea-itrf96-table.html, 1999.

Georgiadou, Y., and A. Kleusberg, On the effect of ionospheric delay on geodetic G{S positioning, *Manuscripta Geodaetica, Vol. 13*, 1-8, 1988.

Goad, C. C., Precise relative position determination using Global Positioning System Carrier phase measurements in a nondifference mode, Proceedings: First International Symposium on Precise Positioning with the Global Positioning System, Rockville, Maryland, USA , 347-356, April 15-19, 1985.

Goad, C. C., and L. Goodman, A modified Hopfield tropospheric refraction correction model, Proceedings of the fall annual meeting of the American Geophysical Union, San Francisco,California, USA, December 12-17, 1974.

GPSCO, Getting started with GPS surveying, Land Information Centre, Bathurst, NSW, 186 pp, 1992

GPS Support Center, http://www.spacecom.af.mil/usspace/gps_support/, 2001.

Gurtner W., and G. Mader, Receiver independent exchange format version 2, *GPS Bulletin, 3(3):* 1-8, 1990.

Gurtner W., G. Mader and D. McArthur, A common exchange format for GPS data, *GPS Bulletin, 2(3):* 1-11, 1989.

Hager, B. H., R. W. King, and M. H. Murray, Measurement of crustal deformation using the Global Positioning System, *Annu. Rev. Earth Planet. Sci.*, 19: 351-382, 1991.

Hall, R., Reconstructing Cenozoic SE Asia, in Tectonic evolution of southeast Asia, eds. R. Hall and D. Blundell, *Geol. Soc. Special Publ. 106*, 153-184, 1996.

Hamburger, M. W., R. K. Cardwell, and B. L. Isacks, Seismotectonics of the northern Philippine island arc, *AGU Geophys. Monograph, 27*, 1-22, 1983.

Heki, K., Horizontal and vertical crustal movements from three-dimensional very long baseline interferometry kinematic reference frame: implication for the reversal timescale revision, *J. Geophys. Res., 101*, 3187-3198, 1996.

Henson, D. J., and E. A. Collier, Effects of the ionosphere on GPS relative geodesy, Proceedings of the IEEE PLANS '86 position location and navigation symposium, Las Vegas. NV, USA, pp 230-237, 1986.

Higgins, M., Transformation from WGS84 to AGD84 - an interim solution, *Department of Mapping and Surveying, Queensland*, 1987.

Hirano, S., T. Nakata, and A. Sangawa, Fault topography and Quaternary faulting along the Philippine fault zone, central Luzon, Philippines, *J. Geography, 95*, 71-93, 1986.

Hofmann-Wellenhof, B., H. Lichtenegger and J. Collins, GPS theory and practice, third edition, Springer-Verlag Wien New York, 355 pp, 1994.

Hopfield, H. S., Two-quadratic tropospheric refractivity profile for correcting satellite data, *J. Geophys. Res., 74 (18)*, 4487-4499, 1969.

International GPS Service for Geodynamics (IGS), http://igscb.jpl.nasa.gov/overview/viewindex.html, 2001.

IPS Radio and Space Services, http://www.ips.gov.au/ 2001

ISC, Bulletin of the International Seismological Centre for July 1990, I.S.C., Newbury, Berkshire, U.K., Vol. 27, No. 7, 1992.

Jones, A.C., The computation and adjustment of the Primary Geodetic Network of the Philippines, NRMDP final report, SAGRIC International, South Australian Dept of Lands, 55 pp, Dec 1991.

Kaplan, E. D. (Ed.), Understanding GPS principles and applications, Artech House, Norwood, Massachusetts, USA, 1996.

Karig, D. E., Plate convergence between the Philippines and the Ryukyu Islands, *Mar. Geol., 14*, 153-168, 1973.

Karig, D. E., Accreted terrains in the northern part of the Philippine archipelago, *Tectonics, 2*, 211-236, 1983.

Kearsley, A.H.W., Evaluation of the geoid in the Philippines, Report to SAGRIC International, NRMDP Philippines, Adelaide, South Australia, 88 pp, 1991.

King, R. W., J. Collins, E. G. Masters, C. Rizos and A. Stolz, Surveying with GPS, Monograph No. 9, School of Geomatic Engineering (formerly surveying), the University of NSW, Sydney, Australia, 1985.

Komjathy, A., *pers. comm.*, Colorado Center for Astrodynamics Research (CCAR), Dept. of Aerospace Engineering, University of Colorado at Boulder, USA, Sep 1996, Jan-Feb 2001.

Kotake, Y., T. Kato, S. Miyazaki, and A. Sengoku, Relative motion of the Philippine Sea plate derived from GPS observations and tectonics of the south-western Japan (in Japanese with English abstract), *Zishin, 51(2)*, 171-180, 1998.

Kouba, J., and Y. Mireault, Analysis Coordinator Report, in IGS 1996 Annual Report, eds. J. F. Zumberge, D. E. Fulton and R. E. Neilan, Jet Propulsion Lab., Calif. Inst. of Technology, Pasadena, Ca, USA, 55-100, 1997.

Kouba, J., J. Ray, M. M. Watkins, IGS Reference Frame Realization, IGS Analysis Centre Workshop Proceedings, Darmstadt, 139-171, 9-11 Feb., 1998.

Kreemer, C., W. E. Holt, S. Goes, and R. Govers, Active deformation in eastern Indonesia and the Philippines from GPS and seismicity data, *J. Geophys. Res., 105:B1*, 663-680, 2000.

Larden, D.R., Harvey, W.M., Feir, R.D. and A.C. Jones, Preliminary evaluation of the national geodetic differential GPS network of the Philippines, Paper 14, Proc., 4th South East Asian Survey Congress, Kuala Lumpur, 3-7 June 1991.

Larson, K. M., J. Freymueller, and S. Philipsen, Global plate velocities from the Global Positioning System, *J. Geophys. Res., 102:B5*, 9961-9981, 1997.

Leick, A., GPS Satellite Surveying, Second Edition, John Wiley and Sons Inc., New York, U.S.A, 560 pp, 1995.

Lewis, S. D., and D. E. Hayes, The tectonics of northward propagating subduction along Eastern Luzon, Philippine Islands, *AGU Geophysical Monograph 27*, 57-78, 1983.

Lewis, S. D., and D. E. Hayes, Plate convergence and deformation, North Luzon ridge, Philippines, *Tectonophys., 168*, 221-237, 1989.

Li, V. C., and J. R. Rice, Crustal deformation in great California earthquake cycles, *J. Geophys. Res., 92:B11*, 11,533-11,551, 1987.

McCabe, R., J. Almasco, and W. Diegor, Geologic and paleomagnetic evidence for a possible Miocene collision in western Panay, central Philippines, *Geology, 10*, 325-329, 1982.

McCaffrey, R., Slip partitioning at convergent plate boundaries of SE Asia, in Tectonic evolution of southeast Asia, eds. R. Hall and D. Blundell, *Geol. Soc. Special Publ. 106*, 3-18, 1996.

Meehan, T. K., J. M. Srinivasan, D. J. Spitzmesser, C. E. Dunn, J. Y. Ten, J. B. Thomas, T. N. Munson and C. B. Duncan, The TurboRogue GPS receiver, Proceedings of the sixth International Geodetic Symposium on satellite positioning, Columbus, OH, USA, 209-218, 17-20 March, 1992.

Michel, G. W., Y. Q. Yu, S. Y. Zhu, C. Reigber, M. Becker, E. Reinhart, W. Simons, B. Ambrosius, C. Vigny, N. Chamot-Rooke, X. Le Pichon, P. Morgan, and S. Matheussen, Crustal motion and block behaviour in SE-Asia from GPS measurements, *Earth Planet Sci. Lett., 187*, 239-244, 2001.

Morante, E. M., and C. R. Allen, Displacement on the Philippine fault during the Ragay Gulf earthquake of March 17, 1973 (abstract), *Geol. Soc. Amer. Abstr. Programs, 5*, 744-745, 1973.

Morante, E. M., The Ragay Gulf earthquake of March 17, 1973, southern Luzon, Philippines, *J. Geol. Soc. Phil., 28:2*, 69-93, 1974.

Morgan, P., Y. Bock, R. Coleman, P. Feng, D. Garrard, G. Johnston, G. Lutton, B. McDowall, M. Pearse, C. Rizos and R. Tiesler, A zero order GPS network for the Australian region, *UNISURV S-46*, School pf Geomatic Engineering, University of NSW, Sydney, Australia, 1996.

Murphy, R. W., The Manila trench–west Taiwan fold belt: a flipped subduction zone?, *Geol. Soc. Malaysia Bull., 6*, 27-42, 1973.

Nakata, T., H. Tsutsumi, R. S. Punongbayan, R. E. Rimando, J. Daligdig, and A. Daag, Surface faulting associated with the Philippine earthquake of 1990 (in Japanese), *Journal of Geography, 99*, 95-112, 1990.

Nakata, T., H. Tsutsumi, R. S. Punongbayan, R. E. Rimando, J. A. Daligdig, A. S. Daag, and G. M. Besana, Surface fault ruptures of the 1990 Luzon earthquake, Philippines, Spec. Publ. No. 25, Research Center for Regional Geography, Hiroshima Univ., 92 p, 1996.

National Aeronautics and Space Administration, Solid Earth Science in the 1990's - Program Plan, NASA TM - 4256, (1), 68 pp, 1991.

National Research Council, Geodetic Monitoring of Tectonic Deformation - Towards a Strategy, Panel on Crustal Movement Measurements, National Academy Press, Wash., D.C., 1981

Newhall, C. G., R. V. Sharp, G. F. Wieczorek, L. Wennerberg, and J. Bicknell, The July 16, 1990, Luzon earthquake, Final Report to U.S. AID from USGS and PHIVOLCS, Oct 29, 1990.

Nur, A., and G. Mavko, Postseismic viscoelastic rebound, Science, 175, 885-887, 1974.

Okada, Y., Surface deformation due to shear and tensile faults in a half-space, *Bull. Seism. Soc. Am., 75*, 1135-1154, 1985.

Parkinson, W. B. and J. J. Spilker Jr., editors, Global Positioning System: theory and applications, volume 163 of Progress in Astronautics and Aeronautics, American Institute of Aeronautics and Astronautics, Inc., Washington, DC, 1996.

Philippine Bureau of Mines, Geological map of the Philippines, scale 1:1,000,000, 9 sheets, Manila, 1963.

Pinch, M. C., and A. E. Peterson, A method for adjusting survey networks in sections, *Canadian Surveyor*, March 1974.

Pollitz, F. F., Postseismic relaxation theory on the spherical Earth, *Bull. Seism. Soc. Am., 82*, 422-453, 1992.

Pollitz, F. F., and I. S. Sacks, Modeling of postseismic relaxation following the great 1857 earthquake, southern California, *Bull. Seism. Soc. Am., 82*, 454-480, 1992.

Pollitz, F. F., R. Bürgmann, and P. Segall, Joint estimation of afterslip rate and postseismic relaxation following the 1989 Loma Prieta earthquake, *J. Geophys. Res., 103:B11*, 26,975-26,992, 1998.

Prescott, W. H., 1981, The determination of displacement fields from geodetic data along a strike slip fault, *J. Geophys. Res., 86:B7*, 6067-6072, 1981.

Rangin, C., X. LePichon, S. Mazzotti, M. Pubellier, N. Chamot-Rooke, M. Aurelio, A. Walpersdorf, and R. Quebral, Plate convergence measured by GPS across the Sundaland/Philippine Sea Plate deformed boundary: the Philippines and eastern Indonesia, *Geophys. J. Int., 139*, 296-316, 1999.

Reilinger, R. E., et al., Coseismic and postseismic fault slip for the 17 August 1999, M = 7.5, Izmit, Turkey earthquake, *Science, 289*, 1519-1524, 2000.

Rizos, C., Potential and limitations of using the Global Positioning System. Report published by Surveying & Mapping Industry Council of NSW, Sydney, NSW, Australia, 58 pp, 1995.

Rothacher, M., B. Beutler, W. Gurtner, A. Geiger, H. G. Kahle, and D. Schneider, The Swiss 1985 GPS campaign, Proceedings of the Fourth International Symposium on Satellite Positioning, Vol. 2, 979-991, Austin, Texas, USA, 1986.

Rothacher, M., B. Beutler, W. Gurtner, E. Brockmann, and L. Mervart, The Bernese GPS software version 3.4, Astronomical Institute, University of Berne, Berne, Switzerland, 1993.

Rothacher, M., and L. Mervart (eds.), Documentation of the Bernese GPS Software Version 4.0, Astronomical Institute, University of Berne, Berne, Switzerland, 418 pp, 1996.

Rowlett, H., and J. Kelleher, Evolving seismic and tectonic patterns along the western margin of the Philippine Sea plate, *J. Geophys. Res., 81*, 3518-3524, 1976.

Saastamoinen, J., Atmospheric correction for the troposphere and stratosphere in radio ranging of satellites, in *Use of artificial satellites for geodesy, AGU Geophysical Monograph 15*, D.C. USA, 1972.

Saastamoinen, J., Contributions to the theory of atmospheric refraction, part II Refraction corrections in satellite geodesy, *Bull. Geod. 107*, 13-34, 1973.

Savage, J. C., Equivalent strike-slip earthquake cycles in half-space and lithosphere-asthenosphere Earth models, *J. Geophys. Res., 95*, 4873-4879, 1990.

Savage, J. C., and R. O. Burford, Accumulation of tectonic strain in California, *Bull. Seism. Soc. Am., 60*, 1877-1896, 1970.

Savage, J. C., and R. O. Burford, Geodetic determination of relative plate motion in central California, *J. Geophys. Res., 78*, 832-845, 1973.

Savage, J. C., and W. H. Prescott, Asthenosphere readjustment and the earthquake cycle, *J. Geophys. Res., 83*, 3369-3376, 1978.

Savage, J. C., and J. L. Svarc, Postseismic deformation associated with the 1992 M_w=7.3 Landers earthquake, southern California, *J. Geophys. Res., 102:B4*, 7565-7577, 1997.

Savage, J. C., and M. Lisowski, Viscoelastic coupling model of the San Andreas fault along the big bend, southern California, *J. Geophys. Res., 103*, 7281-7292, 1998.

Scholz, C. H., The mechanics of earthquakes and faulting, Cambridge Univ. Press, 439 pp, 1990.

Schutz, B. et al., The Southwest Pacific GPS Project: Geodetic results from Burst 1 of the 1990 field campaign, *Bull. Geod. 67*, 224-240, 1993.

Seeber, G., Satellite geodesy: foundations, methods and applications, Walter de Gruyter & Co., New York, USA, 1993.

Segall, P., and R. Harris, Earthquake deformation cycle on the San Andreas fault near Parkfield, California, *J. Geophys. Res., 92:B10*, 10,511-10,525, 1987.

Segall, P., and J. L. Davis, GPS applications for geodynamics and earthquake studies, *Annu. Rev. Earth Planet. Sci.*, 25: 301-336, 1997.

Seno, T., S. Stein, and A. E. Gripp, A model for the motion of the Philippine Sea plate consistent with NUVEL-1 and geological data, *J. Geophys. Res., 98:B10*, 17,941-17,948, 1993.

Shen, Z.-K., D. D. Jackson, Y. Feng, M. Cline, M. Kim, P. Fang, and Y. Bock, Postseismic deformation following the Landers earthquake, California, 28 June 1992, *Bull. Seism. Soc. Am., 84,* 780-791, 1994.

Shen, Z.-K., C. Zhao, A. Yin, Y. Li, D. D. Jackson, P. Fang, and D. Dong, Contemporary crustal deformation in east Asia constrained by Global Positioning System measurements, *J. Geophys. Res., 105:B3,* 5721-5734, 2000.

Silcock, D. M., and J. Beavan, Geodetic constraints on coseismic rupture during the 1990 M_s 7.8 Luzon, Philippines, earthquake, *G-cubed, Vol. 2, paper number 2000GC000101,* 31 July, 2001.

Strang, G., and K. Borre, Linear algebra, geodesy, and GPS, Wellesley-Cambridge Press, 624 pp, 1997.

Taylor, F., http://www.ig.utexas.edu/people/staff/fred, 2002.

Thatcher, W., Nonlinear strain buildup and the earthquake cycle on the San Andreas fault, *J. Geophys. Res., 88:B7,* 5893-5902, 1983.

Thibault, C. A., GPS measurements of crustal deformation in the northern Philippine island arc, M. Sc. thesis, 126 pp., Indiana University, Bloomington, IN, 1999.

Tregoning, P., K. Lambeck, A. Stolz, P. J. Morgan, S. C. McClusky, P. van der Beek, H. McQueen, R. J. Jackson, R. P. Little, A. Laing, and B. Murphy, Determination of current plate motions in Papua New Guinea from Global Positioining System observations, J. Geophys. Res., 103:B6, 12,181-12,205, 1998.

United States Coast and Geodetic Survey (USCGS), Triangulation of the Philippine Islands, Washington D.C., Volumes 1 and 2, 1927.

Vanicek, P., G. Beutler, A. Kleusberg, R. B. Langley, R. Santerre and D. E. Wells, DIPOP: Differential positioning program package for the Global Positioning Sytem, Report 85-005, Geodetic Survey of Canada, 1985.

Webster, I.R., A regional model for the production of ionospheric delay for single frequency users of the Global Positioning System, M.Sc.E. thesis, Department of Surveying Engineering Technical Report No. 166, University of New Brunswick, Frederiction, New Brunswick, Canada, 124pp, 1993.

Wells, D. E., Doppler satellite control, Department of Surveying Engineering, University of New Brunswick, Fredericton, N. B., Canada, 1974.

Wells, D.E., N. Beck, D, Delikaraoglou, A. Kleusberg, E.J. Krakiwsky, G. Lachapelle. R. B. Langley, M. Nakiboglu, K. P. Schwarz, J. M. Tranquilla and P. Vanicek, Guide to GPS Positioning, Second printing with corrections, Canadian GPS Associates, Fredericton, N. b. Canada, 1987.

Wells, D. E., and A. Kleusberg, Kinematic differential Global Positioning System, Contract report for the US Army Engineer Topographic Laboratories, Fort Bevoir, VA, USA, 36 pp, March, 1989.

Wessel, P., and W. H. F. Smith, New, improved version of Generic Mapping Tools released, *Eos, Trans. AGU,* 79, 579, 1998.

Wilson, P., et al., Study provides data on active plate tectonics in Southeast Asia region, *Eos, Trans. AGU,* 79, 545, 548-549, 1998.

Yoshida, Y., and K. Abe, Source mechanism of the Luzon, Philippines earthquake of July 16, 1990, *Geophys. Res. Lett., 19,* 545-548, 1992.

Yu, S.-B., H.-Y. Chen, and L.-C. Kuo, Velocity field of GPS stations in the Taiwan area, *Tectonophysics, 274,* 41-59, 1997.

Yu, S.-B., L.-C. Kuo, R. S. Punongbayan, and E. G. Ramos, GPS observations of crustal deformation in the Taiwan-Luzon region, *Geophys. Res. Lett.*, *26*, 923-926, 1999.

Zhang, J., Y. Bock, H. Johnson, P. Fang, S. Williams, J. Genrich, S. Wdowinski, and J. Behr, Southern California Permanent GPS Geodetic Array: Error analysis of daily position estimates and site velocities, *J. Geophys. Res.*, *102:B8*, 18,035-18,055, 1997.

APPENDIX 1

COMBINATION OF NORMAL EQUATIONS OF DIFFERENT SOLUTIONS
PROGRAM ADDNEQ BERNESE GPS SOFTWARE VERSION 4.0
PICMP93 DAYS 107-111, 115-119

LIST OF STATIONS

TOTAL NUMBER OF STATIONS: 22

NUM	STATION	VELO	R	#FIL	1234567890
4	CGY8			10	WWWWWWWWWW
7	ILN1			5	WWWWW
8	ILO1			5	WWWWW
23	ZGS2			5	WWWWW
13	MRQ1			5	WWWWW
1	ABY3			10	WWWWWWWWWW
21	PNG5			10	WWWWWWWWWW
5	CTN1			5	WWWWW
10	LYT8			4	WWWW
19	PL11			4	WWWW
15	NE44			2	WW
11	MMA1			1	W
20	PMG1			2	WW
16	NVY1			3	WWW
6	IFG1			5	WWWWW
17	NVY3			1	W
9	LUN1			5	WWWWW
22	QZN5			2	WW
3	BLN4			3	WWW
14	NE43			3	WWW
18	NVY4			2	WW
2	ARA1			2	WW

FLAGS: W: WEIGHTS , F: FIXED, N: FREE NETWORK RESTRICTIONS, X: FREE ESTIM.
R: REFERENCE FOR COVARIANCE COMPONENTESTIMATION

A PRIORI SIGMAS FOR STATION COORDINATES / VELOCITIES :

NUM	STATION NAME	SIGMAS IN LOCAL GEODECTIC DATUM COORDINATES (M) NORTH	EAST	UP
4	CGY8	0.01000	0.01000	0.01000
7	ILN1	0.01000	0.01000	0.01000
8	ILO1	0.01000	0.01000	0.01000
23	ZGS2	0.01000	0.01000	0.01000
13	MRQ1	0.01000	0.01000	0.01000
1	ABY3	0.01000	0.01000	0.01000
21	PNG5	0.00100	0.00100	0.00100
5	CTN1	0.01000	0.01000	0.01000
10	LYT8	0.01000	0.01000	0.01000
19	PL11	0.01000	0.01000	0.01000
15	NE44	0.01000	0.01000	0.01000
11	MMA1	0.01000	0.01000	0.01000
20	PMG1	0.01000	0.01000	0.01000
16	NVY1	0.01000	0.01000	0.01000
6	IFG1	0.01000	0.01000	0.01000
17	NVY3	0.01000	0.01000	0.01000
9	LUN1	0.01000	0.01000	0.01000
22	QZN5	0.01000	0.01000	0.01000
3	BLN4	0.01000	0.01000	0.01000
14	NE43	0.01000	0.01000	0.01000
18	NVY4	0.01000	0.01000	0.01000
2	ARA1	0.01000	0.01000	0.01000

TROPOSPHERE MODEL:

TROPOSPHERE MODEL: SAASTAMOINEN
METEO VALUES : EXTRAPOLATED

REFERENCE HEIGHT : 0.00 M TEMPERATURE AT REF. HEIGHT: 18.00 C
PRESSURE AT REF. HEIGHT: 1013.25 MBAR
HUMIDITY AT REF. HEIGHT: 50.00 %

1

STATISTIC OF SOLVED FOR PARAMETERS	#PARAMETERS	#PRE-ELIMINATED	#NO-OBS
STATION COORDINATES	66	0 (BEFORE INV)	0
NUMBER OF SOLVE FOR PARAMETERS	66 0	0	

SHORT SOLUTION STATISTIC

TOTAL NUMBER OF PARAMETERS : 3641
NUMBER OF OBSERVATIONS : 126553
NUMBER OF SINGLE DIFF. FILES : 84

SIGMA OF SINGLE DIFFERENCE OBSERVATION: 0.0050
SIGMA OF COORDINATE GROUP : 0.0202
(ESTIMATION OF A MORE REALISTIC SCALING
FACTOR OF THE COVARIANCE MATRIX)

RESULTS OF COMBINED SOLUTION FOR STATION COORDINATES

TOTAL NUMBER OF STATIONS: 22

MEAN VALUES OF GEOCENTRIC X,Y,Z - COORDINATES
RMS1: FORMAL ACCURACY OF EACH COORDINATE COMPONENT FROM COMBINED SOLUTION
RMS2: RMS OF WEIGHTED AVERAGE OF EACH COORDINATE COMPONENT

EPOCH: 1993-04-18 15:30:23
VELOCITY MODEL INTRODUCED TO INDIVIDUAL SOLUTIONS: ZERO VELOCITY FIELD

NUM	STATION	#FIL	FLG	X (M)	RMS1	RMS2	Y (M)	RMS1	RMS2	Z (M)	RMS1	RMS2	RMS1-XYZ
4	CGY8	10	W	-3197753.9279	0.0018	0.0042	5172251.0481	0.0021	0.0078	1918090.8008	0.0017	0.0038	0.0023
7	ILN1	5	W	-3081613.1108	0.0022	0.0078	5211354.5564	0.0025	0.0091	1999911.2101	0.0018	0.0046	0.0029
8	ILO1	5	W	-3373690.0245	0.0027	0.0068	5282422.4242	0.0029	0.0081	1177534.4548	0.0018	0.0049	0.0031
23	ZGS2	5	W	-3361937.2282	0.0032	0.0126	5365810.2682	0.0034	0.0098	763638.7634	0.0018	0.0043	0.0036
13	MRQ1	5	W	-3274407.4745	0.0024	0.0065	5266929.1431	0.0026	0.0048	1485778.4089	0.0017	0.0068	0.0028
1	ABY3	10	W	-3439974.2943	0.0019	0.0051	5162722.4897	0.0021	0.0063	1476777.0709	0.0017	0.0028	0.0024
21	PNG5	10	W	-3091887.6107	0.0016	0.0002	5300963.2247	0.0016	0.0002	1732686.5627	0.0016	0.0003	0.0016
5	CTN1	5	W	-3639688.4999	0.0034	0.0143	5180308.4739	0.0036	0.0073	773534.1671	0.0019	0.0056	0.0038
10	LYT8	4	W	-3589024.9347	0.0032	0.0114	5124636.7614	0.0034	0.0051	1236306.7310	0.0018	0.0110	0.0037
19	PL11	4	W	-3020765.1356	0.0028	0.0071	5514266.1105	0.0032	0.0046	1068408.8027	0.0018	0.0074	0.0034
15	NE44	2	W	-3163646.1072	0.0024	0.0039	5271531.4884	0.0032	0.0094	1692603.2179	0.0019	0.0038	0.0038
11	MMA1	1	W	-3184192.4749	0.0030	0.0000	5291065.9045	0.0045	0.0000	1590599.1173	0.0022	0.0000	0.0052
20	PMG1	2	W	-3137880.7956	0.0025	0.0047	5298853.7034	0.0034	0.0119	1655110.0505	0.0019	0.0085	0.0040
16	NVY1	3	W	-3161030.5825	0.0022	0.0085	5237487.3979	0.0029	0.0106	1800208.8497	0.0019	0.0037	0.0034
6	IFG1	5	W	-3149064.1382	0.0020	0.0021	5230260.2748	0.0026	0.0036	1844836.4276	0.0018	0.0034	0.0029
17	NVY3	1	W	-3150497.0522	0.0030	0.0000	5257844.4580	0.0043	0.0000	1761153.2266	0.0022	0.0000	0.0051
9	LUN1	5	W	-3085400.2098	0.0020	0.0022	5279092.9100	0.0025	0.0034	1808629.9220	0.0018	0.0031	0.0029
22	QZN5	2	W	-3234384.2387	0.0025	0.0238	5256322.8322	0.0034	0.0224	1604282.5832	0.0019	0.0104	0.0040
3	BLN4	3	W	-3175083.0774	0.0022	0.0086	5274978.7833	0.0029	0.0098	1660428.1932	0.0018	0.0045	0.0033
14	NE43	3	W	-3163764.1522	0.0023	0.0020	5256124.1723	0.0031	0.0037	1740560.4866	0.0019	0.0022	0.0035
18	NVY4	2	W	-3148101.7405	0.0023	0.0007	5258540.0454	0.0032	0.0110	1763927.9875	0.0019	0.0058	0.0037
2	ARA1	2	W	-3213914.9178	0.0025	0.0011	5231687.1645	0.0034	0.0076	1720894.8929	0.0020	0.0065	0.0040

COMPARISON OF COMBINED SOLUTION WITH INDIVIDUAL SOLUTIONS

LIST OF RMS VALUES

COMPARISON OF STATION COORDINATES WITH RESPECT TO THE COMBINED SOLUTION IN MM
- UNWEIGHTED RMS OF INDIVIDUAL COORDINATE RESIDUALS

TOTAL NUMBER OF STATIONS: 22

NUM	STATION	#FIL	C	RMS	1	2	3	4	5	6	7	8	9	10
4	CGY8	10	N	7.8	-1.0	2.1	-1.5	-16.9	9.3	-3.8	2.1	4.7	-6.8	9.3
			E	15.6	-15.5	-13.7	18.5	33.6	7.0	2.3	-2.5	7.6	-11.0	-7.5
			U	25.6	-21.4	1.7	-28.5	10.4	3.0	-29.0	-4.6	9.3	24.6	54.1
7	ILN1	5	N	9.7	0.4	1.8	-4.1	-15.4	11.0					
			E	25.6	3.9	-15.0	18.2	45.3	-1.8					
			U	14.3	-9.1	21.1	-3.8	-8.7	-14.2					
8	ILO1	5	N	10.4	5.8	-2.0	-6.8	-15.4	10.7					
			E	18.8	-28.9	-11.7	-14.8	-0.6	15.0					
			U	15.0	23.0	-8.4	-15.2	8.3	0.3					
23	ZGS2	5	N	8.6	-1.0	4.3	-5.5	-14.3	6.6					
			E	36.7	-67.8	21.9	-7.8	5.4	-14.7					
			U	10.2	1.1	-2.2	-11.7	-2.9	16.3					
13	MRQ1	5	N	12.4	4.2	-3.3	5.3	-21.2	10.3					
			E	13.0	-18.4	-17.8	4.6	-0.8	1.0					
			U	14.2	6.8	-10.8	23.4	-9.7	-0.8					
1	ABY3	10	N	7.0	0.3	-1.9	-5.1	-15.3	6.7	0.5	3.2	2.6	10.5	-2.7
			E	12.5	-18.5	-13.1	-7.1	-6.7	-6.8	-16.6	9.3	14.9	0.9	-13.1
			U	20.1	21.5	-15.9	-20.4	1.5	12.2	16.8	42.7	-12.3	-6.0	-8.1
21	PNG5	10	N	1.0	0.6	0.7	1.2	2.1	0.1	0.9	0.5	0.9	0.4	0.6
			E	0.8	0.5	0.4	-0.5	-1.5	-1.2	0.5	-0.3	-0.1	0.3	0.7
			U	0.9	0.7	1.2	1.8	1.1	0.4	0.2	0.3	0.6	0.6	0.0
5	CTN1	5	N	15.1	15.0	-1.2	-16.8	-17.6	9.3					
			E	30.5	20.2	-54.3	-11.6	15.6	0.3					
			U	15.3	-4.3	-19.8	17.8	11.0	-9.6					
10	LYT8	4	N	20.9	27.8	-8.8	-20.8	5.6						
			E	13.7	-3.3	-17.5	-10.3	11.9						
			U	22.7	11.9	-22.4	-9.7	28.3						
19	PL11	4	N	13.4	-9.3	-12.9	-9.2	14.2						
			E	11.3	-10.5	-16.0	-0.7	4.0						
			U	14.4	1.4	-14.4	3.3	20.0						
15	NE44	2	N	2.3	2.1	-0.9								
			E	9.3	-5.1	7.8								
			U	11.8	11.6	-2.6								
11	MMA1	1	N	0.0	3.2									
			E	0.0	-4.5									
			U	0.0	2.8									
20	PMG1	2	N	8.0	6.8	-4.4								
			E	10.2	-6.4	7.9								
			U	18.3	18.0	-3.1								
16	NVY1	3	N	4.1	3.9	-4.2	0.6							
			E	4.7	-3.7	5.0	2.3							
			U	24.5	-20.9	1.2	27.6							
6	IFG1	5	N	5.0	1.7	-2.8	-4.1	3.3	7.8					
			E	5.7	-1.6	7.7	-2.2	-6.6	-4.4					
			U	9.9	7.6	0.5	-7.4	13.5	9.9					

```
17 NVY3        1 N  0.0                    1.7
               E  0.0                   -3.7
               U  0.0                   -0.6

 9 LUN1        5 N  6.0                2.2  3.8 -8.7  0.9  6.9
               E  5.1                -5.3  1.7  7.4  0.7 -4.1
               U  8.6                10.3 -4.2  4.4  2.6 12.0

22 QZN5        2 N  3.1                   1.2 -2.8
               E 13.3                  13.2 -1.0
               U 47.7                  41.6 -23.4

 3 BLN4        3 N  8.0                  -3.0 -1.9 10.7
               E  6.3                   4.3  1.0 -7.8
               U 21.1                  27.8 -9.3 -5.4

14 NE43        3 N  4.9                  -2.2  4.3  5.0
               E  3.1                  -0.7  3.7 -2.1
               U  5.8                   7.6 -2.7 -1.4

18 NVY4        2 N  5.4                    3.5  4.1
               E  7.5                   4.0 -6.3
               U 14.0                  -4.2 13.3

 2 ARA1        2 N 10.8                   10.8 -0.2
               E  5.2                   0.7 -5.2
               U  7.8                  -1.8  7.6
```

UNWEIGHTED RMS VALUES WITH RESPECT TO THE COMBINED SOLUTION IN MM

TOTAL NUMBER OF STATIONS: 22

```
          #FIL C  RMS   1   2   3   4   5   6   7   8   9  10
```

```
  COMBINATION   10 N  8.1  6.3 10.0  8.7 16.6  9.6  3.4  3.1  4.2  6.3  6.7
                E 14.4 31.1 22.6 13.8 20.0  8.8  6.9  7.7  6.7  5.0  7.0
                U 15.2 15.1 12.6 18.8  8.1 14.6 15.6 21.2 17.5 10.9 20.9
              #STA  22   8  10  10  10  10  10   9   9   9   9
               FAC     3.24 2.86 3.18 3.23 3.47 4.08 3.73 3.50 3.53 3.64
```

OUTLIER DETECTION USING THE MEAN REPEATABILITY RMS OF EACH COMPONENT
DETECTION LEVEL (RESIDUUM/RMS): 3.00
NORTH: 0.024, EAST: 0.043, UP: 0.046 (M)

FILE	STATION	COMPONENT	RESIDUUM(M)	RMS(M)	RMS*FAC(M)	GRP
1	ZGS2	E	-0.0678	0.0055	0.0177	
2	LYT8	N	0.0278	0.0026	0.0073	
4	ILN1	E	0.0453	0.0044	0.0142	

1

UNWEIGHTED RMS VALUES OF THE COMPARISON BETWEEN THE SOLUTIONS IN MM

TOTAL NUMBER OF STATIONS: 22

```
          FIL C    1   2   3   4   5   6   7   8   9
```

```
          2 N     7.8
            E    45.2
            U    25.0
          #STA      8

          3 N    13.3 14.3
            E    31.2 25.0
            U    24.6 25.2
          #STA      8  10
```

4	N	21.0	21.9	12.8					
	E	39.2	35.9	16.3					
	U	17.5	18.2	21.8					
#STA		8	10	10					
5	N	7.7	13.8	16.9	25.7				
	E	29.8	26.8	17.9	21.9				
	U	14.9	19.1	30.3	17.8				
#STA		8	10	10	10				
6	N	2.0	4.5	4.3	14.5	10.3			
	E	12.7	11.6	13.3	23.3	7.8			
	U	6.3	31.7	26.4	29.9	22.9			
#STA		3	3	3	3	3			
7	N	3.0	3.6	6.5	18.8	5.7	6.1		
	E	21.7	17.7	18.8	27.9	13.2	13.5		
	U	19.1	41.7	47.7	31.0	22.2	19.5		
#STA		3	3	3	3	3	8		
8	N	4.3	3.7	7.0	19.8	4.4	6.9	5.8	
	E	28.8	24.9	17.3	23.9	15.4	15.6	8.9	
	U	32.3	6.0	27.4	9.8	17.8	31.4	37.1	
#STA		3	3	3	3	3	6	7	
9	N	8.3	10.8	11.7	19.6	11.7	5.3	6.7	8.0
	E	14.1	10.1	21.6	32.0	13.9	11.6	9.3	10.3
	U	37.9	17.6	38.9	11.4	20.0	29.5	29.3	19.2
#STA		3	3	3	3	3	5	5	7
10	N	7.6	5.1	7.9	20.6	6.6	7.8	7.2	10.6	9.8
	E	6.9	4.4	18.9	29.4	11.3	5.4	13.3	14.7	7.8
	U	57.4	37.5	59.1	31.6	38.9	43.4	39.9	24.4	13.2
#STA		3	3	3	3	3	5	5	7	9

APPENDIX 2

COMBINATION OF NORMAL EQUATIONS OF DIFFERENT SOLUTIONS
PROGRAM ADDNEQ BERNESE GPS SOFTWARE VERSION 4.0
PICMP96 APRIL'99 PROCESSING WITH IGS STATIONS

LIST OF STATIONS

TOTAL NUMBER OF STATIONS: 23

NUM STATION VELO R #FIL 12345

12 MANL 5 WWWWW
4 CGY8 5 WWWWW
31 GUAM 50501M002 5 WWWWW
11 MMA1 5 WWWWW
20 PMG1 4 WWWW
21 PNG5 5 WWWWW
27 TAIW 23601M001 5 WWWWW
40 YAR1 50107M004 5 WWWWW
38 SHAO 21605M002 5 WWWWW
39 TAEJ 23902M001 3 W WW
28 USUD 21729S007 5 WWWWW
30 TIDB 50103M108 5 WWWWW
1 ABY3 3 WWW
26 QZN7 2 WW
36 ARX1 1 W
9 LUN1 2 WW
16 NVY1 2 WW
18 NVY4 3 WWW
15 NE44 2 WW
3 BLN4 2 WW
37 TRE2 2 WW
35 NVX3 1 W
6 IFG1 1 W

FLAGS: W: WEIGHTS , F: FIXED, N: FREE NETWORK RESTRICTIONS, X: FREE ESTIM.
R: REFERENCE FOR COVARIANCE COMPONENTESTIMATION

A PRIORI SIGMAS FOR STATION COORDINATES / VELOCITIES :

		SIGMAS IN LOCAL GEODECTIC DATUM		
		COORDINATES (M)	VELOCITIES (MM/YEAR)	
NUM	STATION NAME	NORTH	EAST	UP
12	MANL	0.01000	0.01000	0.01000
4	CGY8	0.01000	0.01000	0.01000
31	GUAM 50501M002	0.00100	0.00100	0.00100
11	MMA1	0.01000	0.01000	0.01000
20	PMG1	0.01000	0.01000	0.01000
21	PNG5	0.01000	0.01000	0.01000
27	TAIW 23601M001	0.00100	0.00100	0.00100
40	YAR1 50107M004	0.00100	0.00100	0.00100
38	SHAO 21605M002	0.00100	0.00100	0.00100
39	TAEJ 23902M001	0.00100	0.00100	0.00100
28	USUD 21729S007	0.00100	0.00100	0.00100
30	TIDB 50103M108	0.00100	0.00100	0.00100
1	ABY3	0.01000	0.01000	0.01000
26	QZN7	0.01000	0.01000	0.01000
36	ARX1	0.01000	0.01000	0.01000
9	LUN1	0.01000	0.01000	0.01000
16	NVY1	0.01000	0.01000	0.01000
18	NVY4	0.01000	0.01000	0.01000
15	NE44	0.01000	0.01000	0.01000
3	BLN4	0.01000	0.01000	0.01000
37	TRE2	0.01000	0.01000	0.01000
35	NVX3	0.01000	0.01000	0.01000
6	IFG1	0.01000	0.01000	0.01000

SUBSTRACT CENTER INFORMATION DUE TO STACRUX FILE: YES

INCREASING ORBIT LENGTH: NO

TROPOSPHERE MODEL:

TROPOSPHERE MODEL: SAASTAMOINEN
METEO VALUES : EXTRAPOLATED

REFERENCE HEIGHT : 0.00 M TEMPERATURE AT REF. HEIGHT: 18.00 C
PRESSURE AT REF. HEIGHT: 1013.25 MBAR
HUMIDITY AT REF. HEIGHT: 50.00 %

STATISTIC OF SOLVED FOR PARAMETERS	#PARAMETERS	#PRE-ELIMINATED	#NO-OBS
STATION COORDINATES	69	0 (BEFORE INV)	0
NUMBER OF SOLVE FOR PARAMETERS	69	0	0

SHORT SOLUTION STATISTIC

TOTAL NUMBER OF PARAMETERS : 3221
NUMBER OF OBSERVATIONS : 204437
NUMBER OF SINGLE DIFF. FILES : 73

SIGMA OF SINGLE DIFFERENCE OBSERVATION: 0.0055
SIGMA OF COORDINATE GROUP : 0.0255
(ESTIMATION OF A MORE REALISTIC SCALING
FACTOR OF THE COVARIANCE MATRIX)

RESULTS OF COMBINED SOLUTION FOR STATION COORDINATES

TOTAL NUMBER OF STATIONS: 23

MEAN VALUES OF GEOCENTRIC X,Y,Z - COORDINATES
RMS1: FORMAL ACCURACY OF EACH COORDINATE COMPONENT FROM COMBINED SOLUTION
RMS2: RMS OF WEIGHTED AVERAGE OF EACH COORDINATE COMPONENT

EPOCH: 1996-05-16 23:59:45
VELOCITY MODEL INTRODUCED TO INDIVIDUAL SOLUTIONS: ZERO VELOCITY FIELD

NUM	STATION	#FIL	FLG	X (M)	RMS1	RMS2	Y (M)	RMS1	RMS2	Z (M)	RMS1	RMS2	RMS1-XYZ
12	MANL	5	W	-3177118.4101	0.0009	0.0032	5293321.8456	0.0013	0.0023	1597133.1710	0.0006	0.0017	0.0016
4	CGY8	5	W	-3197753.6962	0.0011	0.0049	5172251.0847	0.0016	0.0037	1918090.9213	0.0008	0.0017	0.0020
31	GUAM 50501M002	5	W	-5071312.8124	0.0006	0.0013	3568363.5346	0.0006	0.0012	1488904.2897	0.0004	0.0011	0.0007
11	MMA1	5	W	-3184192.3095	0.0009	0.0047	5291065.9427	0.0015	0.0079	1590599.1577	0.0006	0.0022	0.0018
20	PMG1	4	W	-3137880.6450	0.0011	0.0030	5298853.7265	0.0018	0.0060	1655110.0822	0.0007	0.0053	0.0021
21	PNG5	5	W	-3091887.4765	0.0009	0.0030	5300963.2677	0.0014	0.0035	1732686.5988	0.0006	0.0019	0.0017
27	TAIW 23601M001	5	W	-3024781.9458	0.0005	0.0020	4928936.8685	0.0006	0.0010	2681234.4419	0.0005	0.0012	0.0007
40	YAR1 50107M004	5	W	-2389025.5285	0.0006	0.0027	5043316.8674	0.0006	0.0013	-3078530.8096	0.0005	0.0005	0.0007
38	SHAO 21605M002	5	W	-2831733.2205	0.0005	0.0015	4675666.0772	0.0006	0.0011	3275369.4985	0.0005	0.0009	0.0007
39	TAEJ 23902M001	3	W	-3120422.8759	0.0005	0.0021	4086355.4829	0.0006	0.0019	3761769.5942	0.0006	0.0006	0.0007
28	USUD 21729S007	5	W	-3855262.9654	0.0005	0.0015	3427432.5346	0.0005	0.0019	3741020.3333	0.0005	0.0005	0.0007
30	TIDB 50103M108	5	W	-4460996.1358	0.0006	0.0022	2682557.0831	0.0006	0.0027	-3674443.7733	0.0006	0.0006	0.0007
1	ABY3	3	W	-3439974.1392	0.0012	0.0033	5162722.4957	0.0018	0.0034	1476777.2034	0.0007	0.0018	0.0022
26	QZN7	2	W	-3208785.2846	0.0013	0.0080	5253747.9612	0.0021	0.0150	1662667.7498	0.0008	0.0034	0.0025
36	ARX1	1	W	-3213885.0183	0.0017	0.0000	5231702.4877	0.0027	0.0000	1720905.5356	0.0011	0.0000	0.0032
9	LUN1	2	W	-3085400.0515	0.0013	0.0028	5279092.9358	0.0022	0.0046	1808629.9741	0.0009	0.0005	0.0027
16	NVY1	2	W	-3161030.3785	0.0013	0.0067	5237487.4177	0.0021	0.0054	1800208.9822	0.0009	0.0013	0.0025
18	NVY4	3	W	-3148101.5543	0.0011	0.0022	5258540.0585	0.0017	0.0025	1763928.0688	0.0007	0.0033	0.0021

15	NE44	2	W	-3163645.9249	0.0014	0.0061	5271531.4980	0.0023	0.0044	1692603.2385	0.0009	0.0024	0.0028
3	BLN4	2	W	-3175082.8905	0.0014	0.0034	5274978.8200	0.0022	0.0087	1660428.2207	0.0009	0.0034	0.0027
37	TRE2	2	W	-3116046.4608	0.0014	0.0082	5305708.6836	0.0022	0.0040	1674673.8567	0.0009	0.0053	0.0027
35	NVX3	1	W	-3150497.9354	0.0016	0.0000	5257844.3822	0.0025	0.0000	1761151.6602	0.0010	0.0000	0.0031
6	IFG1	1	W	-3149063.9618	0.0018	0.0000	5230260.3371	0.0028	0.0000	1844836.5543	0.0012	0.0000	0.0034

COMPARISON OF COMBINED SOLUTION WITH INDIVIDUAL SOLUTIONS

****

COMPARISON OF STATION COORDINATES WITH RESPECT TO THE COMBINED SOLUTION IN MM
- UNWEIGHTED RMS OF INDIVIDUAL COORDINATE RESIDUALS

TOTAL NUMBER OF STATIONS: 23

NUM	STATION	#FIL	C	RMS	1	2	3	4	5
12	MANL		5	N	3.6	5.2	1.2	-2.2	-3.2	-3.1
				E	6.9	5.8	-8.1	1.6	9.3	-0.1
				U	5.4	0.9	-5.5	-7.7	-1.1	5.0
4	CGY8		5	N	6.4	-0.9	9.7	0.3	-4.0	-7.0
				E	5.8	0.7	-4.4	0.2	10.7	1.3
				U	10.7	-8.7	-16.7	1.2	8.9	4.7
31	GUAM	50501M002	5	N	2.5	0.6	1.1	0.6	-0.4	-4.7
				E	3.7	4.4	-4.2	2.5	1.6	3.2
				U	1.0	1.5	0.6	0.2	0.8	1.1
11	MMA1		5	N	3.2	1.0	2.1	1.1	-4.1	-4.1
				E	12.6	20.1	-9.5	-3.0	11.3	0.5
				U	25.0	-48.4	-10.7	-6.2	2.3	-1.9
20	PMG1		4	N	8.1	12.7	-0.8	-4.3	-4.4
				E	4.7	-5.1	3.2	-2.1	4.9
				U	20.6	18.0	-5.9	-5.1	29.7
21	PNG5		5	N	5.7	-5.9	7.5	-2.2	-1.6	-5.5
				E	5.8	-2.8	-5.0	2.5	9.6	1.2
				U	9.6	17.3	-2.8	-2.7	-1.7	7.3
27	TAIW	23601M001	5	N	3.0	0.6	-1.8	-0.5	-3.3	4.5
				E	4.3	-0.9	-2.4	1.7	7.9	1.8
				U	1.8	2.1	1.5	1.1	1.6	1.4
40	YAR1	50107M004	5	N	1.3	-1.4	-0.5	-0.9	1.9	-0.1
				E	6.9	-7.3	0.6	-7.5	-6.9	-5.6
				U	0.2	-0.2	-0.1	-0.1	0.3	0.0
38	SHAO	21605M002	5	N	2.3	-3.4	-0.7	-0.9	2.6	1.2
				E	3.9	2.0	-0.7	3.3	-0.3	6.7
				U	0.7	-0.5	-0.8	-0.6	-0.7	-0.3
39	TAEJ	23902M001	3	N	1.4	1.4		-1.2	0.7	
				E	4.9	3.5		5.7	1.9	
				U	0.6	-0.4		-0.5	-0.5	
28	USUD	21729S007	5	N	1.3	-0.1	-0.2	2.1	0.6	-1.4
				E	5.4	7.8	1.9	4.2	5.4	-2.0
				U	0.3	0.3	-0.4	0.4	0.2	-0.1
30	TIDB	50103M108	5	N	1.3	1.2	0.5	0.8	-2.0	-0.9
				E	7.9	-7.8	0.4	-8.6	-6.3	-8.7
				U	1.3	-1.4	-0.6	-1.4	-0.9	-1.3

```
 1 ABY3        3 N  2.2      2.3 -1.3 -1.6
               E  3.7     -1.7  1.7  4.6
               U  7.7      5.5 -6.7  6.6

26 QZN7        2 N 10.5      8.2 -6.6
               E  3.5      0.1 -3.5
               U 21.6     -19.2 10.0

36 ARX1        1 N  0.0      3.1
               E  0.0     -2.7
               U  0.0     -3.1

 9 LUN1        2 N  1.8      1.7  0.1
               E  5.9      2.0 -5.5
               U  4.6     -4.4  1.5

16 NVY1        2 N  4.9      4.2 -2.4
               E  4.0     -3.7  1.5
               U 10.0     -8.9  4.5

18 NVY4        3 N  5.6          3.2 -3.1 -6.6
               E  5.2          2.8  6.8 -0.2
               U  2.2         -0.2 -2.9  1.1

15 NE44        2 N  4.2             -2.4 -3.4
               E  9.0              8.9 -1.4
               U  3.5             -0.6  3.5

 3 BLN4        2 N  4.7             -2.0 -4.3
               E  8.2              8.2  0.3
               U 11.9             -10.1  6.2

37 TRE2        2 N  5.3             -0.1 -5.3
               E  8.5              8.5  0.2
               U 13.0             12.4 -3.9

35 NVX3        1 N  0.0                -4.3
               E  0.0               0.6
               U  0.0               0.5

 6 IFG1        1 N  0.0               -4.0
               E  0.0               0.7
               U  0.0               0.5
```

UNWEIGHTED RMS VALUES WITH RESPECT TO THE COMBINED SOLUTION IN MM

TOTAL NUMBER OF STATIONS: 23

```
          #FIL C  RMS   1    2    3    4    5
```

```
  COMBINATION     5 N  3.6  4.7  4.2  2.5  2.7  4.4
                  E  5.5  7.9  4.2  4.2  7.6  3.4
                  U  8.7 16.6  8.1  4.4  9.0  3.4
                #STA  23   12   16   17   17   16
                 FAC      4.41 3.57 4.71 5.12 4.45
```

OUTLIER DETECTION USING THE MEAN REPEATABILITY RMS OF EACH COMPONENT
DETECTION LEVEL (RESIDUUM/RMS): 3.00
NORTH: 0.011, EAST: 0.016, UP: 0.026 (M)

FILE	STATION	COMPONENT	RESIDUUM(M)	RMS(M)	RMS*FAC(M)	GRP
1	MMA1	E	0.0201	0.0009	0.0039	
1	PMG1	N	0.0127	0.0007	0.0031	

UNWEIGHTED RMS VALUES OF THE COMPARISON BETWEEN THE SOLUTIONS IN MM

TOTAL NUMBER OF STATIONS: 23

FIL C	1	2	3	4
2 N	7.1			
E	11.9			
U	15.8			
#STA	11			
3 N	5.9	5.9		
E	7.5	6.4		
U	16.2	10.5		
#STA	12	15		
4 N	6.7	5.9	3.2	
E	7.0	11.6	6.6	
U	17.5	13.9	11.0	
#STA	12	12	14	
5 N	4.8	8.1	5.1	3.5
E	7.9	7.4	2.9	7.8
U	16.5	9.1	5.5	7.4
#STA	10	10	11	14

APPENDIX 3

COMBINATION OF NORMAL EQUATIONS OF DIFFERENT SOLUTIONS
PROGRAM ADDNEQ BERNESE GPS SOFTWARE VERSION 4.0
PICMP98 APRIL'99 PROCESSING WITH IGS STATIONS

LIST OF STATIONS

TOTAL NUMBER OF STATIONS: 50
NUM STATION VELO R #FIL 1234567890

---

31 GUAM 50501M002 10 WWWWWWWWWW
13 MRQ1 4 WWWW
6 IFG1 2 WW
84 SHAO 21605M002 10 WWWWWWWWWW
86 YAR1 50107M004 10 WWWWWWWWWW
18 NVY4 2 WW
38 ZBS3 2 WW
26 QZN7 2 WW
12 MANL 10 WWWWWWWWWW
20 PMG1 2 WW
85 TAEJ 23902M001 9 WWW WWWWWW
28 USUD 21729S007 10 WWWWWWWWWW
30 TIDB 50103M108 10 WWWWWWWWWW
52 BUAN 3 WWW
15 NE44 3 WWW
54 QZE3 3 WWW
53 PNG3 1 W
4 CGY8 2 WW
81 NVE3 2 WW
21 PNG5 2 WW
82 TRCP 2 WW
3 BLN4 1 W
43 LODP 3 WWW
39 CASP 2 WW
40 DAUP 2 WW
41 DIZP 2 WW
42 GUMP 2 WW
44 MACP 2 WW
45 NABP 2 WW
37 TRE2 2 WW
46 UODP 2 WW
47 ZBS9 2 WW
55 BALT 2 WW
57 SALT 2 WW
59 TGYT 4 WWWW
48 ALAT 2 WW
49 BIGT 2 WW
50 MCLT 2 WW
56 PNKT 2 WW
51 PRPT 2 WW
58 TBGT 4 WWWW
60 TLY2 2 WW
64 CCA5 2 WW
61 BLG4 2 WW
62 CALT 2 WW
63 CAPT 2 WW
65 KAYT 2 WW
66 MTBT 2 WW
67 PINT 2 WW
68 TVST 2 WW

FLAGS: W: WEIGHTS , F: FIXED, N: FREE NETWORK RESTRICTIONS, X: FREE ESTIM.
R: REFERENCE FOR COVARIANCE COMPONENTESTIMATION

A PRIORI SIGMAS FOR STATION COORDINATES / VELOCITIES :

SIGMAS IN LOCAL GEODECTIC DATUM

NUM	STATION NAME	COORDINATES (M) NORTH	EAST	UP	VELOCITIES (MM/YEAR)
31	GUAM 50501M002	0.00500	0.00500	0.00500	
13	MRQ1	0.00500	0.00500	0.00500	
6	IFG1	0.00500	0.00500	0.00500	
84	SHAO 21605M002	0.00100	0.00100	0.00100	
86	YAR1 50107M004	0.00500	0.00500	0.00500	
18	NVY4	0.00500	0.00500	0.00500	
38	ZBS3	0.00500	0.00500	0.00500	
26	QZN7	0.00500	0.00500	0.00500	
12	MANL	0.00050	0.00050	0.00050	
20	PMG1	0.00500	0.00500	0.00500	
85	TAEJ 23902M001	0.00500	0.00500	0.00500	
28	USUD 21729S007	0.00500	0.00500	0.00500	
30	TIDB 50103M108	0.00500	0.00500	0.00500	
52	BUAN	0.00500	0.00500	0.00500	
15	NE44	0.00500	0.00500	0.00500	
54	QZE3	0.00500	0.00500	0.00500	
53	PNG3	0.00500	0.00500	0.00500	
4	CGY8	0.00500	0.00500	0.00500	
81	NVE3	0.00500	0.00500	0.00500	
21	PNG5	0.00500	0.00500	0.00500	
82	TRCP	0.00500	0.00500	0.00500	
3	BLN4	0.00500	0.00500	0.00500	
43	LODP	0.00500	0.00500	0.00500	
39	CASP	0.00500	0.00500	0.00500	
40	DAUP	0.00500	0.00500	0.00500	
41	DIZP	0.00500	0.00500	0.00500	
42	GUMP	0.00500	0.00500	0.00500	
44	MACP	0.00500	0.00500	0.00500	
45	NABP	0.00500	0.00500	0.00500	
37	TRE2	0.00500	0.00500	0.00500	
46	UODP	0.00500	0.00500	0.00500	
47	ZBS9	0.00500	0.00500	0.00500	
55	BALT	0.00500	0.00500	0.00500	
57	SALT	0.00500	0.00500	0.00500	
59	TGYT	0.00500	0.00500	0.00500	
48	ALAT	0.00500	0.00500	0.00500	
49	BIGT	0.00500	0.00500	0.00500	
50	MCLT	0.00500	0.00500	0.00500	
56	PNKT	0.00500	0.00500	0.00500	
51	PRPT	0.00500	0.00500	0.00500	
58	TBGT	0.00500	0.00500	0.00500	
60	TLY2	0.00500	0.00500	0.00500	
64	CCA5	0.00500	0.00500	0.00500	
61	BLG4	0.00500	0.00500	0.00500	
62	CALT	0.00500	0.00500	0.00500	
63	CAPT	0.00500	0.00500	0.00500	
65	KAYT	0.00500	0.00500	0.00500	
66	MTBT	0.00500	0.00500	0.00500	
67	PINT	0.00500	0.00500	0.00500	
68	TVST	0.00500	0.00500	0.00500	

SUBSTRACT CENTER INFORMATION DUE TO STACRUX FILE: YES

INCREASING ORBIT LENGTH: NO

TROPOSPHERE MODEL:

TROPOSPHERE MODEL: SAASTAMOINEN
METEO VALUES : EXTRAPOLATED

REFERENCE HEIGHT : 0.00 M TEMPERATURE AT REF. HEIGHT: 18.00 C
PRESSURE AT REF. HEIGHT: 1013.25 MBAR
HUMIDITY AT REF. HEIGHT: 50.00 %

SHORT SOLUTION STATISTIC

TOTAL NUMBER OF PARAMETERS : 5974
NUMBER OF OBSERVATIONS : 373819
NUMBER OF SINGLE DIFF. FILES : 153

SIGMA OF SINGLE DIFFERENCE OBSERVATION: 0.0054
SIGMA OF COORDINATE GROUP : 0.0216
(ESTIMATION OF A MORE REALISTIC SCALING
FACTOR OF THE COVARIANCE MATRIX)

RESULTS OF COMBINED SOLUTION FOR STATION COORDINATES

TOTAL NUMBER OF STATIONS: 50

MEAN VALUES OF GEOCENTRIC X,Y,Z - COORDINATES
RMS1: FORMAL ACCURACY OF EACH COORDINATE COMPONENT FROM COMBINED SOLUTION
RMS2: RMS OF WEIGHTED AVERAGE OF EACH COORDINATE COMPONENT

EPOCH: 1998-05-21 23:59:45
VELOCITY MODEL INTRODUCED TO INDIVIDUAL SOLUTIONS: ZERO VELOCITY FIELD

NUM	STATION	#FIL	FLG	X (M)	RMS1	RMS2	Y (M)	RMS1	RMS2	Z (M)	RMS1	RMS2	RMS1-XYZ
31	GUAM 50501M002	10	W	-5071312.7964	0.0012	0.0031	3568363.5179	0.0010	0.0029	1488904.2949	0.0005	0.0011	.0016
13	MRQ1	4	W	-3274407.3791	0.0008	0.0022	5266929.0812	0.0012	0.0025	1485778.4615	0.0005	0.0030	0.0015
6	IFG1	2	W	-3149063.9086	0.0012	0.0008	5230260.3384	0.0018	0.0006	1844836.6024	0.0008	0.0029	0.0021
84	SHAO 21605M002	10	W	-2831733.3152	0.0004	0.0008	4675666.0419	0.0006	0.0006	3275369.4797	0.0004	0.0005	0.0007
86	YAR1 50107M004	10	W	-2389025.6547	0.0009	0.0054	5043316.8825	0.0014	0.0048	-3078530.6844	0.0008	0.0019	0.0015
18	NVY4	2	W	-3148101.5165	0.0011	0.0042	5258540.0660	0.0016	0.0051	1763928.1075	0.0007	0.0034	0.0020
38	ZBS3	2	W	-3062287.8067	0.0011	0.0034	5320172.7810	0.0017	0.0078	1726061.1118	0.0007	0.0020	0.0020
26	QZN7	2	W	-3208785.2448	0.0011	0.0031	5253747.9854	0.0016	0.0012	1662667.7832	0.0007	0.0026	0.0020
12	MANL	10	W	-3177118.3415	0.0003	0.0002	5293321.7850	0.0003	0.0007	1597133.1459	0.0003	0.0005	0.0004
20	PMG1	2	W	-3137880.5836	0.0011	0.0036	5298853.6673	0.0017	0.0087	1655110.0591	0.0007	0.0025	0.0020
85	TAEJ 23902M001	9	W	-3120422.9620	0.0007	0.0011	4086355.4471	0.0009	0.0016	3761769.5771	0.0007	0.0014	0.0012
28	USUD 21729S007	10	W	-3855263.0055	0.0008	0.0010	3427432.5381	0.0009	0.0022	3741020.3331	0.0008	0.0013	0.0013
30	TIDB 50103M108	10	W	-4460996.2525	0.0012	0.0072	2682557.1044	0.0012	0.0056	-3674443.6695	0.0009	0.0042	0.0016
52	BUAN	3	W	-3439450.7543	0.0010	0.0015	5168328.3216	0.0014	0.0039	1458974.6723	0.0006	0.0026	0.0017
15	NE44	3	W	-3163645.8881	0.0009	0.0017	5271531.4767	0.0014	0.0028	1692603.2335	0.0006	0.0012	0.0017
54	QZE3	3	W	-3248981.9152	0.0010	0.0011	5238686.9988	0.0015	0.0025	1632131.2987	0.0006	0.0015	0.0018
53	PNG3	1	W	-3075374.5534	0.0013	0.0000	5303613.3194	0.0020	0.0000	1753482.3973	0.0008	0.0000	0.0024
4	CGY8	2	W	-3197753.6340	0.0011	0.0032	5172251.0982	0.0016	0.0102	1918090.9879	0.0007	0.0032	0.0020
81	NVE3	2	W	-3150498.3870	0.0011	0.0020	5257845.6235	0.0016	0.0089	1761146.2922	0.0007	0.0021	0.0020
21	PNG5	2	W	-3091887.4633	0.0011	0.0087	5300963.2659	0.0017	0.0035	1732686.6040	0.0007	0.0046	0.0020
82	TRCP	2	W	-3115707.6823	0.0011	0.0009	5305843.9724	0.0017	0.0007	1674786.4385	0.0007	0.0008	0.0020
3	BLN4	1	W	-3175082.8404	0.0013	0.0000	5274978.8142	0.0020	0.0000	1660428.2143	0.0008	0.0000	0.0024
43	LODP	3	W	-3123723.3546	0.0011	0.0070	5299409.1774	0.0017	0.0034	1679948.4534	0.0007	0.0042	0.0020
39	CASP	2	W	-3101294.4235	0.0016	0.0047	5327157.7932	0.0026	0.0084	1633148.9535	0.0011	0.0021	0.0031
40	DAUP	2	W	-3132573.1343	0.0016	0.0141	5300872.5351	0.0026	0.0180	1658832.6285	0.0011	0.0065	0.0031
41	DIZP	2	W	-3110744.6700	0.0017	0.0055	5320758.5172	0.0028	0.0073	1636458.3383	0.0012	0.0088	0.0033
42	GUMP	2	W	-3125510.6358	0.0016	0.0008	5311601.4063	0.0026	0.0038	1637568.2124	0.0011	0.0021	0.0030
44	MACP	2	W	-3124235.4198	0.0016	0.0017	5305540.6461	0.0025	0.0034	1660249.5165	0.0011	0.0023	0.0030
45	NABP	2	W	-3122720.9151	0.0016	0.0004	5311994.8892	0.0026	0.0025	1642442.8450	0.0011	0.0035	0.0031
37	TRE2	2	W	-3116046.4518	0.0016	0.0028	5305708.7238	0.0026	0.0014	1674673.8676	0.0011	0.0024	0.0031
46	UODP	2	W	-3112859.6212	0.0016	0.0039	5308496.0565	0.0027	0.0088	1671899.5117	0.0011	0.0017	0.0032
47	ZBS9	2	W	-3086604.3483	0.0018	0.0026	5332455.0511	0.0029	0.0037	1643419.2018	0.0013	0.0024	0.0034
55	BALT	2	W	-3197694.2531	0.0011	0.0021	5299481.5519	0.0018	0.0041	1535068.8022	0.0007	0.0036	0.0021
57	SALT	2	W	-3186770.4361	0.0012	0.0027	5307049.5867	0.0018	0.0043	1531545.6019	0.0007	0.0027	0.0022
59	TGYT	4	W	-3181411.9353	0.0008	0.0023	5307495.1495	0.0012	0.0046	1543636.5725	0.0005	0.0020	0.0014
48	ALAT	2	W	-3185461.0864	0.0011	0.0024	5307063.6263	0.0018	0.0043	1534073.2343	0.0007	0.0025	0.0021
49	BIGT	2	W	-3189051.5722	0.0011	0.0020	5304122.0829	0.0018	0.0033	1536758.2737	0.0007	0.0022	0.0021
50	MCLT	2	W	-3187184.0956	0.0012	0.0013	5306004.4139	0.0019	0.0038	1534146.9073	0.0007	0.0023	0.0023
56	PNKT	2	W	-3186808.5491	0.0012	0.0020	5305558.1208	0.0018	0.0039	1536521.4813	0.0007	0.0024	0.0022
51	PRPT	2	W	-3188942.9043	0.0011	0.0018	5303923.2405	0.0018	0.0037	1537692.8282	0.0007	0.0024	0.0021
58	TBGT	4	W	-3187768.3258	0.0009	0.0017	5304902.2292	0.0013	0.0032	1536722.6329	0.0005	0.0017	0.0016
60	TLY2	2	W	-3188771.1196	0.0011	0.0022	5302405.8663	0.0018	0.0044	1543265.6836	0.0007	0.0032	0.0021

64 CCA5	2 W	-3194157.4499	0.0011	0.0091	5305606.7607	0.0017	0.0028	1522197.4650	0.0007	0.0023	0.0021
61 BLG4	2 W	-3183307.9194	0.0011	0.0018	5308689.8333	0.0017	0.0039	1533067.8101	0.0007	0.0027	0.0021
62 CALT	2 W	-3189360.3323	0.0011	0.0005	5304966.1182	0.0018	0.0034	1533329.8570	0.0007	0.0023	0.0021
63 CAPT	2 W	-3189210.5758	0.0012	0.0012	5305288.4444	0.0018	0.0033	1532427.7283	0.0007	0.0024	0.0022
65 KAYT	2 W	-3186179.6325	0.0011	0.0027	5307362.7745	0.0017	0.0051	1531588.1073	0.0007	0.0024	0.0021
66 MTBT	2 W	-3186177.7756	0.0011	0.0026	5307071.5590	0.0018	0.0043	1532741.7875	0.0007	0.0025	0.0021
67 PINT	2 W	-3189372.7453	0.0011	0.0013	5304678.7484	0.0017	0.0016	1534542.6527	0.0007	0.0026	0.0021
68 TVST	2 W	-3187757.3971	0.0011	0.0004	5304935.3450	0.0017	0.0017	1536648.4718	0.0007	0.0023	0.0020

COMPARISON OF COMBINED SOLUTION WITH INDIVIDUAL SOLUTIONS

****

COMPARISON OF STATION COORDINATES WITH RESPECT TO THE COMBINED SOLUTION IN MM
- UNWEIGHTED RMS OF INDIVIDUAL COORDINATE RESIDUALS

TOTAL NUMBER OF STATIONS: 50

NUM	STATION	#FIL	C	RMS	1	2	3	4	5	6	7	8	9	10
31	GUAM	50501M002	10	N	5.1	1.3	-5.1	-3.0	-2.4	-10.6	1.7	-0.1	-1.2	5.3	7.1
				E	7.0	3.3	-4.7	-3.6	-0.1	-1.7	2.0	8.9	-1.2	0.1	17.4
				U	11.1	-4.0	8.1	-2.3	17.4	-1.7	2.4	-7.9	5.2	-24.5	-4.0
13	MRQ1		4	N	5.9	-8.1	-2.4	4.5	-3.4						
				E	2.7	1.4	0.3	-3.8	2.4						
				U	7.2	-9.1	-4.2	1.5	7.0						
6	IFG1		2	N	3.5	-0.2	-3.5								
				E	1.3	-0.3	-1.2								
				U	0.9	0.0	-0.9								
84	SHAO	21605M002	10	N	1.7	-0.5	-3.4	2.2	-1.0	-1.6	1.0	-0.8	-1.9	0.0	0.6
				E	3.0	-4.0	-2.5	-0.1	-5.5	-1.5	-0.9	-2.9	0.1	-1.4	-3.6
				U	0.5	-0.5	-0.3	0.1	-0.4	-0.9	-0.9	0.2	0.0	-0.1	-0.6
86	YAR1	50107M004	10	N	8.1	11.5	-7.6	-0.7	-12.5	-7.6	1.4	-3.2	4.3	8.2	9.5
				E	24.0	-30.2	-0.7	2.6	14.8	-33.5	-5.9	21.9	-42.5	-8.0	-23.5
				U	7.3	-3.6	-8.0	-6.5	-15.5	8.3	3.4	-0.8	-2.9	4.0	3.6
18	NVY4		2	N	5.5	2.1	-5.1								
				E	1.8	-1.8	0.2								
				U	9.5	-9.2	2.4								
38	ZBS3		2	N	4.7	-4.5	-1.1								
				E	1.3	-1.2	0.4								
				U	12.6	11.7	-4.7								
26	QZN7		2	N	3.4	-1.0	-3.3								
				E	3.2	-3.0	1.1								
				U	4.2	-4.1	0.9								
12	MANL		10	N	1.1	-1.4	-0.6	-1.6	-1.1	0.0	-1.2	-0.6	-0.5	-1.0	-1.0
				E	1.7	2.5	1.7	1.2	2.5	1.0	1.4	0.6	1.0	1.6	2.1
				U	1.9	-2.0	-1.9	-1.9	-1.9	-1.8	-1.8	-1.6	-1.8	-1.9	-1.7
20	PMG1		2	N	4.8	1.1	-4.7								
				E	1.9	1.3	-1.5								
				U	13.3	-11.5	6.8								
85	TAEJ	23902M001	9	N	3.2	3.9	-1.9	-1.5		-4.7	1.0	2.2	2.0	0.0	-5.2
				E	4.6	-0.4	-1.3	1.9		3.8	1.5	-0.8	3.2	-4.0	-10.9
				U	5.1	4.7	0.8	8.5		-8.1	5.7	-0.3	0.2	-0.2	3.7
28	USUD	21729S007	10	N	3.6	2.1	0.8	-2.0	-9.0	-1.8	3.5	-1.8	2.2	-0.9	0.6
				E	6.4	-1.3	1.9	2.7	-13.6	5.3	4.3	-1.6	1.3	-5.2	-9.5
				U	5.8	-0.4	-9.7	3.5	4.3	-10.6	2.7	-1.2	-5.7	0.9	4.2
30	TIDB	50103M108	10	N	9.7	-1.7	-16.2	-8.5	-10.8	-11.3	4.3	7.8	-7.3	9.6	6.9
				E	21.7	-24.4	3.3	-11.9	24.6	-35.6	-3.0	21.8	-27.9	-8.8	-17.3
				U	21.4	-30.4	-13.2	-5.6	-29.0	-18.1	-17.0	-9.8	-23.5	-12.2	-27.2

```
52 BUAN      3 N  3.5     -3.0  1.3 -3.7
           E  1.9     -0.6 -1.9  1.8
           U  7.8      0.4 10.5 -3.3

15 NE44      3 N  2.8     -3.2  0.7 -2.4
           E  4.1     -0.1  5.4 -2.3
           U  3.4      2.1  0.3  4.4

54 QZE3      3 N  2.2     -2.8 -0.1 -1.5
           E  1.3      0.9 -1.0  1.2
           U  4.3     -1.9  5.8  0.5

53 PNG3      1 N  0.0     -3.1
           E  0.0     -0.1
           U  0.0     -0.2
 4 CGY8      2 N  7.3         5.1 -5.2
           E 11.6         9.4 -6.9
           U  8.1        -5.6  5.8

81 NVE3      2 N  1.6        -1.2 -1.1
           E  9.0         7.1 -5.5
           U  9.9        -7.4  6.6

21 PNG5      2 N  9.3        -8.6  3.6
           E  9.7         7.9 -5.6
           U  8.2         8.2  0.0

82 TRCP      2 N  1.2        -0.6 -1.0
           E  1.2         0.7 -1.0
           U  1.0         1.0  0.0

 3 BLN4      1 N  0.0           -1.6
           E  0.0          -1.7
           U  0.0           1.1

43 LODP      3 N  9.9           0.3 -11.3  8.1
           E  9.5          -4.7  7.6 -10.1
           U  8.8         -10.0  4.6  -6.0

39 CASP      2 N  6.1              -0.5 -6.0
           E 11.2               4.4 -10.3
           U  8.4               2.3  8.1

40 DAUP      2 N  6.0              -6.0  0.6
           E 30.5              18.5 -24.3
           U 14.2              -6.8  12.5

41 DIZP      2 N 13.4               4.1 -12.8
           E  8.1               2.5  -7.7
           U 10.0               9.6  2.7

42 GUMP      2 N  3.9              -2.4 -3.1
           E  1.9              -0.3 -1.9
           U  5.2               0.3  5.2

44 MACP      2 N  4.4              -1.9 -3.9
           E  4.7               1.5 -4.5
           U  2.9              -0.2  2.9

45 NABP      2 N  6.4               0.3 -6.4
           E  2.5               0.3 -2.5
           U  1.5               0.0  1.5

37 TRE2      2 N  3.5              -3.4 -1.0
           E  3.7               1.5 -3.4
           U  1.8               1.7 -0.6

46 UODP      2 N  5.0              -4.8  1.2
           E  1.5              -1.5  0.0
           U 11.8              11.5  2.9

47 ZBS9      2 N  3.2               0.4 -3.1
           E  5.7               3.0 -4.8
```

	U	3.2		-3.2	-0.1			
55 BALT		2 N	5.5			-0.2	5.5	
	E	1.1		-0.1	-1.1			
	U	7.5		4.6	6.0			
57 SALT		2 N	1.9			1.5	1.2	
	E	2.9		0.4	-2.9			
	U	6.9		5.9	3.6			
59 TGYT		4 N	1.8			2.5	1.2	1.2 -0.7
	E	1.3		-1.1	-1.6	0.9	-0.8	
	U	10.3		15.4	1.9	2.3	8.4	
48 ALAT		2 N	1.7			1.4	0.9	
	E	3.0		0.5	-3.0			
	U	7.2		5.1	5.0			
49 BIGT		2 N	1.8			1.3	1.2	
	E	1.4		-0.9	1.1			
	U	6.8		3.5	5.9			
50 MCLT		2 N	2.2			1.0	1.9	
	E	2.7		0.5	-2.6			
	U	7.2		2.3	6.8			
56 PNKT		2 N	1.7			1.4	0.9	
	E	1.1		-0.1	-1.1			
	U	7.0		4.6	5.2			
51 PRPT		2 N	2.2			1.1	1.9	
	E	0.8		-0.2	-0.8			
	U	6.4		4.5	4.6			
58 TBGT		4 N	1.7			2.1	2.1	0.3 0.3
	E	2.1		-0.3	-2.2	1.6	-2.3	
	U	7.9		8.6	9.7	3.4	2.1	
60 TLY2		2 N	4.2			0.3	4.2	
	E	0.6		-0.4	-0.5			
	U	8.6		4.6	7.2			
64 CCA5		2 N	2.3				2.3	0.3
	E	11.3			-4.8	10.3		
	U	13.2			-1.9	13.0		
61 BLG4		2 N	2.1				1.7	1.1
	E	1.1			-0.6	-0.9		
	U	5.5			5.5	0.5		
62 CALT		2 N	2.6				2.4	-0.9
	E	3.6			0.4	-3.6		
	U	5.6			1.1	5.5		
63 CAPT		2 N	2.2				1.4	1.7
	E	1.9			-0.1	-1.9		
	U	5.7			3.5	4.5		
65 KAYT		2 N	3.5				1.0	3.4
	E	0.9			-0.6	-0.6		
	U	7.7			6.3	-4.5		
66 MTBT		2 N	2.3				1.4	1.8
	E	1.5			-0.3	-1.5		
	U	6.3			6.0	-1.9		
67 PINT		2 N	2.9				2.5	-1.4
	E	2.9			0.1	-2.9		
	U	2.3			2.2	0.6		

68 TVST	2	N	2.4	2.3	-0.6
		E	0.9	-0.8	-0.5
		U	3.0	1.7	2.4

UNWEIGHTED RMS VALUES WITH RESPECT TO THE COMBINED SOLUTION IN MM

TOTAL NUMBER OF STATIONS: 50

#FIL	C	RMS	1	2	3	4	5	6	7	8	9	10
COMBINATION	10	N	4.3	4.6	5.5	4.0	5.4	5.9	4.9	2.5	3.1	3.7	3.9
		E	8.8	11.4	1.8	5.5	8.9	13.4	7.9	8.1	12.8	3.7	9.7
		U	7.6	10.9	5.6	5.8	10.5	7.5	6.4	6.3	7.8	7.6	8.4
#STA	50		13	17	15	16	17	17	17	17	17	17	
FAC			5.12	4.60	4.09	4.09	4.19	3.68	6.29	5.25	5.26	4.76	

OUTLIER DETECTION USING THE MEAN REPEATABILITY RMS OF EACH COMPONENT
DETECTION LEVEL (RESIDUUM/RMS): 3.00
NORTH: 0.013, EAST: 0.026, UP: 0.023 (M)

FILE	STATION	COMPONENT	RESIDUUM(M)	RMS(M)	RMS*FAC(M)	GRP
1	YAR1 50107M004	E	-0.0302	0.0011	0.0056	
5	YAR1 50107M004	E	-0.0335	0.0016	0.0069	
5	TIDB 50103M108	E	-0.0356	0.0018	0.0076	
8	YAR1 50107M004	E	-0.0425	0.0011	0.0059	
8	TIDB 50103M108	E	-0.0279	0.0016	0.0084	

UNWEIGHTED RMS VALUES OF THE COMPARISON BETWEEN THE SOLUTIONS IN MM

TOTAL NUMBER OF STATIONS: 50

FIL	C	1	2	3	4	5	6	7	8	9
2	N	8.2								
	E	12.1								
	U	10.6								
#STA		13								
3	N	7.8	4.9							
	E	13.9	5.6							
	U	10.5	7.7							
#STA		8	11							
4	N	11.7	4.3	6.6						
	E	27.7	10.4	13.9						
	U	12.2	9.1	11.3						
#STA		7	10	14						
5	N	10.7	3.5	4.8	6.8					
	E	6.2	21.0	17.7	32.9					
	U	9.7	8.8	11.9	15.7					
#STA		7	7	7	7					
6	N	5.0	9.9	6.2	10.5	9.3				
	E	13.5	4.6	5.6	16.2	16.7				
	U	6.8	7.7	6.6	11.1	8.3				
#STA		7	7	7	7	17				
7	N	7.4	10.4	7.1	9.9	9.5	3.4			
	E	28.5	13.2	16.8	7.7	33.0	15.7			
	U	8.9	8.1	5.5	15.8	7.6	6.1			
#STA		7	7	7	6	7	7			

8	N	4.0	6.5	3.6	9.2	7.2	5.2	4.7
	E	6.1	21.4	19.6	35.5	5.2	18.2	20.6
	U	5.5	5.1	9.5	9.3	7.0	5.6	6.2
#STA		7	7	7	6	7	7	17

9	N	5.5	13.2	9.0	13.9	12.7	4.3	4.7	6.7
	E	11.4	6.9	6.3	18.6	16.0	5.2	15.6	14.4
	U	11.8	14.8	11.0	22.0	11.3	11.4	8.0	11.9
#STA		7	7	7	6	7	7	9	9

10	N	5.8	12.9	8.8	14.0	12.6	5.0	6.0	6.8	2.4
	E	8.8	16.6	15.7	26.7	14.4	13.5	21.9	12.0	7.7
	U	3.7	10.6	9.9	12.8	8.8	5.0	7.7	6.6	8.5
#STA		7	7	7	6	7	7	9	9	17

APPENDIX 4

The final readjusted PGNet (ITRF96) coordinate set (plus the positional error ellipses) from the NEWGAN adjustment.

Point	Latitude	Longitude	Ellipsoidal	Horiz Standard Ellipse			Height
			Height	Semi major	Semi minor	Orient	Std Dev
ABR 01	N17 36 0.911587	E120 36 54.555542	88.062E	0.085	0.037	83.1	0.075
ABR 02	N17 34 16.374196	E120 54 13.762007	815.494E	0.079	0.035	82.7	0.071
AGN 01	N 9 9 25.851928	E125 33 3.008988	137.966E	0.109	0.040	86.7	0.086
AGN 02	N 8 57 24.858522	E125 24 6.400489	116.987E	0.126	0.048	87.7	0.101
AGS 01	N 8 36 32.535698	E125 54 47.758323	114.392E	0.144	0.048	86.8	0.103
AGS 02	N 8 10 39.007165	E125 59 40.906557	107.641E	0.171	0.050	86.6	0.112
AGS 03	N 8 26 49.237995	E125 43 18.267579	96.597E	0.144	0.046	87.0	0.102
AKN 01	N11 42 24.488247	E122 22 4.799720	89.749E	0.095	0.041	82.0	0.097
AKN 02	N11 48 41.320791	E122 10 16.022664	134.448E	0.094	0.039	84.2	0.083
AKN 03	N11 29 6.924802	E122 18 38.781747	205.111E	0.087	0.035	84.0	0.076
ABY 00	N13 8 52.971336	E123 45 15.999959	77.419E	0.046	0.019	84.1	0.040
ABY 01	N13 11 10.846888	E123 18 18.509508	105.932E	0.074	0.029	83.6	0.064
ABY 02	N13 8 35.418793	E123 45 37.195506	119.126E	0.050	0.021	84.0	0.043
ABY 04	N13 16 32.160624	E124 2 46.384847	193.641E	0.114	0.041	85.5	0.081
ABY 05	N13 0 53.290873	E123 19 12.220419	147.758E	0.139	0.047	91.2	0.093
ATQ 01	N11 54 40.411634	E121 33 1.165519	221.928E	0.117	0.047	86.1	0.098
ATQ 02	N11 15 25.143686	E122 3 42.581270	219.733E	0.087	0.035	83.8	0.077
ATQ 03	N10 56 8.240577	E122 0 19.675781	191.911E	0.082	0.034	84.8	0.074
ATQ 04	N10 26 58.761803	E122 0 38.193367	302.799E	0.071	0.029	85.0	0.064
ARA 01	N15 45 25.786644	E121 33 47.225087	48.113E	0.102	0.030	87.8	0.055
ARA 02	N16 8 36.063436	E121 57 26.684005	51.463E	0.119	0.037	86.4	0.068
ARA 03	N16 24 55.231778	E122 14 22.213324	222.618E	0.117	0.046	84.6	0.091
BSL 01	N 6 42 31.004877	E121 58 15.970309	71.235E	0.086	0.044	88.4	0.072
BSL 02	N 6 24 30.143979	E121 58 2.403589	71.455E	0.113	0.058	89.1	0.096
BSL 03	N 6 39 42.495304	E122 8 25.212156	72.554E	0.094	0.049	90.5	0.079
BSL 04	N 6 41 33.231809	E121 42 23.426743	74.177E	0.113	0.054	88.3	0.087
BTN 01	N14 35 1.549296	E120 34 33.482105	193.145E	0.150	0.047	85.9	0.076
BTN 02	N14 22 46.896470	E120 34 35.408881	237.539E	0.151	0.049	86.0	0.081
BTN 03	N14 26 32.517227	E120 29 54.968446	105.311E	0.157	0.048	86.2	0.081
BTS 02	N20 46 56.420068	E121 50 12.083085	159.145E	0.725	0.229	83.7	0.277
BTS 03	N20 26 17.873089	E121 57 46.034712	46.697E	0.670	0.212	83.6	0.258
BTS 04	N20 18 5.318105	E121 51 30.614502	385.726E	0.669	0.212	83.7	0.257
BTG 01	N13 49 8.110482	E120 57 25.577444	391.761E	0.103	0.039	86.0	0.068
BTG 02	N14 4 56.917423	E120 37 14.659431	46.313E	0.109	0.040	86.1	0.069
BTG 03	N13 40 25.064128	E121 27 4.568874	152.629E	0.105	0.041	86.0	0.067
BTG 04	N13 32 3.395552	E121 5 55.681732	59.264E	0.115	0.046	86.7	0.087
BTG 05	N13 38 8.384302	E121 2 8.999813	48.051E	0.146	0.062	84.5	0.136
BTG 06	N13 38 8.943521	E121 11 43.062896	53.246E	0.118	0.046	87.0	0.085
BTG 07	N13 37 19.634321	E121 4 56.321706	67.592E	0.149	0.066	82.0	0.146
BTG 08	N13 44 30.112358	E120 56 51.550012	48.028E	0.108	0.045	86.1	0.093
BGT 01	N16 23 59.518475	E120 38 46.595973	1288.602E	0.083	0.024	87.1	0.046
BGT 02	N16 35 50.234380	E120 45 44.019739	2154.334E	0.106	0.040	84.9	0.074
BGT 03	N16 35 57.667476	E120 45 45.983498	2163.588E	0.100	0.035	89.0	0.067
BHL 01	N 9 36 22.521267	E123 51 15.909677	248.720E	0.081	0.032	84.2	0.068
BHL 02	N10 7 27.776711	E124 8 51.667180	241.821E	0.080	0.033	83.4	0.070
BHL 03	N 9 39 43.479728	E123 59 17.043351	439.697E	0.083	0.033	83.8	0.071
BHL 04	N 9 44 20.555640	E124 33 13.623762	185.612E	0.090	0.036	83.9	0.076
BKN 01	N 8 13 57.259070	E124 36 10.837042	469.159E	0.114	0.041	87.5	0.089
BKN 02	N 7 47 12.125595	E124 58 0.555753	410.281E	0.139	0.049	88.2	0.106
BKN 03	N 8 9 40.599602	E125 7 10.218547	745.365E	0.131	0.045	88.0	0.099

BKN 04	N 7 29 0.803759	E124 56 37.887918	347.443E	0.133	0.049	88.3	0.101
BKN 05	N 7 55 5.475060	E125 19 34.151233	475.229E	0.126	0.046	88.1	0.097
BLN 01	N14 56 26.655297	E120 52 52.490380	56.383E	0.122	0.034	86.6	0.059
BLN 02	N14 50 47.881897	E120 45 52.910431	45.186E	0.163	0.050	86.1	0.076
BLN 03	N14 54 15.441405	E121 2 34.847428	126.704E	0.120	0.034	86.8	0.061
BLN 04	N15 11 23.955659	E121 2 39.558614	119.584E	0.105	0.030	87.3	0.054
CGY 01	N17 44 6.403296	E121 27 19.555555	85.503E	0.072	0.032	77.2	0.054
CGY 02	N18 52 47.147651	E121 17 34.920142	78.660E	0.156	0.076	70.1	0.172
CGY 03	N18 17 31.460834	E121 49 37.351618	43.582E	0.114	0.053	76.5	0.087
CGY 04	N18 52 33.319771	E121 49 19.345600	73.033E	0.294	0.098	83.7	0.131
CGY 05	N18 30 31.638484	E122 8 59.414336	39.131E	0.251	0.085	83.6	0.115
CGY 06	N17 50 48.731760	E121 54 8.585926	71.928E	0.063	0.034	74.8	0.071
CGY 07	N19 15 35.053084	E121 28 51.227191	37.790E	0.463	0.151	83.3	0.191
CGY 09	N17 57 23.385296	E121 39 34.372451	55.637E	0.070	0.035	76.0	0.061
CGY 10	N18 36 59.552128	E121 2 59.684728	129.750E	0.109	0.053	71.5	0.109
CGY 11	N18 22 41.595382	E121 23 44.060197	46.924E	0.110	0.058	75.7	0.111
CMN 01	N14 19 3.312145	E122 34 16.834964	247.037E	0.249	0.081	85.8	0.114
CMN 02	N14 8 3.897937	E122 58 57.800745	54.643E	0.137	0.057	84.3	0.100
CMS 01	N13 30 28.099170	E123 2 33.112529	54.109E	0.076	0.032	85.6	0.065
CMS 02	N13 45 39.147250	E123 17 10.041304	111.890E	0.079	0.035	86.0	0.068
CMS 03	N13 42 9.491962	E123 45 38.495793	58.166E	0.067	0.030	86.7	0.062
CGN 01	N 9 15 18.425370	E124 43 2.565789	67.023E	0.099	0.038	85.6	0.081
CPZ 01	N11 36 19.617340	E122 42 58.165306	151.990E	0.085	0.035	83.0	0.078
CPZ 02	N11 29 58.229196	E122 42 16.144425	291.684E	0.080	0.033	83.3	0.073
CNS 01	N13 33 8.622277	E124 19 3.143140	69.760E	0.141	0.056	84.8	0.107
CNS 92	N14 1 38.053534	E124 15 52.800732	82.125E	0.200	0.074	86.8	0.139
CVT 01	N14 16 52.700571	E120 59 49.086204	238.657E	0.125	0.040	85.8	0.066
CVT 01	N14 16 53.224657	E120 51 54.195150	154.882E	0.140	0.044	85.7	0.071
CBU 01	N10 59 11.866669	E123 56 47.918573	181.534E	0.076	0.032	82.6	0.067
CBU 02	N 9 31 56.231160	E123 21 33.635662	832.009E	0.087	0.034	85.4	0.071
CBU 03	N10 27 11.956472	E123 42 24.587447	279.393E	0.074	0.030	83.6	0.064
CBU 95	N 9 53 8.155049	E123 35 30.590085	116.528E	0.078	0.031	84.8	0.065
CBU 96	N10 37 37.279572	E124 0 46.114454	314.322E	0.072	0.030	83.2	0.063
CBU 99	N10 37 39.017674	E124 20 20.707450	311.822E	0.078	0.032	82.3	0.068
CBU A0	N10 19 4.895732	E123 53 43.714695	103.336E	0.072	0.029	83.7	0.062
CBU100	N10 19 48.148762	E123 59 21.903727	73.320E	0.130	0.045	91.1	0.093
DVA 01	N 7 41 58.505287	E125 59 13.276767	167.156E	0.163	0.048	87.5	0.114
DVA 02	N 7 28 24.239974	E125 48 10.149897	101.619E	0.118	0.042	88.6	0.086
DVA 03	N 7 35 1.114164	E125 42 18.007250	91.432E	0.123	0.044	88.9	0.093
DVA 04	N 7 8 12.013098	E125 53 52.476881	73.730E	0.169	0.047	88.4	0.115
DVE 01	N 6 53 23.231130	E126 0 22.583538	71.580E	0.118	0.040	88.5	0.081
DVE 02	N 6 39 8.059880	E126 4 10.996650	70.824E	0.132	0.047	88.8	0.093
DVE 03	N 6 57 6.382679	E126 12 25.530038	70.841E	0.141	0.047	88.6	0.100
DVE 04	N 6 16 11.318449	E126 11 34.863569	97.090E	0.182	0.066	88.9	0.130
DVE 05	N 7 12 50.642811	E126 32 22.206190	70.662E	0.216	0.059	88.2	0.149
DVE 06	N 7 52 4.450129	E126 23 1.005001	77.288E	0.163	0.051	87.0	0.118
DVE 07	N 7 37 1.102096	E126 33 57.697651	71.647E	0.173	0.051	87.6	0.123
DVS 01	N 7 4 38.410979	E125 37 36.781225	70.516E	0.099	0.035	88.5	0.069
DVS 02	N 6 58 54.042938	E125 45 26.414964	510.529E	0.104	0.036	88.4	0.072
DVS 03	N 6 44 51.339613	E125 21 25.182222	104.307E	0.078	0.029	88.2	0.056
DVS 04	N 7 16 29.160247	E125 18 54.023777	688.711E	0.080	0.031	88.6	0.059
DVS 05	N 6 23 44.270085	E125 37 6.723255	73.509E	0.104	0.039	88.7	0.078
DVS 06	N 5 55 12.114808	E125 39 19.667819	70.913E	0.135	0.048	87.8	0.096
SME 01	N11 54 19.581998	E125 25 7.776847	62.094E	0.088	0.038	79.1	0.082
SME 02	N12 8 19.958220	E125 26 10.067763	59.937E	0.099	0.045	77.8	0.097
SME 03	N11 36 29.586137	E125 26 44.901850	63.979E	0.083	0.035	81.0	0.071
SME 04	N11 1 54.196685	E125 44 2.981387	66.698E	0.103	0.044	81.1	0.092
SME 05	N11 5 33.615738	E125 30 19.602906	180.036E	0.091	0.039	79.7	0.083
IFG 01	N16 55 14.096937	E121 3 5.532277	1406.908E	0.098	0.036	87.6	0.071

ILN 02	N17 58 5.086880	E120 30 50.225538	136.557E	0.088	0.042	76.1	0.094
ILN 03	N18 5 4.626333	E120 48 52.929619	158.250E	0.080	0.037	75.8	0.083
ILS 01	N17 35 47.412533	E120 23 27.867110	43.343E	0.098	0.043	82.6	0.090
ILS 02	N17 7 52.159121	E120 26 37.414608	45.838E	0.091	0.035	85.6	0.072
ILS 03	N16 58 44.565282	E120 44 18.016414	624.893E	0.088	0.033	85.9	0.065
ILO 02	N11 2 28.065404	E122 54 13.945749	395.587E	0.062	0.025	84.2	0.053
ILO 03	N10 44 17.272366	E122 24 47.028881	148.145E	0.051	0.021	84.4	0.045
ILO 04	N11 12 34.729992	E123 6 56.671207	119.648E	0.068	0.027	84.3	0.057
ILO 05	N11 27 10.093552	E123 15 19.602504	403.703E	0.077	0.031	84.2	0.065
ILO 06	N11 6 54.867975	E122 32 5.439767	165.837E	0.075	0.030	84.3	0.065
ISB 01	N17 7 15.078374	E122 26 27.232008	46.065E	0.317	0.101	85.3	0.132
ISB 02	N16 42 19.060437	E121 33 30.947182	121.590E	0.083	0.030	86.3	0.057
ISB 03	N17 23 12.597510	E122 14 10.433141	48.040E	0.294	0.093	85.1	0.121
ISB 04	N16 30 12.892472	E121 44 13.347215	147.934E	0.100	0.033	86.1	0.061
ISB 05	N17 1 53.594028	E121 51 15.476983	123.789E	0.084	0.038	83.7	0.070
ISB 31	N16 41 28.375445	E121 32 55.395876	159.610E	0.091	0.037	83.6	0.073
ISB 52	N16 59 3.059959	E122 0 30.686277	145.793E	0.121	0.048	85.2	0.091
ISB 53	N17 12 20.141660	E121 36 24.850662	110.134E	0.072	0.037	80.7	0.075
ISB 54	N17 12 20.202375	E121 36 24.869275	110.073E	0.202	0.067	88.8	0.171
KAY 02	N17 24 27.770974	E121 26 36.510120	255.889E	0.060	0.031	80.2	0.059
KAY 03	N18 14 17.887164	E121 22 13.426928	60.043E	0.102	0.052	73.4	0.115
LAG 01	N14 15 46.089914	E121 23 53.457840	54.619E	0.141	0.043	85.7	0.070
LAG 02	N14 26 7.417942	E121 26 57.248341	54.607E	0.133	0.042	85.8	0.067
LAG 03	N14 10 55.759135	E121 8 51.419720	216.480E	0.181	0.058	86.1	0.085
LAG 04	N14 19 58.876519	E121 3 15.559152	69.767E	0.126	0.041	85.9	0.069
LAG 05	N14 20 32.689022	E121 2 58.964479	67.666E	0.126	0.041	85.9	0.069
LAN 01	N 8 16 13.742927	E124 15 29.300026	72.367E	0.113	0.041	87.3	0.091
LAN 02	N 7 54 42.628246	E123 46 6.309449	85.128E	0.126	0.045	87.2	0.096
LAN 03	N 7 47 34.434469	E123 43 0.107197	72.120E	0.147	0.052	87.4	0.110
LAS 01	N 8 0 34.622786	E124 16 53.698756	825.580E	0.123	0.044	87.5	0.099
LAS 02	N 7 47 30.416819	E124 11 37.232286	773.386E	0.147	0.054	88.0	0.120
LAS 03	N 7 35 26.362486	E124 3 58.197019	73.302E	0.141	0.054	88.6	0.123
LUN 01	N16 34 57.199514	E120 18 15.943816	84.037E	0.097	0.029	87.2	0.053
LUN 02	N16 21 32.040704	E120 21 41.192554	97.434E	0.172	0.038	88.5	0.071
LUN 03	N16 15 31.545581	E120 22 3.045886	42.861E	0.153	0.035	88.5	0.064
LYT 01	N11 18 27.815766	E124 41 18.821106	65.234E	0.082	0.035	80.4	0.073
LYT 02	N11 27 18.550921	E124 19 10.721459	93.310E	0.077	0.033	80.0	0.070
LYT 03	N11 0 13.729040	E124 36 32.425153	65.553E	0.083	0.035	80.7	0.074
LYT 04	N11 12 40.308447	E124 23 21.451010	63.944E	0.079	0.033	80.9	0.070
LYT 05	N10 38 0.608186	E124 47 24.123165	108.324E	0.093	0.038	81.4	0.079
LYT 06	N10 44 48.452001	E125 0 48.908758	67.171E	0.080	0.034	80.8	0.069
LYT 07	N11 14 36.467207	E125 0 28.075910	88.684E	0.030	0.012	87.5	0.024
MGD 01	N 7 22 27.540608	E124 16 13.841120	171.331E	0.114	0.044	88.4	0.089
MGD 02	N 7 13 12.417362	E124 14 39.135415	133.831E	0.112	0.044	88.6	0.088
MGD 03	N 7 0 40.399356	E124 9 33.172846	519.358E	0.123	0.048	88.7	0.097
MRQ 02	N13 12 8.358959	E122 1 10.331413	135.063E	0.083	0.035	86.1	0.062
MST 01	N12 21 47.333207	E123 36 28.967302	75.093E	0.074	0.030	84.2	0.058
MST 02	N12 29 4.816440	E123 22 41.340982	208.295E	0.071	0.029	83.7	0.062
MST 04	N11 58 54.695239	E123 13 50.618914	231.418E	0.078	0.032	83.8	0.066
MST 05	N13 9 31.914370	E122 59 43.406597	96.481E	0.079	0.035	87.2	0.072
MST 06	N11 55 51.302575	E123 46 10.407531	75.720E	0.093	0.038	82.8	0.075
MST 93	N11 56 37.526898	E123 44 34.757335	161.108E	0.096	0.040	82.5	0.078
MMA 00	N14 38 6.817085	E121 2 34.963581	99.391E	0.117	0.039	85.6	0.063
MMA 01	N14 32 13.811885	E121 2 23.141840	69.530E	0.118	0.039	85.8	0.065
MMA 05	N14 39 23.124847	E121 4 11.151184	133.125E	0.118	0.040	85.6	0.066
MMA 06	N14 35 53.888241	E120 58 23.141560	62.914E	0.121	0.045	86.0	0.080
MSW 01	N 8 8 25.544283	E123 50 34.398170	71.121E	0.122	0.044	87.2	0.097
MSW 02	N 8 19 56.027979	E123 51 29.471399	70.884E	0.113	0.042	87.2	0.092
MSW 03	N 8 29 10.837063	E123 48 29.125060	70.414E	0.132	0.050	87.0	0.115

MSW 04	N 8 39 25.151108	E123 34 50.402421	68.801E	0.120	0.047	86.8	0.104
MSE 01	N 8 49 48.687258	E125 5 57.376655	71.058E	0.109	0.041	87.1	0.088
MSE 02	N 8 49 44.987539	E125 6 16.423982	94.282E	0.112	0.042	87.1	0.090
MSE 03	N 9 0 1.191885	E124 52 58.922656	69.736E	0.104	0.039	86.7	0.084
MSE 04	N 8 29 47.517819	E124 39 40.202558	88.459E	0.113	0.040	87.5	0.089
MSE 05	N 8 37 8.758335	E124 28 45.657535	71.705E	0.117	0.043	87.4	0.094
MSE 06	N 8 44 30.139874	E124 46 23.893739	70.966E	0.110	0.040	87.3	0.088
MSE 07	N 8 36 48.998025	E124 45 36.750904	73.342E	0.148	0.046	88.7	0.106
MSE 08	N 8 23 26.041652	E124 36 32.140042	289.885E	0.140	0.045	88.0	0.106
MPV 01	N17 5 33.420760	E120 58 8.303778	1230.700E	0.089	0.035	85.6	0.069
NGW 01	N10 57 20.664113	E123 18 46.187992	88.007E	0.075	0.030	84.2	0.064
NGW 02	N10 48 8.295118	E122 58 33.632891	90.797E	0.065	0.026	84.4	0.056
NGW 03	N 9 59 21.271824	E122 48 53.175636	84.761E	0.109	0.043	88.2	0.094
NGW 04	N 9 44 54.623969	E122 24 13.934481	71.986E	0.094	0.039	86.9	0.086
NGW 05	N10 35 20.094434	E123 29 1.168023	64.258E	0.074	0.030	84.2	0.063
NGW 06	N10 54 24.885395	E123 25 2.733358	126.645E	0.071	0.029	83.9	0.062
NGW 07	N10 28 5.484020	E122 49 18.982000	64.653E	0.066	0.027	84.9	0.057
NGW 08	N 9 57 9.547178	E122 42 45.321615	448.955E	0.174	0.080	84.9	0.193
NGE 01	N 9 21 18.162416	E122 50 21.816658	86.690E	0.100	0.039	85.3	0.083
NGE 02	N 9 35 30.153146	E123 8 55.714224	226.507E	0.091	0.035	85.5	0.073
NGE 03	N 9 55 25.214604	E123 10 38.975161	66.578E	0.094	0.036	86.3	0.075
CTN 02	N 7 3 33.394235	E124 40 36.033374	111.406E	0.083	0.034	88.5	0.065
CTN 03	N 7 11 29.662878	E124 32 2.852081	120.667E	0.098	0.040	88.8	0.077
SMN 01	N12 30 24.923346	E124 38 24.911855	60.141E	0.082	0.037	80.1	0.080
SMN 02	N12 23 5.361322	E124 19 38.852622	60.899E	0.069	0.030	81.2	0.062
SMN 03	N12 30 8.952058	E124 17 16.674211	59.150E	0.071	0.031	82.3	0.064
SMN 04	N12 32 45.634015	E125 6 53.482528	69.498E	0.098	0.044	78.5	0.095
SMN 05	N12 30 31.011943	E124 39 40.782457	93.918E	0.080	0.037	80.3	0.078
SMN 06	N12 20 17.040673	E125 1 51.664956	67.449E	0.090	0.040	79.0	0.087
NEJ 43	N15 56 27.223175	E121 2 40.410380	437.557E	0.084	0.026	88.2	0.050
NEJ 44	N15 29 29.579428	E120 58 10.445196	100.768E	0.111	0.036	90.6	0.068
NEJ 45	N15 39 34.339504	E121 13 13.250173	203.086E	0.096	0.028	88.2	0.053
NEJ 47	N15 58 2.683667	E121 2 45.360601	349.840E	0.085	0.026	88.0	0.050
NVY 01	N16 30 8.192032	E121 6 45.502707	419.388E	0.084	0.027	87.6	0.051
NVY 02	N16 19 38.088722	E121 15 39.989548	861.259E	0.085	0.027	86.9	0.049
NVY 03	N16 7 59.141017	E120 55 48.047898	979.003E	0.137	0.046	88.6	0.083
NVY 04	N16 9 31.569177	E120 54 26.865872	1141.608E	0.137	0.046	88.5	0.085
MRW 01	N13 47 18.305355	E120 19 50.754150	118.691E	0.114	0.045	86.6	0.084
MRW 02	N12 12 30.639292	E121 0 36.055664	173.943E	0.082	0.035	86.3	0.069
MRW 03	N12 42 2.391891	E120 52 40.110255	277.786E	0.096	0.040	87.1	0.079
MRW 04	N13 4 46.915151	E120 44 10.176532	93.136E	0.168	0.050	87.7	0.093
MRW 05	N13 13 21.437643	E120 36 25.683206	83.969E	0.111	0.043	86.7	0.081
MRE 01	N13 31 17.636091	E120 59 18.963757	97.805E	0.119	0.045	85.9	0.085
MRE 02	N13 25 46.129551	E121 11 40.007147	50.654E	0.100	0.038	86.1	0.069
MRE 03	N13 1 59.786749	E121 29 32.641824	53.562E	0.079	0.033	86.1	0.064
MRE 04	N12 44 52.031397	E121 29 17.427566	72.844E	0.087	0.037	86.4	0.074
MRE 05	N12 28 14.536658	E121 25 12.519746	216.240E	0.081	0.034	85.9	0.067
PLW 00	N 9 44 57.365399	E118 44 40.389726	71.461E	0.056	0.036	97.2	0.068
PLW 01	N11 59 12.105858	E120 10 53.631017	239.416E	0.118	0.058	88.5	0.108
PLW 02	N12 7 55.932513	E119 56 7.423914	56.307E	0.123	0.060	88.7	0.112
PLW 03	N12 16 22.269018	E120 22 5.296381	192.475E	0.108	0.049	87.1	0.098
PLW 04	N11 9 29.116372	E120 58 23.813522	322.300E	0.086	0.039	86.0	0.088
PLW 05	N10 51 34.712163	E121 4 12.653551	81.786E	0.083	0.037	86.0	0.084
PLW 06	N 9 34 39.500560	E121 11 57.271256	60.395E	0.136	0.056	87.0	0.130
PLW 07	N 9 44 25.437770	E118 44 25.543143	86.244E	0.053	0.034	97.8	0.067
PLW 08	N10 49 42.475504	E119 31 4.465052	61.785E	0.085	0.045	88.6	0.090
PLW 09	N 8 47 27.336282	E117 51 42.161593	53.049E	0.138	0.080	91.7	0.132
PLW 10	N 8 41 13.250827	E117 41 59.681329	52.123E	0.138	0.073	90.6	0.117
PLW 12	N11 57 11.928001	E119 50 7.943475	257.925E	0.125	0.060	88.7	0.113

PLW 13	N 8 30 13.273031	E117 26 0.773908	56.167E	0.165	0.086	91.9	0.137
PLW 14	N 8 26 22.157153	E117 25 45.941002	52.507E	0.152	0.078	91.2	0.124
PLW 15	N 7 59 31.256052	E117 4 27.078556	78.164E	0.194	0.090	91.2	0.152
PLW 16	N 7 58 59.220007	E117 4 13.241984	198.703E	0.193	0.089	91.2	0.149
PLW 17	N 8 46 5.645981	E117 50 8.698304	52.251E	0.126	0.067	90.6	0.106
PLW 18	N 9 16 13.397882	E117 58 49.904718	263.298E	0.111	0.060	90.6	0.093
PLW 19	N 9 8 53.017862	E118 3 38.115218	434.399E	0.108	0.058	90.3	0.087
PLW 20	N 9 26 36.118426	E118 35 16.193802	54.225E	0.075	0.045	92.8	0.074
PLW 21	N 9 43 47.401243	E118 44 0.040187	55.680E	0.063	0.040	99.0	0.075
PLW 22	N 9 4 37.802840	E117 41 54.434468	58.109E	0.138	0.075	89.6	0.132
PLW 23	N10 5 15.153880	E119 12 38.958983	60.293E	0.085	0.049	93.2	0.088
PLW 24	N10 18 57.881235	E119 20 41.782484	54.189E	0.097	0.057	93.0	0.101
PLW 25	N10 19 0.500913	E119 19 48.876249	120.918E	0.090	0.051	92.2	0.091
PLW 26	N10 32 19.282646	E119 46 28.603689	159.668E	0.102	0.056	90.9	0.100
PLW 27	N11 29 29.147629	E119 52 9.527900	51.641E	0.126	0.063	89.3	0.113
PLW 28	N11 15 50.878345	E119 25 21.828178	256.045E	0.116	0.063	90.7	0.114
PLW 29	N11 21 43.649293	E119 24 39.921139	166.559E	0.119	0.065	90.7	0.117
PLW 30	N10 1 14.885832	E118 47 29.514289	77.359E	0.093	0.055	94.7	0.099
PLW 31	N 7 30 37.007876	E117 18 49.904015	53.336E	0.221	0.090	90.1	0.152
PMG 01	N15 8 24.804946	E120 37 59.602123	107.309E	0.114	0.031	87.0	0.055
PNG 02	N16 23 35.800881	E119 52 54.095339	40.545E	0.270	0.085	83.7	0.106
PNG 03	N16 3 47.871388	E120 6 28.464156	81.036E	0.088	0.022	87.0	0.041
PNG 04	N15 54 40.717889	E120 38 30.198032	73.994E	0.069	0.018	87.1	0.035
PNG 06	N16 2 40.234830	E120 19 43.808922	45.389E	0.125	0.029	88.4	0.052
PNG 07	N16 4 22.255037	E120 20 7.975629	59.199E	0.125	0.029	88.4	0.054
QZN 01	N14 6 6.925279	E122 0 55.052097	51.735E	0.214	0.068	86.1	0.096
QZN 02	N14 42 7.956884	E122 19 39.563877	55.505E	0.259	0.082	86.1	0.114
QZN 03	N14 55 30.896290	E121 48 24.349876	70.270E	0.185	0.046	86.6	0.080
QZN 04	N14 37 54.539503	E121 56 24.426674	109.350E	0.180	0.047	86.6	0.076
QZN 05	N14 39 54.059591	E121 36 19.163484	48.608E	0.179	0.046	86.3	0.076
QZN 06	N14 11 17.389359	E121 43 43.267523	50.194E	0.172	0.054	85.8	0.079
QZN 07	N15 12 40.072526	E121 24 53.892692	49.996E	0.129	0.034	86.9	0.061
QZN 08	N13 34 8.925831	E122 34 0.436253	74.467E	0.188	0.067	86.5	0.100
QZN 09	N13 47 9.774643	E122 3 37.946797	120.120E	0.130	0.043	86.6	0.061
QZN 10	N13 35 36.614143	E122 19 30.727700	53.537E	0.173	0.061	86.4	0.090
QZN 11	N13 31 29.736046	E122 24 23.219271	55.516E	0.195	0.068	86.5	0.099
QZN 12	N13 44 20.118682	E122 27 55.858704	55.463E	0.145	0.061	86.8	0.096
QZN 13	N13 9 46.155368	E122 35 57.783758	82.537E	0.071	0.030	85.6	0.057
RZL 01	N14 28 57.077591	E121 11 16.739685	50.277E	0.171	0.055	85.6	0.082
RZL 02	N14 27 48.386336	E121 11 51.635626	124.216E	0.125	0.040	85.9	0.067
RML 01	N12 55 55.819310	E121 43 11.244244	391.621E	0.096	0.041	85.5	0.083
RML 02	N12 47 42.134752	E122 3 7.974583	265.165E	0.082	0.035	86.0	0.069
RML 03	N12 30 4.551198	E122 32 0.792924	79.988E	0.085	0.036	85.8	0.072
RML 04	N12 34 46.315035	E122 15 44.533111	108.303E	0.080	0.033	86.0	0.066
RML 05	N12 20 41.487176	E121 56 12.354029	74.311E	0.094	0.038	85.6	0.077
SMR 01	N11 46 30.644162	E124 52 42.495635	64.859E	0.077	0.033	80.6	0.069
SMR 02	N12 3 45.076193	E124 35 29.992885	62.308E	0.077	0.034	80.0	0.073
SMR 03	N11 56 20.052622	E124 19 2.864639	453.184E	0.077	0.033	80.4	0.070
SMR 04	N11 8 3.856472	E125 12 13.904181	86.816E	0.067	0.029	80.1	0.062
SMR 05	N11 16 48.896820	E125 3 55.689133	110.891E	0.050	0.021	81.8	0.046
SQJ 01	N 9 14 32.439380	E123 37 3.868473	458.171E	0.100	0.039	85.1	0.082
SQJ 02	N 9 13 6.500883	E123 30 44.235613	66.650E	0.105	0.040	85.4	0.085
SRG 01	N12 35 4.968754	E124 5 12.356412	59.028E	0.063	0.027	82.7	0.054
SRG 02	N12 49 31.345516	E123 49 20.053184	179.626E	0.090	0.032	86.5	0.057
SRG 03	N12 58 3.499756	E124 0 10.601663	71.220E	0.055	0.023	83.9	0.047
SRG 04	N12 56 15.550359	E123 31 47.642869	81.298E	0.066	0.027	84.1	0.056
SRG 94	N12 56 15.545059	E123 31 47.643924	81.190E	0.089	0.036	84.9	0.072
CTS 01	N 6 6 52.487796	E125 10 21.040095	112.987E	0.110	0.045	89.8	0.091
CTS 02	N 6 13 26.008847	E124 42 42.408335	790.822E	0.124	0.050	89.6	0.104

CTS 03	N 6 13 35.945894	E124 42 44.728590	827.394E	0.128	0.052	89.7	0.109
CTS 04	N 6 30 1.807763	E124 50 39.934851	135.439E	0.104	0.042	88.9	0.083
CTS 05	N 6 8 42.011693	E125 10 43.525532	117.605E	0.139	0.047	88.7	0.098
CTS 06	N 5 59 16.597223	E124 37 26.944665	75.842E	0.136	0.054	89.6	0.114
CTS 07	N 5 52 26.682975	E125 5 17.072609	78.773E	0.158	0.052	88.1	0.107
CTS 08	N 5 50 16.114407	E125 10 50.368842	117.378E	0.130	0.049	88.8	0.100
LYS 01	N10 8 14.306320	E124 50 37.686936	151.469E	0.090	0.036	83.2	0.076
LYS 02	N10 8 59.519070	E125 7 3.048319	136.892E	0.096	0.039	83.2	0.081
SKT 01	N 6 33 20.331772	E124 3 1.998635	81.723E	0.140	0.056	89.3	0.115
SKT 02	N 6 41 42.262367	E124 40 57.005324	158.769E	0.098	0.039	88.6	0.077
SKT 03	N 6 9 27.186881	E124 16 40.246486	75.471E	0.147	0.059	89.3	0.121
SUL 01	N 6 3 19.018415	E121 0 11.003868	87.438E	0.168	0.080	89.5	0.132
SUL 02	N 6 6 11.473947	E120 57 44.006580	99.670E	0.176	0.084	89.6	0.138
SUL 03	N 6 18 7.983427	E120 35 9.775467	66.479E	0.178	0.085	89.6	0.140
SUL 04	N 5 32 44.498648	E120 48 45.823366	69.472E	0.190	0.089	89.6	0.148
SRN 01	N 9 49 10.282052	E125 26 38.217674	161.621E	0.097	0.038	84.7	0.081
SRN 02	N 9 33 13.973410	E125 34 10.537635	122.448E	0.116	0.044	86.8	0.097
SRN 03	N 9 57 39.228636	E125 35 24.935055	89.930E	0.106	0.043	85.5	0.090
SRN 04	N10 21 36.858682	E125 34 42.022252	69.544E	0.120	0.048	85.9	0.101
SRN 05	N10 1 30.936549	E126 2 29.045761	154.824E	0.137	0.050	87.2	0.110
SRN 06	N 9 36 35.634276	E126 8 11.025683	103.627E	0.128	0.047	87.0	0.103
SRN 07	N 9 38 59.236585	E125 55 12.217061	100.515E	0.120	0.046	86.6	0.100
SRN 08	N 9 32 32.113366	E125 50 26.105287	72.275E	0.120	0.045	86.7	0.095
SRN 09	N 9 36 38.870345	E125 24 6.362095	135.573E	0.107	0.041	86.3	0.086
SRN 10	N 9 39 32.879751	E125 36 10.396711	81.796E	0.167	0.052	87.4	0.113
SRN 11	N 9 34 55.433720	E125 44 2.743466	72.310E	0.160	0.051	87.2	0.109
SRS 01	N 9 16 31.656813	E126 11 27.462775	69.898E	0.132	0.047	87.1	0.101
SRS 02	N 8 48 4.294319	E126 17 38.313043	79.586E	0.149	0.051	86.7	0.107
SRS 03	N 8 12 0.050113	E126 19 38.218853	72.687E	0.161	0.051	86.6	0.115
SRS 04	N 9 4 2.615109	E126 10 26.878530	112.044E	0.182	0.055	86.4	0.115
SRS 05	N 8 56 38.533092	E126 2 31.273564	107.987E	0.132	0.049	86.8	0.102
SRS 06	N 8 27 27.796563	E126 9 41.414327	140.314E	0.231	0.069	86.8	0.137
TRC 01	N15 28 38.648018	E120 35 57.494975	85.217E	0.101	0.028	87.2	0.052
TRC 02	N15 19 23.339537	E120 25 32.462652	242.980E	0.134	0.036	86.6	0.066
TRC 03	N15 36 34.297206	E120 23 1.763329	147.187E	0.135	0.035	86.5	0.065
TTW 01	N 5 1 26.794501	E119 45 56.535070	155.364E	0.205	0.091	89.9	0.155
TTW 02	N 5 16 2.803392	E120 4 44.326441	86.730E	0.202	0.092	90.0	0.156
TTW 03	N 4 40 33.581758	E119 24 57.534914	67.154E	0.237	0.113	89.2	0.192
TTW 04	N 4 48 22.900971	E119 51 50.712926	68.425E	0.215	0.097	89.8	0.163
TTW 05	N 5 2 5.414314	E119 46 30.773104	74.351E	0.210	0.094	90.0	0.159
TTW 06	N 5 1 7.637244	E119 44 50.996957	401.359E	0.209	0.094	89.9	0.159
TTW 07	N 7 1 1.051098	E118 29 22.171654	86.317E	0.186	0.088	90.7	0.145
TTW 08	N 6 4 23.144446	E118 18 44.848744	58.526E	0.234	0.091	89.7	0.157
ZBS 01	N15 24 33.150965	E119 57 8.938823	90.842E	0.223	0.074	84.4	0.105
ZBS 02	N14 59 37.354508	E120 7 14.389633	67.055E	0.169	0.061	82.8	0.091
ZBS 03	N15 48 20.475879	E119 55 28.933549	45.677E	0.148	0.060	80.9	0.092
ZGN 01	N 8 35 12.957919	E123 20 39.521459	79.087E	0.109	0.043	86.5	0.091
ZGN 02	N 8 30 52.317929	E123 3 45.958710	74.968E	0.139	0.068	88.5	0.124
ZGN 03	N 8 14 2.913402	E122 59 52.447820	81.261E	0.136	0.062	88.0	0.113
ZGN 04	N 8 8 16.811367	E122 40 34.326718	67.658E	0.156	0.073	87.8	0.128
ZGN 05	N 7 58 51.559090	E122 24 19.768998	222.699E	0.137	0.062	87.6	0.111
ZGN 06	N 7 42 29.002175	E122 8 11.783590	72.654E	0.129	0.061	87.7	0.111
ZGN 07	N 7 17 31.462758	E122 3 57.173233	74.960E	0.071	0.035	88.3	0.059
ZGS 01	N 8 4 23.468662	E123 29 19.980577	89.172E	0.125	0.047	87.4	0.095
ZGS 03	N 7 34 45.210424	E123 10 2.881451	71.277E	0.136	0.058	87.8	0.107
ZGS 04	N 7 44 20.317118	E123 28 4.949309	172.524E	0.148	0.057	87.5	0.112
ZGS 05	N 7 49 3.372292	E123 23 35.123202	452.909E	0.168	0.054	86.9	0.109
ZGS 06	N 7 49 41.070124	E123 25 50.803520	134.705E	0.131	0.050	87.4	0.099
ZGS 07	N 7 51 28.944908	E123 2 55.838463	170.658E	0.137	0.058	87.7	0.106

ZGS 08	N 7 25 30.103431	E122 48 33.729327	87.634E	0.144	0.062	87.5	0.110
ZGS 09	N 7 35 13.949699	E122 48 8.224755	86.542E	0.147	0.066	87.6	0.118
ZGS 10	N 7 46 25.358207	E122 34 48.138749	142.223E	0.137	0.058	87.4	0.105
ZGS 11	N 7 22 40.217717	E122 17 23.319030	94.353E	0.100	0.045	87.8	0.077
ZGS 12	N 7 15 21.835955	E122 15 46.690680	176.213E	0.090	0.040	87.8	0.067
MRQ 01	N13 33 36.032960	E121 52 7.982200	319.029E	.001	0.001	0.0	0.001
ABY 03	N13 28 36.030432	E123 40 33.320669	161.740E	0.001	0.001	0.0	0.001
CGY 08	N17 37 2.567887	E121 43 35.424730	82.055E	0.001	0.001	0.0	0.001
ILN 01	N18 23 41.343889	E120 35 49.049710	41.120E	0.001	0.001	0.0	0.001
ILO 01	N10 42 36.552947	E122 33 53.576580	84.001E	0.001	0.001	0.1	0.001
CTN 01	N 7 0 44.446117	E125 5 30.857450	367.189E	0.001	0.001	0.3	0.001
PLW 11	N 9 42 27.861430	E118 42 51.582540	55.774E	0.001	0.001	0.0	0.001
PNG 05	N15 52 3.650304	E120 15 13.274470	139.874E	0.001	0.001	0.0	0.001
ZGS 02	N 6 55 21.094629	E122 4 8.813160	77.155E	0.001	0.001	0.1	0.001
LYT 08	N11 15 4.950184	E125 0 19.325201	88.229E	0.001	0.001	0.1	0.001

APPENDIX 5

Pre 1990 Luzon Earthquake WGS84 Coordinates from a free net adjustment of PGNet GPS data using NEWGAN software

Result Format

Point	φ	λ	h	**Horiz**	**Standard**	**Ellipse**	**Height**
				Semi major	Semi minor	Orient	Std Dev
	X	Y	Z				

ABR 01 N 17 36 10.71175 E 120 36 54.53986 90.383 0.031 0.029 263.6 0.010
-3097083.013 5233722.438 1916573.833

QZN 07 N 15 12 39.91491 E 121 24 53.88416 51.540 0.299 0.118 84.3 0.189
-3208787.127 5253750.456 1662663.385

TRC 01 N 15 28 38.48284 E 120 35 57.49344 87.310 0.216 0.102 81.8 0.173
-3129720.858 5292215.738 1691086.076

ARA 01 N 15 45 25.61777 E 121 33 47.23851 49.503 0.188 0.094 82.7 0.166
-3213917.091 5231689.856 1720890.071

ARA 02 N 16 8 35.89651 E 121 57 26.66730 52.743 0.192 0.097 82.2 0.173
-3243628.861 5199488.098 1761980.878

BGT 01 N 16 23 59.35230 E 120 38 46.59619 1290.336 0.170 0.082 83.9 0.150
-3120358.174 5266524.701 1789579.861

BGT 02 N 16 35 50.06075 E 120 45 44.01510 2156.015 0.165 0.078 84.7 0.139
-3128259.948 5255579.626 1810779.031

BLN 01 N 14 56 26.49805 E 120 52 52.48874 58.255 0.217 0.103 81.4 0.177
-3163706.420 5290096.797 1633775.755

BLN 02 N 14 50 47.72571 E 120 45 52.91226 47.050 0.252 0.110 82.7 0.184
-3154302.359 5298811.681 1623710.274

BLN 03 N 14 54 15.28783 E 121 2 34.84164 128.465 0.220 0.105 81.3 0.184
-3179199.989 5282091.452 1629896.967

BLN 04 N 15 11 23.80524 E 121 2 39.56130 121.373 0.230 0.112 79.1 0.206
-3175084.890 5274981.220 1660424.178

IFG 01 N 16 55 13.90957 E 121 3 5.51913 1408.952 0.148 0.073 84.4 0.133
-3149065.550 5230263.712 1844831.184

ILS 02 N 17 7 51.96410 E 120 26 37.40160 48.183 0.127 0.064 84.9 0.114
-3089288.202 5256369.952 1866717.722

ILS 03 N 16 58 44.37630 E 120 44 18.00349 627.094 0.129 0.065 84.5 0.117
-3119081.690 5245135.065 1850793.210

ISB 02 N 16 42 18.88133 E 121 33 30.92694 123.184 0.172 0.088 83.0 0.164
-3198191.542 5207014.649 1821649.888

ISB 04 N 16 30 12.71917 E 121 44 13.33126 149.494 0.179 0.091 82.6 0.167
-3217761.835 5202475.384 1800265.359

Result Format

Point	ϕ	λ	h	Horiz Standard	Ellipse	Height
				Semi major	Semi minor Orient	Std Dev
	X	Y	Z			

LAG 02 N 14 26 7.26665 E 121 26 57.23248 56.242 0.308 0.124 83.8 0.199
-3223387.817 5270568.036 1579688.228

LUN 01 N 16 34 57.01208 E 120 18 15.94592 85.944 0.158 0.077 84.4 0.141
-3085402.035 5279095.839 1808624.863

MMA 00 N 14 38 6.66480 E 121 2 34.96067 101.046 0.231 0.108 81.3 0.183
-3183103.251 5288569.631 1601102.402

MMA 05 N 14 39 22.97259 E 121 4 11.14851 134.746 0.230 0.108 81.3 0.183
-3185279.922 5286604.670 1603380.065

MPV 01 N 17 5 33.23013 E 120 58 8.28743 1232.839 0.144 0.071 84.3 0.131
-3138572.710 5229876.065 1862989.748

NEJ 43 N 15 56 26.97844 E 121 2 40.45562 439.266 0.179 0.089 83.4 0.157
-3163767.243 5256126.876 1740553.421

NEJ 44 N 15 29 29.43521 E 120 58 10.44505 102.516 0.204 0.098 81.9 0.170
-3163647.704 5271534.126 1692599.440

NEJ 45 N 15 39 34.13017 E 121 13 13.31884 205.163 0.185 0.093 82.8 0.167
-3184156.541 5253452.102 1710531.585

NVY 01 N 16 30 7.99504 E 121 6 45.48670 421.234 0.167 0.084 83.8 0.150
-3161031.992 5237490.859 1800203.307

NVY 02 N 16 19 37.89710 E 121 15 39.97833 862.910 0.171 0.086 83.1 0.159
-3177653.748 5234323.539 1781746.662

NVY 03 N 16 7 58.87212 E 120 55 48.06860 980.941 0.189 0.095 84.2 0.179
-3150499.653 5257847.830 1761145.543

NVY 04 N 16 9 31.30605 E 120 54 26.86625 1142.9410.190 0.095 84.2 0.179
-3148103.511 5258543.186 1763920.300

PMG 01 N 15 8 24.64455 E 120 37 59.60705 109.446 0.227 0.105 82.1 0.177
-3137883.559 5298856.188 1655106.008

PNG 03 N 16 3 47.68869 E 120 6 28.45655 83.278 0.232 0.103 81.8 0.170
-3075376.560 5303616.442 1753477.693

PNG 04 N 15 54 40.55900 E 120 38 30.19123 75.773 0.198 0.094 82.3 0.163
-3127012.439 5278713.033 1737307.956

PNG 05 N 15 52 3.47539 E 120 15 13.27551 142.038 0.217 0.100 81.9 0.169
-3091889.400 5300966.290 1732682.037

QZN 01 N 14 6 6.78100 E 122 0 55.02183 52.774 0.448 0.162 85.0 0.241
-3280119.312 5246173.648 1543929.797

QZN 03 N 14 55 30.74079 E 121 48 24.32296 71.454 0.349 0.133 85.0 0.207
-3248981.373 5238691.063 1632123.285

Result Format

Point	ϕ	λ	h	**Horiz**	**Standard**	**Ellipse**	**Height**
				Semi major	Semi minor	Orient	Std Dev
	X	Y	Z				

QZN 04 N 14 37 54.39281 E 121 56 24.39974 110.333 0.410 0.151 84.9 0.228
-3265566.776 5238174.873 1600739.800

QZN 05 N 14 39 53.90633 E 121 36 19.14184 50.049 0.321 0.126 84.2 0.200
-3234385.828 5256326.064 1604278.431

QZN 06 N 14 11 17.24221 E 121 43 43.24630 51.431 0.378 0.142 84.5 0.218
-3252609.083 5260531.345 1553181.809

TRC 02 N 15 19 23.17047 E 120 25 32.46612 245.054 0.221 0.103 81.9 0.178
-3116042.486 5305714.908 1674671.850

TRC 03 N 15 36 34.12521 E 120 23 1.76801 149.431 0.219 0.103 81.6 0.181
-3107844.395 5300620.564 1705188.230

APPENDIX 6

Post 1990 Luzon Earthquake WGS84 Coordinates from a free net adjustment of PGNet GPS data using NEWGAN software

Result Format

Point	ϕ λ h	**Horiz** Semi major	**Standard** Semi minor	**Ellipse** Orient	**Height** Std Dev
	X Y Z				
ABR 01	N 17 36 10.71175 E 120 36 54.53986	90.383	0.031	0.029 180.0	0.010
	-3097083.013 5233722.438 1916573.833				
QZN 07	N 15 12 39.90811 E 121 24 53.87411	51.579	0.249	0.081 88.0	0.144
	-3208786.919 5253750.691 1662663.193				
TRC 01	N 15 28 38.47549 E 120 35 57.48576	87.187	0.231	0.078 88.3	0.140
	-3129720.632 5292215.805 1691085.826				
ARA 01	N 15 45 25.61699 E 121 33 47.19938	49.822	0.222	0.077 88.4	0.136
	-3213916.263 5231690.733 1720890.134				
ARA 02	N 16 8 35.89066 E 121 57 26.64112	53.185	0.244	0.080 87.9	0.142
	-3243628.453 5199488.913 1761980.828				
BGT 01	N 16 23 59.33318 E 120 38 46.57799	1290.794	0.204	0.074 88.5	0.129
	-3120358.018 5266525.498 1789579.426				
BGT 03	N 16 35 57.48154 E 120 45 45.96248	2165.859	0.205	0.074 88.6	0.134
	-3128281.050 5255502.184 1811000.529				
BLN 01	N 14 56 26.49049 E 120 52 52.47995	58.027	0.260	0.083 87.9	0.148
	-3163706.113 5290096.794 1633775.472				
BLN 03	N 14 54 15.27818 E 121 2 34.83746	128.325	0.252	0.081 88.1	0.145
	-3179199.851 5282091.466 1629896.644				
BLN 04	N 15 11 23.78918 E 121 2 39.54567	121.274	0.236	0.080 88.4	0.142
	-3175084.507 5274981.490 1660423.676				
IFG 01	N 16 55 13.90924 E 121 3 5.50602	1409.111	0.197	0.072 88.5	0.129
	-3149065.297 5230264.045 1844831.221				
ILS 02	N 17 7 51.96475 E 120 26 37.40121	48.269	0.164	0.064 88.4	0.099
	-3089288.231 5256370.023 1866717.767				
ILS 03	N 16 58 44.37508 E 120 44 17.99738	627.208	0.180	0.068 88.5	0.118
	-3119081.596 5245135.260 1850793.207				
ISB 02	N 16 42 18.87865 E 121 33 30.91311	123.607	0.208	0.075 88.4	0.133
	-3198191.418 5207015.228 1821649.931				
ISB 04	N 16 30 12.71366 E 121 44 13.31122	149.822	0.230	0.078 88.1	0.138
	-3217761.520 5202476.005 1800265.290				
ISB 54	N 17 12 20.01495 E 121 36 24.83478	112.118	0.262	0.091 88.8	0.200
	-3194112.362 5190555.114 1874609.926				

Result Format

Point	ϕ	λ	h	Horiz Standard	Ellipse		Height
				Semi major	Semi minor	Orient	Std Dev
	X	Y	Z				

LUN 01 N 16 34 57.01041 E 120 18 15.92968 86.438 0.201 0.073 88.4 0.128
-3085401.865 5279096.504 1808624.955

LUN 02 N 16 21 31.85450 E 120 21 41.17808 99.731 0.255 0.080 88.6 0.141
-3094206.853 5282089.723 1784893.622

LUN 03 N 16 15 31.36066 E 120 22 3.03210 45.135 0.242 0.078 88.7 0.137
-3096313.162 5284401.543 1774242.691

MPV 01 N 17 5 33.22988 E 120 58 8.28000 1232.986 0.189 0.070 88.3 0.125
-3138572.596 5229876.300 1862989.784

NEJ 43 N 15 56 27.04888 E 121 2 40.39078 439.516 0.215 0.076 88.5 0.134
-3163765.408 5256127.567 1740555.572

NEJ 44 N 15 29 29.40930 E 120 58 10.43055 102.613 0.233 0.081 89.1 0.144
-3163647.491 5271534.611 1692598.698

NEJ 45 N 15 39 34.16911 E 121 13 13.23029 204.891 0.222 0.077 88.5 0.136
-3184153.983 5253452.969 1710532.664

NEJ 47 N 15 58 2.50571 E 121 2 45.33836 351.797 0.219 0.076 88.2 0.133
-3163432.022 5255288.393 1743352.808

NVY 01 N 16 30 8.01002 E 121 6 45.47564 421.524 0.204 0.074 88.5 0.131
-3161031.787 5237491.154 1800203.831

NVY 02 N 16 19 37.90966 E 121 15 39.96221 863.262 0.208 0.074 88.3 0.131
-3177653.458 5234323.983 1781747.132

NVY 03 N 16 7 58.96319 E 120 55 48.02783 981.067 0.238 0.084 88.5 0.149
-3150498.276 5257847.889 1761148.267

NVY 04 N 16 9 31.39093 E 120 54 26.84588 1143.697 0.240 0.084 88.5 0.150
-3148102.992 5258543.497 1763923.017

PMG 01 N 15 8 24.63661 E 120 37 59.59596 109.159 0.240 0.080 88.2 0.142
-3137883.166 5298856.173 1655105.698

PNG 03 N 16 3 47.68903 E 120 6 28.45648 83.296 0.233 0.078 88.0 0.139
-3075376.565 5303616.455 1753477.708

PNG 04 N 15 54 40.54096 E 120 38 30.18415 76.046 0.218 0.076 88.4 0.135
-3127012.469 5278713.497 1737307.497

PNG 05 N 15 52 3.47256 E 120 15 13.26700 142.038 0.227 0.078 88.2 0.137
-3091889.194 5300966.438 1732681.953

PNG 06 N 16 2 40.05399 E 120 19 43.79850 47.555 0.248 0.080 88.2 0.142
-3096076.987 5292185.236 1751469.868

PNG 07 N 16 4 22.07413 E 120 20 7.96578 61.389 0.252 0.080 88.2 0.142
-3096265.613 5291085.210 1754487.319

Result Format

Point	ϕ	λ	h	**Horiz**	**Standard**	**Ellipse**	**Height**
				Semi major	Semi minor	Orient	Std Dev
	X	Y	Z				

QZN 03 N 14 55 30.73701 E 121 48 24.32394 71.713 0.317 0.091 87.3 0.168
-3248981.546 5238691.286 1632123.239

QZN 04 N 14 37 54.38405 E 121 56 24.39932 110.663 0.335 0.094 87.4 0.173
-3265566.970 5238175.208 1600739.623

QZN 05 N 14 39 53.90174 E 121 36 19.14291 50.084 0.339 0.094 87.2 0.174
-3234385.892 5256326.107 1604278.303

TRC 02 N 15 19 23.16801 E 120 25 32.46128 244.907 0.251 0.082 88.1 0.146
-3116042.300 5305714.876 1674671.738

TRC 03 N 15 36 34.12189 E 120 23 1.75610 149.265 0.248 0.081 88.0 0.145
-3107844.022 5300620.629 1705188.087

Appendix 7

Digitised UTM Zone 51 N (WGS84) coordinates of the mapped rupture trace of the 1990 Luzon Earthquake from south near Gabaldon (point 1) to north near Kayapa (point 215)

	UTM (WGS84) Zone 51 N Coordinates	
Luzon EQ Fault (Digitised)	**Easting** (metres)	**Northing** (metres)
1	323840	11705366
2	323519	11705475
3	323267	11705623
4	322984	11705926
5	322697	11706274
6	322393	11706552
7	322065	11706777
8	321690	11707027
9	321195	11707193
10	320732	11707641
11	320549	11707840
12	320243	11708175
13	320073	11708742
14	319883	11709407
15	319646	11710303
16	319596	11710455
17	319377	11710987
18	319257	11711277
19	319028	11711768
20	318907	11711952
21	318733	11712172
22	318563	11712401
23	318343	11712595
24	318076	11712848
25	317692	11713497
26	317249	11714194
27	317276	11714188
28	316836	11714910
29	316639	11715192
30	316520	11715353
31	316359	11715564
32	315881	11716090
33	315474	11716517
34	315079	11716929
35	314699	11717344
36	314248	11717852
37	313992	11718136
38	313776	11718329
39	313366	11718618
40	312912	11718882
41	312467	11719192
42	312470	11719142
43	311971	11719505

	UTM (WGS84) Zone 51 N Coordinates	
Luzon EQ Fault (Digitised)	**Easting** (metres)	**Northing** (metres)
44	311432	11719840
45	310986	11720148
46	310434	11720485
47	310111	11720712
48	309911	11720873
49	309613	11721222
50	309234	11721650
51	308824	11722082
52	308532	11722414
53	308031	11723067
54	307503	11723682
55	307113	11724197
56	306671	11724719
57	306299	11725190
58	305833	11725856
59	305479	11726331
60	305270	11726616
61	305168	11726780
62	304855	11727230
63	304397	11727858
64	303876	11728665
65	303497	11729149
66	303213	11729591
67	303059	11729845
68	302873	11730117
69	302531	11730491
70	302090	11731118
71	301702	11731655
72	301350	11732067
73	301102	11732389
74	300709	11732852
75	300187	11733519
76	299876	11733919
77	299658	11734178
78	299149	11734791
79	298801	11735267
80	298437	11735678
81	297972	11736213
82	297602	11736702
83	297429	11736911
84	297238	11737135
85	297021	11737345
86	296858	11737483
87	296370	11738058
88	295996	11738592
89	295668	11738983
90	295454	11739287
91	295034	11739817
92	294843	11740148
93	294761	11740318
94	294519	11740641
95	294318	11740998

	UTM (WGS84) Zone 51 N Coordinates	
Luzon EQ Fault (Digitised)	**Easting** (metres)	**Northing** (metres)
96	294155	11741277
97	297234	11737134
98	293978	11742053
99	293707	11742793
100	293433	11743531
101	293302	11743955
102	293133	11744651
103	292914	11745087
104	292482	11745732
105	292253	11746106
106	291931	11746740
107	291641	11747272
108	291257	11747788
109	290942	11748381
110	290623	11749038
111	290398	11749586
112	290260	11750100
113	290015	11750720
114	289824	11751241
115	289441	11751995
116	289160	11752621
117	288962	11753061
118	288794	11753339
119	288376	11754154
120	288031	11754821
121	287784	11755267
122	287681	11755687
123	287581	11756083
124	287164	11756940
125	286946	11757324
126	286861	11757714
127	286582	11758163
128	286294	11758444
129	286136	11758712
130	286024	11758959
131	286032	11759014
132	285775	11759581
133	285587	11760017
134	285335	11760641
135	285187	11761083
136	285045	11761405
137	284728	11762148
138	284552	11762621
139	284465	11762816
140	284345	11763007
141	284023	11763774
142	283759	11764324
143	283533	11764685
144	283362	11765088
145	283167	11765411
146	283062	11766024

UTM (WGS84) Zone 51 N Coordinates

Luzon EQ Fault (Digitised)	**Easting** (metres)	**Northing** (metres)
147	282938	11766504
148	282852	11766818
149	282723	11767059
150	282562	11767408
151	282450	11767737
152	282334	11768268
153	282185	11768980
154	282044	11769476
155	281926	11769792
156	281888	11769830
157	281714	11770236
158	281584	11770797
159	281440	11771399
160	281268	11772354
161	281162	11772845
162	280994	11773416
163	280926	11773861
164	280939	11774140
165	280875	11774693
166	280719	11775079
167	280646	11775473
168	280521	11775957
169	280392	11776452
170	280235	11776760
171	280200	11777151
172	280115	11777510
173	279842	11777817
174	279500	11778309
175	279173	11778819
176	278919	11779162
177	278748	11779491
178	278547	11779891
179	278372	11780274
180	278211	11780613
181	278118	11780880
182	277988	11781470
183	277818	11781765
184	277680	11782168
185	277422	11782965
186	277242	11783615
187	277096	11783946
188	276854	11784358
189	276636	11784760
190	276523	11785086
191	276455	11785509
192	276404	11785941
193	276337	11786251
194	276108	11786733
195	275964	11787108
196	275801	11787484
197	275541	11788503

	UTM (WGS84) Zone 51 N Coordinates	
Luzon EQ Fault (Digitised)	**Easting** (metres)	**Northing** (metres)
198	275397	11789245
199	275244	11789847
200	275136	11790405
201	275029	11790899
202	274975	11791476
203	274862	11792188
204	274652	11792830
205	274621	11793423
206	274630	11793995
207	274565	11794545
208	274507	11795115
209	274579	11795482
210	274619	11795788
211	274793	11796355
212	274969	11796771
213	275114	11797168
214	275162	11797390
215	275192	11797570